Article

Unextractable fossil fuels in a 1.5 °C world

Dan Welsby[1✉], James Price[2], Steve Pye[2] & Paul Ekins[1]

Parties to the 2015 Paris Agreement pledged to limit global warming to well below 2 °C and to pursue efforts to limit the temperature increase to 1.5 °C relative to pre-industrial times[1]. However, fossil fuels continue to dominate the global energy system and a sharp decline in their use must be realized to keep the temperature increase below 1.5 °C (refs. [2–7]). Here we use a global energy systems model[8] to assess the amount of fossil fuels that would need to be left in the ground, regionally and globally, to allow for a 50 per cent probability of limiting warming to 1.5 °C. By 2050, we find that nearly 60 per cent of oil and fossil methane gas, and 90 per cent of coal must remain unextracted to keep within a 1.5 °C carbon budget. This is a large increase in the unextractable estimates for a 2 °C carbon budget[9], particularly for oil, for which an additional 25 per cent of reserves must remain unextracted. Furthermore, we estimate that oil and gas production must decline globally by 3 per cent each year until 2050. This implies that most regions must reach peak production now or during the next decade, rendering many operational and planned fossil fuel projects unviable. We probably present an underestimate of the production changes required, because a greater than 50 per cent probability of limiting warming to 1.5 °C requires more carbon to stay in the ground and because of uncertainties around the timely deployment of negative emission technologies at scale.

In 2015, McGlade and Ekins[9] set out the limits to fossil fuel extraction under stringent climate targets. They estimated that one-third of oil reserves, almost half of fossil methane gas reserves and over 80% of current coal reserves should remain in the ground in 2050 to limit warming to 2 °C. They also highlighted that some countries would need to leave much higher proportions of fossil fuel reserves in the ground than others. Since 2015, the Paris Agreement and the Intergovernmental Panel on Climate Change (IPCC) have helped to refocus the debate on warming limits of 1.5 °C (refs. [1,10]). Multiple scenarios have been published, showing the additional effort required to limit global CO_2 emissions to net zero by around 2050 to meet this target[11]. In this Article, we extend the earlier 2015 work to estimate the levels of unextractable fossil fuel reserves out to 2100 under a 1.5 °C scenario (50% probability), using a 2018–2100 carbon budget of 580 $GtCO_2$ (ref. [3]). We also provide insights into the required decline of fossil fuel production at a regional level, which will necessitate a range of policy interventions. We define unextractable fossil fuels as the volumes that need to stay in the ground, regardless of end use (that is, combusted or non-combusted), to keep within our 1.5 °C carbon budget.

Paris Agreement-compliant fossil fuel prospects

Fossil fuels continue to dominate the global energy system, accounting for 81% of primary energy demand[12]. After decades of growth, their rate of production and use will need to reverse and decline rapidly to meet internationally agreed climate goals. There are some promising signs, with global coal production peaking in 2013, and oil output estimated to have peaked in 2019 or be nearing peak demand, even by some industry commentators[13].

The plateauing of production and subsequent decline will mean that large amounts of fossil fuel reserves, prospects that are seen today as economic, will never be extracted. This has important implications for producers who may be banking on monetizing those reserves in the future, and current and prospective investors. Investments made today in fossil fuel energy therefore risk being stranded[14]. However, there continues to be a disconnect between the production outlook of different countries and corporate entities and the necessary pathway to limit average temperature increases[2].

A number of analyses have explored how fossil fuels fit into an energy system under a 1.5 °C target. The IPCC's *Special Report on Global Warming of 1.5 °C* estimates coal use only representing 1–7% of primary energy use in 2050, while oil and fossil methane gas see declines relative to 2020 levels by 39–77% and 13–62%, respectively[3]. Despite strong declines, the use of fossil fuels continues at lower levels, reflecting the assumed inertia in the system and continued use of fossil fuels in hard-to-mitigate sectors. Luderer et al.[4] estimate that, despite large-scale efforts, CO_2 emissions from fossil fuels will probably exceed the 1.5 °C carbon budget and require high levels of carbon dioxide removals (CDR). Grubler et al.[5] explored efforts to reduce energy demand, substantially reducing the role of fossil fuels and removing the need for CDR deployment.

The extent of fossil fuel decline in the coming decades remains uncertain, influenced by factors such as the rapidity of the rollout of clean technologies and decisions about the retirement of (and new investment in) fossil fuel infrastructure. Indeed, while dependent on lifetimes and operating patterns, existing fossil fuel infrastructure already places a 1.5 °C target at risk owing to implied 'committed' future CO_2 emissions[6]. The possible extent of CDR further complicates this

[1]Institute for Sustainable Resources, University College London, London, UK. [2]UCL Energy Institute, University College London, London, UK. ✉e-mail: daniel.welsby.14@ucl.ac.uk

picture. At high levels, this may allow for more persistent use of fossil fuels, but such assumptions have attracted considerable controversy[7].

Although a number of studies have explored fossil fuel reductions under a 1.5 °C target, none have estimated the fossil fuel reserves and resources that have to remain in the ground. Here, using global energy systems model TIAM-UCL, we assess the levels of fossil fuels that would remain unextractable in 2050 and 2100.

Unextractable reserves under a 1.5 °C target

Unextractable oil, fossil methane gas and coal reserves are estimated as the percentage of the 2018 reserve base that is not extracted to achieve a 50% probability of keeping the global temperature increase to 1.5 °C. We estimate this to be 58% for oil, 56% for fossil methane gas and 89% for coal in 2050. This means that very high shares of reserves considered economic today would not be extracted under a global 1.5 °C target. These estimates are considerably higher than those made by McGlade and Ekins[9], who estimated unextractable reserves at 33% and 49% for oil and fossil methane gas, respectively (Supplementary Fig. 3). This reflects the stronger climate ambition assumed in this analysis, plus a more positive outlook for low-carbon technology deployment, such as zero-emission vehicles and renewable energy.

Continued use of fossil fuels after 2050 sees these estimates reduce by 2100. For oil, the global estimate drops to 42% in 2100. The reduction is smaller for fossil methane gas, reducing from 56% to 47%. The majority of fossil fuels extracted after 2050 are used as feedstocks in the petrochemical sector, and as fuel in the aviation sector in the case of oil. Feedstock use, which has a substantially lower carbon intensity than combustion, accounts for 65% and 68% of total oil and fossil methane gas use, respectively, in 2100 under a 1.5 °C carbon budget. However, it also reflects limited consideration of targeted actions to reduce feedstock use that, if available, would limit the dependence on CDR.

Unextractable shares vary substantially by region, relative to the global estimates (Fig. 1, Table 1). The largest reserve holders, such as the Middle East (MEA) (for oil and fossil methane gas) and Russia and other former Soviet states (FSU) (for fossil methane gas) have the strongest influence on the global picture, and therefore have estimates close to or marginally above the global average. For oil, Canada has much higher unextractable estimates than in other regions, at 83%. This includes 84% of the 49 billion barrels (Gb) of Canadian oil sands we estimate as proven reserves. By contrast, the FSU region has a relatively low unextractable share of total oil reserves (38% in 2050), reflecting their cost-effectiveness.

Given its role as a key exporter and with the lowest-cost reserve base, MEA sees unextractable reserves of 62% in 2050, reducing to 38% by 2100. As previously mentioned, oil consumption after 2050 is dominated by non-combustible feedstocks and therefore action to reduce demand for oil-based products, such as plastics[15], would substantially change this picture for producers[16] including MEA. It is evident that large incumbent producers dominate the production picture going forwards, with the vast majority of undeveloped (particularly unconventional) oil remaining unused.

Unextractable estimates for coal show less regional variation, although they are lowest in those regions that utilize most coal in the next 30 years, notably India, China and other parts of Asia (ODA). However, coal consumption declines rapidly even in these regions (see Supplementary Information section 6 for additional detail on coal decline).

A sensitivity analysis on key model assumptions was undertaken to explore the effect on unextractable reserve estimates (Supplementary Information section 3). These include the rate of carbon capture and storage (CCS) deployment, availability of bioenergy, and growth in future energy service demands in aviation and the chemical sector given the challenges in their decarbonization. We find that the sensitivities do not affect the unextractable estimates substantially, suggesting that the headline results are relatively robust to uncertainties across key

assumptions. Of the sensitivities, the availability of biomass (and therefore negative emissions potential from bioenergy with CCS (BECCS)) has the most impact on unextractable estimates. Where higher biomass availability is assumed, unextractable estimates in 2050 for oil, fossil methane gas and coal are 55% (−3%), 53% (−3%), and 87% (−2%), respectively (change relative to central scenario in brackets).

Broadening out unextractable estimates to resources is important because a share of non-reserve resources will come online in future years, and contribute to overall production and eventual emissions (Supplementary Information section 1). For unconventional oil, their large size (as well as less-favourable economics and higher carbon intensity) means that 99% of these resources remain unextractable. A higher share of unconventional gas also remains unextractable (86%), relative to conventional resources (74%), again due to higher extractions costs in most regions, with the exception of North America. Arctic oil and fossil methane gas resources across all regions where these are located remain undeveloped.

Production decline of major producing regions

Underlying the regional unextractable estimates of both reserves and the wider resource base are regional production trajectories. Figure 2 shows the outlook to 2050 for the five largest oil-and fossil methane gas-producing regions. The outlook is one of decline, with 2020 marking both global peak oil and fossil methane gas production, with decline thereafter to 2050 of 2.8% and 3.2%, respectively (Supplementary Fig. 7).

Apart from the USA, all oil producing regions see strong declines to 2050 (Fig. 2a). The USA sees production growth to 2025, peaking at 16.9 million barrels per day, before constant decline out to 2050. This initial increase is due to several factors including falling imports of oil into the USA, the continued use of oil in the transport sector before strong growth in low-emission vehicles and the flexibility of light tight oil due to its production dynamics (that is, high production growth and decline rates from tight oil wells).

For CSA, production shows modest decline of 1.1% per year to 2025, before a more rapid rate of decline of 3.5% out to 2050. The early slow decline reflects Brazilian fields with final investment decisions off-setting production decline in mature producing assets[17]. MEA, the largest oil producer, sees a decline of over 50% by 2050 (relative to 2020). Given the huge reserves in the region, most production to 2050 is from designated reserves (85–91% in any given year). Elsewhere, oil production in Africa and the FSU exhibits constant decline from 2020 out to 2050 at rates of 3.5% and 3.1%, respectively, driven by declining domestic demand and oil demand destruction in key importing regions (for example, Europe).

Regional fossil methane gas production is a more complex story owing to its use to meet demand growth in emerging markets, and as an alternative to coal use in the industrial sector, notably in China and ODA (Fig. 2b). Production in the USA peaks in 2020 and sees rapid decline through 2050, with an annual derived decline rate of 8.1%. This mirrors a rapid decline in the domestic market, with complete phase out of use in the power sector by 2040. In addition, the high share of unconventional gas in the production mix exhibits faster decline than for other major producers. This has important implications for US liquefied fossil methane gas exports, with prospects of low utilization rates of infrastructure, and limited prospect for future additional liquefaction capacity. The FSU region sees peak gas production in 2020, but with production decline across legacy gas fields in Western Siberia and Central Asia moderated by the production increases from export projects to predominantly Asian (and particularly Chinese) markets and a shift of production to the Yamal Peninsula and East Siberia.

Three of the regions in Fig. 2b see fossil methane gas production growth out to the 2030s, before decline. For the Middle East, this reflects the competitiveness of exporters in the region. For Africa, this
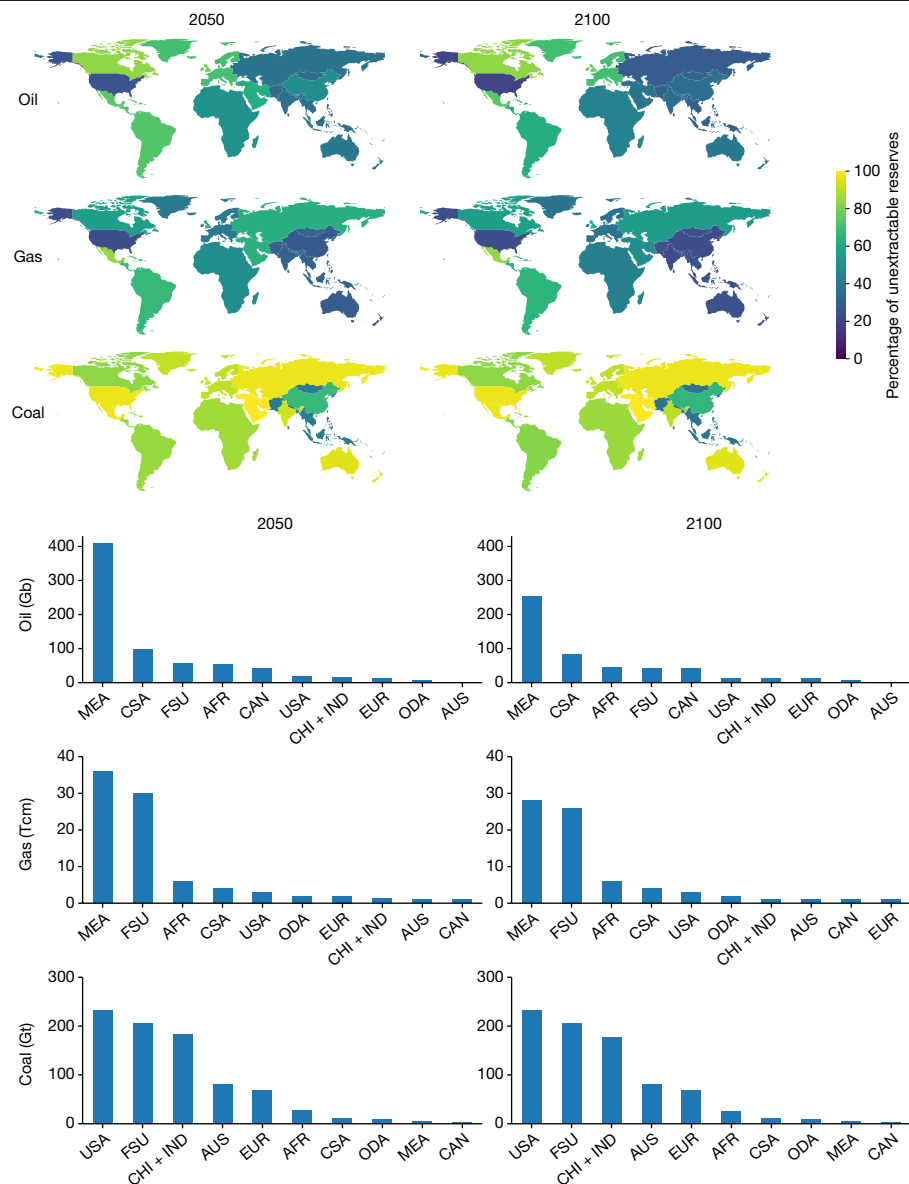
Fig. 1 | Unextractable reserves of fossil fuels by region in 2050 and 2100 under a 1.5 °C scenario. Left, 2050. Right, 2100. Top, Maps of the percentage of unextractable reserves of oil, fossil methane gas and coal (from top to bottom) disaggregated into the model regions. We note that 13 out of 16 TIAM regions are plotted with the Western and Eastern EU aggregated together, and South Korea and Japan are not shown owing to their negligible reserves. Bottom, The absolute amount of each fossil fuel reserve that must remain unextracted. In some cases the order of regions on the x axis changes between 2050 and 2100 owing to similar levels of unextractable reserves in 2050 and small differences in cumulative production after 2050 leading to regions switching places. Reserves are defined as both technically and economically proven given current market conditions. They can be further subcategorized: currently producing, undeveloped but post/pending final investment decision and undeveloped but sufficient field appraisal to meet SPE definition of technically and economically proven[27]. Additional detail on the definition of reserves in this work is provided in the Methods. The mapping software used was Python version 3.8 (Python Software Foundation). The y-axis units are billion barrels (Gb), trillion m³ (Tcm) and billion tonnes (Gt) for oil, gas and coal, respectively.

growth is driven by increased demand for electricity, higher industrial demand (partially displacing oil) and modest growth in exports to 2035. For ODA, fossil methane gas gains domestic market share as coal is rapidly phased out of industry. However, there is considerable uncertainty around the geological and economic feasibility of undeveloped resources, particularly for the two largest producers in ODA: Indonesia and Malaysia. The profiles for Africa and ODA also suggest substantial transition risk, particularly as post-2035 production rapidly declines at rates of 5.7% and 6.6%, respectively. This decline is due to the ramp-up in renewables crowding fossil methane gas out of the power sector and the increasing electrification of industry. This transition risk also extends to large exporters, given rapidly changing import dynamics in regions such as China. For example, Chinese gas demand peaks at

700 billion m³ (60% of which is imported) in 2035, before reverting to 2018 levels by 2050.

Reassessing fossil fuel production

The need to forgo future production means country producers, fossil energy companies and their investors need to seriously reassess their production outlooks. This is particularly true for countries that are fiscally reliant on fossil fuels, to allow for a managed diversification of their economies. Many regions are facing peak production now or over the next decade, and the development of new low-carbon sectors of their economies that will provide employment and revenues will therefore be key. For regions that are heavily dependent on fossil

Table 1 | Unextractable reserves of fossil fuels by region under the 1.5 °C scenario

Region	Oil				Fossil methane gas				Coal			
	2050		2100		2050		2100		2050		2100	
	(%)	(Gb)	(%)	(Gb)	(%)	(Tcm)	(%)	(Tcm)	(%)	(Gt)	(%)	(Gt)
Africa (AFR)	51	53	44	46	49	6	43	6	86	27	85	26
Australia and other OECD Pacific (AUS)	40	2	40	2	29	0.7	25	0.6	95	80	95	80
Canada (CAN)	83%	43	83%	43	56%	1.1	56%	1.1	83%	4	83%	4
China and India (CHI + IND)	47%	17	36%	13	29%	1.3	24%	1.1	76%	182	73%	177
Russia and former Soviet states (FSU)	38%	57	29%	44	63%	30	55%	26	97%	205	97%	205
Central and South America (CSA)	73%	98	62%	84	67%	4	65%	4	84%	11	82%	11
Europe (EUR)	72%	12	72%	12	43%	2	40%	1	90%	69	90%	69
Middle East (MEA)	62%	409	38%	253	64%	36	49%	28	100%	5	100%	5
Other Developing Asia (ODA)	36%	8	31%	7	32%	2	25%	2	42%	10	39%	9
USA	26%	18	20%	14	24%	2.8	24%	2.8	97%	233	97%	232
Global	58%	740	42%	541	56%	87	47%	73	89%	826	88%	818

Reserves are defined as both technically and economically proven given current market conditions. The header rows show the time horizon for which unextractable fossil fuels are assessed. Each row then shows the proportion and absolute volume of fossil fuel reserves which must remain unextracted for each column with the units in parentheses. Additional detail on the definition of reserves in this work is provided in the Methods. For a breakdown of countries included in the aggregated regions of TIAM-UCL, see Supplementary Table 26. OECD, Organisation for Economic Co-operation and Development.

fuels for fiscal revenue, this analysis echoes recent work suggesting huge transition risk unless economies diversify rapidly[18]. For example, Middle Eastern oil production needs to peak in 2020, which in combination with lower oil prices from demand destruction signifies large reductions in fiscal revenue, with Iraq, Bahrain, Saudi Arabia and Kuwait relying on fossil fuels for 65–85% of total government revenues at present.

Central to pushing this transition forwards will be the domestic policy measures required to both restrict production and reduce demand[19].

Increasing attention is being focused on supply-side policies that can complement carbon pricing and regulatory instruments that focus on demand[20]. Such policies act to curtail the extraction of fossil fuels and can include subsidy removal, production taxes, penalties for regulatory non-compliance and bans on new exploration and production[21]. The development of international initiatives, such as the proposed non-proliferation treaty on fossil fuels[22], is also key as they could serve to foster global action, as could existing frameworks such as the United Nations Framework Convention on Climate Change[23].
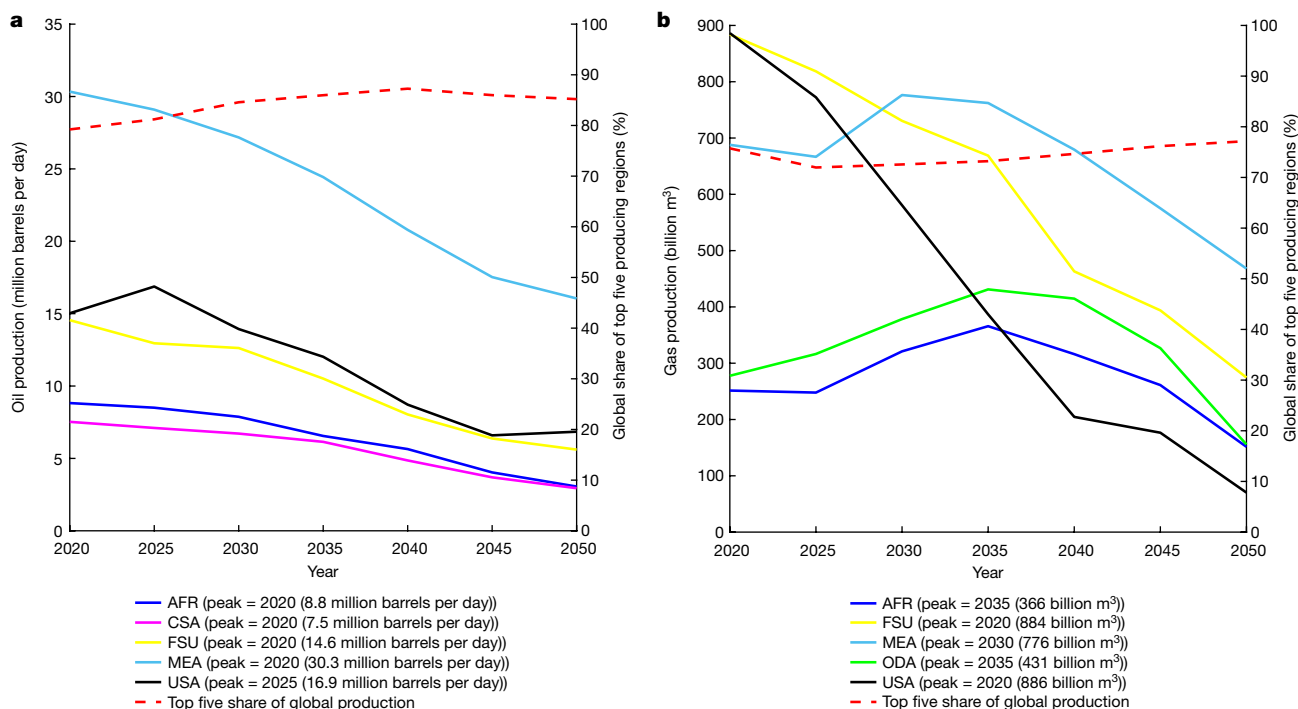

Fig. 2 | Production profiles for regions producing major oil and fossil methane gas for 2020–2050. a, Total oil production. **b**, Total fossil methane gas production. The left-hand *y* axis shows the production from each of the five largest oil (**a**) and gas (**b**)-producing regions, whereas the right-hand *y* axis shows the global share captured by these incumbent producers. The legend shows the year and volume of peak production for each region in parentheses.

Article

The recent downturn in oil and fossil methane gas demand due to COVID-19 provides an opportune moment for governments to shift strategy[2]. The crisis has further exposed the vulnerability of the oil and gas sector in particular, and raised concerns about its profitability in the future[24,25]. With many fossil fuel energy companies revising their outlooks downwards in 2020, this makes new investments risky. These risks are compounded by the momentum towards low-carbon technologies, with continued falls in renewable energy costs and battery technology. Governments who have historically benefited should take the lead, with other countries that have a high dependency on fossil fuels but low capacity for transition—or those forgoing extractive activities—needing to be supported to follow this lead[26].

The bleak picture painted by our scenarios for the global fossil fuel industry is very probably an underestimate of what is required and, as a result, production would need to be curtailed even faster. This is because our scenarios use a carbon budget associated with a 50% probability of limiting warming to 1.5 °C, which does not consider uncertainties around, for example, Earth system feedbacks[3]; therefore, to ensure more certainty of stabilizing at this temperature, more carbon needs to stay in the ground. Furthermore, it relies on CDR of approximately 4.4 (5.9) GtCO$_2$ per year by 2050 (2100). Given the substantial uncertainties around the scaling of CDR, this dependency risks underestimating the required rate of emissions reduction.

Online content

Any methods, additional references, Nature Research reporting summaries, source data, extended data, supplementary information, acknowledgements, peer review information; details of author contributions and competing interests; and statements of data and code availability are available at https://doi.org/10.1038/s41586-021-03821-8.

1. *Adoption of the Paris Agreement* https://unfccc.int/resource/docs/2015/cop21/eng/l09r01.pdf (United Nations, 2015).
2. *The Production Gap Report: 2020 Special Report* http://productiongap.org/2020report (SEI, IISD, ODI, E3G & UNEP, 2020).
3. Rogelj, J. et al. in *Special Report on Global Warming of 1.5 °C* (eds Masson-Delmotte, V. et al.) (IPCC, WMO, 2018).
4. Luderer, G. et al. Residual fossil CO$_2$ emissions in 1.5–2°C pathways. *Nat. Clim. Change* **8**, 626–633 (2018).
5. Grubler, A. et al. A low energy demand scenario for meeting the 1.5 °C target and sustainable development goals without negative emission technologies. *Nat. Energy* **3**, 515–527 (2018).
6. Tong, D. et al. Committed emissions from existing energy infrastructure jeopardize 1.5 °C climate target. *Nature* **572**, 373–377 (2019).
7. Anderson, K. & Peters, G. The trouble with negative emissions. *Science* **354**, 182–183 (2016).
8. Pye, S. et al. An equitable redistribution of unburnable carbon. *Nat. Commun.* **11**, 3968 (2020).
9. McGlade, C. & Ekins, P. The geographical distribution of fossil fuels unused when limiting global warming to 2 °C. *Nature* **517**, 187–190 (2015).
10. Masson-Delmotte, V. et al. (eds) *Special Report on Global Warming of 1.5 °C* (IPCC, WMO, 2018).
11. Rogelj, J. et al. Scenarios towards limiting global mean temperature increase below 1.5 °C. *Nat. Clim. Change* **8**, 325–332 (2018).
12. *World Energy Outlook 2019* (IEA, 2019).
13. *BP Energy Outlook: 2020 Edition* https://www.bp.com/content/dam/bp/business-sites/en/global/corporate/pdfs/energy-economics/energy-outlook/bp-energy-outlook-2020.pdf (BP, 2020).
14. *Unburnable Carbon 2013: Wasted Capital and Stranded Assets* (Carbon Tracker & Grantham Research Institute of Climate Change and the Environment, 2013).
15. Lau, W. W. Y. et al. Evaluating scenarios toward zero plastic pollution. *Science* **369**, 1455–1461 (2020).
16. *The Future's Not in Plastics: Why Plastics Demand Won't Rescue the Oil Sector* https://carbontracker.org/reports/the-futures-not-in-plastics/ (Carbon Tracker Initiative, 2020).
17. Godoi, J. M. A. & dos Santos Matai, P. H. L. Enhanced oil recovery with carbon dioxide geosequestration: first steps at Pre-salt in Brazil. *J. Petrol. Explor. Prod.* **11**, 1429–1441 (2021).
18. *Beyond Petrostates: The Burning Need to Cut Oil Dependence in the Energy Transition* https://carbontracker.org/reports/petrostates-energy-transition-report/ (Carbon Tracker Initiative, 2021).
19. Green, F. & Denniss, R. Cutting with both arms of the scissors: the economic and political case for restrictive supply-side climate policies. *Clim. Change* **150**, 73–87 (2018).
20. Erickson, P., Lazarus, M. & Piggot, G. Limiting fossil fuel production as the next big step in climate policy. *Nat. Clim. Change* **8**, 1037–1043 (2018).
21. Lazarus, M. & van Asselt, H. Fossil fuel supply and climate policy: exploring the road less taken. *Clim. Change* **150**, 1–13 (2018).
22. Newell, P. & Simms, A. Towards a fossil fuel non-proliferation treaty. *Clim. Policy* **20**, 1043–1054 (2020).
23. Piggot, G., Erickson, P., van Asselt, H. & Lazarus, M. Swimming upstream: addressing fossil fuel supply under the UNFCCC. *Clim. Policy* **18**, 1189–1202 (2018).
24. *World Energy Outlook 2020* (IEA, 2020).
25. *Decline and Fall: The Size & Vulnerability of the Fossil Fuel System* https://carbontracker.org/reports/decline-and-fall/ (Carbon Tracker Initiative, 2020).
26. Muttitt, G. & Kartha, S. Equity, climate justice and fossil fuel extraction: principles for a managed phase out. *Clim. Policy* **20**, 1024–1042 (2020).
27. *Petroleum Resources Management System* http://info.specommunications.org/rs/833-LLT-087/images/PRMgmtSystem_V1.01Nov27.pdf?mkt_tok=ODMzLUxMVC0wODcAAAF9dSrG2UNYnY2eBC7yyN17I25FkaA9i2XvL5kjWdgP6mXak-NSn63rWtB1NFtduvqTfPhyTxIcU92WlXrHa762rjvWID3PytxB3BUUJLfhomzKAA (Society of Petroleum Engineers, 2018).

Methods

We first describe the TIAM-UCL model, before presenting our approach to modelling scenarios. The remainder of the Methods focuses on key issues of definition around geological categories and techno-economic classifications of fossil fuels.

Description of TIAM-UCL

To explore the question of unextractable fossil fuel reserves and resources under a 1.5 °C carbon budget, we used the TIMES Integrated Assessment Model at University College London (TIAM-UCL)[8,9,28,29]. This model provides a representation of the global energy system, capturing primary energy sources (oil, fossil methane gas, coal, nuclear, biomass and renewables) from production through to their conversion (electricity production, hydrogen and biofuel production, oil refining), transport and distribution, and their eventual use to meet energy service demands across a range of economic sectors. Using a scenario-based approach, the evolution of the system over time to meet future energy service demands can be simulated, driven by a least-cost objective. The model uses the TIMES modelling framework, which is described in detail in Supplementary Information section 7.

The model represents the countries of the world as 16 regions (Supplementary Table 26), allowing for more detailed characterization of regional energy sectors and the trade flows between regions. Upstream sectors within regions that contain members of OPEC are modelled separately, for example, the upstream sector in the Central and South America (CSA) region will be split between OPEC (Venezuela) and non-OPEC countries. Regional coal, oil and fossil methane gas prices are generated within the model. These incorporate the marginal cost of production, scarcity rents (for example, the benefit forgone by using a resource now as opposed to in the future, assuming discount rates), rents arising from other imposed constraints (such as depletion rates) and transportation costs, but not fiscal regimes. This means that the full price formation, which includes taxes and subsidies, is not captured in TIAM-UCL, and remains a contested limitation of this type of model[30].

A key strength of TIAM-UCL is the representation of the regional fossil resource base (Supplementary Information section 5). For oil reserves and resources, these are categorized into current conventional proved (1P) reserves in fields that are in production or are scheduled to be developed, reserve growth, undiscovered oil, Arctic oil, light tight oil, gas liquids, natural bitumen and extra-heavy oil. The latter two categories represent unconventional oil resources. For fossil methane gas, these resources are categorized into current conventional 1P reserves that are in fields in production or are scheduled to be developed, reserve growth, undiscovered gas, Arctic gas, associated gas, tight gas, coal-bed methane and shale gas. The categorization of resources and associated definitions are described later in the Methods. For oil and fossil methane gas, individual supply cost curves for each of the categories are estimated for each region (Extended Data Fig. 1a, b). These supply cost curves in TIAM-UCL refer to all capital and operating expenditure associated with exploration through production, but do not include fiscal regimes or additional transportation costs[31]. Crucially, the upstream emissions associated with the extraction of different fossil fuels are also captured in the model.

The model has various technological options to remove emissions from the atmosphere via negative emissions, including a set of bioenergy with carbon capture and storage (BECCS) technologies, in power generation, industry, and H_2 and biofuel production. The primary limiting factor on this suite of technologies is the global bioenergy resource potential, set at a maximum 112 EJ per year, in line with the recent UK Committee on Climate Change (CCC) biomass report[32]. This is a lower level than the biomass resource available in many other integrated assessment scenarios for 1.5 °C (which can be up to 400 EJ per year)[33,34], and is more representative of an upper estimate of the global resource

of truly low-carbon sustainable biomass based on many ecological studies[35] (Supplementary Table 20). In addition to technological solutions for capturing carbon from the atmosphere, TIAM-UCL also models CO_2 emissions from land use, land-use change and forestry (LULUCF) at the regional level on the basis of exogenously defined data from the IMAGE model[36]. Here we use a trajectory based on that model's Shared Socio-economic Pathway 2 (SSP2) RCP2.6 scenario, which leads to global net negative CO_2 emissions from LULUCF from 2060 onwards.

In TIAM-UCL, exogenous future demands for energy services (including mobility, lighting, residential, commercial and industrial heat and cooling) drive the evolution of the system so that energy supply meets the energy service demands across the whole time horizon (that is, 2005–2100), which have increased through population and economic growth. For this Article, we use energy service demands derived from SSP2[37]. The model was also run with an elastic demand function, with energy service demands reducing as the marginal price of satisfying the energy service increases. Decisions around what energy sector investments to make across regions are determined using the cost-effectiveness of investments, taking into account the existing system today, energy resource potential, technology availability and, crucially, policy constraints such as emissions reduction targets. The model time horizon runs to 2100, in line with the timescale typically used for climate stabilization.

In conjunction with a cumulative CO_2 budget, an upper limit is placed on annual CH_4 and N_2O emissions based on pathways from the IPCC's *Special Report on Global Warming of 1.5 °C* scenario database[11] We select all pathways that have a warming at or below 1.5 °C in 2100 and take an average across these scenarios to derive a CH_4 and N_2O emissions trajectory that is in line with a 1.5 °C world. Further information on key assumptions used in the model is provided in Supplementary Information section 6. The TIAM-UCL model version used for this analysis was 4.1.1, and was run using TIMES code 4.2.2 with GAMS 27.2. The model solver used was CPLEX 12.9.0.0.

Scenario specification

Extended Data Table 1 describes the scenarios used in this work and some key sensitivities to explore the effect on unextractable fossil fuels under a 1.5-°C-consistent carbon budget. For a 50% probability, this is estimated at 580 $GtCO_2$ (from 2018)[3]. With regard to sensitivities, three key parameters were varied; (1) the rate at which carbon capture and storage technologies can deploy; (2) the availability of bioenergy and therefore the potential for negative emissions through BECCS; and (3) the future energy service demands in aviation and the chemical sector, which provide a considerable challenge to decarbonize given their current total reliance on fossil fuels.

The lower level of bioenergy on sustainability grounds, compared with other IAM models[38], combined with a constrained role for direct air capture (DAC), puts the global emissions trajectory in our central scenario between the P2 and P3 archetypes set out in the IPCC's special report on 1.5 °C. Here, in our central case, BECCS sequesters 287 $GtCO_2$ cumulatively out to 2100, compared with 151 and 414 $GtCO_2$ for P2 and P3 scenarios, respectively. Annually, BECCS use is 5 $GtCO_2$ in 2100 with a further 0.9 $GtCO_2$ being captured by DAC. This scale of engineered removals mean the central 1.5D scenario is on the edge of what is feasible (that is, it does not require a backstop to remove CO_2) within the current version of TIAM-UCL.

As such, while CDR has an important role in our scenarios, aside from 1.5D-HiBio, we do not see cases in which global net negative emissions are in the range of 10−20 $GtCO_2$ per year in the second half of the century, which would enable a large carbon budget exceedance before net zero. This in turn inherently limits the amount that global surface temperatures can exceed or overshoot 1.5 °C before 2100 and, to some extent, reduces exposure to the sizable long-term risks associated with reliance on extensive negative emissions after 2050 as envisaged by P3 and P4 type scenarios[39].

Article

For the low-demand scenarios, we derived an exponential annual growth rate for aviation (domestic and international) and the chemical sector using Grubler et al.[5], considering regional variation between OECD and non-OECD regions. These growth rates were then applied to the calibrated historical data in TIAM-UCL and extrapolated forwards to 2050 and 2100. These two sub-sectors were chosen due to relatively high residual emissions, and because the specific policy direction can influence consumer demand (for example, passenger demand for aviation and demand for plastics). More detail on the low-energy-service demand trajectories, and how these differ from our central 1.5 °C scenario, can be found in Supplementary Information section 3.

Defining geological categories and techno-economic classifications of fossil fuel resources

It is crucial that definitions for reporting are clearly set out, given the regular use of both geological and techno-economic terminology in previous sections, and their differing use in the literature.

Conventional and unconventional oil and fossil methane gas. Conventional oil in TIAM-UCL is defined as having an American Petroleum Institute (API) index greater than 10°; this reflects the 'density' of the oil and therefore its flow characteristics in the hydrocarbon-bearing reservoir[31]. Conventional oil also includes light tight oil, gas liquids and Arctic oil. Unconventional oil, which includes ultra-heavy oil and bitumen, generally has an API < 10° and therefore is extremely viscous with a very high density, typically requiring additional processing and upgrading to produce synthetic crude oil (SCO), which is comparable to conventional crude oil. The additional energy required for upgrading results in a more carbon-intensive product and often at higher costs than conventional oils (shown in Extended Data Fig. 1a). TIAM-UCL also includes shale oil (kerogen), which we classify as unconventional. However, none of this is produced in any scenario conducted for this work, and therefore we have not included it within our unextractable resource estimates.

Conventional fossil methane gas refers to those resources in well-defined reservoirs, which do not require additional stimulation to recover economical volumes. It can be found in both gas-only reservoirs and associated with oil (associated fossil methane gas, either forming a gas cap or dissolved in the oil stream). Unconventional fossil methane gas refers to the gas-bearing reservoir, and whether additional technologies are required to initiate commercial flow rates such as hydraulic fracturing. In TIAM-UCL, this includes shale (low-permeability shale source rock), tight (sandstone reservoirs with extremely low permeability) and coal bed methane (absorbed within coal matrices).

Conventional oil and fossil methane gas are split further into four main production categories, with (1) providing the bulk of our reserve estimates, and the other three categories (2–4) included as resources.

(1) Reserves. These include resources technically and economically proven at prevailing market rates. If the field is not developed, sufficient appraisal needs to have occurred to satisfy the condition of technically and economically proven. As described below, oil and gas reserves are considered on a 1P basis.

(2) Reserve additions. These are discovered but undeveloped accumulations that are either sub-economic, abandoned or reservoirs in producing fields that have not yet been developed due to technical constraints or insufficient geological testing. Therefore, these can become reserves through improved efficiency, technical improvements, fossil fuel price increases and additional geological testing.

(3) New discoveries. These resources of conventional oil and fossil methane gas can be geologically inferred to be recoverable (usually under different probabilities) without taking costs into account.

(4) Arctic oil and fossil methane gas. These include undiscovered and undeveloped conventional resources in the Arctic region. As discussed by McGlade[31], the categorization of Arctic resources is based on economic viability (that is, whether the field has been developed or

any interest in development has been indicated), with the geographical extent defined by the USGS[40].

Unconventional oil and gas do not have the same disaggregation in terms of resource steps, with no distinct 'proved reserves' step for unconventional oil and gas as with conventional reserves, but instead three different cost steps for the overall resource base. Therefore, we have identified volumes of unconventional oil and gas that we categorize as reserves, with the relevant cumulative production from these steps accounted for in the calculation of unextractable fossil fuel reserves.

Coal. Unlike oil and fossil methane gas production, which naturally decline through time, coal is not susceptible to the same geological cost–depletion characteristics. Although considerably more attention is paid in this paper to oil and fossil methane gas, coal reserve levels were compared with recent data from the BGR[41]. Given the rapid phase-out of coal across our 1.5 °C scenarios, a systematic review of uncertainties in the availability and cost of coal reserves and resources was not undertaken. However, static reserve and resource numbers were cross-checked with the BGR as mentioned.

Reserve estimates for oil and fossil methane gas. Oil and fossil methane gas reserves are assumed to be recoverable with current technologies at current market prices or are now producing. They are typically provided with a given probability of the reported volume being recovered at current market prices: the notation for this is 1P, 2P and 3P, reflecting proved, probable and possible reserves. 1P reserves would be the most conservative, with a 90% probability of at least the reported volume being recovered. 2P reserves have a 50% probability, whereas 3P are the most speculative with a 10% probability of the reported volume being recovered.

In this Article, for reserve estimates we use the methods described by D.W. (manuscript in preparation) for fossil methane gas and used a combination of publicly available data and the methods set out by McGlade[31] for oil (described in further detail in Supplementary Information section 5). Both used discrete estimates of proven reserves, and combined these (assuming various degrees of correlation) using Monte Carlo simulations. For fossil methane gas, using a 1P basis, outputs from the reserve uncertainty distributions were then combined with a field-level cost database, which was extended to non-producing fields using linear regression models. For oil, we have updated and recalibrated McGlade's study using 1P estimates from public sources given that these are the most up-to-date available. This allows us to account for reserves of light tight oil in the USA[42], while maintaining the robust assessment of uncertainty conducted by McGlade[31]. The definitions follow SPE guidelines on what constitutes proved reserves to the greatest possible extent[27]. For example, McGlade[31] identified several key examples (the Middle East, Venezuela and Canada) where publicly reported estimates of oil reserves are probably exaggerated, including due to countries booking reserves for political leverage[43], and which provide the bulk of the variation between our 1P estimates and those reported by public sources[12,44–46]. D.W. (manuscript in preparation) also identified the example of Russia, where publicly reported 'proved' gas reserves (under an SPE definition) actually seem in reality to refer to Russian reporting standards where field economics are not considered within the definition of reserves[47,48]. The bottom-up assessment of reserves, using field-level data and accounting for the inherent volumetric uncertainty using probability distributions, is the main driver behind the systematically lower reserve numbers in this work compared with other publicly reporting sources. A detailed explanation of the method used to estimate reserves is provided in Supplementary Information section 5.

Resource estimates for oil and fossil methane gas. Resource estimates used in TIAM-UCL are based on the category of technically

recoverable resources. These are a subset of ultimately recoverable resources, in that technologies assumed to be used in recovery are relatively static (that is, do not evolve). Oil resources were originally defined on an ultimately recoverable resources basis. Owing to the sensitivity of resource estimates to the recovery factor, a Monte Carlo simulation method was used that combined uncertainty distributions of recovery factors with in-place unconventional volumes to generate aggregated country- and region-level volumes of ultimately recoverable unconventional oil[9,31]. Since their original estimation, updates have been undertaken to consider historical production (since 2010) and changes in both estimates of recoverable volumes and costs. For example, the revised volumes of ultimately recoverable extra-heavy oil and bitumen (EHOB) have been reconciled with recent technically recoverable resource estimates from the IEA[12].

For unconventional gas, there is a wide range of literature now estimating technically recoverable resources at individual play levels (at least for shale gas). Therefore, play-level uncertainty ranges of technically recoverable shale resources were constructed and combined using a Monte Carlo simulation to generate regional estimates of technically recoverable shale gas (D.W., manuscript in preparation). These were then combined with cost–depletion curves derived from statistically significant drivers of field supply costs for individual shale plays. This process is illustrated in Supplementary Fig. 12. For tight-gas and coal-bed methane, country-level ranges were combined in a similar manner to generate regional estimates of technically recoverable resources.

Estimation approach for unextractable reserves and resources.
The representation of fossil fuels in TIAM-UCL is driven by detailed bottom-up analysis of both the cost and availability of different geological categories of oil and fossil methane gas. McGlade[31] and D.W. (manuscript in preparation) constructed supply cost curves for each region and resource category in TIAM-UCL using robust statistical methods to estimate the availability and cost of oil and fossil methane gas.

The supply cost curves of different fossil fuel resources in TIAM-UCL are shown in Extended Data Fig. 1, with oil, fossil methane gas and coal split into the regions of TIAM-UCL. Additional information is provided in Supplementary Information section 5. These supply costs represent costs associated with getting the fossil fuels out of the ground, but do not include transportation costs or taxes under different fiscal regimes. Therefore, they should not be considered as break-even prices. The oil supply cost curve (Extended Data Fig. 1a) reflects the supply cost for a representative barrel of oil energy equivalent (boe), as the mining processes yield different energy commodities. For example, conventional oil reserves output a barrel of crude oil, whereas oil sand production processes output a barrel of bitumen, which may then have to be upgraded if it is to be used for certain downstream uses. This requires additional energy inputs and technology processes, the additional costs of which are not included in the supply curve although are captured in the processing sector of TIAM-UCL.

To provide full transparency and flexibility across the full hydrocarbon resource base, we extended our analysis in this study to unextractable fossil fuel resources (that is, not just reserves), taking into account production from across the supply cost curves shown in Extended Data Fig. 1. Crucially, fossil fuels are not necessarily extracted in cost order along the supply curve because additional constraints (at a region and resource category level) are included, which control both the rate of production expansion and decline.

Constraints are based on McGlade[31], McGlade and Ekins[9] and D.W. (manuscript in preparation), with each constructed from bottom-up databases of oil and gas fields (and individual wells for US shale gas), and allow TIAM-UCL to provide an empirically robust representation of the 'depletion' characteristics of oil and fossil methane gas production. The decline and growth constraints are used to model both geological and techno-economic characteristics of oil and gas

mining technologies, as well as some degree of inertia within the system. Additional information on how these constraints function, as well as underlying data assumptions, is provided in Supplementary Information section 5.

In this Article, resources beyond reserves are considered when estimating unextractable fossil fuels for a number of reasons. First, the dynamic nature of reserves means that resources can shift across the techno-economic feasibility matrix in either direction (that is, resources can become reserves and vice versa). Therefore, considering the whole resource base allows us to expand away from the relatively restrictive definition of reserves, albeit necessarily increasing the uncertainty range away from the most certain recoverable volumes. Second, not all fossil fuel production, particularly when moving out to 2100, is from the reserves base, due to constraints on production growth and decline, and trade. The full resource base needs consideration to capture non-reserve volumes. Finally, when analysing fossil fuel extraction under a 1.5-°C-consistent carbon budget, it is not just the supply cost hierarchy of different reserves and resources that drives the regional distribution of production, but also the volume of CO_2 (and other greenhouse gases) associated with those resources, and therefore the potential emissions from extraction and consumption.

Data availability
The results data and key source data in the figures (including in the Supplementary Information) are available via Zenodo at https://doi.org/10.5281/zenodo.5118971. Source data are provided with this paper.

Code availability
The underlying code (mathematical equations) for the model is available via GitHub (https://github.com/etsap-TIMES/TIMES_model). The full model database is also available via Zenodo (https://doi.org/10.5281/zenodo.5118971). Given the complexity of the model, further guidance will be provided on model assumptions upon reasonable request from the corresponding author.

28. McCollum, D. L. et al. Interaction of consumer preferences and climate policies in the global transition to low-carbon vehicles. *Nat. Energy* **3**, 664–673 (2018).
29. Marangoni, G. et al. Sensitivity of projected long-term CO_2 emissions across the Shared Socioeconomic Pathways. *Nat. Clim. Change* **7**, 113–117 (2017).
30. Erickson, P. et al. Why fossil fuel producer subsidies matter. *Nature* **578**, E1–E4 (2020).
31. McGlade, C. *Uncertainties in the Outlook for Oil and Gas*. PhD thesis, UCL (2013).
32. *Biomass in a Low-Carbon Economy* https://www.theccc.org.uk/publication/biomass-in-a-low-carbon-economy/ (CCC, 2018).
33. Huppmann, D., Rogelj, J., Kriegler, E., Krey, V. & Riahi, K. A new scenario resource for integrated 1.5 °C research. *Nat. Clim. Change* **8**, 1027–1030 (2018).
34. Fuss, S. et al. Negative emissions—part 2: costs, potentials and side effects. *Environ. Res. Lett.* **13**, 063002 (2018).
35. Creutzig, F. et al. Bioenergy and climate change mitigation: an assessment. *Glob. Change Biol. Bioenergy* **7**, 916–944 (2015).
36. *Integrated Assessment of Global Environmental Change with IMAGE 3.0: Model Description and Policy Applications* https://www.pbl.nl/en/publications/integrated-assessment-of-global-environmental-change-with-IMAGE-3.0 (PBL, 2014).
37. Fricko, O. et al. The marker quantification of the Shared Socioeconomic Pathway 2: a middle-of-the-road scenario for the 21st century. *Glob. Environ. Change* **42**, 251–267 (2017).
38. Bauer, N. et al. Global energy sector emission reductions and bioenergy use: overview of the bioenergy demand phase of the EMF-33 model comparison. *Clim. Change* **163**, 1553–1568 (2020).
39. Fuss, S. et al. Betting on negative emissions. *Nat. Clim. Change* **4**, 850–853 (2014).
40. Gautier, D. & Moore, T. in *The 2008 Circum-Arctic Resource Appraisal* Professional Paper No. 1824 (eds Gautier, D. & Moore, T.) (USGS, 2017).
41. *BGR Energy Study 2019: Data and Developments Concerning German and Global Energy Supplies* https://www.bgr.bund.de/EN/Themen/Energie/Downloads/energiestudie_2019_en.pdf;jsessionid=A73E36C969C2253E194ADF4E2484C95A.1_cid321?__blob=publicationFile&v=6 (BGR, 2020).
42. *Assumptions to the Annual Energy Outlook 2020: Oil and Gas Supply Module* https://www.eia.gov/outlooks/aeo/assumptions/pdf/oilgas.pdf (EIA, 2020).
43. Laherrère, J. Future of oil supplies. *Energy Explor. Exploit.* **21**, 227–267 (2003).
44. *OPEC Annual Statistical Bulletin 2019* https://www.opec.org/opec_web/static_files_project/media/downloads/publications/ASB_2019.pdf (OPEC, 2019).

Article

45. *Statistical Review of World Energy* https://www.bp.com/content/dam/bp/business-sites/en/global/corporate/pdfs/energy-economics/statistical-review/bp-stats-review-2020-full-report.pdf (BP, 2020).
46. *Energy Study 2016: Reserves, Resources and Availability of Energy Resources* (BGR, 2016).
47. *Russian Energy 2015* https://ac.gov.ru/files/publication/a/10205.pdf (Analytical Centre for the Government of the Russian Federation, 2016).
48. *Natural Gas Information 2019* https://www.iea.org/reports/natural-gas-information-2019 (2019).

Author contributions All authors were involved in the design approach to the research. D.W. and J.P. undertook the scenario modelling and analysed the results. All authors contributed to the development of early drafts of the paper, and to writing the final paper.

Competing interests The authors declare no competing interests.

Additional information
Supplementary information The online version contains supplementary material available at https://doi.org/10.1038/s41586-021-03821-8.
Correspondence and requests for materials should be addressed to D.W.
Peer review information *Nature* thanks Dieter Franke, Gang He and Michael Lazarus for their contribution to the peer review of this work. Peer reviewer reports are available.
Reprints and permissions information is available at http://www.nature.com/reprints.
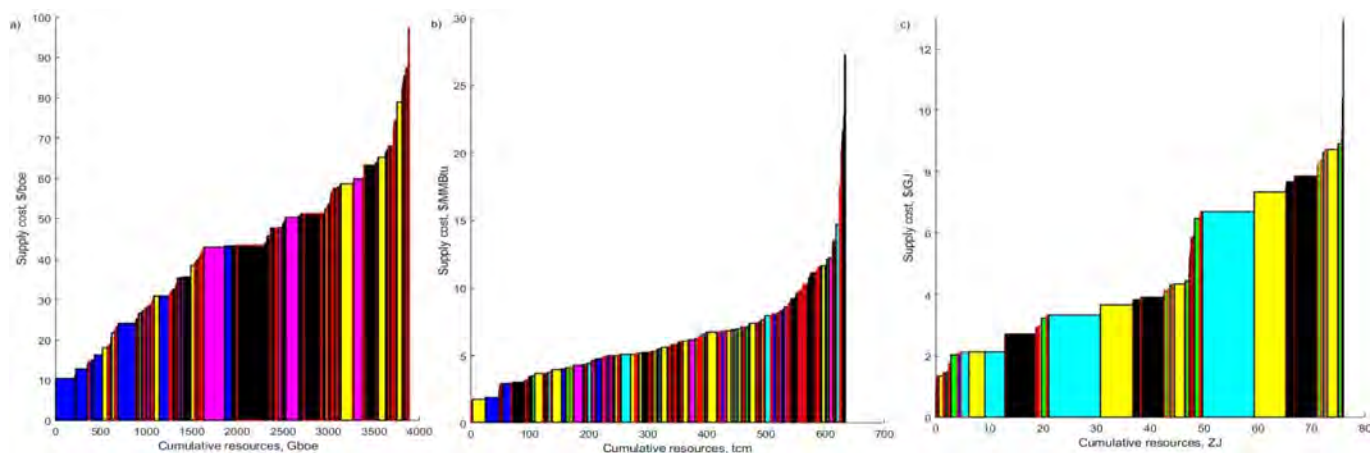
Extended Data Fig. 1 | Supply cost curves split by region in TIAM-UCL.
a–**c**, Curves for oil (**a**), fossil methane gas (**b**) and coal (**c**). Costs are given on an energy-content basis (barrel of oil equivalent for oil, British thermal units for gas and joules for coal), on a US$$_{2005}$ basis. For oil, different mining processes output different commodities (for example, oil sands mining initially (pre-upgrading) outputs a barrel of bitumen) hence the use of the energy-content cost basis. For gas, associated gas is not included in Extended Data Fig. 1b as it is a by-product of oil production.

Article

Extended Data Table 1 | Description of the scenarios explored in this work

Scenario	Key assumptions
1.5D	Central 1.5°C scenario (50% probability)
1.5D-LoCCS	Growth rates for carbon capture technologies are constrained to 2.5% per year (compared to 5% in 1.5D). This is 5.6 $GtCO_2$ of sequestration per year in 2050.
1.5D-HiCCS	Growth rates for carbon capture technologies relaxed to a maximum of 10% per year (compared to 5% in 1.5D). CCS also start deploying at 2025, compared to 2030 in 1.5D. This is 7.8 $GtCO_2$ of sequestration per year in 2050.
1.5D-HiBio	Solid biomass and bio crop availability is increased to 213 EJ in 2050 (from 112 EJ in the central scenario)
1.5D-LoDem	Departed from SSP2 demands for aviation and chemical sector based on Grubler et al.[5]. Selected energy service demands are chosen based on the challenges of mitigation in these sectors post-2050.

Summary for Policymakers

SPM

Summary
for Policymakers

Drafting Authors:

Nerilie Abram (Australia), Carolina Adler (Switzerland/Australia), Nathaniel L. Bindoff (Australia), Lijing Cheng (China), So-Min Cheong (Republic of Korea), William W. L. Cheung (Canada), Matthew Collins (UK), Chris Derksen (Canada), Alexey Ekaykin (Russian Federation), Thomas Frölicher (Switzerland), Matthias Garschagen (Germany), Jean-Pierre Gattuso (France), Bruce Glavovic (New Zealand), Stephan Gruber (Canada/Germany), Valeria Guinder (Argentina), Robert Hallberg (USA), Sherilee Harper (Canada), Nathalie Hilmi (Monaco/France), Jochen Hinkel (Germany), Yukiko Hirabayashi (Japan), Regine Hock (USA), Anne Hollowed (USA), Helene Jacot Des Combes (Fiji), James Kairo (Kenya), Alexandre K. Magnan (France), Valérie Masson-Delmotte (France), J.B. Robin Matthews (UK), Kathleen McInnes (Australia), Michael Meredith (UK), Katja Mintenbeck (Germany), Samuel Morin (France), Andrew Okem (South Africa/Nigeria), Michael Oppenheimer (USA), Ben Orlove (USA), Jan Petzold (Germany), Anna Pirani (Italy), Elvira Poloczanska (UK/Australia), Hans-Otto Pörtner (Germany), Anjal Prakash (Nepal/India), Golam Rasul (Nepal), Evelia Rivera-Arriaga (Mexico), Debra C. Roberts (South Africa), Edward A.G. Schuur (USA), Zita Sebesvari (Hungary/Germany), Martin Sommerkorn (Norway/Germany), Michael Sutherland (Trinidad and Tobago), Alessandro Tagliabue (UK), Roderik Van De Wal (Netherlands), Phil Williamson (UK), Rong Yu (China), Panmao Zhai (China)

Draft Contributing Authors:

Andrés Alegría (Honduras), Robert M. DeConto (USA), Andreas Fischlin (Switzerland), Shengping He (Norway/China), Miriam Jackson (Norway), Martin Künsting (Germany), Erwin Lambert (Netherlands), Pierre-Marie Lefeuvre (Norway/France), Alexander Milner (UK), Jess Melbourne-Thomas (Australia), Benoit Meyssignac (France), Maike Nicolai (Germany), Hamish Pritchard (UK), Heidi Steltzer (USA), Nora M. Weyer (Germany)

Introduction

This Special Report on the Ocean and Cryosphere[1] in a Changing Climate (SROCC) was prepared following an IPCC Panel decision in 2016 to prepare three Special Reports during the Sixth Assessment Cycle[2]. By assessing new scientific literature[3], the SROCC[4] responds to government and observer organization proposals. The SROCC follows the other two Special Reports on Global Warming of 1.5°C (SR1.5) and on Climate Change and Land (SRCCL)[5] and the Intergovernmental Science Policy Platform on Biodiversity and Ecosystem Services (IPBES) Global Assessment Report on Biodiversity and Ecosystem Services.

This Summary for Policymakers (SPM) compiles key findings of the report and is structured in three parts: SPM.A: Observed Changes and Impacts, SPM.B: Projected Changes and Risks, and SPM.C: Implementing Responses to Ocean and Cryosphere Change. To assist navigation of the SPM, icons indicate where content can be found. Confidence in key findings is reported using IPCC calibrated language[6] and the underlying scientific basis for each key finding is indicated by references to sections of the underlying report.

Key of icons to indicate content

High mountain cryosphere

Polar regions

Coasts and sea level rise

Ocean

---

[1]   The cryosphere is defined in this report (Annex I: Glossary) as the components of the Earth System at and below the land and ocean surface that are frozen, including snow cover, glaciers, ice sheets, ice shelves, icebergs, sea ice, lake ice, river ice, permafrost, and seasonally frozen ground.

[2]   The decision to prepare a Special Report on Climate Change and Oceans and the Cryosphere was made at the Forty-Third Session of the IPCC in Nairobi, Kenya, 11–13 April 2016.

[3]   Cut-off dates: 15 October 2018 for manuscript submission, 15 May 2019 for acceptance for publication.

[4]   The SROCC is produced under the scientific leadership of Working Group I and Working Group II. In line with the approved outline, mitigation options (Working Group III) are not assessed with the exception of the mitigation potential of blue carbon (coastal ecosystems).

[5]   The full titles of these two Special Reports are: "Global Warming of 1.5°C. An IPCC special report on the impacts of global warming of 1.5°C above pre-industrial levels and related global greenhouse gas emission pathways, in the context of strengthening the global response to the threat of climate change, sustainable development, and efforts to eradicate poverty"; "Climate Change and Land: an IPCC special report on climate change, desertification, land degradation, sustainable land management, food security, and greenhouse gas fluxes in terrestrial ecosystems".

[6]   Each finding is grounded in an evaluation of underlying evidence and agreement. A level of confidence is expressed using five qualifiers: very low, low, medium, high and very high, and typeset in italics, e.g., *medium confidence*. The following terms have been used to indicate the assessed likelihood of an outcome or a result: virtually certain 99–100% probability, very likely 90–100%, likely 66–100%, about as likely as not 33–66%, unlikely 0–33%, very unlikely 0–10%, exceptionally unlikely 0–1%. Assessed likelihood is typeset in italics, e.g., *very likely*. This is consistent with AR5 and the other AR6 Special Reports. Additional terms (extremely likely 95–100%, more likely than not >50–100%, more unlikely than likely 0–<50%, extremely unlikely 0–5%) are used when appropriate. This Report also uses the term '*likely* range' or '*very likely* range' to indicate that the assessed likelihood of an outcome lies within the 17–83% or 5–95% probability range. {1.9.2, Figure 1.4}

Startup Box | The Importance of the Ocean and Cryosphere for People

All people on Earth depend directly or indirectly on the ocean and cryosphere. The global ocean covers 71% of the Earth surface and contains about 97% of the Earth's water. The cryosphere refers to frozen components of the Earth system[1]. Around 10% of Earth's land area is covered by glaciers or ice sheets. The ocean and cryosphere support unique habitats, and are interconnected with other components of the climate system through global exchange of water, energy and carbon. The projected responses of the ocean and cryosphere to past and current human-induced greenhouse gas emissions and ongoing global warming include climate feedbacks, changes over decades to millennia that cannot be avoided, thresholds of abrupt change, and irreversibility. {Box 1.1, 1.2}

Human communities in close connection with coastal environments, small islands (including Small Island Developing States, SIDS), polar areas and high mountains[7] are particularly exposed to ocean and cryosphere change, such as sea level rise, extreme sea level and shrinking cryosphere. Other communities further from the coast are also exposed to changes in the ocean, such as through extreme weather events. Today, around 4 million people live permanently in the Arctic region, of whom 10% are Indigenous. The low-lying coastal zone[8] is currently home to around 680 million people (nearly 10% of the 2010 global population), projected to reach more than one billion by 2050. SIDS are home to 65 million people. Around 670 million people (nearly 10% of the 2010 global population), including Indigenous peoples, live in high mountain regions in all continents except Antarctica. In high mountain regions, population is projected to reach between 740 and 840 million by 2050 (about 8.4–8.7% of the projected global population). {1.1, 2.1, 3.1, Cross-Chapter Box 9, Figure 2.1}

In addition to their role within the climate system, such as the uptake and redistribution of natural and anthropogenic carbon dioxide (CO_2) and heat, as well as ecosystem support, services provided to people by the ocean and/or cryosphere include food and water supply, renewable energy, and benefits for health and well-being, cultural values, tourism, trade, and transport. The state of the ocean and cryosphere interacts with each aspect of sustainability reflected in the United Nations Sustainable Development Goals (SDGs). {1.1, 1.2, 1.5}

---

[7] High mountain areas include all mountain regions where glaciers, snow or permafrost are prominent features of the landscape. For a list of high mountain regions covered in this report, see Chapter 2. Population in high mountain regions is calculated for areas less than 100 kilometres from glaciers or permafrost in high mountain areas assessed in this report. {2.1} Projections for 2050 give the range of population in these regions across all five of the Shared Socioeconomic Pathways. {Cross-Chapter Box 1 in Chapter 1}

[8] Population in the low elevation coastal zone is calculated for land areas connected to the coast, including small island states, that are less than 10 metres above sea level. {Cross-Chapter Box 9} Projections for 2050 give the range of population in these regions across all five of the Shared Socioeconomic Pathways. {Cross-Chapter Box 1 in Chapter 1}

A.   Observed Changes and Impacts

Observed Physical Changes

A.1   **Over the last decades, global warming has led to widespread shrinking of the cryosphere, with mass loss from ice sheets and glaciers (*very high confidence*), reductions in snow cover (*high confidence*) and Arctic sea ice extent and thickness (*very high confidence*), and increased permafrost temperature (*very high confidence*). {2.2, 3.2, 3.3, 3.4, Figures SPM.1, SPM.2}**

A.1.1   Ice sheets and glaciers worldwide have lost mass (*very high confidence*). Between 2006 and 2015, the Greenland Ice Sheet[9] lost ice mass at an average rate of 278 ± 11 Gt yr^{-1} (equivalent to 0.77 ± 0.03 mm yr^{-1} of global sea level rise)[10], mostly due to surface melting (*high confidence*). In 2006–2015, the Antarctic Ice Sheet lost mass at an average rate of 155 ± 19 Gt yr^{-1} (0.43 ± 0.05 mm yr^{-1}), mostly due to rapid thinning and retreat of major outlet glaciers draining the West Antarctic Ice Sheet (*very high confidence*). Glaciers worldwide outside Greenland and Antarctica lost mass at an average rate of 220 ± 30 Gt yr^{-1} (equivalent to 0.61 ± 0.08 mm yr^{-1} sea level rise) in 2006–2015. {3.3.1, 4.2.3, Appendix 2.A, Figure SPM.1}

A.1.2   Arctic June snow cover extent on land declined by $13.4 \pm 5.4\%$ per decade from 1967 to 2018, a total loss of approximately 2.5 million km^2, predominantly due to surface air temperature increase (*high confidence*). In nearly all high mountain areas, the depth, extent and duration of snow cover have declined over recent decades, especially at lower elevation (*high confidence*). {2.2.2, 3.4.1, Figure SPM.1}

A.1.3   Permafrost temperatures have increased to record high levels (1980s–present) (*very high confidence*) including the recent increase by $0.29°C \pm 0.12°C$ from 2007 to 2016 averaged across polar and high mountain regions globally. Arctic and boreal permafrost contain 1460–1600 Gt organic carbon, almost twice the carbon in the atmosphere (*medium confidence*). There is *medium evidence* with *low agreement* whether northern permafrost regions are currently releasing additional net methane and CO_2 due to thaw. Permafrost thaw and glacier retreat have decreased the stability of high mountain slopes (*high confidence*). {2.2.4, 2.3.2, 3.4.1, 3.4.3, Figure SPM.1}

A.1.4   Between 1979 and 2018, Arctic sea ice extent has *very likely* decreased for all months of the year. September sea ice reductions are *very likely* $12.8 \pm 2.3\%$ per decade. These sea ice changes in September are *likely* unprecedented for at least 1000 years. Arctic sea ice has thinned, concurrent with a transition to younger ice: between 1979 and 2018, the areal proportion of multi-year ice at least five years old has declined by approximately 90% (*very high confidence*). Feedbacks from the loss of summer sea ice and spring snow cover on land have contributed to amplified warming in the Arctic (*high confidence*) where surface air temperature *likely* increased by more than double the global average over the last two decades. Changes in Arctic sea ice have the potential to influence mid-latitude weather (*medium confidence*), but there is *low confidence* in the detection of this influence for specific weather types. Antarctic sea ice extent overall has had no statistically significant trend (1979–2018) due to contrasting regional signals and large interannual variability (*high confidence*). {3.2.1, 6.3.1, Box 3.1, Box 3.2, SPM A.1.2, Figures SPM.1, SPM.2}

---

[9]   Including peripheral glaciers.

[10]   360 Gt ice corresponds to 1 mm of global mean sea level.

Past and future changes in the ocean and cryosphere

Historical changes (observed and modelled) and projections under RCP2.6 and RCP8.5 for key indicators

Legend: Historical (observed) | Historical (modelled) | Projected (RCP2.6) | Projected (RCP8.5)
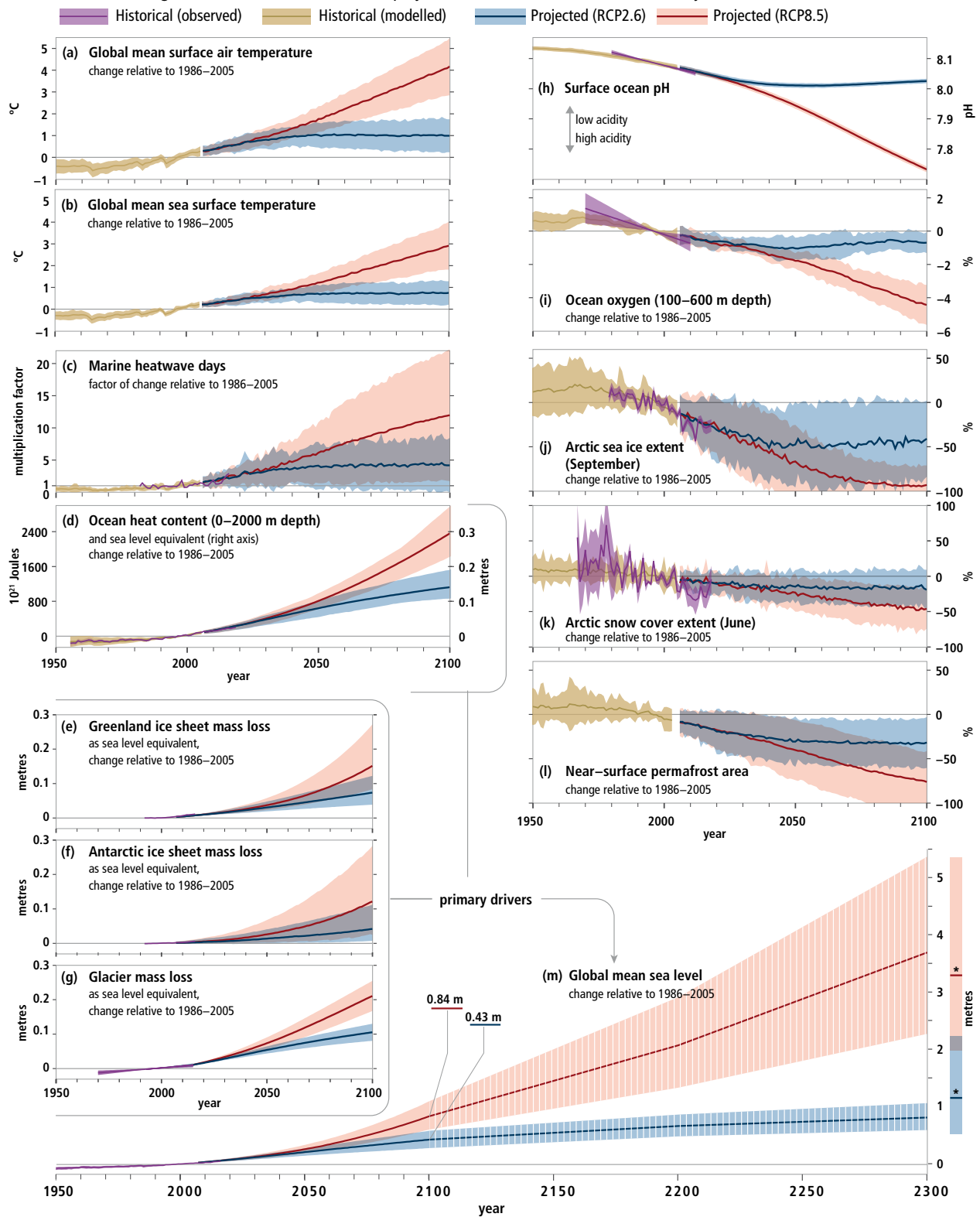
Figure SPM.1 | Observed and modelled historical changes in the ocean and cryosphere since 1950[11], and projected future changes under low (RCP2.6) and high (RCP8.5) greenhouse gas emissions scenarios. {Box SPM.1}

---

[11] This does not imply that the changes started in 1950. Changes in some variables have occurred since the pre-industrial period.

Figure SPM.1 (continued): Changes are shown for: **(a)** Global mean surface air temperature change with *likely* range. {Box SPM.1, Cross-Chapter Box 1 in Chapter 1} **Ocean-related changes** with *very likely* ranges for **(b)** Global mean sea surface temperature change {Box 5.1, 5.2.2}; **(c)** Change factor in surface ocean marine heatwave days {6.4.1}; **(d)** Global ocean heat content change (0–2000 m depth). An approximate steric sea level equivalent is shown with the right axis by multiplying the ocean heat content by the global-mean thermal expansion coefficient ($\varepsilon \approx 0.125$ m per 10^{24} Joules)[12] for observed warming since 1970 {Figure 5.1}; **(h)** Global mean surface pH (on the total scale). Assessed observational trends are compiled from open ocean time series sites longer than 15 years {Box 5.1, Figure 5.6, 5.2.2}; and **(i)** Global mean ocean oxygen change (100–600 m depth). Assessed observational trends span 1970–2010 centered on 1996 {Figure 5.8, 5.2.2}. **Sea level changes** with *likely* ranges for **(m)** Global mean sea level change. Hashed shading reflects *low confidence* in sea level projections beyond 2100 and bars at 2300 reflect expert elicitation on the range of possible sea level change {4.2.3, Figure 4.2}; and components from **(e,f)** Greenland and Antarctic ice sheet mass loss {3.3.1}; and **(g)** Glacier mass loss {Cross-Chapter Box 6 in Chapter 2, Table 4.1}. Further **cryosphere-related changes** with *very likely* ranges for **(j)** Arctic sea ice extent change for September[13] {3.2.1, 3.2.2 Figure 3.3}; **(k)** Arctic snow cover change for June (land areas north of 60ºN) {3.4.1, 3.4.2, Figure 3.10}; and **(l)** Change in near-surface (within 3–4 m) permafrost area in the Northern Hemisphere {3.4.1, 3.4.2, Figure 3.10}. Assessments of projected changes under the intermediate RCP4.5 and RCP6.0 scenarios are not available for all variables considered here, but where available can be found in the underlying report. {For RCP4.5 see: 2.2.2, Cross-Chapter Box 6 in Chapter 2, 3.2.2, 3.4.2, 4.2.3, for RCP6.0 see Cross-Chapter Box 1 in Chapter 1}

Box SPM.1 | Use of Climate Change Scenarios in SROCC

Assessments of projected future changes in this report are based largely on CMIP5[14] climate model projections using Representative Concentration Pathways (RCPs). RCPs are scenarios that include time series of emissions and concentrations of the full suite of greenhouse gases (GHGs) and aerosols and chemically active gases, as well as land use / land cover. RCPs provide only one set of many possible scenarios that would lead to different levels of global warming. {Annex I: Glossary}

This report uses mainly RCP2.6 and RCP8.5 in its assessment, reflecting the available literature. RCP2.6 represents a low greenhouse gas emissions, high mitigation future, that in CMIP5 simulations gives a two in three chance of limiting global warming to below 2ºC by 2100[15]. By contrast, RCP8.5 is a high greenhouse gas emissions scenario in the absence of policies to combat climate change, leading to continued and sustained growth in atmospheric greenhouse gas concentrations. Compared to the total set of RCPs, RCP8.5 corresponds to the pathway with the highest greenhouse gas emissions. The underlying chapters also reference other scenarios, including RCP4.5 and RCP6.0 that have intermediate levels of greenhouse gas emissions and result in intermediate levels of warming. {Annex I: Glossary, Cross-Chapter Box 1 in Chapter 1}

Table SPM.1 provides estimates of total warming since the pre-industrial period under four different RCPs for key assessment intervals used in SROCC. The warming from the 1850–1900 period until 1986–2005 has been assessed as 0.63ºC (0.57ºC to 0.69ºC *likely* range) using observations of near-surface air temperature over the ocean and over land.[16] Consistent with the approach in AR5, modelled future changes in global mean surface air temperature relative to 1986–2005 are added to this observed warming. {Cross-Chapter Box 1 in Chapter 1}

Table SPM.1 | Projected global mean surface temperature change relative to 1850–1900 for two time periods under four RCPs[15] {Cross-Chapter Box 1 in Chapter 1}

Scenario	Near-term: 2031–2050		End-of-century: 2081–2100	
	Mean (°C)	*Likely* range (°C)	Mean (°C)	*Likely* range (°C)
RCP2.6	1.6	1.1 to 2.0	1.6	0.9 to 2.4
RCP4.5	1.7	1.3 to 2.2	2.5	1.7 to 3.3
RCP6.0	1.6	1.2 to 2.0	2.9	2.0 to 3.8
RCP8.5	2.0	1.5 to 2.4	4.3	3.2 to 5.4

---

[12] This scaling factor (global-mean ocean expansion as sea level rise in metres per unit heat) varies by about 10% between different models, and it will systematically increase by about 10% by 2100 under RCP8.5 forcing due to ocean warming increasing the average thermal expansion coefficient. {4.2.1, 4.2.2, 5.2.2}

[13] Antarctic sea ice is not shown here due to *low confidence* in future projections. {3.2.2}

[14] CMIP5 is Phase 5 of the Coupled Model Intercomparison Project (Annex I: Glossary).

[15] A pathway with lower emissions (RCP1.9), which would correspond to a lower level of projected warming than RCP2.6, was not part of CMIP5.

[16] In some instances this report assesses changes relative to 2006–2015. The warming from the 1850–1900 period until 2006–2015 has been assessed as 0.87ºC (0.75 to 0.99ºC *likely* range). {Cross-Chapter Box 1 in Chapter 1}

A.2   It is *virtually certain* that the global ocean has warmed unabated since 1970 and has taken up more than 90% of the excess heat in the climate system (*high confidence*). Since 1993, the rate of ocean warming has more than doubled (*likely*). Marine heatwaves have *very likely* doubled in frequency since 1982 and are increasing in intensity (*very high confidence*). By absorbing more CO_2, the ocean has undergone increasing surface acidification (*virtually certain*). A loss of oxygen has occurred from the surface to 1000 m (*medium confidence*). {1.4, 3.2, 5.2, 6.4, 6.7, Figures SPM.1, SPM.2}

A.2.1.   The ocean warming trend documented in the IPCC Fifth Assessment Report (AR5) has continued. Since 1993 the rate of ocean warming and thus heat uptake has more than doubled (*likely*) from 3.22 ± 1.61 ZJ yr^{-1} (0–700 m depth) and 0.97 ± 0.64 ZJ yr^{-1} (700–2000 m) between 1969 and 1993, to 6.28 ± 0.48 ZJ yr^{-1} (0–700 m) and 3.86 ± 2.09 ZJ yr^{-1} (700–2000 m) between 1993 and 2017[17], and is attributed to anthropogenic forcing (*very likely*). {1.4.1, 5.2.2, Table 5.1, Figure SPM.1}

A.2.2   The Southern Ocean accounted for 35–43% of the total heat gain in the upper 2000 m global ocean between 1970 and 2017 (*high confidence*). Its share increased to 45–62% between 2005 and 2017 (*high confidence*). The deep ocean below 2000 m has warmed since 1992 (*likely*), especially in the Southern Ocean. {1.4, 3.2.1, 5.2.2, Table 5.1, Figure SPM.2}

A.2.3   Globally, marine heat-related events have increased; marine heatwaves[18], defined when the daily sea surface temperature exceeds the local 99th percentile over the period 1982 to 2016, have doubled in frequency and have become longer-lasting, more intense and more extensive (*very likely*). It is *very likely* that between 84–90% of marine heatwaves that occurred between 2006 and 2015 are attributable to the anthropogenic temperature increase. {Table 6.2, 6.4, Figures SPM.1, SPM.2}

A.2.4   Density stratification[19] has increased in the upper 200 m of the ocean since 1970 (*very likely*). Observed surface ocean warming and high latitude addition of freshwater are making the surface ocean less dense relative to deeper parts of the ocean (*high confidence*) and inhibiting mixing between surface and deeper waters (*high confidence*). The mean stratification of the upper 200 m has increased by 2.3 ± 0.1% (*very likely* range) from the 1971–1990 average to the 1998–2017 average. {5.2.2}

A.2.5   The ocean has taken up between 20–30% (*very likely*) of total anthropogenic CO_2 emissions since the 1980s causing further ocean acidification. Open ocean surface pH has declined by a *very likely* range of 0.017–0.027 pH units per decade since the late 1980s[20], with the decline in surface ocean pH *very likely* to have already emerged from background natural variability for more than 95% of the ocean surface area. {3.2.1, 5.2.2, Box 5.1, Figures SPM.1, SPM.2}

---

[17]   ZJ is Zettajoule and is equal to 10^{21} Joules. Warming the entire ocean by 1°C requires about 5500 ZJ; 144 ZJ would warm the top 100 m by about 1°C.

[18]   A marine heatwave is a period of extreme warm near-sea surface temperature that persists for days to months and can extend up to thousands of kilometres (Annex I: Glossary).

[19]   In this report density stratification is defined as the density contrast between shallower and deeper layers. Increased stratification reduces the vertical exchange of heat, salinity, oxygen, carbon, and nutrients.

[20]   Based on in-situ records longer than fifteen years.

A.2.6   Datasets spanning 1970–2010 show that the open ocean has lost oxygen by a *very likely* range of 0.5–3.3% over the upper 1000 m, alongside a *likely* expansion of the volume of oxygen minimum zones by 3–8% (*medium confidence*). Oxygen loss is primarily due to increasing ocean stratification, changing ventilation and biogeochemistry (*high confidence*). {5.2.2, Figures SPM.1, SPM.2}

A.2.7   Observations, both in situ (2004–2017) and based on sea surface temperature reconstructions, indicate that the Atlantic Meridional Overturning Circulation (AMOC)[21] has weakened relative to 1850–1900 (*medium confidence*). There is insufficient data to quantify the magnitude of the weakening, or to properly attribute it to anthropogenic forcing due to the limited length of the observational record. Although attribution is currently not possible, CMIP5 model simulations of the period 1850–2015, on average, exhibit a weakening AMOC when driven by anthropogenic forcing. {6.7}

A.3   Global mean sea level (GMSL) is rising, with acceleration in recent decades due to increasing rates of ice loss from the Greenland and Antarctic ice sheets (*very high confidence*), as well as continued glacier mass loss and ocean thermal expansion. Increases in tropical cyclone winds and rainfall, and increases in extreme waves, combined with relative sea level rise, exacerbate extreme sea level events and coastal hazards (*high confidence*). {3.3, 4.2, 6.2, 6.3, 6.8, Figures SPM.1, SPM.2, SPM.4, SPM.5}

A.3.1   Total GMSL rise for 1902–2015 is 0.16 m (*likely* range 0.12–0.21 m). The rate of GMSL rise for 2006–2015 of 3.6 mm yr^{-1} (3.1–4.1 mm yr^{-1}, *very likely* range), is unprecedented over the last century (*high confidence*), and about 2.5 times the rate for 1901–1990 of 1.4 mm yr^{-1} (0.8– 2.0 mm yr^{-1}, *very likely* range). The sum of ice sheet and glacier contributions over the period 2006–2015 is the dominant source of sea level rise (1.8 mm yr^{-1}, *very likely* range 1.7–1.9 mm yr^{-1}), exceeding the effect of thermal expansion of ocean water (1.4 mm yr^{-1}, *very likely* range 1.1–1.7 mm yr^{-1})[22] (*very high confidence*). The dominant cause of global mean sea level rise since 1970 is anthropogenic forcing (*high confidence*). {4.2.1, 4.2.2, Figure SPM.1}

A.3.2   Sea level rise has accelerated (*extremely likely*) due to the combined increased ice loss from the Greenland and Antarctic ice sheets (*very high confidence*). Mass loss from the Antarctic ice sheet over the period 2007–2016 tripled relative to 1997–2006. For Greenland, mass loss doubled over the same period (*likely, medium confidence*). {3.3.1, Figures SPM.1, SPM.2, SPM A.1.1}

A.3.3   Acceleration of ice flow and retreat in Antarctica, which has the potential to lead to sea level rise of several metres within a few centuries, is observed in the Amundsen Sea Embayment of West Antarctica and in Wilkes Land, East Antarctica (*very high confidence*). These changes may be the onset of an irreversible[23] ice sheet instability. Uncertainty related to the onset of ice sheet instability arises from limited observations, inadequate model representation of ice sheet processes, and limited understanding of the complex interactions between the atmosphere, ocean and the ice sheet. {3.3.1, Cross-Chapter Box 8 in Chapter 3, 4.2.3}

A.3.4   Sea level rise is not globally uniform and varies regionally. Regional differences, within ±30% of the global mean sea level rise, result from land ice loss and variations in ocean warming and circulation. Differences from the global mean can be greater in areas of rapid vertical land movement including from local human activities (e.g. extraction of groundwater). (*high confidence*) {4.2.2, 5.2.2, 6.2.2, 6.3.1, 6.8.2, Figure SPM.2}

---

[21]   The Atlantic Meridional Overturning Circulation (AMOC) is the main current system in the South and North Atlantic Oceans (Annex I: Glossary).

[22]   The total rate of sea level rise is greater than the sum of cryosphere and ocean contributions due to uncertainties in the estimate of landwater storage change.

[23]   The recovery time scale is hundreds to thousands of years (Annex I: Glossary).

A.3.5   Extreme wave heights, which contribute to extreme sea level events, coastal erosion and flooding, have increased in the Southern and North Atlantic Oceans by around 1.0 cm yr^{-1} and 0.8 cm yr^{-1} over the period 1985–2018 (*medium confidence*). Sea ice loss in the Arctic has also increased wave heights over the period 1992–2014 (*medium confidence*). {4.2.2, 6.2, 6.3, 6.8, Box 6.1}

A.3.6   Anthropogenic climate change has increased observed precipitation (*medium confidence*), winds (*low confidence*), and extreme sea level events (*high confidence*) associated with some tropical cyclones, which has increased intensity of multiple extreme events and associated cascading impacts (*high confidence*). Anthropogenic climate change may have contributed to a poleward migration of maximum tropical cyclone intensity in the western North Pacific in recent decades related to anthropogenically-forced tropical expansion (*low confidence*). There is emerging evidence for an increase in annual global proportion of Category 4 or 5 tropical cyclones in recent decades (*low confidence*). {6.2, Table 6.2, 6.3, 6.8, Box 6.1}

Observed Impacts on Ecosystems

A.4   **Cryospheric and associated hydrological changes have impacted terrestrial and freshwater species and ecosystems in high mountain and polar regions through the appearance of land previously covered by ice, changes in snow cover, and thawing permafrost. These changes have contributed to changing the seasonal activities, abundance and distribution of ecologically, culturally, and economically important plant and animal species, ecological disturbances, and ecosystem functioning. (*high confidence*) {2.3.2, 2.3.3, 3.4.1, 3.4.3, Box 3.4, Figure SPM.2}**

A.4.1   Over the last century some species of plants and animals have increased in abundance, shifted their range, and established in new areas as glaciers receded and the snow-free season lengthened (*high confidence*). Together with warming, these changes have increased locally the number of species in high mountains, as lower-elevation species migrate upslope (*very high confidence*). Some cold-adapted or snow-dependent species have declined in abundance, increasing their risk of extinction, notably on mountain summits (*high confidence*). In polar and mountain regions, many species have altered seasonal activities especially in late winter and spring (*high confidence*). {2.3.3, Box 3.4}

A.4.2   Increased wildfire and abrupt permafrost thaw, as well as changes in Arctic and mountain hydrology have altered frequency and intensity of ecosystem disturbances (*high confidence*). This has included positive and negative impacts on vegetation and wildlife such as reindeer and salmon (*high confidence*). {2.3.3, 3.4.1, 3.4.3}

A.4.3   Across tundra, satellite observations show an overall greening, often indicative of increased plant productivity (*high confidence*). Some browning areas in tundra and boreal forest are indicative that productivity has decreased (*high confidence*). These changes have negatively affected provisioning, regulating and cultural ecosystem services, with also some transient positive impacts for provisioning services, in both high mountains (*medium confidence*) and polar regions (*high confidence*). {2.3.1, 2.3.3, 3.4.1, 3.4.3, Annex I: Glossary}

A.5   **Since about 1950 many marine species across various groups have undergone shifts in geographical range and seasonal activities in response to ocean warming, sea ice change and biogeochemical changes, such as oxygen loss, to their habitats (*high confidence*). This has resulted in shifts in species composition, abundance and biomass production of ecosystems, from the equator to the poles. Altered interactions between species have caused cascading impacts on ecosystem structure and functioning (*medium confidence*). In some marine ecosystems species are impacted by both the effects of fishing and climate changes (*medium confidence*). {3.2.3, 3.2.4, Box 3.4, 5.2.3, 5.3, 5.4.1, Figure SPM.2}**

A.5.1   Rates of poleward shifts in distributions across different marine species since the 1950s are 52 ± 33 km per decade and 29 ± 16 km per decade (*very likely* ranges) for organisms in the epipelagic (upper 200 m from sea surface) and seafloor ecosystems, respectively. The rate and direction of observed shifts in distributions are shaped by local temperature, oxygen, and ocean currents across depth, latitudinal and longitudinal gradients (*high confidence*). Warming-induced species range expansions have led to altered ecosystem structure and functioning such as in the North Atlantic, Northeast Pacific and Arctic (*medium confidence*). {5.2.3, 5.3.2, 5.3.6, Box 3.4, Figure SPM.2}

A.5.2   In recent decades, Arctic net primary production has increased in ice-free waters (*high confidence*) and spring phytoplankton blooms are occurring earlier in the year in response to sea ice change and nutrient availability with spatially variable positive and negative consequences for marine ecosystems (*medium confidence*). In the Antarctic, such changes are spatially heterogeneous and have been associated with rapid local environmental change, including retreating glaciers and sea ice change (*medium confidence*). Changes in the seasonal activities, production and distribution of some Arctic zooplankton and a southward shift in the distribution of the Antarctic krill population in the South Atlantic are associated with climate-linked environmental changes (*medium confidence*). In polar regions, ice associated marine mammals and seabirds have experienced habitat contraction linked to sea ice changes (*high confidence*) and impacts on foraging success due to climate impacts on prey distributions (*medium confidence*). Cascading effects of multiple climate-related drivers on polar zooplankton have affected food web structure and function, biodiversity as well as fisheries (*high confidence*). {3.2.3, 3.2.4, Box 3.4, 5.2.3, Figure SPM.2}

A.5.3   Eastern Boundary Upwelling Systems (EBUS) are amongst the most productive ocean ecosystems. Increasing ocean acidification and oxygen loss are negatively impacting two of the four major upwelling systems: the California Current and Humboldt Current (*high confidence*). Ocean acidification and decrease in oxygen level in the California Current upwelling system have altered ecosystem structure, with direct negative impacts on biomass production and species composition (*medium confidence*). {Box 5.3, Figure SPM.2}

A.5.4   Ocean warming in the 20th century and beyond has contributed to an overall decrease in maximum catch potential (*medium confidence*), compounding the impacts from overfishing for some fish stocks (*high confidence*). In many regions, declines in the abundance of fish and shellfish stocks due to direct and indirect effects of global warming and biogeochemical changes have already contributed to reduced fisheries catches (*high confidence*). In some areas, changing ocean conditions have contributed to the expansion of suitable habitat and/or increases in the abundance of some species (*high confidence*). These changes have been accompanied by changes in species composition of fisheries catches since the 1970s in many ecosystems (*medium confidence*). {3.2.3, 5.4.1, Figure SPM.2}

A.6   Coastal ecosystems are affected by ocean warming, including intensified marine heatwaves, acidification, loss of oxygen, salinity intrusion and sea level rise, in combination with adverse effects from human activities on ocean and land (*high confidence*). Impacts are already observed on habitat area and biodiversity, as well as ecosystem functioning and services (*high confidence*). {4.3.2, 4.3.3, 5.3, 5.4.1, 6.4.2, Figure SPM.2}

A.6.1   Vegetated coastal ecosystems protect the coastline from storms and erosion and help buffer the impacts of sea level rise. Nearly 50% of coastal wetlands have been lost over the last 100 years, as a result of the combined effects of localised human pressures, sea level rise, warming and extreme climate events (*high confidence*). Vegetated coastal ecosystems are important carbon stores; their loss is responsible for the current release of 0.04–1.46 GtC yr^{-1} (*medium confidence*). In response to warming, distribution ranges of seagrass meadows and kelp forests are expanding at high latitudes and contracting at low latitudes since the late 1970s (*high confidence*), and in some areas episodic losses occur following heatwaves (*medium confidence*). Large-scale mangrove mortality that is related to warming since the 1960s has been partially offset by their encroachment into subtropical saltmarshes as a result of increase in temperature, causing the loss of open areas with herbaceous plants that provide food and habitat for dependent fauna (*high confidence*). {4.3.3, 5.3.2, 5.3.6, 5.4.1, 5.5.1, Figure SPM.2}

A.6.2   Increased sea water intrusion in estuaries due to sea level rise has driven upstream redistribution of marine species (*medium confidence*) and caused a reduction of suitable habitats for estuarine communities (*medium confidence*). Increased nutrient and organic matter loads in estuaries since the 1970s from intensive human development and riverine loads have exacerbated the stimulating effects of ocean warming on bacterial respiration, leading to expansion of low oxygen areas (*high confidence*). {5.3.1}

A.6.3   The impacts of sea level rise on coastal ecosystems include habitat contraction, geographical shift of associated species, and loss of biodiversity and ecosystem functionality. Impacts are exacerbated by direct human disturbances, and where anthropogenic barriers prevent landward shift of marshes and mangroves (termed coastal squeeze) (*high confidence*). Depending on local geomorphology and sediment supply, marshes and mangroves can grow vertically at rates equal to or greater than current mean sea level rise (*high confidence*). {4.3.2, 4.3.3, 5.3.2, 5.3.7, 5.4.1}

A.6.4   Warm-water coral reefs and rocky shores dominated by immobile, calcifying (e.g., shell and skeleton producing) organisms such as corals, barnacles and mussels, are currently impacted by extreme temperatures and ocean acidification (*high confidence*). Marine heatwaves have already resulted in large-scale coral bleaching events at increasing frequency (*very high confidence*) causing worldwide reef degradation since 1997, and recovery is slow (more than 15 years) if it occurs (*high confidence*). Prolonged periods of high environmental temperature and dehydration of the organisms pose high risk to rocky shore ecosystems (*high confidence*). {SR.1.5; 5.3.4, 5.3.5, 6.4.2, Figure SPM.2}

Observed regional impacts from changes in the ocean and the cryosphere

Ocean

	Arctic	EBUS [1]	North Atlantic	North Pacific	South Atlantic	South Pacific	Southern Ocean	Temperate Indian Ocean	Tropical Atlantic	Tropical Indian Ocean	Tropical Pacific
Physical changes (Greenhouse Gases)											
Temperature	●●	●	●●	●●	●●	●●	●●	●●	●●	●●	●
Oxygen		●	●	●	●	●	●	●	●	●	●
Ocean pH	●●●	●●●	●●●	●●●	●●●	●●●	●●●	●●●	●●●	●●●	●●●
Sea ice extent	●●●						●				
Sea level	●	●●	●●	●●	●●	●●		●●	●●	●●	●●
Ecosystems (Climate Change)											
Upper water column	●●	●	●●●	●●	●●	●●	●●	●	●●	●	●●
Coral		●			●●●				●●●	●●●	●●●
Coastal wetlands			●●	●●	●●	●●		●●	●●	●●	●●
Kelp forest	●●	●●	●●	●●	●	●		●			●
Rocky shores			●●●	●●				●●			
Deep sea				●							
Polar benthos	●●						●●				
Sea ice-associated	●●						●●				
Human systems and ecosystem services											
Fisheries	●●	●	●●●	●	●	●		●	●●	●	●
Tourism	●●	●		●		●	●	●	●		●
Habitat services	●●	●	●●	●●	●	●●		●	●●	●●	●●
Transportation/shipping	●●										
Cultural services	●●		●●	●							
Coastal carbon sequestration		●●	●●	●	●			●	●	●●	●

LEGEND

Physical changes
- increase
- decrease
- increase and decrease

Systems
- positive
- negative
- positive and negative

- no assessment

Attribution confidence
- ●●● high
- ●● medium
- ● low

[1] Eastern Boundary Upwelling Systems (Benguela Current, Canary Current, California Current, and Humboldt Current); {Box 5.3}

High mountain and polar land regions

	Himalaya, Tibetan Plateau and other High Mountain Asia [2]	Low Latitudes [3]	Southern Andes	New Zealand	Western Canada and USA	European Alps and Pyrenees	Caucasus	Scandinavia [4]	Iceland	Russian Arctic	Alaska [5]	Arctic Canada and Greenland	Antarctica
Physical changes													
Water availability	●●●	●●●	●●		●●●	●●	●	●●	●●	●●	●●●		
Flood	●				●	●							
Landslide	●			●	●	●●●		●	●		●●		
Avalanche	●					●●	●						
Ground subsidence										●●	●●	●●	
Ecosystems													
Tundra	●●●	●			●●	●●		●●		●●	●●	●●	●
Forest	●●				●●					●●	●●	●●	
Lakes/ponds										●	●		
Rivers/streams		●	●	●	●●	●●●			●				
Human systems and ecosystem services													
Tourism	●●	●			●●●	●●		●			●		
Agriculture	●●	●	●					●					
Infrastructure	●●●				●●●					●●	●●	●●	
Migration [6]	●	●									●●		
Cultural services	●●	●●			●	●●●		●		●		●●	

[2] including Hindu Kush, Karakoram, Hengduan Shan, and Tien Shan; [3] tropical Andes, Mexico, eastern Africa, and Indonesia;
[4] includes Finland, Norway, and Sweden; [5] includes adjacent areas in Yukon Territory and British Columbia, Canada; [6] Migration refers to an increase or decrease in net migration, not to beneficial/adverse value.

Figure SPM.2 | Synthesis of observed regional hazards and impacts in ocean[24] (top) and high mountain and polar land regions (bottom) assessed in SROCC. For each region, physical changes, impacts on key ecosystems, and impacts on human systems and ecosystem function and services are shown. For physical changes, yellow/green refers to an increase/decrease, respectively, in amount or frequency of the measured variable. For impacts on ecosystems, human systems and ecosystems services blue or red depicts whether an observed impact is positive (beneficial) or negative (adverse), respectively, to the given system or service. Cells assigned 'increase and decrease' indicate that within that region, both increase and decrease of physical changes are found, but are not necessarily equal; the same holds for cells showing 'positive and negative' attributable impacts. For ocean regions, the confidence level refers to the confidence in attributing observed changes to changes in greenhouse gas forcing for physical changes and to climate change for ecosystem, human systems, and ecosystem services. For high mountain and polar land regions, the level of confidence in attributing physical changes and impacts at least partly to a change in the cryosphere is shown. No assessment means: not applicable, not assessed at regional scale, or the evidence is insufficient for assessment. The physical changes in the ocean are defined as: Temperature change in 0–700 m layer of the ocean except for Southern Ocean (0–2000 m) and Arctic Ocean (upper mixed layer and major inflowing branches); Oxygen in the 0–1200 m layer or oxygen minimum layer; Ocean pH as surface pH (decreasing pH corresponds to increasing ocean acidification). Ecosystems in the ocean: Coral refers to warm-water coral reefs and cold-water corals. The 'upper water column' category refers to epipelagic zone for all ocean regions except Polar Regions, where the impacts on some pelagic organisms in open water deeper than the upper 200 m were included. Coastal wetland includes salt marshes, mangroves and seagrasses. Kelp forests are habitats of a specific group of macroalgae. Rocky shores are coastal habitats dominated by immobile calcified organisms such as mussels and barnacles. Deep sea is seafloor ecosystems that are 3000–6000 m deep. Sea-ice associated includes ecosystems in, on and below sea ice. Habitat services refer to supporting structures and services (e.g., habitat, biodiversity, primary production). Coastal Carbon Sequestration refers to the uptake and storage of carbon by coastal blue carbon ecosystems. Ecosystems on Land: Tundra refers to tundra and alpine meadows, and includes terrestrial Antarctic ecosystems.

---

[24] Marginal seas are not assessed individually as ocean regions in this report.

Figure SPM.2 (continued): Migration refers to an increase or decrease in net migration, not to beneficial/adverse value. Impacts on tourism refer to the operating conditions for the tourism sector. Cultural services include cultural identity, sense of home, and spiritual, intrinsic and aesthetic values, as well as contributions from glacier archaeology. The underlying information is given for land regions in tables SM2.6, SM2.7, SM2.8, SM3.8, SM3.9, and SM3.10, and for ocean regions in tables SM5.10, SM5.11, SM3.8, SM3.9, and SM3.10. {2.3.1, 2.3.2, 2.3.3, 2.3.4, 2.3.5, 2.3.6, 2.3.7, Figure 2.1, 3.2.1, 3.2.3, 3.2.4, 3.3.3, 3.4.1, 3.4.3, 3.5.2, Box 3.4, 4.2.2, 5.2.2, 5.2.3, 5.3.3, 5.4, 5.6, Figure 5.24, Box 5.3}

Observed Impacts on People and Ecosystem Services

A.7   **Since the mid-20th century, the shrinking cryosphere in the Arctic and high mountain areas has led to predominantly negative impacts on food security, water resources, water quality, livelihoods, health and well-being, infrastructure, transportation, tourism and recreation, as well as culture of human societies, particularly for Indigenous peoples (*high confidence*). Costs and benefits have been unequally distributed across populations and regions. Adaptation efforts have benefited from the inclusion of Indigenous knowledge and local knowledge (*high confidence*). {1.1, 1.5, 1.6.2, 2.3, 2.4, 3.4, 3.5, Figure SPM.2}**

A.7.1   Food and water security have been negatively impacted by changes in snow cover, lake and river ice, and permafrost in many Arctic regions (*high confidence*). These changes have disrupted access to, and food availability within, herding, hunting, fishing, and gathering areas, harming the livelihoods and cultural identity of Arctic residents including Indigenous populations (*high confidence*). Glacier retreat and snow cover changes have contributed to localized declines in agricultural yields in some high mountain regions, including Hindu Kush Himalaya and the tropical Andes (*medium confidence*). {2.3.1, 2.3.7, Box 2.4, 3.4.1, 3.4.2, 3.4.3, 3.5.2, Figure SPM.2}

A.7.2   In the Arctic, negative impacts of cryosphere change on human health have included increased risk of food- and waterborne diseases, malnutrition, injury, and mental health challenges especially among Indigenous peoples (*high confidence*). In some high mountain areas, water quality has been affected by contaminants, particularly mercury, released from melting glaciers and thawing permafrost (*medium confidence*). Health-related adaptation efforts in the Arctic range from local to international in scale, and successes have been underpinned by Indigenous knowledge (*high confidence*). {1.8, Cross-Chapter Box 4 in Chapter 1, 2.3.1, 3.4.3}

A.7.3   Arctic residents, especially Indigenous peoples, have adjusted the timing of activities to respond to changes in seasonality and safety of land, ice, and snow travel conditions. Municipalities and industry are beginning to address infrastructure failures associated with flooding and thawing permafrost and some coastal communities have planned for relocation (*high confidence*). Limited funding, skills, capacity, and institutional support to engage meaningfully in planning processes have challenged adaptation (*high confidence*). {3.5.2, 3.5.4, Cross-Chapter Box 9}

A.7.4   Summertime Arctic ship-based transportation (including tourism) increased over the past two decades concurrent with sea ice reductions (*high confidence*). This has implications for global trade and economies linked to traditional shipping corridors, and poses risks to Arctic marine ecosystems and coastal communities (*high confidence*), such as from invasive species and local pollution. {3.2.1, 3.2.4, 3.5.4, 5.4.2, Figure SPM.2}

A.7.5   In past decades, exposure of people and infrastructure to natural hazards has increased due to growing population, tourism and socioeconomic development (*high confidence*). Some disasters have been linked to changes in the cryosphere, for example in the Andes, high mountain Asia, Caucasus and European Alps (*medium confidence*). {2.3.2, Figure SPM.2}

A.7.6   Changes in snow and glaciers have changed the amount and seasonality of runoff and water resources in snow dominated and glacier-fed river basins (*very high confidence*). Hydropower facilities have experienced changes in seasonality and both increases and decreases in water input from high mountain areas, for

example, in central Europe, Iceland, Western USA/Canada, and tropical Andes (*medium confidence*). However, there is only *limited evidence* of resulting impacts on operations and energy production. {SPM B.1.4, 2.3.1}

A.7.7   High mountain aesthetic and cultural aspects have been negatively impacted by glacier and snow cover decline (e.g. in the Himalaya, East Africa, the tropical Andes) (*medium confidence*). Tourism and recreation, including ski and glacier tourism, hiking, and mountaineering, have also been negatively impacted in many mountain regions (*medium confidence*). In some places, artificial snowmaking has reduced negative impacts on ski tourism (*medium confidence*). {2.3.5, 2.3.6, Figure SPM.2}

A.8   Changes in the ocean have impacted marine ecosystems and ecosystem services with regionally diverse outcomes, challenging their governance (*high confidence*). Both positive and negative impacts result for food security through fisheries (*medium confidence*), local cultures and livelihoods (*medium confidence*), and tourism and recreation (*medium confidence*). The impacts on ecosystem services have negative consequences for health and well-being (*medium confidence*), and for Indigenous peoples and local communities dependent on fisheries (*high confidence*). {1.1, 1.5, 3.2.1, 5.4.1, 5.4.2, Figure SPM.2}

A.8.1   Warming-induced changes in the spatial distribution and abundance of some fish and shellfish stocks have had positive and negative impacts on catches, economic benefits, livelihoods, and local culture (*high confidence*). There are negative consequences for Indigenous peoples and local communities that are dependent on fisheries (*high confidence*). Shifts in species distributions and abundance has challenged international and national ocean and fisheries governance, including in the Arctic, North Atlantic and Pacific, in terms of regulating fishing to secure ecosystem integrity and sharing of resources between fishing entities (*high confidence*). {3.2.4, 3.5.3, 5.4.2, 5.5.2, Figure SPM.2}

A.8.2   Harmful algal blooms display range expansion and increased frequency in coastal areas since the 1980s in response to both climatic and non-climatic drivers such as increased riverine nutrients run-off (*high confidence*). The observed trends in harmful algal blooms are attributed partly to the effects of ocean warming, marine heatwaves, oxygen loss, eutrophication and pollution (*high confidence*). Harmful algal blooms have had negative impacts on food security, tourism, local economy, and human health (*high confidence*). The human communities who are more vulnerable to these biological hazards are those in areas without sustained monitoring programs and dedicated early warning systems for harmful algal blooms (*medium confidence*). {Box 5.4, 5.4.2, 6.4.2}

A.9   Coastal communities are exposed to multiple climate-related hazards, including tropical cyclones, extreme sea levels and flooding, marine heatwaves, sea ice loss, and permafrost thaw (*high confidence*). A diversity of responses has been implemented worldwide, mostly after extreme events, but also some in anticipation of future sea level rise, e.g., in the case of large infrastructure. {3.2.4, 3.4.3, 4.3.2, 4.3.3, 4.3.4, 4.4.2, 5.4.2, 6.2, 6.4.2, 6.8, Box 6.1, Cross Chapter Box 9, Figure SPM.5}

A.9.1   Attribution of current coastal impacts on people to sea level rise remains difficult in most locations since impacts were exacerbated by human-induced non-climatic drivers, such as land subsidence (e.g., groundwater extraction), pollution, habitat degradation, reef and sand mining (*high confidence*). {4.3.2, 4.3.3}

A.9.2   Coastal protection through hard measures, such as dikes, seawalls, and surge barriers, is widespread in many coastal cities and deltas. Ecosystem-based and hybrid approaches combining ecosystems and built infrastructure are becoming more popular worldwide. Coastal advance, which refers to the creation of new land by building seawards (e.g., land reclamation), has a long history in most areas where there are dense coastal

populations and a shortage of land. Coastal retreat, which refers to the removal of human occupation of coastal areas, is also observed, but is generally restricted to small human communities or occurs to create coastal wetland habitat. The effectiveness of the responses to sea level rise are assessed in Figure SPM.5. {3.5.3, 4.3.3, 4.4.2, 6.3.3, 6.9.1, Cross-Chapter Box 9}

B.   Projected Changes and Risks

Projected Physical Changes[25]

B.1 **Global-scale glacier mass loss, permafrost thaw, and decline in snow cover and Arctic sea ice extent are projected to continue in the near-term (2031–2050) due to surface air temperature increases (*high confidence*), with unavoidable consequences for river runoff and local hazards (*high confidence*). The Greenland and Antarctic Ice Sheets are projected to lose mass at an increasing rate throughout the 21st century and beyond (*high confidence*). The rates and magnitudes of these cryospheric changes are projected to increase further in the second half of the 21st century in a high greenhouse gas emissions scenario (*high confidence*). Strong reductions in greenhouse gas emissions in the coming decades are projected to reduce further changes after 2050 (*high confidence*). {2.2, 2.3, Cross-Chapter Box 6 in Chapter 2, 3.3, 3.4, Figure SPM.1, SPM Box SPM.1}**

B.1.1   Projected glacier mass reductions between 2015 and 2100 (excluding the ice sheets) range from 18 ± 7% (*likely* range) for RCP2.6 to 36 ± 11% (*likely* range) for RCP8.5, corresponding to a sea level contribution of 94 ± 25 mm (*likely* range) sea level equivalent for RCP2.6, and 200 ± 44 mm (*likely* range) for RCP8.5 (*medium confidence*). Regions with mostly smaller glaciers (e.g., Central Europe, Caucasus, North Asia, Scandinavia, tropical Andes, Mexico, eastern Africa and Indonesia), are projected to lose more than 80% of their current ice mass by 2100 under RCP8.5 (*medium confidence*), and many glaciers are projected to disappear regardless of future emissions (*very high confidence*). {Cross-Chapter Box 6 in Chapter 2, Figure SPM.1}

B.1.2   In 2100, the Greenland Ice Sheet's projected contribution to GMSL rise is 0.07 m (0.04–0.12 m, *likely* range) under RCP2.6, and 0.15 m (0.08–0.27 m, *likely* range) under RCP8.5. In 2100, the Antarctic Ice Sheet is projected to contribute 0.04 m (0.01–0.11 m, *likely* range) under RCP2.6, and 0.12 m (0.03–0.28 m, *likely* range) under RCP8.5. The Greenland Ice Sheet is currently contributing more to sea level rise than the Antarctic Ice Sheet (*high confidence*), but Antarctica could become a larger contributor by the end of the 21st century as a consequence of rapid retreat (*low confidence*). Beyond 2100, increasing divergence between Greenland and Antarctica's relative contributions to GMSL rise under RCP8.5 has important consequences for the pace of relative sea level rise in the Northern Hemisphere. {3.3.1, 4.2.3, 4.2.5, 4.3.3, Cross-Chapter Box 8 in Chapter 3, Figure SPM.1}

B.1.3   Arctic autumn and spring snow cover are projected to decrease by 5–10%, relative to 1986–2005, in the near-term (2031–2050), followed by no further losses under RCP2.6, but an additional 15–25% loss by the end of century under RCP8.5 (*high confidence*). In high mountain areas, projected decreases in low elevation mean winter snow depth, compared to 1986–2005, are *likely* 10–40% by 2031–2050, regardless of emissions scenario (*high confidence*). For 2081–2100, this projected decrease is *likely* 10–40% for RCP2.6 and 50–90% for RCP8.5. {2.2.2, 3.3.2, 3.4.2, Figure SPM.1}

---

[25]   This report primarily uses RCP2.6 and RCP8.5 for the following reasons: These scenarios largely represent the assessed range for the topics covered in this report; they largely represent what is covered in the assessed literature, based on CMIP5; and they allow a consistent narrative about projected changes. RCP4.5 and RCP6.0 are not available for all topics addressed in the report. {Box SPM.1}

B.1.4 Widespread permafrost thaw is projected for this century (*very high confidence*) and beyond. By 2100, projected near-surface (within 3–4 m) permafrost area shows a decrease of 24 ± 16% (*likely* range) for RCP2.6 and 69 ± 20% (*likely* range) for RCP8.5. The RCP8.5 scenario leads to the cumulative release of tens to hundreds of billions of tons (GtC) of permafrost carbon as CO_2[26] and methane to the atmosphere by 2100 with the potential to exacerbate climate change (*medium confidence*). Lower emissions scenarios dampen the response of carbon emissions from the permafrost region (*high confidence*). Methane contributes a small fraction of the total additional carbon release but is significant because of its higher warming potential. Increased plant growth is projected to replenish soil carbon in part, but will not match carbon releases over the long term (*medium confidence*). {2.2.4, 3.4.2, 3.4.3, Figure SPM.1, Cross-Chapter Box 5 in Chapter 1}

B.1.5 In many high mountain areas, glacier retreat and permafrost thaw are projected to further decrease the stability of slopes, and the number and area of glacier lakes will continue to increase (*high confidence*). Floods due to glacier lake outburst or rain-on-snow, landslides and snow avalanches, are projected to occur also in new locations or different seasons (*high confidence*). {2.3.2}

B.1.6 River runoff in snow-dominated or glacier-fed high mountain basins is projected to change regardless of emissions scenario (*very high confidence*), with increases in average winter runoff (*high confidence)* and earlier spring peaks (*very high confidence*). In all emissions scenarios, average annual and summer runoff from glaciers are projected to peak at or before the end of the 21st century (*high confidence*), e.g., around mid-century in High Mountain Asia, followed by a decline in glacier runoff. In regions with little glacier cover (e.g., tropical Andes, European Alps) most glaciers have already passed this peak (*high confidence*). Projected declines in glacier runoff by 2100 (RCP8.5) can reduce basin runoff by 10% or more in at least one month of the melt season in several large river basins, especially in High Mountain Asia during the dry season (*low confidence*). {2.3.1}

B.1.7 Arctic sea ice loss is projected to continue through mid-century, with differences thereafter depending on the magnitude of global warming: for stabilised global warming of 1.5°C the annual probability of a sea ice-free September by the end of century is approximately 1%, which rises to 10–35% for stabilised global warming of 2°C (*high confidence*). There is *low confidence* in projections for Antarctic sea ice. {3.2.2, Figure SPM.1}

B.2 Over the 21st century, the ocean is projected to transition to unprecedented conditions with increased temperatures (*virtually certain*), greater upper ocean stratification (*very likely*), further acidification (*virtually certain*), oxygen decline (*medium confidence*), and altered net primary production (*low confidence*). Marine heatwaves (*very high confidence)* and extreme El Niño and La Niña events (*medium confidence)* are projected to become more frequent. The Atlantic Meridional Overturning Circulation (AMOC) is projected to weaken (*very likely*). The rates and magnitudes of these changes will be smaller under scenarios with low greenhouse gas emissions (*very likely*). {3.2, 5.2, 6.4, 6.5, 6.7, Box 5.1, Figures SPM.1, SPM.3}

B.2.1 The ocean will continue to warm throughout the 21st century (*virtually certain*). By 2100, the top 2000 m of the ocean are projected to take up 5–7 times more heat under RCP8.5 (or 2–4 times more under RCP2.6) than the observed accumulated ocean heat uptake since 1970 (*very likely*). The annual mean density stratification[19] of the top 200 m, averaged between 60°S and 60°N, is projected to increase by 12–30% for RCP8.5 and 1–9% for RCP2.6, for 2081–2100 relative to 1986–2005 (*very likely*), inhibiting vertical nutrient, carbon and oxygen fluxes. {5.2.2, Figure SPM.1}

---

[26] For context, total annual anthropogenic CO_2 emissions were 10.8 ± 0.8 GtC yr^{-1} (39.6 ± 2.9 $GtCO_2$ yr^{-1}) on average over the period 2008–2017. Total annual anthropogenic methane emissions were 0.35 ± 0.01 $GtCH_4$ yr^{-1}, on average over the period 2003–2012. {5.5.1}

B.2.2   By 2081–2100 under RCP8.5, ocean oxygen content (*medium confidence*), upper ocean nitrate content (*medium confidence*), net primary production (*low confidence*) and carbon export (*medium confidence*) are projected to decline globally by *very likely* ranges of 3–4%, 9–14%, 4–11% and 9–16% respectively, relative to 2006–2015. Under RCP2.6, globally projected changes by 2081–2100 are smaller compared to RCP8.5 for oxygen loss (*very likely*), nutrient availability (*about as likely as not*) and net primary production (*high confidence*). {5.2.2, Box 5.1, Figures SPM.1, SPM.3}

B.2.3   Continued carbon uptake by the ocean by 2100 is *virtually certain* to exacerbate ocean acidification. Open ocean surface pH is projected to decrease by around 0.3 pH units by 2081–2100, relative to 2006–2015, under RCP8.5 (*virtually certain*). For RCP8.5, there are elevated risks for keystone aragonite shell-forming species due to crossing an aragonite stability threshold year-round in the Polar and sub-Polar Oceans by 2081–2100 (*very likely*). For RCP2.6, these conditions will be avoided this century (*very likely*), but some eastern boundary upwelling systems are projected to remain vulnerable (*high confidence*). {3.2.3, 5.2.2, Box 5.1, Box 5.3, Figure SPM.1}

B.2.4   Climate conditions, unprecedented since the preindustrial period, are developing in the ocean, elevating risks for open ocean ecosystems. Surface acidification and warming have already emerged in the historical period (*very likely*). Oxygen loss between 100 and 600 m depth is projected to emerge over 59–80% of the ocean area by 2031–2050 under RCP8.5 (*very likely*). The projected time of emergence for five primary drivers of marine ecosystem change (surface warming and acidification, oxygen loss, nitrate content and net primary production change) are all prior to 2100 for over 60% of the ocean area under RCP8.5 and over 30% under RCP2.6 (*very likely*). {Annex I: Glossary, Box 5.1, Box 5.1 Figure 1}

B.2.5   Marine heatwaves are projected to further increase in frequency, duration, spatial extent and intensity (maximum temperature) (*very high confidence*). Climate models project increases in the frequency of marine heatwaves by 2081–2100, relative to 1850–1900, by approximately 50 times under RCP8.5 and 20 times under RCP2.6 (*medium confidence*). The largest increases in frequency are projected for the Arctic and the tropical oceans (*medium confidence*). The intensity of marine heatwaves is projected to increase about 10-fold under RCP8.5 by 2081–2100, relative to 1850–1900 (*medium confidence*). {6.4, Figure SPM.1}

B.2.6   Extreme El Niño and La Niña events are projected to *likely* increase in frequency in the 21st century and to *likely* intensify existing hazards, with drier or wetter responses in several regions across the globe. Extreme El Niño events are projected to occur about as twice as often under both RCP2.6 and RCP8.5 in the 21st century when compared to the 20th century (*medium confidence*). Projections indicate that extreme Indian Ocean Dipole events also increase in frequency (*low confidence*). {6.5, Figures 6.5, 6.6}

B.2.7   The AMOC is projected to weaken in the 21st century under all RCPs (*very likely*), although a collapse is *very unlikely* (*medium confidence)*. Based on CMIP5 projections, by 2300, an AMOC collapse is *about as likely as not* for high emissions scenarios and *very unlikely* for lower ones (*medium confidence)*. Any substantial weakening of the AMOC is projected to cause a decrease in marine productivity in the North Atlantic (*medium confidence*), more storms in Northern Europe (*medium confidence*), less Sahelian summer rainfall (*high confidence*) and South Asian summer rainfall (*medium confidence*), a reduced number of tropical cyclones in the Atlantic (*medium confidence*), and an increase in regional sea level along the northeast coast of North America (*medium confidence*). Such changes would be in addition to the global warming signal. {6.7, Figures 6.8–6.10}

B.3 **Sea level continues to rise at an increasing rate. Extreme sea level events that are historically rare (once per century in the recent past) are projected to occur frequently (at least once per year) at many locations by 2050 in all RCP scenarios, especially in tropical regions (*high confidence*). The increasing frequency of high water levels can have severe impacts in many locations depending on exposure (*high confidence*). Sea level rise is projected to continue beyond 2100 in all RCP scenarios. For a high emissions scenario (RCP8.5), projections of global sea level rise by 2100 are greater than in AR5 due to a larger contribution from the Antarctic Ice Sheet (*medium confidence*). In coming centuries under RCP8.5, sea-level rise is projected to exceed rates of several centimetres per year resulting in multi-metre rise (*medium confidence*), while for RCP2.6 sea level rise is projected to be limited to around 1 m in 2300 (*low confidence*). Extreme sea levels and coastal hazards will be exacerbated by projected increases in tropical cyclone intensity and precipitation (*high confidence*). Projected changes in waves and tides vary locally in whether they amplify or ameliorate these hazards (*medium confidence*). {Cross-Chapter Box 5 in Chapter 1, Cross-Chapter Box 8 in Chapter 3, 4.1, 4.2, 5.2.2, 6.3.1, Figures SPM.1, SPM.4, SPM.5}**

B.3.1   The global mean sea level (GMSL) rise under RCP2.6 is projected to be 0.39 m (0.26–0.53 m, *likely* range) for the period 2081–2100, and 0.43 m (0.29–0.59 m, *likely* range) in 2100 with respect to 1986–2005. For RCP8.5, the corresponding GMSL rise is 0.71 m (0.51–0.92 m, *likely* range) for 2081–2100 and 0.84 m (0.61–1.10 m, *likely* range) in 2100. Mean sea level rise projections are higher by 0.1 m compared to AR5 under RCP8.5 in 2100, and the *likely* range extends beyond 1 m in 2100 due to a larger projected ice loss from the Antarctic Ice Sheet (*medium confidence*). The uncertainty at the end of the century is mainly determined by the ice sheets, especially in Antarctica. {4.2.3, Figures SPM.1, SPM.5}

B.3.2   Sea level projections show regional differences around GMSL. Processes not driven by recent climate change, such as local subsidence caused by natural processes and human activities, are important to relative sea level changes at the coast (*high confidence*). While the relative importance of climate-driven sea level rise is projected to increase over time, local processes need to be considered for projections and impacts of sea level (*high confidence*). {SPM A.3.4, 4.2.1, 4.2.2, Figure SPM.5}

B.3.3   The rate of global mean sea level rise is projected to reach 15 mm yr^{-1} (10–20 mm yr^{-1}, *likely* range) under RCP8.5 in 2100, and to exceed several centimetres per year in the 22nd century. Under RCP2.6, the rate is projected to reach 4 mm yr^{-1} (2–6 mm yr^{-1}, *likely* range) in 2100. Model studies indicate multi-meter rise in sea level by 2300 (2.3–5.4 m for RCP8.5 and 0.6–1.07 m under RCP2.6) (*low confidence*), indicating the importance of reduced emissions for limiting sea level rise. Processes controlling the timing of future ice-shelf loss and the extent of ice sheet instabilities could increase Antarctica's contribution to sea level rise to values substantially higher than the *likely* range on century and longer time-scales (*low confidence*). Considering the consequences of sea level rise that a collapse of parts of the Antarctic Ice Sheet entails, this high impact risk merits attention. {Cross-Chapter Box 5 in Chapter 1, Cross-Chapter Box 8 in Chapter 3, 4.1, 4.2.3}

B.3.4   Global mean sea level rise will cause the frequency of extreme sea level events at most locations to increase. Local sea levels that historically occurred once per century (historical centennial events) are projected to occur at least annually at most locations by 2100 under all RCP scenarios (*high confidence*). Many low-lying megacities and small islands (including SIDS) are projected to experience historical centennial events at least annually by 2050 under RCP2.6, RCP4.5 and RCP8.5. The year when the historical centennial event becomes an annual event in the mid-latitudes occurs soonest in RCP8.5, next in RCP4.5 and latest in RCP2.6. The increasing frequency of high water levels can have severe impacts in many locations depending on the level of exposure (*high confidence*). {4.2.3, 6.3, Figures SPM.4, SPM.5}

B.3.5   Significant wave heights (the average height from trough to crest of the highest one-third of waves) are projected to increase across the Southern Ocean and tropical eastern Pacific (*high confidence*) and Baltic Sea (*medium confidence*) and decrease over the North Atlantic and Mediterranean Sea under RCP8.5 (*high confidence*). Coastal tidal amplitudes and patterns are projected to change due to sea level rise and coastal adaptation measures (*very likely*). Projected changes in waves arising from changes in weather patterns, and changes in tides due to sea level rise, can locally enhance or ameliorate coastal hazards (*medium confidence*). {6.3.1, 5.2.2}

B.3.6   The average intensity of tropical cyclones, the proportion of Category 4 and 5 tropical cyclones and the associated average precipitation rates are projected to increase for a 2°C global temperature rise above any baseline period (*medium confidence*). Rising mean sea levels will contribute to higher extreme sea levels associated with tropical cyclones (*very high confidence*). Coastal hazards will be exacerbated by an increase in the average intensity, magnitude of storm surge and precipitation rates of tropical cyclones. There are greater increases projected under RCP8.5 than under RCP2.6 from around mid-century to 2100 (*medium confidence*). There is *low confidence* in changes in the future frequency of tropical cyclones at the global scale. {6.3.1}

Projected Risks for Ecosystems

B.4   **Future land cryosphere changes will continue to alter terrestrial and freshwater ecosystems in high mountain and polar regions with major shifts in species distributions resulting in changes in ecosystem structure and functioning, and eventual loss of globally unique biodiversity (*medium confidence*). Wildfire is projected to increase significantly for the rest of this century across most tundra and boreal regions, and also in some mountain regions (*medium confidence*). {2.3.3, Box 3.4, 3.4.3}**

B.4.1   In high mountain regions, further upslope migration by lower-elevation species, range contractions, and increased mortality will lead to population declines of many alpine species, especially glacier- or snow-dependent species (*high confidence*), with local and eventual global species loss (*medium confidence*). The persistence of alpine species and sustaining ecosystem services depends on appropriate conservation and adaptation measures (*high confidence*). {2.3.3}

B.4.2   On Arctic land, a loss of globally unique biodiversity is projected as limited refugia exist for some High-Arctic species and hence they are outcompeted by more temperate species (*medium confidence*). Woody shrubs and trees are projected to expand to cover 24–52% of Arctic tundra by 2050 (*medium confidence*). The boreal forest is projected to expand at its northern edge, while diminishing at its southern edge where it is replaced by lower biomass woodland/shrublands (*medium confidence*). {3.4.3, Box 3.4}

B.4.3   Permafrost thaw and decrease in snow will affect Arctic and mountain hydrology and wildfire, with impacts on vegetation and wildlife (*medium confidence)*. About 20% of Arctic land permafrost is vulnerable to abrupt permafrost thaw and ground subsidence, which is projected to increase small lake area by over 50% by 2100 for RCP8.5 (*medium confidence*). Even as the overall regional water cycle is projected to intensify, including increased precipitation, evapotranspiration, and river discharge to the Arctic Ocean, decreases in snow and permafrost may lead to soil drying with consequences for ecosystem productivity and disturbances (*medium confidence*). Wildfire is projected to increase for the rest of this century across most tundra and boreal regions, and also in some mountain regions, while interactions between climate and shifting vegetation will influence future fire intensity and frequency (*medium confidence*). {2.3.3, 3.4.1, 3.4.2, 3.4.3, SPM B.1}

B.5   **A decrease in global biomass of marine animal communities, their production, and fisheries catch potential, and a shift in species composition are projected over the 21st century in ocean ecosystems from the surface to the deep seafloor under all emission scenarios (*medium confidence*). The rate and magnitude of decline are projected to be highest in the tropics (*high confidence*), whereas impacts remain diverse in polar regions (*medium confidence*) and increase for high emissions scenarios. Ocean acidification (*medium confidence*), oxygen loss (*medium confidence*) and reduced sea ice extent (*medium confidence*) as well as non-climatic human activities (*medium confidence*) have the potential to exacerbate these warming-induced ecosystem impacts. {3.2.3, 3.3.3, 5.2.2, 5.2.3, 5.2.4, 5.4.1, Figure SPM.3}**

B.5.1   Projected ocean warming and changes in net primary production alter biomass, production and community structure of marine ecosystems. The global-scale biomass of marine animals across the foodweb is projected to decrease by 15.0 ± 5.9% (*very likely* range) and the maximum catch potential of fisheries by 20.5–24.1% by the end of the 21st century relative to 1986–2005 under RCP8.5 (*medium confidence*). These changes are projected to be *very likely* three to four times larger under RCP8.5 than RCP2.6. {3.2.3, 3.3.3, 5.2.2, 5.2.3, 5.4.1, Figure SPM.3}

B.5.2   Under enhanced stratification reduced nutrient supply is projected to cause tropical ocean net primary production to decline by 7–16% (*very likely* range) for RCP8.5 by 2081–2100 (*medium confidence*). In tropical regions, marine animal biomass and production are projected to decrease more than the global average under all emissions scenarios in the 21st century (*high confidence*). Warming and sea ice changes are projected to increase marine net primary production in the Arctic (*medium confidence*) and around Antarctica (*low confidence*), modified by changing nutrient supply due to shifts in upwelling and stratification. Globally, the sinking flux of organic matter from the upper ocean is projected to decrease, linked largely due to changes in net primary production (*high confidence*). As a result, 95% or more of the deep sea (3000–6000 m depth) seafloor area and cold-water coral ecosystems are projected to experience declines in benthic biomass under RCP8.5 (*medium confidence*). {3.2.3, 5.2.2. 5.2.4, Figure SPM.1}

B.5.3   Warming, ocean acidification, reduced seasonal sea ice extent and continued loss of multi-year sea ice are projected to impact polar marine ecosystems through direct and indirect effects on habitats, populations and their viability (*medium confidence*). The geographical range of Arctic marine species, including marine mammals, birds and fish is projected to contract, while the range of some sub-Arctic fish communities is projected to expand, further increasing pressure on high-Arctic species (*medium confidence*). In the Southern Ocean, the habitat of Antarctic krill, a key prey species for penguins, seals and whales, is projected to contract southwards under both RCP2.6 and RCP8.5 (*medium confidence*). {3.2.2, 3.2.3, 5.2.3}

B.5.4   Ocean warming, oxygen loss, acidification and a decrease in flux of organic carbon from the surface to the deep ocean are projected to harm habitat-forming cold-water corals, which support high biodiversity, partly through decreased calcification, increased dissolution of skeletons, and bioerosion (*medium confidence*). Vulnerability and risks are highest where and when temperature and oxygen conditions both reach values outside species' tolerance ranges (*medium confidence*). {Box 5.2, Figure SPM.3}

Projected changes, impacts and risks for ocean ecosystems as a result of climate change

(a) Simulated net primary production

RCP2.6   RCP8.5

Value in mol C m^{-2} yr^{-1} (1986–2005)

0   10   20   >25

(b) Simulated total animal biomass

Value in normalized index (1986–2005)

0   0.5   1   > 3

(c) Maximum fisheries catch potential

Observed values in tonnes* (1986–2005)

0   0.15   55   >275,000

* See figure caption for details

Percent change
Average by 2081–2100, relative to 1986–2005

model disagreement

no data

<—50   −40   −30   −20   −10   0   10   20   30   40   >50

(d) Impacts and risks to ocean ecosystems from climate change

Global mean sea surface temperature (SST) change relative to pre-industrial levels (°C)

Global mean surface temperature (GMST) change relative to pre-industrial levels (°C)

present day

Warm water corals | Kelp forests | Seagrass meadows | Epipelagic** | Rocky shores | Salt marshes | Cold water corals | Estuaries | Sandy beaches | Mangrove forests | Abyssal plains

Level of added impacts/risks

— **Very high** —— **Purple:** Very high probability of severe impacts/risks and the presence of significant irreversibility or the persistence of climate-related hazards, combined with persistence of climate-related hazards, combined with limited ability to adapt due to the nature of the hazard or impacts/risks.

— **High** —— **Red:** Significant and widespread impacts/risks.

— **Moderate** —— **Yellow:** Impacts/risks are detectable and attributable to climate change with at least medium confidence.

— **Undetectable** —— **White:** Impacts/risks are undetectable.

Confidence level for transition

•••• = Very high
••• = High
•• = Medium
• = Low
| = Transition range

**see figure caption for definition

Figure SPM.3 | Projected changes, impacts and risks for ocean regions and ecosystems.

SPM

Figure SPM.3 (continued): **(a)** depth integrated net primary production (NPP from CMIP5[27]), **(b)** total animal biomass (depth integrated, including fishes and invertebrates from FISHMIP[28]), **(c)** maximum fisheries catch potential and **(d)** impacts and risks for coastal and open ocean ecosystems. The three left panels represent the simulated (a,b) and observed (c) mean values for the recent past (1986–2005), the middle and right panels represent projected changes (%) by 2081–2100 relative to recent past under low (RCP2.6) and high (RCP8.5) greenhouse gas emissions scenario {Box SPM.1}, respectively. Total animal biomass in the recent past (b, left panel) represents the projected total animal biomass by each spatial pixel relative to the global average. (c) *Average observed fisheries catch in the recent past (based on data from the Sea Around Us global fisheries database); projected changes in maximum fisheries catch potential in shelf seas are based on the average outputs from two fisheries and marine ecosystem models. To indicate areas of model inconsistency, shaded areas represent regions where models disagree in the direction of change for more than: (a) and (b) 3 out of 10 model projections, and (c) one out of two models. Although unshaded, the projected change in the Arctic and Antarctic regions in (b) total animal biomass and (c) fisheries catch potential have *low confidence* due to uncertainties associated with modelling multiple interacting drivers and ecosystem responses. Projections presented in (b) and (c) are driven by changes in ocean physical and biogeochemical conditions e.g., temperature, oxygen level, and net primary production projected from CMIP5 Earth system models. **The epipelagic refers to the uppermost part of the ocean with depth <200 m from the surface where there is enough sunlight to allow photosynthesis. (d) Assessment of risks for coastal and open ocean ecosystems based on observed and projected climate impacts on ecosystem structure, functioning and biodiversity. Impacts and risks are shown in relation to changes in Global Mean Surface Temperature (GMST) relative to pre-industrial level. Since assessments of risks and impacts are based on global mean Sea Surface Temperature (SST), the corresponding SST levels are shown[29]. The assessment of risk transitions is described in Chapter 5 Sections 5.2, 5.3, 5.2.5 and 5.3.7 and Supplementary Materials SM5.3, Table SM5.6, Table SM5.8 and other parts of the underlying report. The figure indicates assessed risks at approximate warming levels and increasing climate-related hazards in the ocean: ocean warming, acidification, deoxygenation, increased density stratification, changes in carbon fluxes, sea level rise, and increased frequency and/or intensity of extreme events. The assessment considers the natural adaptive capacity of the ecosystems, their exposure and vulnerability. Impact and risk levels do not consider risk reduction strategies such as human interventions, or future changes in non-climatic drivers. Risks for ecosystems were assessed by considering biological, biogeochemical, geomorphological and physical aspects. Higher risks associated with compound effects of climate hazards include habitat and biodiversity loss, changes in species composition and distribution ranges, and impacts/risks on ecosystem structure and functioning, including changes in animal/plant biomass and density, productivity, carbon fluxes, and sediment transport. As part of the assessment, literature was compiled and data extracted into a summary table. A multi-round expert elicitation process was undertaken with independent evaluation of threshold judgement, and a final consensus discussion. Further information on methods and underlying literature can be found in Chapter 5, Sections 5.2 and 5.3 and Supplementary Material. {3.2.3, 3.2.4, 5.2, 5.3, 5.2.5, 5.3.7, SM5.6, SM5.8, Figure 5.16, Cross Chapter Box 1 in Chapter 1 Table CCB1}

B.6   **Risks of severe impacts on biodiversity, structure and function of coastal ecosystems are projected to be higher for elevated temperatures under high compared to low emissions scenarios in the 21st century and beyond. Projected ecosystem responses include losses of species habitat and diversity, and degradation of ecosystem functions. The capacity of organisms and ecosystems to adjust and adapt is higher at lower emissions scenarios (*high confidence*). For sensitive ecosystems such as seagrass meadows and kelp forests, high risks are projected if global warming exceeds 2°C above pre-industrial temperature, combined with other climate-related hazards (*high confidence*). Warm-water corals are at high risk already and are projected to transition to very high risk even if global warming is limited to 1.5°C (*very high confidence*). {4.3.3, 5.3, 5.5, Figure SPM.3}**

B.6.1   All coastal ecosystems assessed are projected to face increasing risk level, from moderate to high risk under RCP2.6 to high to very high risk under RCP8.5 by 2100. Intertidal rocky shore ecosystems are projected to be at very high risk by 2100 under RCP8.5 (*medium confidence*) due to exposure to warming, especially during marine heatwaves, as well as to acidification, sea level rise, loss of calcifying species and biodiversity (*high confidence*). Ocean acidification challenges these ecosystems and further limits their habitat suitability (*medium confidence*) by inhibiting recovery through reduced calcification and enhanced bioerosion. The decline of kelp forests is projected to continue in temperate regions due to warming, particularly under the projected intensification of marine heatwaves, with high risk of local extinctions under RCP8.5 (*medium confidence*). {5.3, 5.3.5, 5.3.6, 5.3.7, 6.4.2, Figure SPM.3}

B.6.2   Seagrass meadows and saltmarshes and associated carbon stores are at moderate risk at 1.5°C global warming and increase with further warming (*medium confidence).* Globally, 20–90% of current coastal wetlands are projected to be lost by 2100, depending on projected sea level rise, regional differences and wetland types, especially where vertical growth is already constrained by reduced sediment supply and landward migration is constrained by steep topography or human modification of shorelines (*high confidence*). {4.3.3, 5.3.2, Figure SPM.3, SPM A.6.1}

---

[27]   NPP is estimated from the Coupled Models Intercomparison Project 5 (CMIP5).

[28]   Total animal biomass is from the Fisheries and Marine Ecosystem Models Intercomparison Project (FISHMIP).

[29]   The conversion between GMST and SST is based on a scaling factor of 1.44 derived from changes in an ensemble of RCP8.5 simulations; this scaling factor has an uncertainty of about 4% due to differences between the RCP2.6 and RCP8.5 scenarios. {Table SPM.1}

B.6.3   Ocean warming, sea level rise and tidal changes are projected to expand salinization and hypoxia in estuaries (*high confidence*) with high risks for some biota leading to migration, reduced survival, and local extinction under high emission scenarios (*medium confidence*). These impacts are projected to be more pronounced in more vulnerable eutrophic and shallow estuaries with low tidal range in temperate and high latitude regions (*medium confidence*). {5.2.2, 5.3.1, Figure SPM.3}

B.6.4   Almost all warm-water coral reefs are projected to suffer significant losses of area and local extinctions, even if global warming is limited to 1.5°C (*high confidence*). The species composition and diversity of remaining reef communities is projected to differ from present-day reefs (*very high confidence*). {5.3.4, 5.4.1, Figure SPM.3}

Projected Risks for People and Ecosystem Services

B.7   Future cryosphere changes on land are projected to affect water resources and their uses, such as hydropower (*high confidence*) and irrigated agriculture in and downstream of high mountain areas (*medium confidence*), as well as livelihoods in the Arctic (*medium confidence*). Changes in floods, avalanches, landslides, and ground destabilization are projected to increase risk for infrastructure, cultural, tourism, and recreational assets (*medium confidence*). {2.3, 2.3.1, 3.4.3}

B.7.1   Disaster risks to human settlements and livelihood options in high mountain areas and the Arctic are expected to increase (*medium confidence*), due to future changes in hazards such as floods, fires, landslides, avalanches, unreliable ice and snow conditions, and increased exposure of people and infrastructure (*high confidence*). Current engineered risk reduction approaches are projected to be less effective as hazards change in character (*medium confidence*). Significant risk reduction and adaptation strategies help avoid increased impacts from mountain flood and landslide hazards as exposure and vulnerability are increasing in many mountain regions during this century (*high confidence*). {2.3.2, 3.4.3, 3.5.2}

B.7.2   Permafrost thaw-induced subsidence of the land surface is projected to impact overlying urban and rural communication and transportation infrastructure in the Arctic and in high mountain areas (*medium confidence*). The majority of Arctic infrastructure is located in regions where permafrost thaw is projected to intensify by mid-century. Retrofitting and redesigning infrastructure has the potential to halve the costs arising from permafrost thaw and related climate-change impacts by 2100 (*medium confidence*). {2.3.4, 3.4.1, 3.4.3}

B.7.3   High mountain tourism, recreation and cultural assets are projected to be negatively affected by future cryospheric changes (*high confidence*). Current snowmaking technologies are projected to be less effective in reducing risks to ski tourism in a warmer climate in most parts of Europe, North America, and Japan, in particular at 2°C global warming and beyond (*high confidence*). {2.3.5, 2.3.6}

B.8   Future shifts in fish distribution and decreases in their abundance and fisheries catch potential due to climate change are projected to affect income, livelihoods, and food security of marine resource-dependent communities (*medium confidence*). Long-term loss and degradation of marine ecosystems compromises the ocean's role in cultural, recreational, and intrinsic values important for human identity and well-being (*medium confidence*). {3.2.4, 3.4.3, 5.4.1, 5.4.2, 6.4}

B.8.1   Projected geographical shifts and decreases of global marine animal biomass and fish catch potential are more pronounced under RCP8.5 relative to RCP2.6 elevating the risk for income and livelihoods of dependent human communities, particularly in areas that are economically vulnerable (*medium confidence*). The projected redistribution of resources and abundance increases the risk of conflicts among fisheries, authorities or communities (*medium confidence*). Challenges to fisheries governance are widespread under RCP8.5 with regional hotspots such as the Arctic and tropical Pacific Ocean (*medium confidence*). {3.5.2, 5.4.1, 5.4.2, 5.5.2, 5.5.3, 6.4.2, Figure SPM.3}

B.8.2   The decline in warm-water coral reefs is projected to greatly compromise the services they provide to society, such as food provision (*high confidence*), coastal protection (*high confidence*) and tourism (*medium confidence*). Increases in the risks for seafood security (*medium confidence*) associated with decreases in seafood availability are projected to elevate the risk to nutritional health in some communities highly dependent on seafood (*medium confidence*), such as those in the Arctic, West Africa, and Small Island Developing States. Such impacts compound any risks from other shifts in diets and food systems caused by social and economic changes and climate change over land (*medium confidence*). {3.4.3, 5.4.2, 6.4.2}

B.8.3   Global warming compromises seafood safety (*medium confidence*) through human exposure to elevated bioaccumulation of persistent organic pollutants and mercury in marine plants and animals (*medium confidence*), increasing prevalence of waterborne *Vibrio* pathogens (*medium confidence*), and heightened likelihood of harmful algal blooms (*medium confidence*). These risks are projected to be particularly large for human communities with high consumption of seafood, including coastal Indigenous communities (*medium confidence*), and for economic sectors such as fisheries, aquaculture, and tourism (*high confidence*). {3.4.3, 5.4.2, Box 5.3}

B.8.4   Climate change impacts on marine ecosystems and their services put key cultural dimensions of lives and livelihoods at risk (*medium confidence*), including through shifts in the distribution or abundance of harvested species and diminished access to fishing or hunting areas. This includes potentially rapid and irreversible loss of culture and local knowledge and Indigenous knowledge, and negative impacts on traditional diets and food security, aesthetic aspects, and marine recreational activities (*medium confidence*). {3.4.3, 3.5.3, 5.4.2}

B.9 **Increased mean and extreme sea level, alongside ocean warming and acidification, are projected to exacerbate risks for human communities in low-lying coastal areas (*high confidence*). In Arctic human communities without rapid land uplift, and in urban atoll islands, risks are projected to be moderate to high even under a low emissions scenario (RCP2.6) (*medium confidence*), including reaching adaptation limits (*high confidence*). Under a high emissions scenario (RCP8.5), delta regions and resource rich coastal cities are projected to experience moderate to high risk levels after 2050 under current adaptation (*medium confidence*). Ambitious adaptation including transformative governance is expected to reduce risk (*high confidence*), but with context-specific benefits. {4.3.3, 4.3.4, SM4.3, 6.9.2, Cross-Chapter Box 9, Figure SPM.5}**

B.9.1   In the absence of more ambitious adaptation efforts compared to today, and under current trends of increasing exposure and vulnerability of coastal communities, risks, such as erosion and land loss, flooding, salinization, and cascading impacts due to mean sea level rise and extreme events are projected to significantly increase throughout this century under all greenhouse gas emissions scenarios (*very high confidence*). Under the same assumptions, annual coastal flood damages are projected to increase by 2–3 orders of magnitude by 2100 compared to today (*high confidence*). {4.3.3, 4.3.4, Box 6.1, 6.8, SM.4.3, Figures SPM.4, SPM.5}

B.9.2   High to very high risks are approached for vulnerable communities in coral reef environments, urban atoll islands and low-lying Arctic locations from sea level rise well before the end of this century in case of high emissions scenarios. This entails adaptation limits being reached, which are the points at which an actor's objectives (or system needs) cannot be secured from intolerable risks through adaptive actions (*high confidence*). Reaching adaptation limits (e.g., biophysical, geographical, financial, technical, social, political, and institutional) depends on the emissions scenario and context-specific risk tolerance, and is projected to expand to more areas beyond 2100, due to the long-term commitment of sea level rise (*medium confidence*). Some island nations are *likely* to become uninhabitable due to climate-related ocean and cryosphere change (*medium confidence*), but habitability thresholds remain extremely difficult to assess. {4.3.4, 4.4.2, 4.4.3, 5.5.2, Cross-Chapter Box 9, SM.4.3, SPM C.1, Glossary, Figure SPM.5}

B.9.3   Globally, a slower rate of climate-related ocean and cryosphere change provides greater adaptation opportunities (*high confidence*). While there is *high confidence* that ambitious adaptation, including governance for transformative change, has the potential to reduce risks in many locations, such benefits can vary between locations. At global scale, coastal protection can reduce flood risk by 2–3 orders of magnitude during the 21st century, but depends on investments on the order of tens to several hundreds of billions of US$ per year (*high confidence*). While such investments are generally cost efficient for densely populated urban areas, rural and poorer areas may be challenged to afford such investments with relative annual costs for some small island states amounting to several percent of GDP (*high confidence*). Even with major adaptation efforts, residual risks and associated losses are projected to occur (*medium confidence*), but context-specific limits to adaptation and residual risks remain difficult to assess. {4.1.3, 4.2.2.4, 4.3.1, 4.3.2, 4.3.4., 4.4.3, 6.9.1, 6.9.2, Cross-Chapter Boxes 1–2 in Chapter 1, SM.4.3, Figure SPM.5}

Extreme sea level events

Due to projected global mean sea level (GMSL) rise, local sea levels that historically occurred once per century (historical centennial events, HCEs) are projected to become at least annual events at most locations during the 21st century. The height of a HCE varies widely, and depending on the level of exposure can already cause severe impacts. Impacts can continue to increase with rising frequency of HCEs.

(a) Schematic effect of regional sea level rise on projected extreme sea level events (not to scale)

(b) Year when HCEs are projected to recur once per year on average

(c) Difference between RCP8.5 and RCP2.6

The difference map shows locations where the HCE becomes annual at least 10 years later under RCP2.6 than under RCP8.5.
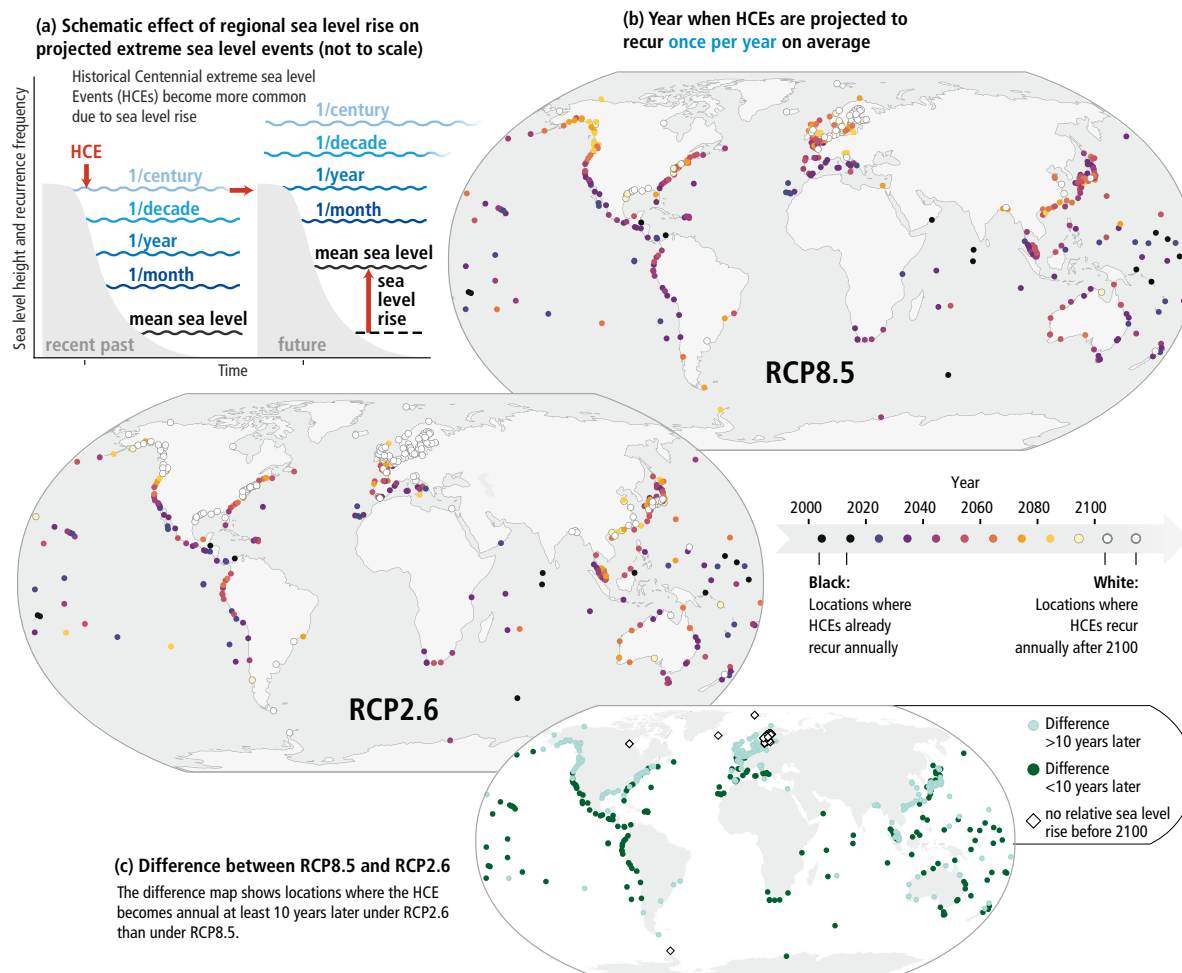
Figure SPM.4 | The effect of regional sea level rise on extreme sea level events at coastal locations. **(a)** Schematic illustration of extreme sea level events and their average recurrence in the recent past (1986–2005) and the future. As a consequence of mean sea level rise, local sea levels that historically occurred once per century (historical centennial events, HCEs) are projected to recur more frequently in the future. **(b)** The year in which HCEs are expected to recur once per year on average under RCP8.5 and RCP2.6, at the 439 individual coastal locations where the observational record is sufficient. The absence of a circle indicates an inability to perform an assessment due to a lack of data but does not indicate absence of exposure and risk. The darker the circle, the earlier this transition is expected. The *likely* range is ±10 years for locations where this transition is expected before 2100. White circles (33% of locations under RCP2.6 and 10% under RCP8.5) indicate that HCEs are not expected to recur once per year before 2100. **(c)** An indication at which locations this transition of HCEs to annual events is projected to occur more than 10 years later under RCP2.6 compared to RCP8.5. As the scenarios lead to small differences by 2050 in many locations results are not shown here for RCP4.5 but they are available in Chapter 4. {4.2.3, Figure 4.10, Figure 4.12}

C. Implementing Responses to Ocean and Cryosphere Change

Challenges

C.1 **Impacts of climate-related changes in the ocean and cryosphere increasingly challenge current governance efforts to develop and implement adaptation responses from local to global scales, and in some cases pushing them to their limits. People with the highest exposure and vulnerability are often those with lowest capacity to respond (*high confidence*). {1.5, 1.7, Cross-Chapter Boxes 2–3 in Chapter 1, 2.3.1, 2.3.2, 2.3.3, 2.4, 3.2.4, 3.4.3, 3.5.2, 3.5.3, 4.1, 4.3.3, 4.4.3, 5.5.2, 5.5.3, 6.9}**

C.1.1 The temporal scales of climate change impacts in ocean and cryosphere and their societal consequences operate on time horizons which are longer than those of governance arrangements (e.g., planning cycles, public and corporate decision making cycles, and financial instruments). Such temporal differences challenge the ability of societies to adequately prepare for and respond to long-term changes including shifts in the frequency and intensity of extreme events (*high confidence*). Examples include changing landslides and floods in high mountain regions and risks to important species and ecosystems in the Arctic, as well as to low-lying nations and islands, small island nations, other coastal regions and to coral reef ecosystems. {2.3.2, 3.5.2, 3.5.4, 4.4.3, 5.2, 5.3, 5.4, 5.5.1, 5.5.2, 5.5.3, 6.9}

C.1.2 Governance arrangements (e.g., marine protected areas, spatial plans and water management systems) are, in many contexts, too fragmented across administrative boundaries and sectors to provide integrated responses to the increasing and cascading risks from climate-related changes in the ocean and/or cryosphere (*high confidence*). The capacity of governance systems in polar and ocean regions to respond to climate change impacts has strengthened recently, but this development is not sufficiently rapid or robust to adequately address the scale of increasing projected risks (*high confidence*). In high mountains, coastal regions and small islands, there are also difficulties in coordinating climate adaptation responses, due to the many interactions of climatic and non-climatic risk drivers (such as inaccessibility, demographic and settlement trends, or land subsidence caused by local activities) across scales, sectors and policy domains (*high confidence*). {2.3.1, 3.5.3, 4.4.3, 5.4.2, 5.5.2, 5.5.3, Box 5.6, 6.9, Cross-Chapter Box 3 in Chapter 1}

C.1.3 There are a broad range of identified barriers and limits for adaptation to climate change in ecosystems (*high confidence*). Limitations include the space that ecosystems require, non-climatic drivers and human impacts that need to be addressed as part of the adaptation response, the lowering of adaptive capacity of ecosystems because of climate change, and the slower ecosystem recovery rates relative to the recurrence of climate impacts, availability of technology, knowledge and financial support, and existing governance arrangements (*medium confidence*). {3.5.4, 5.5.2}

C.1.4 Financial, technological, institutional and other barriers exist for implementing responses to current and projected negative impacts of climate-related changes in the ocean and cryosphere, impeding resilience building and risk reduction measures (*high confidence*). Whether such barriers reduce adaptation effectiveness or correspond to adaptation limits depends on context specific circumstances, the rate and scale of climate changes and on the ability of societies to turn their adaptive capacity into effective adaptation responses. Adaptive capacity continues to differ between as well as within communities and societies (*high confidence*). People with highest exposure and vulnerability to current and future hazards from ocean and cryosphere changes are often also those with lowest adaptive capacity, particularly in low-lying islands and coasts, Arctic and high mountain regions with development challenges (*high confidence*). {2.3.1, 2.3.2, 2.3.7, Box 2.4, 3.5.2, 4.3.4, 4.4.2, 4.4.3, 5.5.2, 6.9, Cross-Chapter Boxes 2 and 3 in Chapter 1, Cross-Chapter Box 9}

Strengthening Response Options

C.2   The far-reaching services and options provided by ocean and cryosphere-related ecosystems can be supported by protection, restoration, precautionary ecosystem-based management of renewable resource use, and the reduction of pollution and other stressors (*high confidence*). Integrated water management (*medium confidence*) and ecosystem-based adaptation (*high confidence*) approaches lower climate risks locally and provide multiple societal benefits. However, ecological, financial, institutional and governance constraints for such actions exist (*high confidence*), and in many contexts ecosystem-based adaptation will only be effective under the lowest levels of warming (*high confidence*). {2.3.1, 2.3.3, 3.2.4, 3.5.2, 3.5.4, 4.4.2, 5.2.2, 5.4.2, 5.5.1, 5.5.2, Figure SPM.5}

C.2.1   Networks of protected areas help maintain ecosystem services, including carbon uptake and storage, and enable future ecosystem-based adaptation options by facilitating the poleward and altitudinal movements of species, populations, and ecosystems that occur in response to warming and sea level rise (*medium confidence*). Geographic barriers, ecosystem degradation, habitat fragmentation and barriers to regional cooperation limit the potential for such networks to support future species range shifts in marine, high mountain and polar land regions (*high confidence*). {2.3.3, 3.2.3, 3.3.2, 3.5.4, 5.5.2, Box 3.4}

C.2.2   Terrestrial and marine habitat restoration, and ecosystem management tools such as assisted species relocation and coral gardening, can be locally effective in enhancing ecosystem-based adaptation (*high confidence*). Such actions are most successful when they are community-supported, are science-based whilst also using local knowledge and Indigenous knowledge, have long-term support that includes the reduction or removal of non-climatic stressors, and under the lowest levels of warming (*high confidence*). For example, coral reef restoration options may be ineffective if global warming exceeds 1.5°C, because corals are already at high risk (*very high confidence*) at current levels of warming. {2.3.3, 4.4.2, 5.3.7, 5.5.1, 5.5.2, Box 5.5, Figure SPM.3}

C.2.3   Strengthening precautionary approaches, such as rebuilding overexploited or depleted fisheries, and responsiveness of existing fisheries management strategies reduces negative climate change impacts on fisheries, with benefits for regional economies and livelihoods (*medium confidence*). Fisheries management that regularly assesses and updates measures over time, informed by assessments of future ecosystem trends, reduces risks for fisheries (*medium confidence*) but has limited ability to address ecosystem change. {3.2.4, 3.5.2, 5.4.2, 5.5.2, 5.5.3, Figure SPM.5}

C.2.4   Restoration of vegetated coastal ecosystems, such as mangroves, tidal marshes and seagrass meadows (coastal 'blue carbon' ecosystems), could provide climate change mitigation through increased carbon uptake and storage of around 0.5% of current global emissions annually (*medium confidence*). Improved protection and management can reduce carbon emissions from these ecosystems. Together, these actions also have multiple other benefits, such as providing storm protection, improving water quality, and benefiting biodiversity and fisheries (*high confidence*). Improving the quantification of carbon storage and greenhouse gas fluxes of these coastal ecosystems will reduce current uncertainties around measurement, reporting and verification (*high confidence*). {Box 4.3, 5.4, 5.5.1, 5.5.2, Annex I: Glossary}

C.2.5   Ocean renewable energy can support climate change mitigation, and can comprise energy extraction from offshore winds, tides, waves, thermal and salinity gradient and algal biofuels. The emerging demand for alternative energy sources is expected to generate economic opportunities for the ocean renewable energy sector (*high confidence*), although their potential may also be affected by climate change (*low confidence*). {5.4.2, 5.5.1, Figure 5.23}

C.2.6   Integrated water management approaches across multiple scales can be effective at addressing impacts and leveraging opportunities from cryosphere changes in high mountain areas. These approaches also support water resource management through the development and optimization of multi-purpose storage and release of water from reservoirs (*medium confidence*), with consideration of potentially negative impacts to ecosystems and communities. Diversification of tourism activities throughout the year supports adaptation in high mountain economies (*medium confidence*). {2.3.1, 2.3.5}

C.3   Coastal communities face challenging choices in crafting context-specific and integrated responses to sea level rise that balance costs, benefits and trade-offs of available options and that can be adjusted over time (*high confidence*). All types of options, including protection, accommodation, ecosystem-based adaptation, coastal advance and retreat, wherever possible, can play important roles in such integrated responses (*high confidence*). {4.4.2, 4.4.3, 4.4.4, 6.9.1, Cross-Chapter Box 9, Figure SPM.5}

C.3.1   The higher the sea levels rise, the more challenging is coastal protection, mainly due to economic, financial and social barriers rather than due to technical limits (*high confidence*). In the coming decades, reducing local drivers of exposure and vulnerability such as coastal urbanization and human-induced subsidence constitute effective responses (*high confidence*). Where space is limited, and the value of exposed assets is high (e.g., in cities), hard protection (e.g., dikes) is *likely* to be a cost-efficient response option during the 21st century taking into account the specifics of the context (*high confidence*), but resource-limited areas may not be able to afford such investments. Where space is available, ecosystem-based adaptation can reduce coastal risk and provide multiple other benefits such as carbon storage, improved water quality, biodiversity conservation and livelihood support (*medium confidence*). {4.3.2, 4.4.2, Box 4.1, Cross-Chapter Box 9, Figure SPM.5}

C.3.2   Some coastal accommodation measures, such as early warning systems and flood-proofing of buildings, are often both low cost and highly cost-efficient under current sea levels (*high confidence*). Under projected sea level rise and increase in coastal hazards some of these measures become less effective unless combined with other measures (*high confidence*). All types of options, including protection, accommodation, ecosystem-based adaptation, coastal advance and planned relocation, if alternative localities are available, can play important roles in such integrated responses (*high confidence*). Where the community affected is small, or in the aftermath of a disaster, reducing risk by coastal planned relocations is worth considering if safe alternative localities are available. Such planned relocation can be socially, culturally, financially and politically constrained (*very high confidence*). {4.4.2, Box 4.1, Cross-Chapter Box 9, SPM B.3}

C.3.3   Responses to sea level rise and associated risk reduction present society with profound governance challenges, resulting from the uncertainty about the magnitude and rate of future sea level rise, vexing trade-offs between societal goals (e.g., safety, conservation, economic development, intra- and inter-generational equity), limited resources, and conflicting interests and values among diverse stakeholders (*high confidence*). These challenges can be eased using locally appropriate combinations of decision analysis, land-use planning, public participation, diverse knowledge systems and conflict resolution approaches that are adjusted over time as circumstances change (*high confidence*). {Cross-Chapter Box 5 in Chapter 1, 4.4.3, 4.4.4, 6.9}

C.3.4   Despite the large uncertainties about the magnitude and rate of post 2050 sea level rise, many coastal decisions with time horizons of decades to over a century are being made now (e.g., critical infrastructure, coastal protection works, city planning) and can be improved by taking relative sea level rise into account, favouring flexible responses (i.e., those that can be adapted over time) supported by monitoring systems for early warning signals, periodically adjusting decisions (i.e., adaptive decision making), using robust decision-making approaches, expert judgement, scenario-building, and multiple knowledge systems (*high confidence*). The sea level rise range that needs to be considered for planning and implementing coastal responses depends on the risk tolerance of

stakeholders. Stakeholders with higher risk tolerance (e.g., those planning for investments that can be very easily adapted to unforeseen conditions) often prefer to use the *likely* range of projections, while stakeholders with a lower risk tolerance (e.g., those deciding on critical infrastructure) also consider global and local mean sea level above the upper end of the *likely* range (globally 1.1 m under RCP8.5 by 2100) and from methods characterised by lower confidence such as from expert elicitation. {1.8.1, 1.9.2, 4.2.3, 4.4.4, Figure 4.2, Cross-Chapter Box 5 in Chapter 1, Figure SPM.5, SPM B.3}

Sea level rise risk and responses

The term response is used here instead of adaptation because some responses, such as retreat, may or may not be considered to be adaptation.

(a) Risk in 2100 under different sea level rise and response scenarios

Risk for illustrative geographies based on mean sea level changes *(medium confidence)*
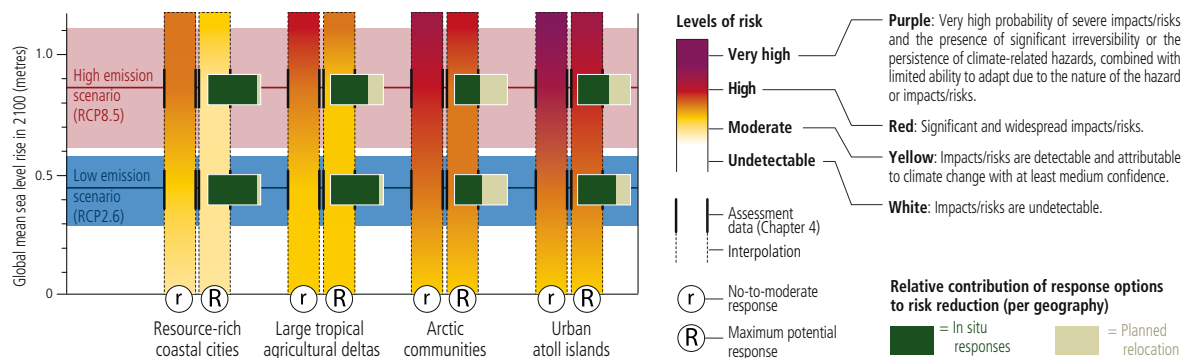
In this assessment, the term response refers to in situ responses to sea level rise (hard engineered coastal defenses, restoration of degraded ecosystems, subsidence limitation) and planned relocation. Planned relocation in this assessment refers to proactive managed retreat or resettlement only at a local scale, and according to the specificities of a particular context (e.g., in urban atoll islands: within the island, in a neighbouring island or in artificially raised islands). Forced displacement and international migration are not considered in this assessment.

The illustrative geographies are based on a limited number of case studies well covered by the peer reviewed literature. The realisation of risk will depend on context specificities.

Sea level rise scenarios: RCP4.5 and RCP6.0 are not considered in this risk assessment because the literature underpinning this assessment is only available for RCP2.6 and RCP8.5.

(b) Benefits of responses to sea level rise and mitigation
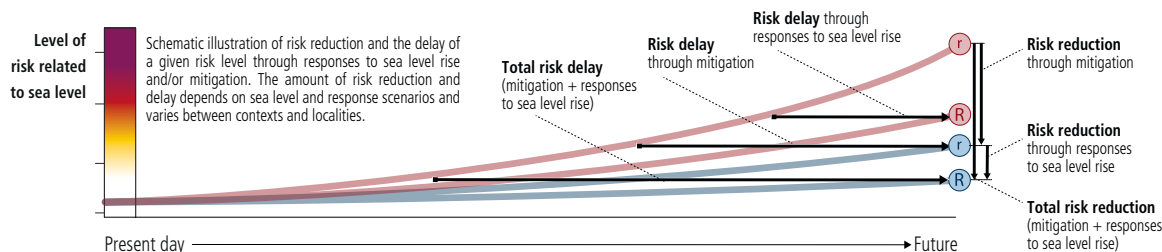
Figure SPM.5 | a, b

(c) Responses to rising mean and extreme sea levels

The table illustrates responses and their characteristics. It is not exhaustive. Whether a response is applicable depends on geography and context.

Confidence levels (assessed for effectiveness): ●●●● = Very High   ●●●= High   ●● = Medium   ●= Low

Responses		Potential effectiveness in terms of reducing sea level rise (SLR) risks (technical/biophysical limits)	Advantages (beyond risk reduction)	Co–benefits	Drawbacks	Economic efficiency	Governance challenges
Hard protection		Up to multiple metres of SLR {4.4.2.2.4} ●●●	Predictable levels of safety {4.4.2.2.4}	Multifunctional dikes such as for recreation, or other land use {4.4.2.2.5}	Destruction of habitat through coastal squeeze, flooding & erosion downdrift, lock–in, disastrous consequence in case of defence failure {4.3.2.4, 4.4.2.2.5}	High if the value of assets behind protection is high, as found in many urban and densely populated coastal areas {4.4.2.2.7}	Often unaffordable for poorer areas. Conflicts between objectives (e.g., conservation, safety and tourism), conflicts about the distribution of public budgets, lack of finance {4.3.3.2, 4.4.2.2.6}
Sediment– based protection		Effective but depends on sediment availability {4.4.2.2.4} ●●●	High flexibility {4.4.2.2.4}	Preservation of beaches for recreation/tourism {4.4.2.2.5}	Destruction of habitat, where sediment is sourced {4.4.2.2.5}	High if tourism revenues are high {4.4.2.2.7}	Conflicts about the distribution of public budgets {4.4.2.2.6}
Ecosystem based adaptation	**Coral conservation** **Coral restoration**	Effective up to 0.5 cm yr⁻¹ SLR. ●● Strongly limited by ocean warming and acidification. Constrained at 1.5°C warming and lost at 2°C at many places. {4.3.3.5.2, 4.4.2.3.2, 5.3.4} ●●●	Opportunity for community involvement, {4.4.2.3.1}	Habitat gain, biodiversity, carbon sequestration, income from tourism, enhanced fishery productivity, improved water quality. Provision of food, medicine, fuel, wood and cultural benefits {4.4.2.3.5}	Long–term effectiveness depends on ocean warming, acidification and emission scenarios {4.3.3.5.2., 4.4.2.3.2}	Limited evidence on benefit–cost ratios; Depends on population density and the availability of land {4.4.2.3.7}	Permits for implementation are difficult to obtain. Lack of finance. Lack of enforcement of conservation policies. EbA options dismissed due to short–term economic interest, availability of land {4.4.2.3.6}
	Wetland conservation (Marshes, Mangroves)	Effective up to 0.5–1 cm yr⁻¹ SLR, ●● decreased at 2°C {4.3.3.5.1, 4.4.2.3.2, 5.3.7} ●●●			Safety levels less predictable, development benefits not realized {4.4.2.3.5, 4.4.2.3.2}		
	Wetland restoration (Marshes, Mangroves)				Safety levels less predictable, a lot of land required, barriers for landward expan–sion of ecosystems has to be removed {4.4.2.3.5, 4.4.2.3.2}		
Coastal advance		Up to multiple metres of SLR {4.4.2.2.4} ●●●	Predictable levels of safety {4.4.2.2.4}	Generates land and land sale revenues that can be used to finance adaptation {4.4.2.4.5}	Groundwater salinisa–tion, enhanced erosion and loss of coastal ecosystems and habitat {4.4.2.4.5}	Very high if land prices are high as found in many urban coasts {4.4.2.4.7}	Often unaffordable for poorer areas. Social conflicts with regards to access and distribution of new land {4.4.2.4.6}
Coastal accommodation (Flood–proofing buildings, early warning systems for flood events, etc.)		Very effective for small SLR {4.4.2.5.4} ●●●	Mature technology; sediments deposited during floods can raise elevation {4.4.2.5.5}	Maintains landscape connectivity {4.4.2.5.5}	Does not prevent flooding/impacts {4.4.2.5.5}	Very high for early warning systems and building–scale measures {4.4.2.5.7}	Early warning systems require effective insti–tutional arrangements {4.4.2.6.6}
Retreat	**Planned relocation**	Effective if alternative safe localities are available {4.4.2.6.4} ●●●	Sea level risks at origin can be eliminated {4.4.2.6.4}	Access to improved services (health, education, housing), job opportunities and economic growth {4.4.2.6.5}	Loss of social cohesion, cultural identity and well–being. Depressed services (health, education, housing), job opportunities and economic growth {4.4.2.6.5}	Limited evidence [4.4.2.6.7]	Reconciling the divergent interests arising from relocating people from point of origin and destination {4.4.2.6.6}
	Forced displacement	Addresses only immediate risk at place of origin	Not applicable	Not applicable	Range from loss of life to loss of livelihoods and sovereignty {4.4.2.6.5}	Not applicable	Raises complex humanitarian questions on livelihoods, human rights and equity {4.4.2.6.6}

(d) Choosing and enabling sea level rise responses

Generic steps of adaptive decision making

Stage setting → **Dynamic plan** → **Implementation** → **Monitoring and corrective action**

Stage setting
Identify risks, objectives, options, uncertainties and criteria for evaluating options

Dynamic plan
Develop initial plan (combinations of options over time) plus corrective actions to be carried out based on observed situation

Implementation
of initial plan and monitoring system for progressing change and success

Monitoring and corrective action
Monitor and take corrective action upon observed situation

Enabling conditions
- Long–term perspective
- Cross–scale coordination
- Address vulnerability and equity
- Inclusive public participation
- Capability to address complexity

Figure SPM.5 | c, d

Figure SPM.5 | Sea level rise risks and responses. The term response is used here instead of adaptation because some responses, such as retreat, may or may not be considered to be adaptation. **(a)** shows the combined risk of coastal flooding, erosion and salinization for illustrative geographies in 2100, due to changing mean and extreme sea levels under RCP2.6 and RCP8.5 and under two response scenarios. Risks under RCPs 4.5 and 6.0 were not assessed due to a lack of literature for the assessed geographies. The assessment does not account for changes in extreme sea level beyond those directly induced by mean sea level rise; risk levels could increase if other changes in extreme sea levels were considered (e.g., due to changes in cyclone intensity). Panel a) considers a socioeconomic scenario with relatively stable coastal population density over the century. {SM4.3.2} Risks to illustrative geographies have been assessed based on relative sea level changes projected for a set of specific examples: New York City, Shanghai and Rotterdam for resource-rich coastal cities covering a wide range of response experiences; South Tarawa, Fongafale and Male' for urban atoll islands; Mekong and Ganges-Brahmaputra-Meghna for large tropical agricultural deltas; and Bykovskiy, Shishmaref, Kivalina, Tuktoyaktuk and Shingle Point for Arctic communities located in regions remote from rapid glacio-isostatic adjustment. {4.2, 4.3.4, SM4.2} The assessment distinguishes between two contrasting response scenarios. "No-to-moderate response" describes efforts as of today (i.e., no further significant action or new types of actions). "Maximum potential response" represents a combination of responses implemented to their full extent and thus significant additional efforts compared to today, assuming minimal financial, social and political barriers. The assessment has been conducted for each sea level rise and response scenario, as indicated by the burning embers in the figure; in-between risk levels are interpolated. {4.3.3} The assessment criteria include exposure and vulnerability (density of assets, level of degradation of terrestrial and marine buffer ecosystems), coastal hazards (flooding, shoreline erosion, salinization), in-situ responses (hard engineered coastal defenses, ecosystem restoration or creation of new natural buffers areas, and subsidence management) and planned relocation. Planned relocation refers to managed retreat or resettlement as described in Chapter 4, i.e., proactive and local-scale measures to reduce risk by relocating people, assets and infrastructure. Forced displacement is not considered in this assessment. Panel **(a)** also highlights the relative contributions of in-situ responses and planned relocation to the total risk reduction. **(b)** schematically illustrates the risk reduction (vertical arrows) and risk delay (horizontal arrows) through mitigation and/or responses to sea level rise. **(c)** summarizes and assesses responses to sea level rise in terms of their effectiveness, costs, co-benefits, drawbacks, economic efficiency and associated governance challenges. {4.4.2} **(d)** presents generic steps of an adaptive decision-making approach, as well as key enabling conditions for responses to sea level rise. {4.4.4, 4.4.5}

Enabling Conditions

C.4   Enabling climate resilience and sustainable development depends critically on urgent and ambitious emissions reductions coupled with coordinated sustained and increasingly ambitious adaptation actions (*very high confidence*). Key enablers for implementing effective responses to climate-related changes in the ocean and cryosphere include intensifying cooperation and coordination among governing authorities across spatial scales and planning horizons. Education and climate literacy, monitoring and forecasting, use of all available knowledge sources, sharing of data, information and knowledge, finance, addressing social vulnerability and equity, and institutional support are also essential. Such investments enable capacity-building, social learning, and participation in context-specific adaptation, as well as the negotiation of trade-offs and realisation of co-benefits in reducing short-term risks and building long-term resilience and sustainability. (*high confidence*). This report reflects the state of science for ocean and cryosphere for low levels of global warming (1.5°C), as also assessed in earlier IPCC and IPBES reports. {1.1, 1.5, 1.8.3, 2.3.1, 2.3.2, 2.4, Figure 2.7, 2.5, 3.5.2, 3.5.4, 4.4, 5.2.2, Box 5.3, 5.4.2, 5.5.2, 6.4.3, 6.5.3, 6.8, 6.9, Cross-Chapter Box 9, Figure SPM.5}

C.4.1   In light of observed and projected changes in the ocean and cryosphere, many nations will face challenges to adapt, even with ambitious mitigation (*very high confidence*). In a high emissions scenario, many ocean- and cryosphere-dependent communities are projected to face adaptation limits (e.g. biophysical, geographical, financial, technical, social, political and institutional) during the second half of the 21st century. Low emission pathways, for comparison, limit the risks from ocean and cryosphere changes in this century and beyond and enable more effective responses (*high confidence*), whilst also creating co-benefits. Profound economic and institutional transformative change will enable Climate Resilient Development Pathways in the ocean and cryosphere context (*high confidence*). {1.1, 1.4–1.7, Cross-Chapter Boxes 1–3 in Chapter 1, 2.3.1, 2.4, Box 3.2, Figure 3.4, Cross-Chapter Box 7 in Chapter 3, 3.4.3, 4.2.2, 4.2.3, 4.3.4, 4.4.2, 4.4.3, 4.4.6, 5.4.2, 5.5.3, 6.9.2, Cross-Chapter Box 9, Figure SPM.5}

C.4.2   Intensifying cooperation and coordination among governing authorities across scales, jurisdictions, sectors, policy domains and planning horizons can enable effective responses to changes in the ocean, cryosphere and to sea level rise (*high confidence*). Regional cooperation, including treaties and conventions, can support adaptation action; however, the extent to which responding to impacts and losses arising from changes

in the ocean and cryosphere is enabled through regional policy frameworks is currently limited *(high confidence)*. Institutional arrangements that provide strong multiscale linkages with local and Indigenous communities benefit adaptation *(high confidence)*. Coordination and complementarity between national and transboundary regional policies can support efforts to address risks to resource security and management, such as water and fisheries *(medium confidence)*. {2.3.1, 2.3.2, 2.4, Box 2.4, 2.5, 3.5.2, 3.5.3, 3.5.4, 4.4.4, 4.4.5, Table 4.9, 5.5.2, 6.9.2}

C.4.3   Experience to date – for example, in responding to sea level rise, water-related risks in some high mountains, and climate change risks in the Arctic – also reveal the enabling influence of taking a long-term perspective when making short-term decisions, explicitly accounting for uncertainty of context-specific risks beyond 2050 *(high confidence)*, and building governance capabilities to tackle complex risks *(medium confidence)*. {2.3.1, 3.5.4, 4.4.4, 4.4.5, Table 4.9, 5.5.2, 6.9, Figure SPM.5}

C.4.4   Investments in education and capacity building at various levels and scales facilitates social learning and long-term capability for context-specific responses to reduce risk and enhance resilience *(high confidence)*. Specific activities include utilization of multiple knowledge systems and regional climate information into decision making, and the engagement of local communities, Indigenous peoples, and relevant stakeholders in adaptive governance arrangements and planning frameworks *(medium confidence).* Promotion of climate literacy and drawing on local, Indigenous and scientific knowledge systems enables public awareness, understanding and social learning about locality-specific risk and response potential *(high confidence)*. Such investments can develop, and in many cases transform existing institutions and enable informed, interactive and adaptive governance arrangements *(high confidence)*. {1.8.3, 2.3.2, Figure 2.7, Box 2.4, 2.4, 3.5.2, 3.5.4, 4.4.4, 4.4.5, Table 4.9, 5.5.2, 6.9}

C.4.5   Context-specific monitoring and forecasting of changes in the ocean and the cryosphere informs adaptation planning and implementation, and facilitates robust decisions on trade-offs between short- and long-term gains *(medium confidence)*. Sustained long-term monitoring, sharing of data, information and knowledge and improved context-specific forecasts, including early warning systems to predict more extreme El Niño/La Niña events, tropical cyclones, and marine heatwaves, help to manage negative impacts from ocean changes such as losses in fisheries, and adverse impacts on human health, food security, agriculture, coral reefs, aquaculture, wildfire, tourism, conservation, drought and flood *(high confidence)*. {2.4, 2.5, 3.5.2, 4.4.4, 5.5.2, 6.3.1, 6.3.3, 6.4.3, 6.5.3, 6.9}

C.4.6   Prioritising measures to address social vulnerability and equity underpins efforts to promote fair and just climate resilience and sustainable development *(high confidence)*, and can be helped by creating safe community settings for meaningful public participation, deliberation and conflict resolution *(medium confidence)*. {Box 2.4, 4.4.4, 4.4.5, Table 4.9, Figure SPM.5}

C.4.7   This assessment of the ocean and cryosphere in a changing climate reveals the benefits of ambitious mitigation and effective adaptation for sustainable development and, conversely, the escalating costs and risks of delayed action. The potential to chart Climate Resilient Development Pathways varies within and among ocean, high mountain and polar land regions. Realising this potential depends on transformative change. This highlights the urgency of prioritising timely, ambitious, coordinated and enduring action *(very high confidence)*. {1.1, 1.8, Cross-Chapter Box 1 in Chapter 1, 2.3, 2.4, 3.5, 4.2.1, 4.2.2, 4.3.4, 4.4, Table 4.9, 5.5, 6.9, Cross-Chapter Box 9, Figure SPM.5}

DOCUMENT 15

DEPARTMENT OF PLANNING, INDUSTRY & ENVIRONMENT

Climate change impacts in the NSW and ACT Alpine region

Impacts on biodiversity

environment.nsw.gov.au

Cover photo: Winter landscape in Kosciuszko National Park. John Spencer/DPIE

This report should be cited as:

Love J, Thapa R, Drielsma M and Robb J 2019, *Climate change impacts in the NSW and ACT Alpine region: Impacts on biodiversity*, NSW Department of Planning, Industry and Environment, Sydney, Australia.

Find out more about your environment at:

www.environment.nsw.gov.au

Contents

List of tables

List of figures

List of shortened forms

ACT	Australian Capital Territory
BCC	Bioclimatic Class
BIAP	Biodiversity Impacts and Adaptation Project
CSIRO	Commonwealth Scientific and Industrial Research Organisation
EHA	effective habitat area
FPC	foliage projective cover
DPIE	Department of Planning, Industry and Environment
GCM	Global Climate Model
GDM	Generalised Dissimilarity Model
GIS	geographic information system
KNP	Kosciuszko National Park
KTPs	Key Threatening Processes
MCAS-S	Multi-Criteria Analysis Shell for Spatial Decision Support
NARCliM	NSW/ACT Regional Climate Modelling project
NPWS	NSW National Parks and Wildlife Service
NSW	New South Wales
NVM	Native Vegetation Management
OEH	Office of Environment and Heritage
REMP	Rapid Evaluation of Metapopulation Persistence
RCM	Regional Climate Model
RGB	red green blue
SoS	*Saving our Species*
UNE	University of New England
3CMP	climate ready metapopulation analysis

Summary of findings

Impacts on biodiversity in the NSW and ACT Alpine region

1. Alpine vegetation communities are projected to experience 21–70% change in species composition in the far future (2060 to 2079). Alpine Herbfields, Montane Bogs and Fens, Grassy Woodlands and Wet Sclerophyll Forest are projected to decrease in area and compositional suitability as climatic conditions transition to those better suiting species of Subalpine Woodland and Dry Sclerophyll Forest, which are predicted to expand accordingly.

2. Key flora species are predicted to be impacted by future changes in climate, including plants listed as critically endangered: the black-hooded sun orchid (*Thelymitra atronitida*), Kelton's leek orchid (*Prasophyllum keltonii*) and *Prasophyllum bagoense*. These species will be under increasing pressure as climate change proceeds.

3. Other threatened flora species predicted to be impacted are pale pomaderris, suggan buggan mallee, feldmark grass, anemone buttercup, austral pillwort, mauve burr-daisy, slender greenhood, Max Mueller's burr-daisy, shining cudweed, leafy anchor plant, Monaro golden daisy, slender greenhood, Kiandra leek orchid.

4. Mammals from habitats predicted to be most impacted by future climate change include southern myotis (*Myotis macropus*), eastern pygmy possum (*Cercartetus nanus*), mountain pygmy possum (*Burramys parvus*), broad-toothed rat (*Mastacomys fuscus*), smoky mouse (*Pseudomys fumeus*), spotted-tailed quoll (*Dasyurus maculatus*) and brush-tailed rock-wallaby (*Petrogale penicillate*).

5. The Australian painted snipe (*Rostratula australis*) is an endangered bird species that occupies montane lakes, and bogs and fens. These areas are likely to contract under the projected future climate, potentially placing the snipe at greater risk from habitat loss. Other bird species listed as vulnerable are projected to be impacted by climate change. Most utilise a variety of habitats and the advantage of high mobility may provide some flexibility as they are confronted with changing climatic conditions.

6. Subalpine Woodlands, Alpine Heaths and Herbfields, and Alpine Bogs and Fens are habitat for several species of frogs listed as critically endangered. These vegetation classes also provide habitat for the endangered alpine she-oak skink (*Cyclodomorphus praealtus*) and the Guthega skink (*Liopholis guthega*). These habitats are predicted to experience large change by 2060 to 2079. It is predicted that the southern corroboree frog (*Pseudophryne corroboree*) and alpine tree frog (*Litoria verreauxii alpina*) will also be severely impacted.

7. Where habitat condition and connectivity permit, some of the region's biodiversity will have the opportunity to migrate to emerging suitable habitats at higher altitudes. This may lead to conflicting management priorities, as native species compete for resources. Although the velocity of change is expected to be less than in other parts of the state, consequences may be greater as the Alpine region sits at the edge of a major environmental gradient. There is nowhere for species to migrate beyond mountain tops as temperatures increase and colder high elevation climate envelopes contract. This presents unique challenges to the conservation of alpine biodiversity.

8. Species already listed as threatened may need novel management interventions to persist through near and far future climate. It is likely more species and their ecosystems will need special management in the future even though they may appear to have sufficient habitat and stable populations at present. Where species are isolated or without the ability to propagate and colonise emerging areas of suitable habitat, assisted relocation may be necessary.

1.   Introduction

1.1   Background

Alpine regions throughout the world are important biodiversity hotspots with high levels of endemism. During the last five decades, unprecedented changes to ecosystems have occurred globally due to changing climate and human activities (Millennium Ecosystem Assessment 2005; Chapin et al. 2009). Accelerating climate change combined with other anthropogenic disturbances leads to habitat loss and alteration, as well as shifts in species compositions and assemblages. This process threatens biodiversity and ultimately the resilience of ecosystems and entire regions (Chapin et al. 2009). Alpine biodiversity is highly vulnerable to the impacts of climate change (IPCC 2007; Buytaert et al. 2011).

Predicting the response of alpine biodiversity to climate change has become a research priority (Hennessy et al. 2007; Worboys et al. 2010; Morrison & Pickering 2013). Conserving the Alpine region's biodiversity requires understanding potential future risks and anticipating biodiversity's response to climatic and ecological changes (Pereira at al. 2010).

Climate projections are predicting increased variability in climate, above average temperature and longer dry seasons (IPCC 2007; Buytaert et al. 2011). High variability will disrupt ecosystem functions, resulting in higher rates of species loss and turnover (Boulanger et al. 2007; Buytaert et al. 2009). Australian native vegetation is naturally dynamic, transitioning along the different phases of an adaptive cycle after a disturbance (Thapa et al. 2016). Severe or ongoing disturbance and climate change cause ecosystem processes to cross thresholds, leading to state change; for example, from grassland to woodland (Wolf et al. 2007). Changes such as temperature increases, sea level rise and changing patterns of precipitation may also result in 'multi-directional' species movement (VanDerWal et al. 2013). Species are generally expected to follow climatic niches, the area in which climatic conditions are suitable, by shifting to higher altitudes or latitudes. Successful response of individual species to these changes depends on their adaptive capacity and that of the ecosystems they inhabit.

When landscape effects (distances and habitat fragmentation) are considered, it becomes apparent that biodiversity cannot always keep pace with the rate of environmental change, or find migratory pathways to more suitable habitat. Without management intervention, this will lead to local or global extinctions. Some areas that have lost their historic biota and where neighbouring communities are unable to colonise will become home to novel communities that have not previously existed. Pioneer species may appear from elsewhere or from a previously suppressed seed bank, and new or invasive species may colonise the system. This could be in the form of unprecedented weed invasions (Whalley et al. 2011).

Despite representing only 0.16% of Australia's land surface, the NSW and ACT Alpine region is disproportionately important nationally and internationally due to its conservation significance, economic values, provision of ecosystems goods and services (Worboys et al. 2010; Morrison & Pickering 2013), and its social and cultural heritage (Morrison & Pickering 2013). The region is trending towards higher temperatures and decreasing precipitation, resulting in dramatic changes to existing ecosystems, and to the ski/tourism and hydropower generation industries (Hennessy et al. 2007; Worboys et al. 2010). These changes will adversely impact on economies downstream as agriculture, tourism and hydropower all rely on a secure supply of water from upstream.

Endemic alpine species are often dependent on adequate snow cover for their habitats (Pickering et al. 2004; Hughes L 2011). The endangered mountain pygmy possum is expected to suffer substantial habitat loss due to changes in snow cover (Hughes 2011). Species interactions may be affected and there may be increased predation by foxes and cats associated with decreased snow cover (Hughes 2011). This may also threaten vulnerable broad-toothed rat populations, as this species has a narrow environmental tolerance and would be at increased risk of predation.

With increasing summer temperatures and decreasing precipitation, the intensity of bushfires in the NSW and ACT Alpine region is expected to rise. It is predicted that by 2020 the intensity of fires may increase by 65% under the worst-case scenario, and by 300% by 2050 (Lucas et al. 2007). The NSW and ACT Regional Climate Modelling (NARCliM) projections have predicted that the Alpine region is likely to experience higher temperatures, fewer cold nights, lower precipitation and lower snowfall in the near and far futures. The frequency and intensity of extreme events, such as floods, erosion and fire, are also expected to increase, irreversibly influencing the composition, structure and function of the alpine ecosystems.

Ecosystem processes change at multiple scales (Forman & Godron 1986; Turner 2005) as different controls and processes are characteristic of each scale in time and space (Wu 1999) and are differentiated by biotic and abiotic structure (Pickett & Cadenasso 1995). Understanding how and why ecosystems change requires an understanding of the key drivers that operate at different scales and is central to ecosystem science (Sutherland et al. 2013). Spatial scale is a window through which ecosystems can be viewed (Wiens 1989; Parsons & Thoms 2007). What is seen at any scale is related to the size of the window through which the system is viewed (Wiens 1989) and to the way the scales of observation used relate to the hierarchical organisation of processes operating within the system (Dollar et al. 2007). Thus, this analysis is discussed in the context of three regions of varying scale (Figure 1), allowing important ecological processes to be adequately framed, and providing a broader context to our interpretations of ecosystem behaviour.

This report is part of a larger project delivered by the NSW Department of Planning, Industry and Environment (DPIE) on the various impacts from climate change on the NSW and ACT Alpine region, hereafter referred to as the Alpine region.
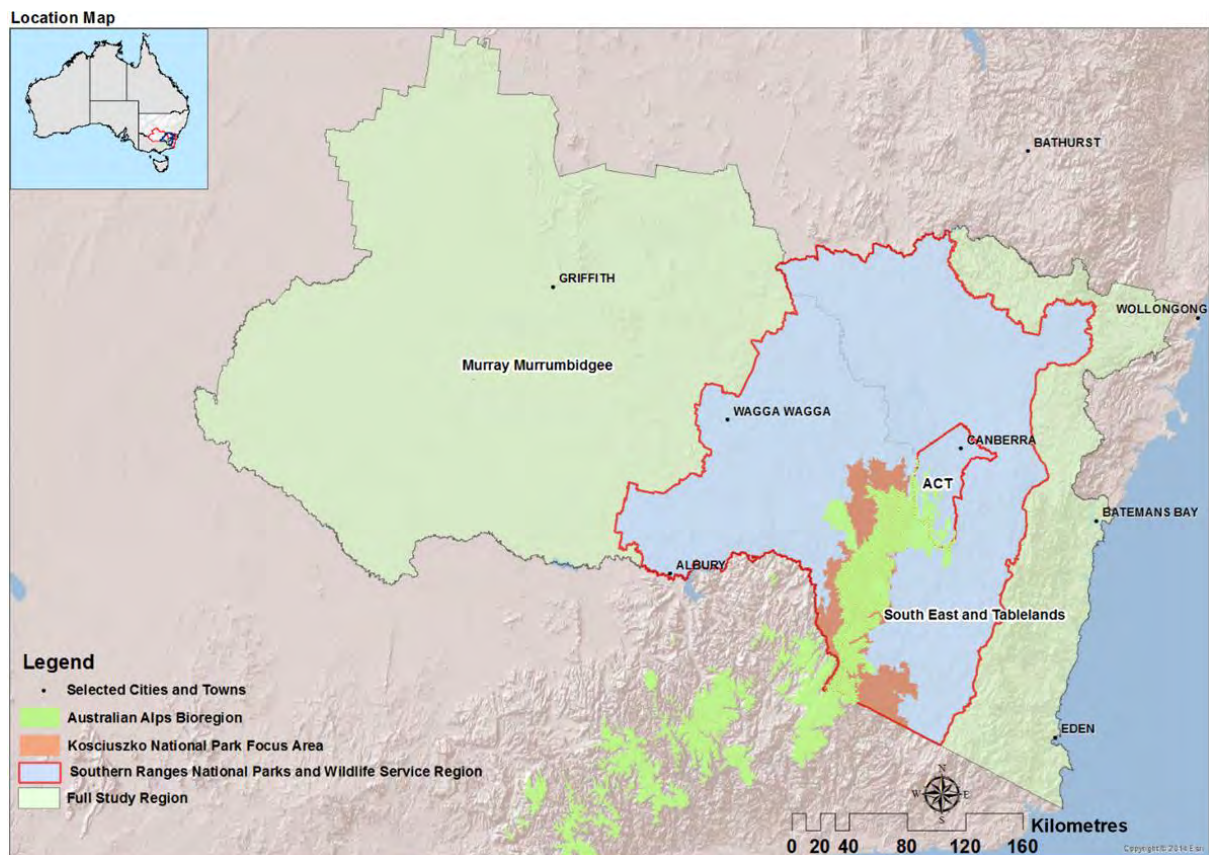
Figure 1   **Study areas used to assess the biodiversity impacts of climate change in the Alpine region at three spatial scales**

The three spatial scales are: full study region (light green), Southern Ranges National Parks and Wildlife Service region (light blue) and Kosciuszko National Park focus area (orange). The Australian Alps bioregion is also shown (green).

1.2   Objectives

This study used recent biodiversity impacts and adaptation modelling of the direct influence of climate change on species composition and the resulting impacts on biodiversity persistence to report on the impacts for biodiversity in the Alpine region and surrounding areas. This assessment reports on how the recent historic (baseline period 1990 to 2009) biodiversity of the Alpine region is likely be impacted under NARCliM modelled near future (2020 to 2039) and far future (2060 to 2079) climate projections. The adaptive capacity of alpine vegetation classes and the habitats of threatened flora and fauna are assessed by considering their current condition, and levels of habitat fragmentation and connectivity. The benefits that result from potential biodiversity conservation or restoration actions are also reported to support biodiversity management in the alpine and surrounding region aimed at delivering better long-term biodiversity outcomes.

1.3   Outputs

Output	Details	Key user
Report	Five sections detailing climate change impacts on the region's biodiversity including vegetation communities and fauna	Biodiversity conservation policy and management sectors; private sector that contributes to biodiversity conservation; those interested in understanding more about climate change impacts on biodiversity
Maps and tables	Twenty-six figures and 14 tables representing analysis findings	Biodiversity conservation policy and management sectors; private sector contributing to biodiversity conservation; researchers in the fields of ecology, resilience, climate change
Spatial and tabular data	The spatial and tabular data underpinning the findings of this analysis (see Appendix A for a complete list of source data)	Researchers who work in the fields of ecology, resilience, climate change; those wishing to conduct further analysis or reporting on the available data

1.4   Focus region

The Alpine region is located in the south-eastern corner of mainland Australia, forms the southern end of the Great Dividing Range and covers a total area of 1.64 million hectares that extend over 500 kilometres (Morrison & Pickering 2013). The highest peak, Mount Kosciuszko, rises to an altitude of 2228 metres. There are 11 national parks and reserves within the region and it extends across most of the Alpine bioregion (Crabb 2003). Kosciuszko National Park (KNP) and its plant communities are recognised by UNESCO as a World Biosphere Reserve and the park is listed in the National Heritage List (ISC 2004).

The climate within the Alpine region is highly variable. The annual average temperature in the areas surrounding KNP is 4°C. The summer average temperature ranges from 10–12°C with an average maximum range of 14–16°C. In comparison, the average minimum winter temperature ranges from –6 to –4°C. Average minimum and maximum annual rainfall varies considerably, both spatially and temporally.

The long-term temperature has been increasing since the 1990s (Hennessy et al. 2007). The mean temperature has risen by 0.5°C per decade since 1990 and is projected to increase by 2.6–3°C by 2070 (AdaptNSW website). Long-term rainfall is also highly variable and is projected to decrease in winter and spring and increase in autumn (AdaptNSW website; Hennessy et al 2007). The predicted increase in temperature and decrease in precipitation will likely result in dramatic changes in existing ecosystem functions and cause the loss of

ecosystem services (Hennessy et al. 2007; Worboys et al. 2010). Further, these changes in climate may result in loss of endemic alpine herbfields, bogs and fens and change in species richness.

The focus of this study is KNP, which is also viewed in the context of the Southern Ranges National Parks and Wildlife Service (NPWS) region and the full study region, which takes in the coast to the east and the NSW Murray River catchment area to the west. Considering cross-scale effects is considered essential to successful natural resource management (Walker & Salt 2012) and the use of three different regions is intended to provide a more complete picture of biodiversity in the Alpine region and how it responds to the impacts of climate change.

Changes in ecosystems are rarely simple, as responses to drivers of change are mediated through a range of interactions and feedbacks between biotic and abiotic components and processes. Understanding the patterns of response at different scales is critical to our ability to manage the complex ecosystems of the Alpine region, and to be able to make predictions about their future conditions.

2.   Method

To report climate change impacts on alpine biodiversity, this study primarily draws on information from the Biodiversity Impacts and Adaptation Project (BIAP) (OEH 2016; Drielsma et al. 2017), which extended '3C' modelling for biodiversity under future climate (Drielsma et al. 2015) by including 12 additional NARCliM simulations. The BIAP forecasted broad impacts of climate change on biodiversity across eastern Australia and identified adaptation opportunities to minimise biodiversity loss. This analysis also draws on regional-scale connectivity modelling performed by DPIE for the south-east (Love et al. 2015) and Riverina (Love et al. 2017) Local Land Services and presents draft species occupancy modelling currently being prepared for the NSW *Saving our Species* (SoS) program.

The 3C modelling for biodiversity under future climate project extended under BIAP was part of the Australian Government's Regional Natural Resource Management Planning for Climate Change, stream 2. More information about 3C and its products are available online on the <u>TerraNova Climate Change Adaptation Information Hub</u>.

2.1   Source of data

NARCliM simulations from four Coupled Model Intercomparison Project phase 3 (CMIP3) Global Climate Models (GCMs) were used to drive three Regional Climate Models (RCMs) to form a 12-member GCM/RCM ensemble (Evans et al. 2014). The four selected GCMs cover a broad range of possible climate outcomes. This includes MIROC3.2, which is a warm/wet scenario, ECHAM5, a hot/similar precipitation scenario, CCCMA3.1, a hot/wet scenario, and CSIRO-Mk3.0, a warm/dry scenario. For future projections, the Special Report on Emissions Scenarios (SRES) business-as-usual A2 scenario was used (IPCC 2000). The three selected RCMs are three physics scheme combinations of the Weather Research and Forecasting (WRF) model. Each simulation consists of three 20-year runs (1990 to 2009, 2020 to 2039, and 2060 to 2079). The four GCMs were chosen based on a number of criteria: i) adequate performance when simulating historic climate; ii) most independent; iii) cover the largest range of plausible future precipitation and temperature changes for Australia. The three RCMs correspond to three different physics scheme combinations of the WRF V3.3 model (Skamarock et al. 2008), which were also chosen for adequate skill and error independence, following a comprehensive analysis of 36 different combinations of physics parameterisations over eight significant East Coast Lows (ECLs) (Evans et al. 2012; Ji et al. 2014). For the selected three RCMs, the WRF Double Moment 5-class (WDM5) microphysics scheme and NOAH land surface scheme are used in all cases. Refer to Evans et al. (2014) for more details on each physics scheme.

We acknowledge that the results are model dependent (as all model studies are) but through the use of this carefully selected ensemble we have attempted to minimise this dependence. By using this model selection process, we have shown that it is possible to create relatively small ensembles that are able to reproduce the ensemble mean and variance from the large parent ensemble (i.e. the many GCMs) as well as minimise the overall error (Evans et al. 2013a).

Some initial evaluation of NARCliM simulations shows that they have strong skill in simulating the precipitation and temperature of Australia, with a small cold bias and overestimation of precipitation on the Great Dividing Range (Evans et al. 2013b; Ji et al. 2016). The differing responses of the different RCMs confirm the utility of considering model independence when choosing the RCMs. The RCM response to large-scale modes of variability also agrees well with observations (Fita et al. 2016). Through these evaluations we found that while there is a spread in model predictions, all models perform adequately with no single model performing the best for all variables and metrics. The use of the full ensemble provides a measure of robustness such that any result that is common through all models in the ensemble is considered to have higher confidence.

Data for this analysis (listed in Appendix A) were sourced from BIAP and 3C derived products and DPIE corporate datasets such as the BioNet Atlas and the NSW vegetation map version 3. The findings from BIAP will be available alongside snapshots for other impact and adaptation themes on the AdaptNSW website. More detailed findings, products and data arising from BIAP will be downloadable via the AdaptNSW data portal.

The statewide native vegetation condition layer (Appendix B, *B1. Current vegetation condition*) was originally developed for the NSW Native Vegetation Management (NVM) benefits analyses (Drielsma et al. 2010; Drielsma et al. 2012) and extended under BIAP. Effective habitat area (EHA) mapping uses the cost–benefit approach (Drielsma et al. 2007a; Drielsma et al. 2014). Habitat connectivity (Appendix B, *B3. Habitat connectivity*) and metapopulation analysis (Appendix B, *B4. Climate ready metapopulation analysis*) were sourced from the 3C project and additional fine-scale analysis undertaken for Local Land Services (Love et al. 2015; Love et al. 2017) using the spatial links tool (Drielsma et al. 2007b). The biodiversity benefits mapping, including conservation and revegetation benefits (Appendix B, *B6. Conservation manage benefits* and *B7. Revegetation benefits*) are sourced from BIAP and the projected changes in benefits over time (Appendix B, *B8. Relative change in benefits*) are sourced from 3C. The 3C products were modelled between 2000 and 2050.

Keith (2002) has derived a NSW wide composite spatial data layer differentiating vegetation types from a classification of 106 native vegetation classes and shows vegetation types for extant native vegetation across NSW and the ACT (Keith 2002, data.environment.nsw.gov.au). Each class is composed of related plant communities with structural and compositional similarities and common habitat characteristics. At the time of our analysis this layer provided the most consistent and complete mapping of vegetation types across the entire analysis region.

Draft species occupancy models (Section 3.7) were supplied from 'Spatial prioritisation for species resilience' (OEH & UNE unpub.), a research project currently being undertaken for SoS. *Saving our Species* is an ongoing statewide program addressing the growing number of plants and animals in New South Wales facing extinction.

Species occupancy models are currently draft products and are provided as examples of additional information relevant to managing the region's biodiversity (OEH & UNE unpub.).

2.2   Analysis

This analysis used existing spatial products relating to biodiversity resilience and adaptive capacity, climate change impacts, and management to aid adaptation, to report on measures for vegetation classes and threatened flora and fauna considered to be important indicators of the impacts of climate change on biodiversity in the Alpine region.

This analysis reported on climate change impacts for:

- the mapped extents of 13 vegetation classes most relevant to the Alpine region, out of the 68 vegetation classes mapped as occurring in the full study region

- site occurrence records for 11 threatened flora and 23 threatened fauna species from within the full study area that are under the greatest pressure from future climate change, with a focus on those that occur in the KNP

- estimated dissimilarity in species composition between current and future climate projections, reported at each location (grid cell). This analysis estimated and mapped how unsuitable each location will become in the near (2020 to 2039) and far future (2060 to 2079) NARCliM projection periods for the species it currently supports, and how compositionally dissimilar the vegetation that is best suited to future conditions is, to that which currently occurs

- changes to the expected biodiversity benefits across the region. Expected biodiversity benefits measure the expected gains in regional biodiversity persistence that result from retaining intact habitats or restoring lost habitats. Using 3C modelling (Drielsma et al. 2015), we report on how climate change is expected to change these benefits between the recent past (2000 baseline) and 2050.

In addition, three spatial products relating to the resilience of biodiversity and its current capacity to respond to climate change were reported:

- current vegetation condition (as of 2012) – estimating how intact or degraded native vegetation at each location (grid cell) or region is, relative to a maximum potential 'pristine' state

- effective habitat area – measuring the habitat's spatial context, which integrates the condition of vegetation at each location (grid cell) with measures of its connectivity to, and the condition of, surrounding habitat

- habitat connectivity – measuring how the placement and structure of habitat is most likely to facilitate the movement of biodiversity through the landscape.

Initially, datasets from past DPIE (previously Office of Environment and Heritage) projects (including 3C Modelling, BIAP and regional-scale products) were assessed in terms of their relevance to measuring climate change impacts on alpine biodiversity and their suitability for reporting within the applied framework. The selected products, while predominantly developed to provide statewide coverage, were considered suitable for regional-scale analysis and most suitable for reporting the biodiversity impacts of climate change in the Alpine region.

All raster data were converted to Lamberts conformal coordinate systems in ArcMap 10.1, with a spatial resolution of 250 metres used for consistency. The method of extracting values from existing products involved intersecting raster layers using GIS analysis tools in ArcGIS 10.1. The analysis primarily consisted of developing statistics using the spatial analysis zonal statistics toolset. This toolset was used to summarise raster layers within the mapped extents of vegetation classes. Threatened species records were extracted from the BioNet Atlas and similarly used for reporting impact related spatial information.

Maps and graphs in this report, and associated data, were all prepared using ArcMap 10.1, R Studio and Microsoft Excel.

2.3   Bioclimatic Class envelopes

The modelling of biodiversity impacts under climate change relies on a representation of biodiversity provided here by spatially interpolated Bioclimatic Class (BCC) envelopes. BCCs are a data driven classification of biodiversity based on a Generalised Dissimilarity Model (GDM) produced for the NARCliM region (OEH 2016) and based on vascular plant records and environmental predictor surfaces. BCCs were developed specifically as a surrogate for biodiversity as they allow unconstrained modelling of biodiversity shifts in response to dynamic climate variables, without needing to relate back to existing vegetation communities that may be displaced or not exist at all under future climates. The probabilistic rendering of BCC envelopes (henceforth referred to as BCC envelopes or 'envelopes') across space (Figure 2) allows for the expected disaggregation of existing relationships as overlaps between classes and the species they represent change and new compositional overlaps emerge (Drielsma et al. 2015; Drielsma et al. 2017).

The compositional similarity between individual BCC envelopes is displayed graphically by employing relative RGB colouring, whereby classes with similar species composition are portrayed with similar colour (e.g. Figure 2). Species composition is the result of a history of relationships, events and variables, some relatively static such as geology and terrain, others dynamic such as patterns of weather and fire regime. The BCC envelopes spatially define biophysical capability to support each BCC. Each location has been allocated probabilistically to each envelope at the 1990 to 2009 baseline, and projected at 2020 to 2039 and 2060 to 2079 for each of the NARCliM climate futures. As the climatic conditions at a location change, envelopes shift, favouring shifts in BCC distribution, subject to the possibility of migration. This is displayed as a change in colour over time at any location (shown in Figure 3 for the three RCMs under the CSIRO-Mk3.0 GCM for 2020 to 2039 and 2060 to 2079).

At the 1990 to 2009 baseline period, we expect that the distribution of each BCC aligns closely to its corresponding envelope. Subsequent predicted shifts do not signify a complete or sudden turnover of all species. At least in the short term, transitions are generally between BCC envelopes with similar species composition, indicated graphically by a subtle change in colour. Actualised transitions will occur over time whereby a proportion of species leave or enter each location, while others may be able to adapt and remain. However, species and ultimately whole communities will diminish if: envelopes disappear completely; the velocity of change is too high for successful migrations to occur; or environmental gradients are naturally or anthropogenically truncated or fragmented.

BCC envelopes are used to represent the potential composition and distribution of biodiversity across the full study region. To accommodate reporting, BCC envelopes were overlaid with vegetation classes (Section 2.4). This allowed reporting of what changes in biodiversity the Alpine region can expect with future changing climate in the context of known and identifiable vegetation types. Figure 3 shows BCC envelope distributions under the baseline period and the CSIRO-Mk3.0 GCM for the three RCMs for the near and far future separately.

Overall, the distribution of BCC envelopes is predicted to change dramatically across the full study region in the far future relative to the baseline period; however, changes in BCC envelopes differ greatly under the 12 NARCliM scenarios. Across both climate futures, the most dramatic changes are consistently observed between Wagga Wagga and Griffith. In the higher altitude alpine areas, the velocity of change is slower, shown by smaller geographic shifts in BCC envelopes with transitions to relatively similar BCCs over near and far future periods; however, biodiversity represented by classes contracting at higher altitudes lacks emerging suitable habitats in the future; therefore, species in these areas may be more at risk from change. Along the Alpine regions of New South Wales and the ACT, the greatest compositional changes in BCCs are predicted along the south-eastern, south-western and the northern edges of KNP.
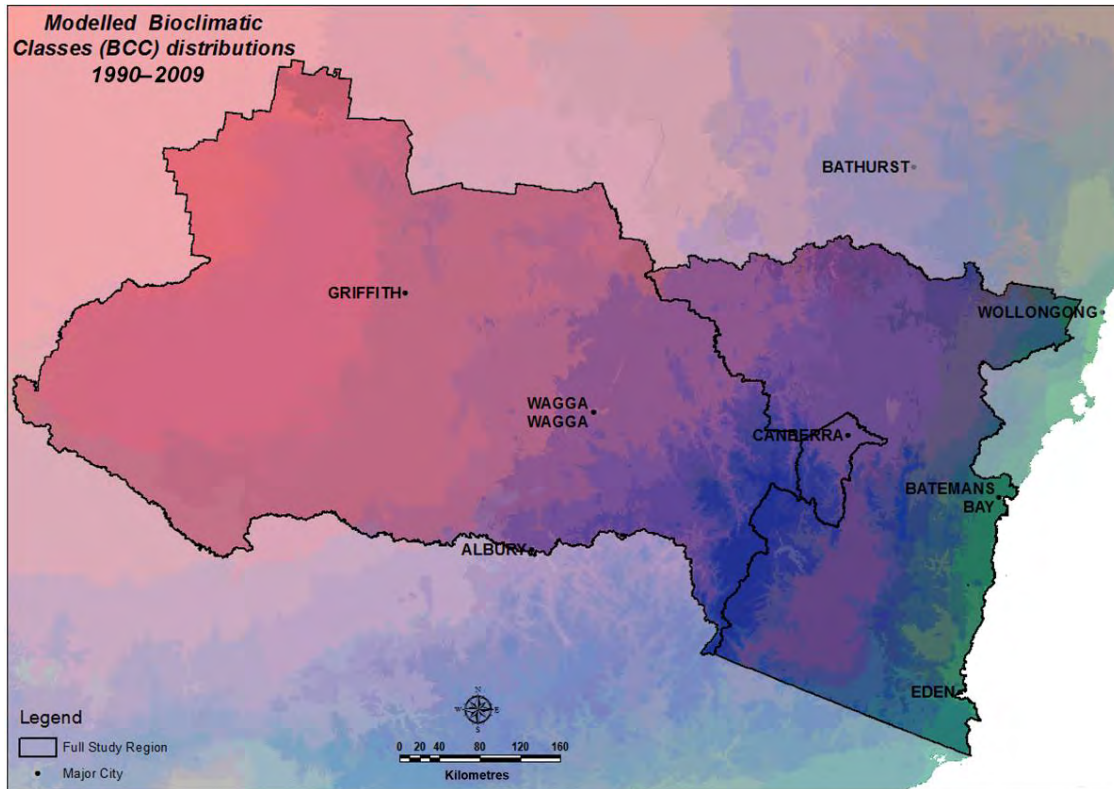
Figure 2 **Modelled Bioclimatic Class (BCC) envelope distributions for the full study region for the 1990 to 2009 baseline period**
Colours of similar hue represent BCCs with similar species compositions.
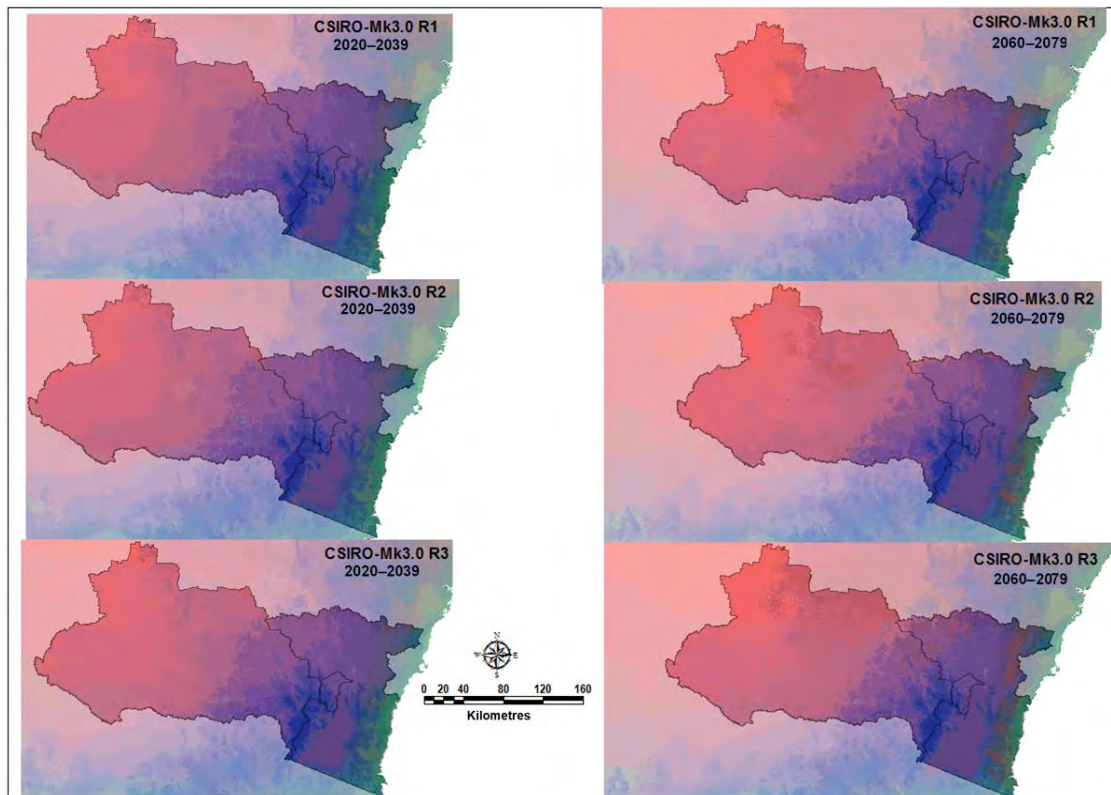
Figure 3 **Modelled Bioclimatic Class envelope distributions for the full study region under the CSIRO-Mk3.0 GCM showing differences under the three RCMs for the near future (2020 to 2039) and far future (2060 to 2079)**
Colours of similar hue represent BCCs with similar species compositions.

2.4   NSW vegetation classes

BCC envelopes are useful for climate impact and adaptation modelling as their distributions can routinely be recalculated for any time-step of any climate scenario where projected climate variables are available; however, BCCs are not a familiar or relatable classification scheme so we have intersected their distribution with the current distributions of vegetation classes (Figure 4) (Keith 2002; Keith & Simpson 2017) for reporting. This aids in assessing and communicating impacts and possible adaptation strategies by relating analysis results to well-known surrogates.

There are 68 vegetation classes within the full study region. Thirty-one are within the NPWS estate and 18 of these are found in KNP. The Alpine region is dominated by Subalpine Woodlands with a total area of approximately 3.5 million hectares. Montane Wet Sclerophyll Forest occupies over 78,000 hectares, followed by Alpine Heaths with approximately 72,000 hectares. Alpine Fjaeldmarks has the smallest extent of all alpine vegetation classes.

Out of the 68 vegetation classes in the full study region, the 13 most related to alpine biodiversity (Table 1 and Figure 4) were selected for impact analysis and reporting. The mapped extents of these 13 classes were intersected with the current distribution of 79 BCC envelopes (Table 2) to observe how changes in BCC envelopes modelled under climate change may relate to impacts on different vegetation types (Figure 5). They are also intersected with the full suite of spatial products used to report on the impacts of climate change and biodiversity's ability to successfully respond.
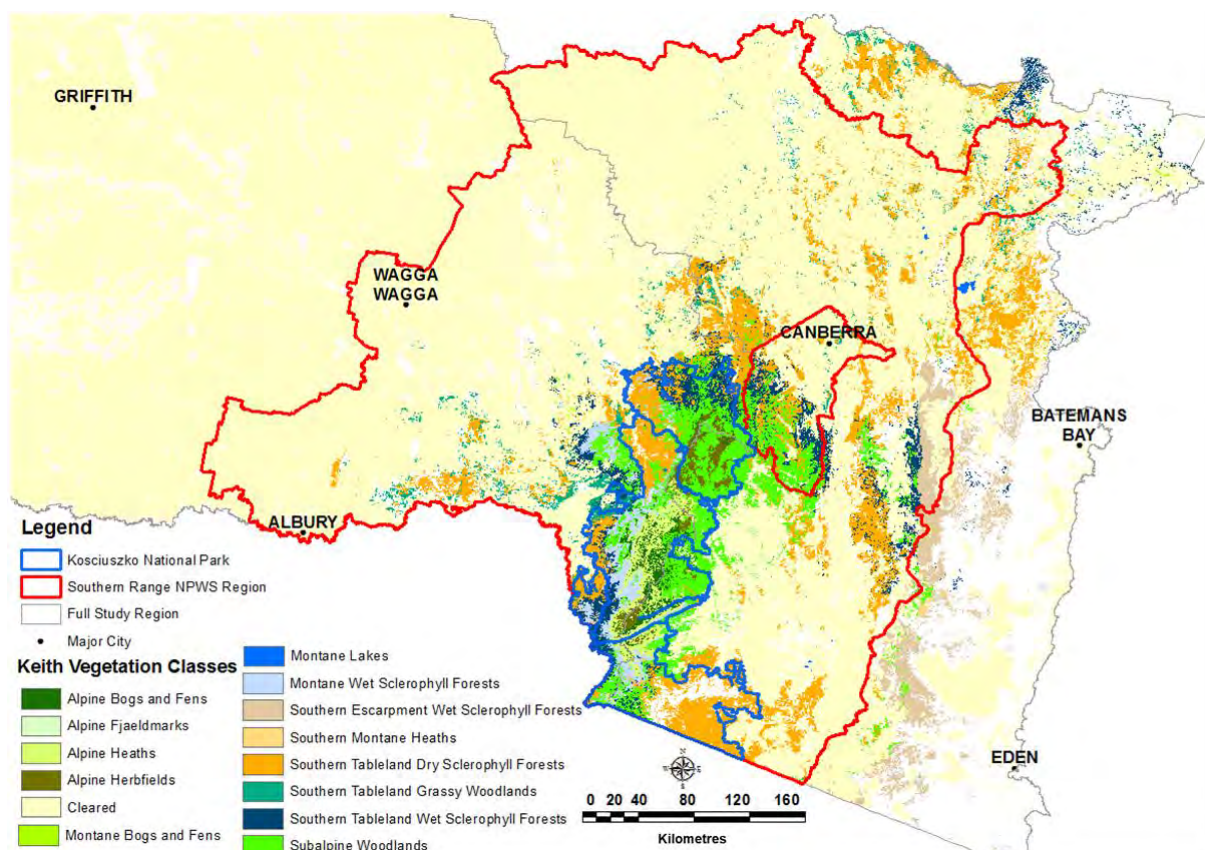
Figure 4   **The mapped extent of the 13 alpine related vegetation classes selected for reporting, extracted from the NSW vegetation map version 3.0 (Keith 2002; Keith & Simpson 2017)**

Table 1 **The 13 vegetation classes in the Alpine region selected for reporting, and their mapped extent**

Vegetation class	Area (ha)
Alpine Bogs and Fens	40,431
Alpine Fjaeldmarks	175
Alpine Heaths	71,781
Alpine Herbfields	39,113
Montane Bogs and Fens	12,625
Montane Lakes	2,906
Montane Wet Sclerophyll Forests	78,119
Southern Escarpment Wet Sclerophyll Forests	195,275
Southern Montane Heaths	8,281
Southern Tableland Dry Sclerophyll Forests	692,644
Southern Tableland Grassy Woodlands	105,231
Southern Tableland Wet Sclerophyll Forests	197,288
Subalpine Woodlands	366,619
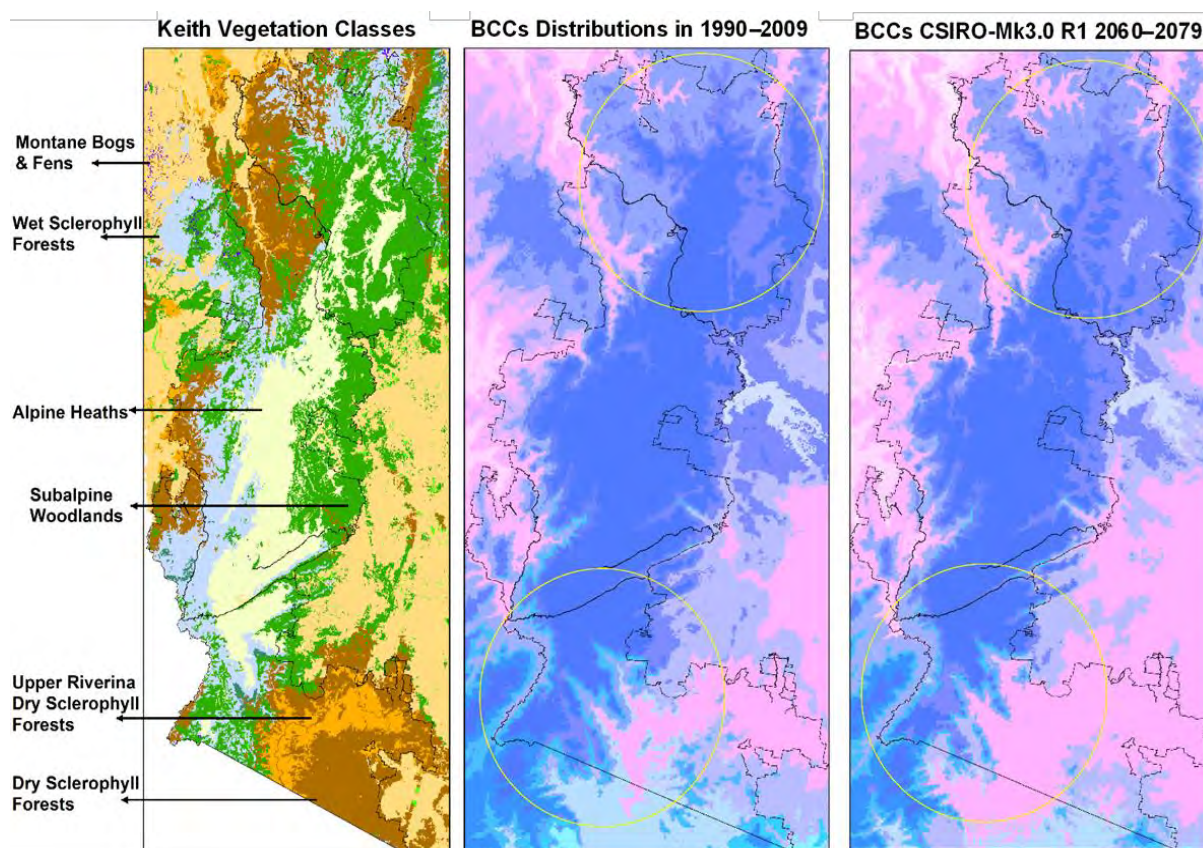
Figure 5 **Keith vegetation classes in the Alpine region (left), with comparisons of modelled Bioclimatic Class envelope distributions at the baseline period (1990 to 2009) (centre) and CSIRO-Mk3.0 R1 GCM for 2060 to 2079 (right)**

Colours of similar hue represent BCCs with similar species composition.

Table 2 **The 79 Bioclimatic Classes present in the full study region and their respective areas in the 1990 to 2009 baseline period**

Colours of similar hue represent BCCs with similar species composition.

BCC Class	No of pixels	Area (hectares)	Colour	BCC Class	No of pixels	Area (hectares)	Colour	BCC Class	No of pixels	Area (hectares)	Colour
1	2072	12950.00	1	73	209909	1311931.25	73	157	150	937.5	157
10	421	2631.25	10	74	2	12.5	74	158	5986	37412.5	158
11	699	4368.75	11	80	67174	419837.5	80	161	43166	269787.5	161
14	50	312.50	14	90	27267	170418.75	90	164	14090	88062.5	164
16	476	2975.00	16	91	16791	104943.75	91	165	150095	938093.75	165
17	356	2225.00	17	94	30239	188993.75	94	170	562	3512.5	170
19	2727	17043.75	19	95	56259	351618.75	95	177	2223	13893.75	177
21	7922	49512.50	21	96	23	143.75	96	190	10707	66918.75	190
23	128285	801781.25	23	100	48462	302887.5	100	191	62971	393568.75	191
24	12076	75475.00	24	104	87	543.75	104	192	18188	113675	192
27	3	18.75	27	105	2	12.5	105	202	52	325.00	202
31	26797	167481.25	31	106	36125	225781.25	106	207	1266	7912.50	207
35	5586	34912.50	35	109	15428	96425	109	208	64	400.00	208
40	13128	82050.00	40	110	11	68.75	110	217	2025	12656.25	217
42	471342	2945887.50	42	114	14534	90837.5	114	221	11446	71537.50	221
43	81137	507106.25	43	116	270899	1693118.75	116	223	9046	56537.50	223
46	16413	102581.25	46	120	1267	7918.75	120	228	62	387.50	228
47	32134	200837.50	47	122	47066	294162.5	122	233	1098	6862.50	233
52	93539	584618.75	52	125	6	37.5	125	234	1787	11168.75	234
53	2521	15756.25	53	131	36595	228718.75	131	244	928	5800.00	244
55	3138	19612.50	55	135	934	5837.5	135	247	1417	8856.25	247
58	3104	19400.00	58	137	13149	82181.25	137	248	1843	11518.75	248
64	15388	96175.00	64	143	12078	75487.5	143	250	6	37.50	250
65	18	112.50	65	146	937	5856.25	146				
68	23945	149656.25	68	149	3774	23587.5	149				
70	16006	100037.50	70	150	508979	3181118.75	150				
71	20	125.00	71	154	3191	19943.75	154				
72	3524	22025.00	72	156	23707	148168.75	156				

Within our study area there are 79 BCCs altogether with a total area of 17,168,125 hectares.

2.5 BioNet Atlas records

Occurrence records for 11 threatened flora species (Table 3) and 23 threatened fauna species (Table 4) were extracted for reporting from the NSW DPIE BioNet Atlas records. These species were selected due to their high level of future climate impact when assessed, compared with other threatened species in the region.

Table 3 **Threatened flora from the Alpine region selected for reporting**

Common name	Scientific name
Anemone buttercup	*Ranunculus anemoneus*
Austral pillwort	*Pilularia novae-hollandiae*
Cotoneaster pomaderris	*Pomaderris cotoneaster*
Feldmark grass	*Rytidosperma pumilum*
Leafy anchor plant	*Discaria nitida*
Mauve burr-daisy	*Calotis glandulosa*
Monaro golden daisy	*Rutidosis leiolepis*
Pale pomaderris	*Pomaderris pallida*
Shining cudweed	*Argyrotegium nitidulum*
Slender greenhood	*Pterostylis foliata*
Suggan buggan mallee	*Eucalyptus saxatilis*

Table 4 **Threatened fauna from the Alpine region selected for reporting**

Common name	Scientific name
Alpine she-oak skink	*Cyclodomorphus praealtus*
Alpine tree frog	*Litoria verreauxii alpina*
Australian painted snipe	*Rostratula australis*
Booroolong frog	*Litoria booroolongensis*
Broad-toothed rat	*Mastacomys fuscus*
Brown treecreeper (eastern subspecies)	*Climacteris picumnus victoriae*
Brush-tailed rock-wallaby	*Petrogale penicillata*
Dusky woodswallow	*Artamus cyanopterus cyanopterus*
Eastern pygmy possum	*Cercartetus nanus*
Eastern quoll	*Dasyurus viverrinus*
Glossy black-cockatoo	*Calyptorhynchus lathami*
Hooded robin (south-eastern form)	*Melanodryas cucullata cucullata*
Mountain pygmy possum	*Burramys parvus*
Northern corroboree frog	*Pseudophryne pengilleyi*
Smoky mouse	*Pseudomys fumeus*
Sooty owl	*Tyto tenebricosa*
Southern bell frog	*Litoria raniformis*
Southern corroboree frog	*Pseudophryne corroboree*
Southern myotis	*Myotis macropus*
Spotted-tailed quoll	*Dasyurus maculatus*
Turquoise parrot	*Neophema pulchella*
White-bellied sea-eagle	*Haliaeetus leucogaster*
White-fronted chat	*Epthianura albifrons*

2.6 *Saving our Species* dynamic occupancy modelling

Examples of relevant species occupancy modelling currently being developed for the SoS program are also provided. Projected species occupancy modelling based on NARCliM climate models is being used to identify priority areas for conservation action that will benefit multiple threatened fauna species. This work extended habitat suitability modelling developed by Macquarie University by using the Rapid Evaluation of Metapopulation Persistence (REMP, Drielsma & Ferrier 2009), a raster-based metapopulation process model that accounts for local extinctions and colonisations from adjoining areas, subject to the arrangement of habitat in the region. This prioritisation work provides guidance on where and what types of conservation actions will most benefit biodiversity. It also provides information on population viability and how this is likely to change under different climate scenarios.

2.7 Quality control

Inputs for this study were sourced from either the BIAP project or DPIE corporate systems. The BIAP and 3C data have been through control processes that ensure they are suitable for public release. Descriptions of inputs are provided in Appendix B. Source data from DPIE corporate systems are also specified and the source origin should be referred to for data quality statements. There is no way of assessing the accuracy of NARCliM climate projections adopted for BIAP, or products that are based on these. Instead, modelling a range of projected climate futures and where possible reporting on multi-model mean or other aggregation statistics to identify areas of agreement between models was considered a suitable approach to address future climate uncertainty.

Software used for BIAP, including the biodiversity forecasting tool (Drielsma et al. 2014), REMP (Drielsma & Ferrier 2009) and spatial links software (Drielsma et al. 2007b) are considered mature and well-tested, and the methodologies they employ are all peer reviewed and published. Additional spatial analysis was performed in ArcMap 10.1 software using the standard suite of data management and spatial analysis tools. Where inputs are based on in-house or 3rd party processes that are not part of the standard ArcMap 10.1 suite of tools, either complete descriptions are provided, or documented methodology cited. Where task automation such as batch processing has been employed, the methods used, inputs and outputs at each stage have been thoroughly assessed to ensure correct software behaviour.

All derived products have been reviewed internally by multiple team members prior to delivery. Outputs and other intermediate or derived data have been manually assessed to ensure they accurately represent the information they intend to provide. During analysis, internal file naming, folder structure and versioning conventions were adopted that reflect those developed and used during the NARCliM region wide BIAP analysis.

A complete draft version of this report was externally peer reviewed by Professor Nick Reid from the University of New England (UNE) prior to finalising. Comments and recommendations were addressed (available on request).

2.8 Data storage and access

All output data were converted to raster format (ArcGIS ESRI grid) and supplied to the MCAS-S (Multi-Criteria Analysis Shell for Spatial Decision Support) datapacks for distribution and storage. All input data to the model and by-products are stored on hard disk drives. All data are in the NARCliM coordinate system. The extent of the datasets includes the Murray-Murrumbidgee state planning region, ACT and South East and Tablelands with the boundary at top: –32.671254, left: 143.317445, right: 150.745676, and bottom: –37.505077.

Where suitable, derived products (including spatial and tabular data) have been named using the NARCliM Impact Science – Directory and File Naming Convention. Where this is not applicable, descriptive product names have been applied to derived data. Refer to Appendix A for product details.

3. Results

3.1 Predicted impacts on biodiversity

The BIAP analysis (Drielsma et al. 2015; Drielsma et al. 2017) of NARCliM and 3C climate futures reports that by 2070 CE, habitats in New South Wales will be 30–60% less suitable for the composition of species they currently support. Similar impacts are reflected in the alpine and surrounding areas of the full study region. It was found that near and far future climate change will most greatly impact biodiversity through the central part of the full study region, between Wagga Wagga and Griffith (Sections 3.3 and Appendix B, *B4. Climate ready metapopulation analysis*). Habitats in these areas have already been severely impacted by past land clearing (Sections 3.2 and Appendix B, *B1. Current vegetation condition*), limiting the capacity of species and ecosystems to respond successfully to climate change.

In the higher altitude areas of the Southern Ranges NPWS region, the greatest climate induced impacts are expected along the south-eastern extent and areas surrounding the ACT. Impacts on biodiversity in the KNP are expected to be relatively gradual when compared with other areas in the full study region; however, consequences for biodiversity are likely to be greater as suitable habitats for species and ecosystems are contracting with nowhere for new suitable habitats to emerge.

Table 5 summarises the results of this analysis for the 13 selected vegetation classes occurring in the Alpine region. Additionally, these results are presented as a series of charts and maps (Figure 6 to Figure 11). Table 6 and Table 7 provide summaries for the 11 threatened flora and 23 threatened fauna species selected for reporting (Section 2.5). These measure the current status of each vegetation class or habitat for each species, providing an indication of their adaptive capacity by assessing their current condition, level of fragmentation (EHA) and its contribution to habitat connectivity; how different future species composition within each class or habitat is likely to be under future climatic conditions; and the relative benefit of restoring or revegetating degraded habitat or maintaining the condition of relatively intact remnants.

3.2 Adaptive capacity of current vegetation classes

Current vegetation condition modelling (Appendix B, *B1. Current vegetation condition*) suggests that biodiversity in the central part of the full study region, while experiencing the greatest impacts from climate change, will also be less resilient to change due to the habitat loss and degradation that has already occurred. This was especially evident between Wagga Wagga and Griffith, where large areas of habitat have been removed or heavily modified (Figure 16), primarily to support agricultural production.

Overall, the lowest vegetation condition values were observed in agricultural land in the central and western parts of the full study region, and higher condition values were observed within the Southern Ranges NPWS region and the KNP (Figure 16). The more intact and connected habitats in the east of the full study region are expected to better support species and ecosystems responding to climate change.

The mean vegetation condition values for each of the 68 vegetation classes occurring in the full study region ranged from 33–86, from a possible range of 0–100. The condition of vegetation classes within KNP was generally the highest out of those in the full study region; however, this varies considerably. The mean condition values of the 13 vegetation classes selected for reporting (Table 5) ranged from 50–86 indicating they are currently in moderate (~50) to very good (>75) condition, suggesting a general capacity to remain resilient in the face of climate change.

Montane Lakes, Grassy Woodland, Montane Bogs and Fens had the lowest mean condition values (Table 5) suggesting their capacity to adapt to change in the near to far future is lower than the other selected vegetation classes. These classes will need considered management to protect them from future impacts of changing climate and to ensure the persistence of the species they support. Dry and Wet Sclerophyll Forests and Subalpine Woodlands have mean condition values of 71, 77 and 75 respectively, indicating that although they are not in a pristine state, being relatively intact they're likely to have more resilience to climate change with a greater likelihood of species persisting.

As with condition, EHA values vary greatly across the full study region, ranging from low (0) to high (98) (Figure 17), covering almost the full range of possible values (0–100). The 13 selected vegetation classes have mean EHA values ranging from 63–91 (Table 5), which are higher than their mean condition values, suggesting that while some degradation has occurred, they occur in areas with relatively well-connected and functionally-intact habitats.

The lowest EHA (Appendix B, *B2. Effective habitat area*) observed amongst the 13 selected classes was for Montane Lakes (mean EHA of 63). Grassy Woodlands, Montane Bogs and Fens and Dry Sclerophyll Forests had mean EHA values of 72, 77 and 78 respectively (Table 5). The remaining selected vegetation classes all have relatively good spatial context with mean EHA values above 80.

Out of the 13 selected vegetation classes, Montane Lakes, Grassy Woodlands, Dry and Wet Sclerophyll Forests and Montane Bogs and Fens have the lowest mean connectivity (Appendix B, *B3. Habitat connectivity*) values of 95, 111, 128 and 139 (out of a possible 255) respectively (Table 5). As a result, species (both flora and fauna) in these classes have limited ability to disperse through the landscape, reducing their capacity to reach emerging areas of suitable habitat and undertake successful migratory responses to climate change.

Out of the 13 selected vegetation classes, the resilience of Montane Lakes to future climate change is expected to be the most negatively impacted by surrounding habitat fragmentation and loss of connectivity. Their widespread but locally restricted nature is likely to compound climate change impacts by limiting access to emerging suitable habitats. The unique environmental characteristics associated with such habitats also limit the likelihood of similar environments capable of supporting propagules emerging under future climate.

Climate ready metapopulation analysis (Appendix B, *B4. Climate ready metapopulation analysis*) undertaken for the 3C project identifies areas in the study region that are relatively stable under climate change and support depleted (highly cleared or degraded) ecosystems into the future, or have the capacity to passively transition between depleted ecosystems by allowing colonisation and unhindered movement of biodiversity as BCC envelopes shift. Figure 19 shows a band of high value (green) that includes Griffith and Wagga Wagga indicating a functional 'climate corridor' with potential to facilitate the movement of species (and thus communities) from west to east. However, north–south movements are impeded by unsuitable environmental conditions and land uses in the western part of the study region.

3.3　　Impacts of climate change on vegetation classes

The significance of the Alpine region to the overall biodiversity of New South Wales is highlighted by the fact that more than one third of the state's BCCs are found in the full study region. Of the 250 BCCs covering the entire NARCliM extent, 79 were recorded between the far south coast and the western plains for the baseline period of 1990 to 2009 (Table 2).

The distribution of BCC envelopes is projected to change dramatically across the full study region in 2060 to 2079 relative to 1990 to 2009 (e.g. Figure 3); however, changes in BCC envelopes differ greatly under the 12 NARCliM scenarios. Across both climate futures, the most dramatic changes are consistently observed between Wagga Wagga and Griffith. In the higher altitude alpine areas, the velocity of change is slower, with smaller geographic shifts in BCC envelopes and transitions to relatively similar BCCs for both future periods; however, biodiversity represented by classes contracting at higher altitudes lacks emerging suitable habitats in the future. Along the alpine regions of New South Wales and the ACT, the greatest changes in BCC envelopes are predicted along the south-eastern, south-western and the northern edges of KNP.

In and around the alpine regions, BCC envelopes are mostly small in extent, and are predicted to move slowly and in multiple directions – influenced by terrain, with most shifts towards higher altitudes (see Figure 6). In comparison, on the mostly flat terrain further west, between Wagga Wagga and Griffith, BCC envelopes are larger in extent and they shift mostly southwards at a relatively rapid velocity, with some easterly movement on the south-west slopes between Wagga Wagga and the Alpine region.
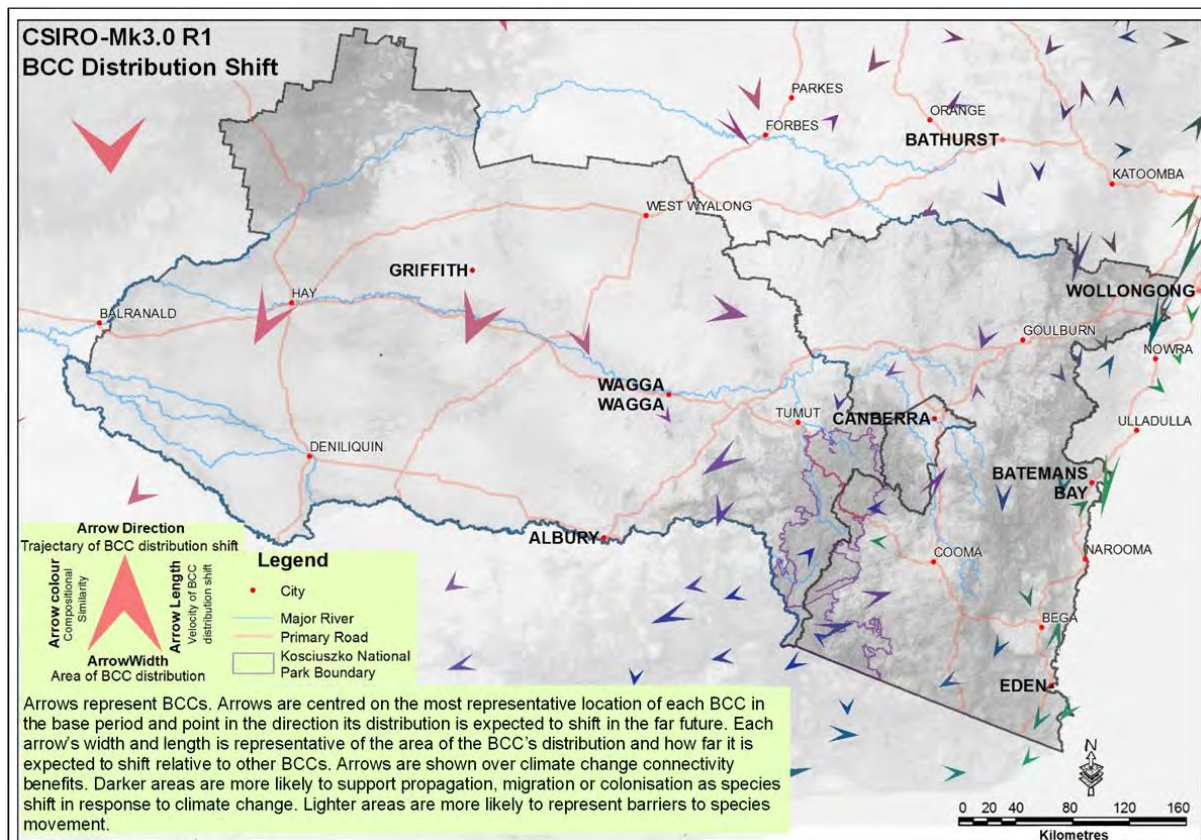

Figure 6　　**Bioclimatic Class envelopes shifting under the CSIRO-Mk3.0 GCM R1, shown as arrows representing their current extent (arrow width), trajectory (arrow directions) and relative velocity at which they're expected to shift (arrow length) under this scenario**

Figure 6 illustrates the dynamic process of BCC envelope distribution shifts based on the CSIRO-Mk3.0 GCM R1 model. Each arrow is located at the spatial centroid of the BCC envelope it represents for 1990 to 2009. The arrows point in the direction of the centroid's projected shift for 2060 to 2079, the arrow's length indicates the velocity of the shift (longer arrows indicating higher velocity) and its width represents the envelope's spatial extent for 1990 to 2009. The arrows pointing towards the KNP boundary show the shift of BCCs to higher altitudes (Figure 6). Arrows are shown over a base-map of 3C climate change connectivity (Appendix B, *B3. Habitat connectivity*). Darker areas have higher connectivity and are more likely to support actual propagation, migration or colonisation as BCC envelopes shift in response to climate change.

When existing vegetation class mapping is overlaid with BCCs, Montane Lakes, Alpine Herb fields, Southern Escarpment Wet Sclerophyll Forests, Southern Tablelands Grassy Woodlands, Montane Bogs and Fens and Southern Tableland Wet Sclerophyll Forests are most aligned with BCCs that are largely projected to decrease in area in the far future (Figure 5). This is because environmental conditions transition to those more suited to supporting Subalpine Woodland and Southern Tableland Dry Sclerophyll Forest. The BCC envelopes that are currently most aligned with Subalpine Woodland and Southern Tableland Dry Sclerophyll Forest are predicted to expand in the region accordingly.

In the KNP and surrounding high altitude areas of the Southern Ranges NPWS region habitats are expected to experience a slower decline in suitability for existing species and ecosystems than lower altitude western and coastal areas of the full study region (Figure 8 and Figure 9). This relative stability over time highlights the importance of the Alpine region for biodiversity conservation.

The compositional dissimilarity (Appendix B, *B5. Climate impacts – dissimilarity with baseline biodiversity*) of a location (grid cell) measures its expected change in species composition over time. Compositional dissimilarity values range from 0–1 and have been scaled here by multiplying by 1000. A location with a value of 0 indicates that no change in species composition is expected over the specified period, while a value of 1000 indicates that no species currently occurring at the location are expected to occur there in the future. The compositional dissimilarity (x1000) for the 13 selected vegetation classes averaged across the NARCliM models shows that in the near future (2020 to 2039) the greatest compositional changes are projected in the Montane Lakes, Grassy Woodlands, Montane Bogs and Fens (Table 5).

For the far future (2060 to 2079), the species composition of Montane Lakes, Montane Heaths, Wet and Dry Sclerophyll Forest, Grassy Woodland and Montane Bogs and Fens are projected to undergo greater change than other vegetation classes within the Alpine region (Table 5). The compositional dissimilarity for the extents of these classes for 2060 to 2079 relative to 1990 to 2009 ranges between of 300 and 600, with mean values between 400 and 500.

Grassy Woodland's projected compositional dissimilarity for 2020 to 2039 relative to 1990 to 2009 is 330, increasing to 420 for 2060 to 2079. Likewise, Escarpment Wet Sclerophyll Forest projected compositional dissimilarity for 2020 to 2039 relative to 1990 to 2009 is 330, increasing to 440 for 2060 to 2079. The compositional dissimilarity of Montane Lakes is also projected to change from 370 in 2020 to 2039 to 480 in the 2060 to 2079 projection period. The NARCliM models project that areas currently supporting Grassy Woodlands, Alpine Herbfields, Escarpment Wet Sclerophyll Forest and Montane Lakes will experience the greatest changes in species composition for 2060 to 2079.

The vegetation of the Alpine region is projected to remain relatively stable in composition for 2060 to 2079 when compared with vegetation across the full study region and further to the west, as well as other parts of New South Wales; however, future compositional dissimilarity is likely to result in greater species loss rather than distribution shifts as contractions of suitable habitat occur, and no new areas of suitable habitat emerge.

3.4 Vegetation management for climate change adaptation

Biodiversity benefits measure the benefit to regional biodiversity persistence that occurs if certain management is undertaken at each location (grid cell). Conservation benefits measure the outcome of retaining existing intact habitat, proportional to the avoided loss that would result from its removal. Revegetation benefits measure the gain that would result from revegetating or actively restoring the species that would have occurred or are likely to occur in areas of degraded habitat. These benefits consider the representativeness and condition of habitat at each location (grid cell), and how well connected it is to other surrounding habitat (up to a 5 km radius). They also consider changes in species composition under the future climate projections and the resulting change in benefits up to 2050 (Drielsma et al. 2015).

Within the selected vegetation classes, mean conservation benefit values (Appendix B, *B6. Conservation manage benefits*) were lowest for Montane Lakes, Alpine Herbfields, Alpine Heaths, Montane Bogs and Fens (Table 5). This suggests that despite the long-term threat to these ecosystems, there is relatively less urgency to undertake conservation action in these areas due to a slower rate of change relative to that impacting other vegetation classes. However, this does not imply that species and ecosystems represented in these vegetation types are not under threat. Conservation benefits increase in higher altitude areas from the 2000 baseline to 2050. This trend is likely to continue beyond 2050 and these vegetation types will face ongoing pressure.

Under current management and future climate, Montane Lakes and Grassy Woodlands will benefit the most from revegetation (Table 5) relative to the other selected vegetation classes, due to their current level of condition and fragmentation. The highest revegetation benefits (Appendix B, *B7. Revegetation benefits*) in the full study region occur further west where a greater proportion of the original habitat has been lost or degraded. Between now and 2050, the expected benefits from conservation actions only increase, not decrease, across the full study region (Appendix B, *B8. Relative change in benefits*), indicating increasing pressure on biodiversity from climate change, and therefore an increasing need to undertake actions intended to benefit regional biodiversity persistence.

Important alpine habitats with benefits already in the upper range are increasing disproportionally in relation to habitats in lower slopes and the plains to the west. This highlights the increasing role for alpine areas in biodiversity conservation. As BCCs shift altitudinally in response to increasing temperatures, these areas will need to accommodate retreating climate refugees from other areas, while also remaining the last refuge of species that already depend on alpine environments. As these areas act as climate refugia, they are likely to become increasingly important for regional biodiversity conservation.

The least change in benefits occurs in the central part of the full study region where high levels of habitat loss and degradation have already occurred. These are areas where the benefits to be gained from retaining remaining intact habitat and restoring heavily cleared and degraded habitat types are already relatively high but increase less over the period to 2050, relative to other areas (including higher altitude areas such as KNP). Biodiversity investment in these areas would provide the greatest benefit now and in the future; however, there is less change in the relative benefit of conserving or revegetating habitats in these areas, much of which are likely to remain under agricultural land uses.

Table 5 **Measures used to assess the biodiversity impacts of climate change showing mean values for the 13 selected vegetation classes**

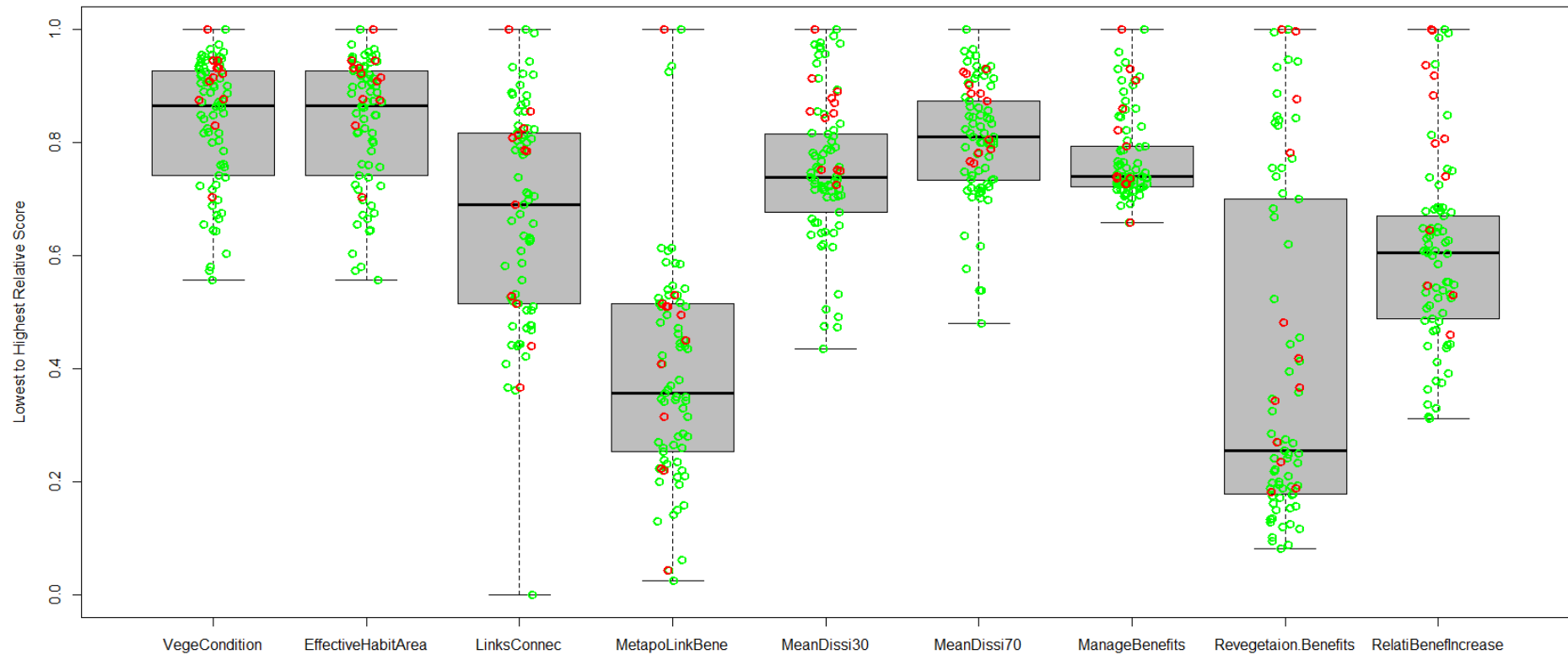| Vegetation class	Area (ha)	Vegetation condition (0–100)	Effective habitat area (0–100)	Habitat connectivity (0–255)	Meta-population links (0–1000)	Composition dissimilarity 2020–2039 change (0–1000)	Composition dissimilarity 2060–2079 change (0–1000)	Conservation benefits 2060–2079 change (0–255)	Revegetation benefits 2060–2079 change (0–255)	Benefits change 2050 change (0–1000)
Alpine Bogs and Fens	40,431	79	85	153	826	245	231	81	43	409
Alpine Fjaeldmarks	175	86	90	150	467	224	287	87	25	405
Alpine Heaths	71,781	77	84	147	742	244	320	77	46	407
Alpine Herbfields	39,113	74	83	145	833	260	344	77	56	384
Montane Bogs and Fens	12,625	68	77	128	693	325	414	79	76	281
Montane Lakes	2,906	50	63	95	516	365	476	73	124	249
Montane Wet Sclerophyll Forests	78,119	80	86	140	640	253	366	80	46	348
Southern Escarpment Wet Sclerophyll Forests	195,275	81	86	150	834	332	438	82	47	297
Southern Montane Heaths	8,281	77	84	144	795	353	448	87	58	279
Southern Tableland Dry Sclerophyll Forests	692,644	96	78	128	693	330	429	93	78	248
Southern Tableland Grassy Woodlands	105,231	63	72	101	545	330	424	85	92	226
Southern Tableland Wet Sclerophyll Forests	197,288	77	83	139	721	318	415	87	57	280
Subalpine Woodlands	366,619	75	82	141	798	274	379	83	59	333

Figure 7 **Box plot showing the 1st and 3rd quartiles and the mean values of vegetation classes within the nine different biodiversity variables assessed**

All variables have been standardised to between 0 and 1. The open green circles show all 68 vegetation classes within the full study region, and the red open circles show the 13 selected vegetation classes.

Figure 8 **Compositional dissimilarity for 2020 to 2039 relative to 1990 to 2009 averaged across NARCliM models (CSIRO-Mk3.0 R1, CCCMA3.1 R1 R2 R3, ECHAM5 R1 R2 R3 and MIROC3.2 R1 R2 R3)**

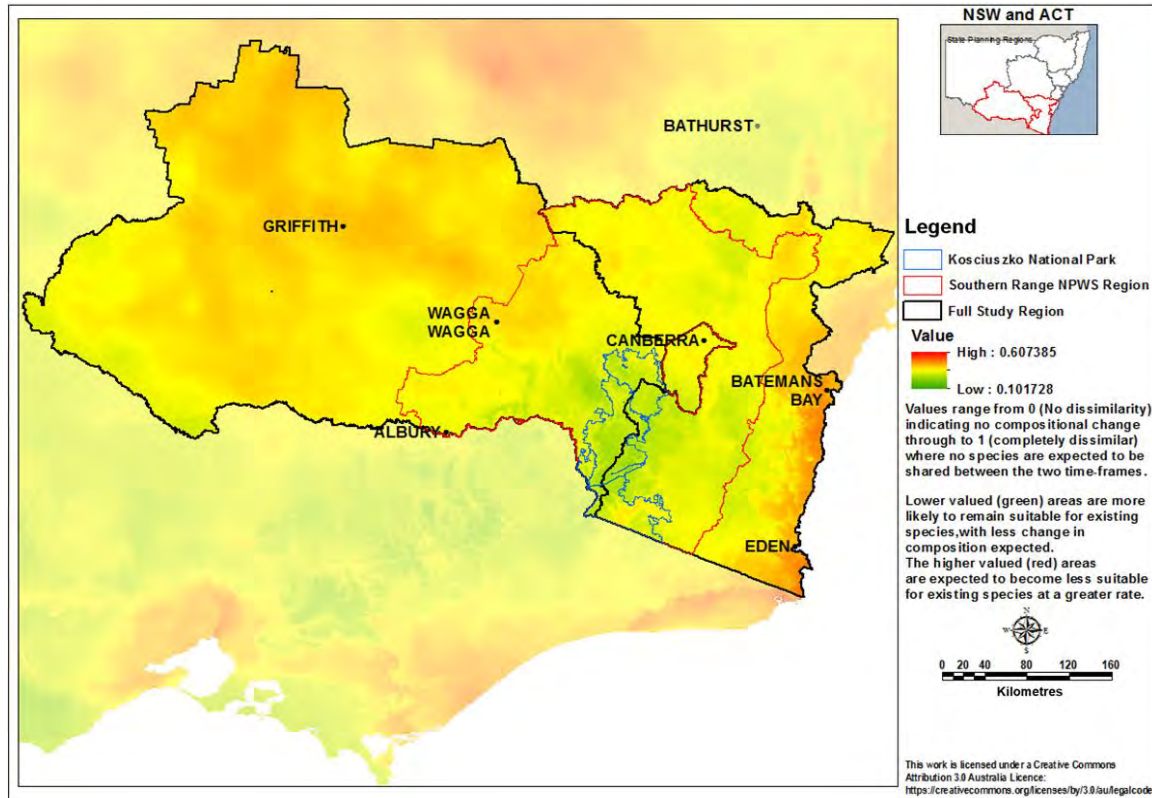**Figure 9** **Compositional dissimilarity for 2060 to 2079 relative to 1990 to 2009 averaged across NARCliM models (CSIRO-Mk3.0 R1, CCCMA3.1 R1 R2 R3, ECHAM5 R1 R2 R3 and MIROC3.2 R1 R2 R3)**
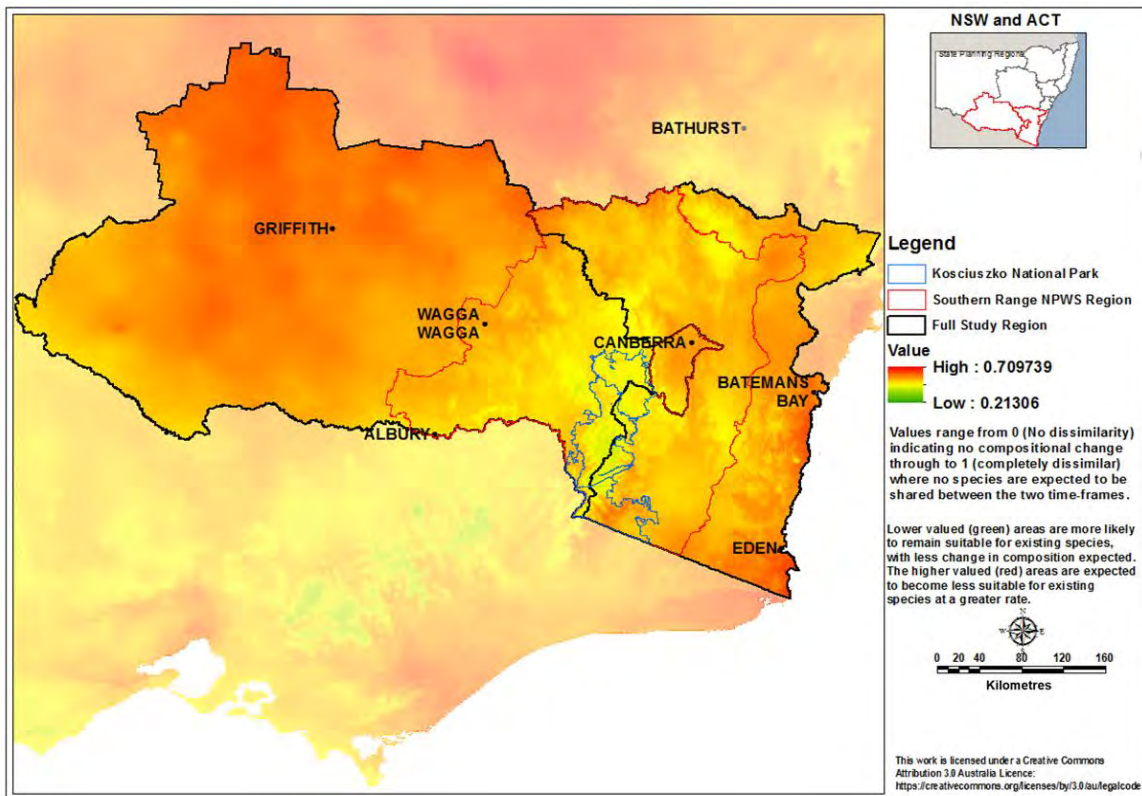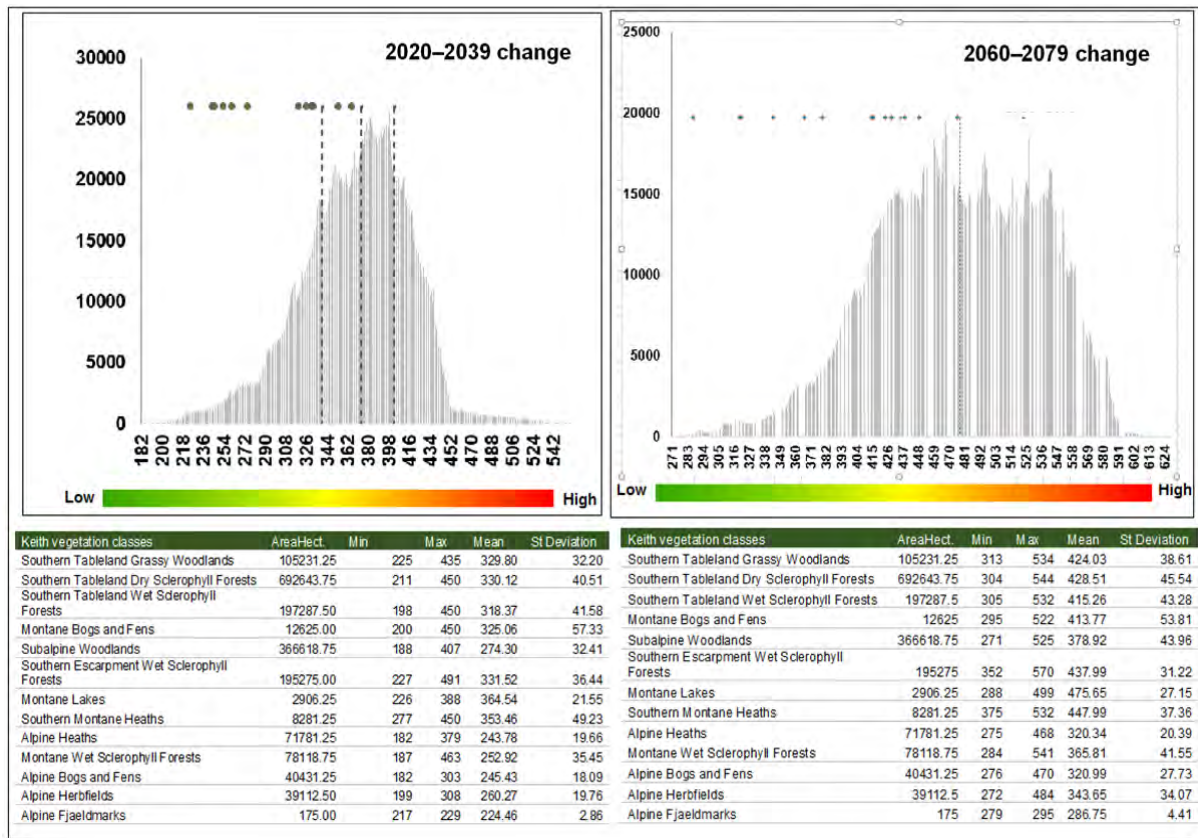
Figure 10   Charts showing the distribution of mean compositional dissimilarity values (x1000) for 2020 to 2039 relative to 1990 to 2009 (left) and 2060 to 2079 relative to 1990 to 2009 (right)

The open circles above the charts show the spread of selected vegetation class mean values as shown in the table below the charts, and the dotted lines within the histograms show the mean, 1st and 3rd quantiles of the two mean dissimilarity raster layers.
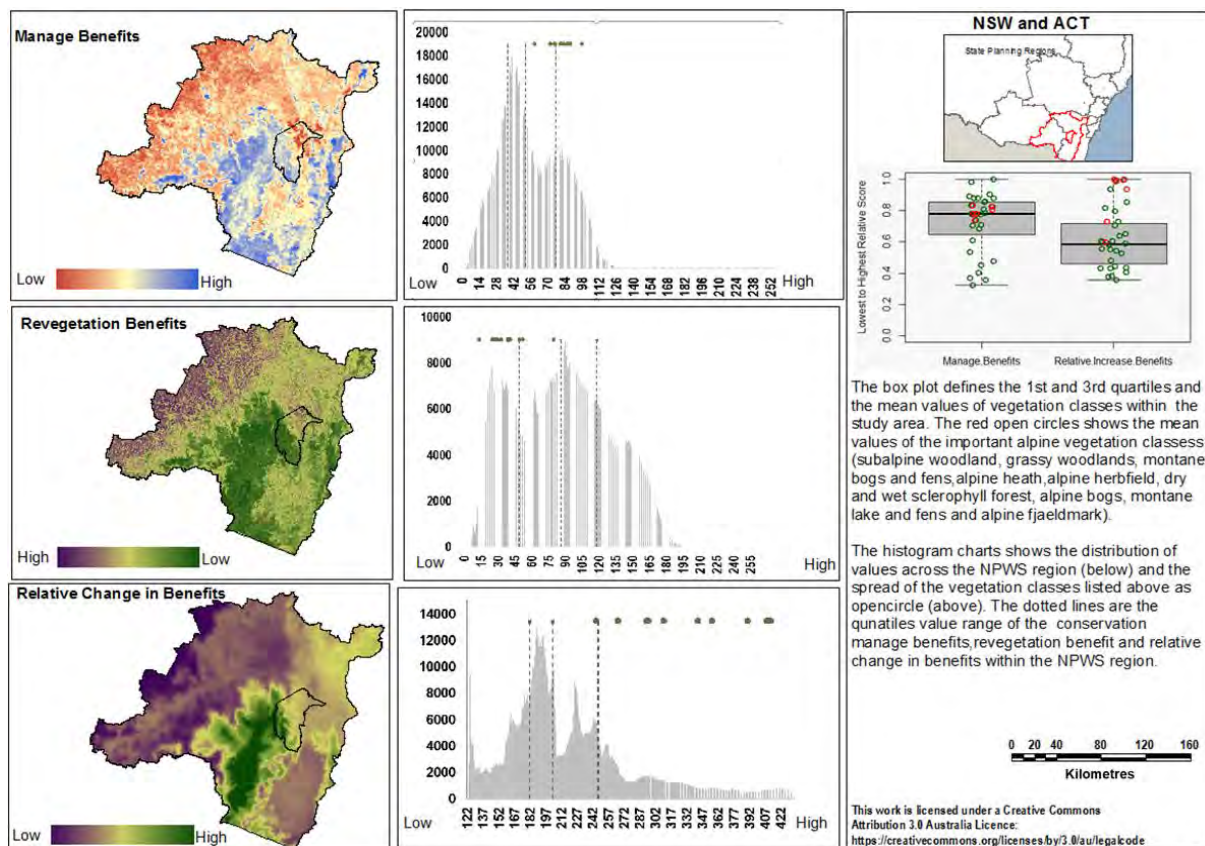
Figure 11   **Maps and charts showing the distribution of values within conservation benefits, relative change in benefits and CSIRO-Mk3.0 layers for 2060 to 2079 relative to 1990 to 2009**

The open circles in the box plot are the spread of the selected vegetation classes mean values and the dotted lines within the histograms are the quantiles of the three raster layers (left-hand corner).

3.5   Predicted impacts on threatened flora

Threatened floral species that are in further danger from future climate change within the Alpine region and selected for reporting in this study are listed in Table 3. Of these species, austral pillwort occurs in areas with the lowest mean vegetation condition (31) and lowest mean EHA (48), and also the lowest mean habitat connectivity (71). Austral pillwort also has the second highest dissimilarity (361) for 2020 to 2039, and highest dissimilarity (473) for 2060 to 2079 of these species (Table 6), indicating it has less intact suitable habitat remaining in its current environment and that its habitat is likely to become less suitable under climate change when compared with other threatened flora species. Likewise, cotoneaster pomaderris has a mean dissimilarity value of 363 projected for 2020 to 2039 (the highest of the selected species) and 462 for 2060 to 2079, suggesting its current habitat is also likely to become much less suitable in the far future projection period (Table 6).

All threatened flora in the Alpine region will need considered management plans that address the impacts of climate change. Where conditions supporting these species cease to exist, new conservation techniques that may challenge convention will be required. This may involve relocating to areas where future environmental conditions can support these species, though they may never have naturally occurred, selectively breading to produce individuals better able to adapt to future conditions, or in extreme cases, the preservation of specimens in artificial environments. As many endemic alpine species depend on a shrinking niche of environmental conditions, there will be increasing cases where conservation is not practical, and the acceptance of extinction becomes a more common reality.

3.6   Predicted Impacts on threatened fauna

A total of 164 threatened faunal species have been identified as occurring within the full study region (based on BioNet Atlas records). This comprises 93 bird species, 45 species of mammals, 14 species of amphibian, 10 reptiles, and two species of insects. The 23 threatened species under the greatest pressure from future climate change within the Alpine region, with a focus on KNP, are listed in Table 4. Some are endemic alpine species that are dependent on cold temperatures and adequate snow cover for their habitats. In terms of conservation, these species require concentrated attention. Currently, they occur in low numbers and this analysis suggests they are predicted to be impacted heavily by future climate change.

Species found in lower mean vegetation condition or effective habitat area are more likely to already be under pressure from habitat degradation or fragmentation. For species that occur in higher revegetation benefit areas, investment in increasing or improving habitat is likely to also benefit the representation or configuration of important native vegetation and improve regional biodiversity outcomes. Managing remaining good quality habitat for species in areas of high biodiversity benefits (see Appendix B, *B6. Conservation manage benefits* and *B7. Revegetation benefits*) is also expected to contribute to better regional biodiversity outcomes.

For those species located in areas of higher mean dissimilarity in both projection periods (Table 7), greater compositional change in their existing habitat is expected and the species or ecosystems they depend on may cease to exist in situ. These species will be under greater pressure to move to emerging suitable habitat or adapt to a changing environment. Where species occur in higher connectivity areas (Table 7), the landscape in which their habitat occurs may facilitate suitable dispersal and migration, allowing species to range-shift in response to changing environmental conditions.

For those species occurring in lower connectivity landscapes, bolstering or restoring lost connectivity will be more necessary to allow species to shift in response to climate change. Where this occurs in areas with high mean revegetation benefit values (Table 7), additional regional-scale biodiversity benefits are also likely to result. Where habitat fragmentation impedes the ability of species to respond to changing environmental conditions, other interventions such as translocation to emerging areas of suitable habitat may become necessary to avoid extinction.

Table 6 **Measures used to assess the biodiversity impacts of climate change showing mean values for selected threatened flora**

Threatened flora species	Vegetation condition (0–100)	Effective habitat area (0–100)	Habitat connectivity (0–255)	Composition dissimilarity 2020–2039 change (0–1000)	Composition dissimilarity 2060–2079 change (0–1000)	Conservation benefits 2060–2079 change (0–255)	Revegetation benefits 2060–2079 change (0–255)	Relative change in benefits 2050 change
Anemone buttercup	84	89	149	229	292	85	28	408
Austral pillwort	31	48	71	361	473	57	154	155
Cotoneaster pomaderris	76	82	139	363	462	94	66	243
Feldmark grass	95	93	155	223	289	95	13	404
Leafy anchor plant	69	78	134	274	391	75	69	347
Mauve burr-daisy	53	67	115	288	407	62	106	269
Monaro golden daisy	62	73	124	287	382	67	88	319
Pale pomaderris	61	71	107	355	471	90	100	233
Shining cudweed	85	90	160	233	296	87	28	412
Slender greenhood	83	87	142	293	385	95	50	292
Suggan buggan mallee	77	83	154	332	462	91	65	251

Table 7 **Measures used to assess the biodiversity impacts of climate change showing mean values for selected threatened fauna species**

Threatened fauna species	Vegetation condition (0–100)	Effective habitat area (0–100)	Habitat connectivity (0–255)	Composition dissimilarity 2020–2039 change (0–1000)	Composition dissimilarity 2060–2079 change (0–1000)	Conservation benefits 2060–2079 change (0–255)	Revegetation benefits 2060–2079 change (0–255)	Relative change in benefits 2050 change
Southern bell frog	33	51	66	369	490	67	157	158
Australian painted snipe	36	53	83	374	487	72	154	196
White-fronted chat	45	60	82	387	503	84	142	218

Threatened fauna species	Vegetation condition (0–100)	Effective habitat area (0–100)	Habitat connectivity (0–255)	Composition dissimilarity 2020–2039 change (0–1000)	Composition dissimilarity 2060–2079 change (0–1000)	Conservation benefits 2060–2079 change (0–255)	Revegetation benefits 2060–2079 change (0–255)	Relative change in benefits 2050 change
Glossy black-cockatoo	51	82	120	439	514	74	48	243
Brown treecreeper (eastern subspecies)	51	62	77	366	462	99	138	165
Dusky woodswallow	52	65	90	360	454	75	110	202
Hooded robin (south-eastern form)	54	65	88	370	478	96	127	183
White-bellied sea-eagle	56	69	81	447	520	67	76	227
Eastern quoll	56	69	96	294	434	98	94	297
Turquoise parrot	56	67	90	362	447	98	116	172
Booroolong frog	59	72	106	336	416	82	90	226
Southern myotis	63	71	101	412	501	86	93	217
Brush-tailed rock-wallaby	69	78	131	348	472	81	84	232
Spotted-tailed quoll	70	79	130	359	459	79	66	257
Eastern pygmy possum	75	81	122	368	461	78	53	257
Broad-toothed rat	76	84	146	263	343	78	52	386
Northern corroboree frog	76	84	131	303	357	80	52	332
Alpine tree frog	77	84	145	251	349	81	51	378
Mountain pygmy possum	78	85	144	249	326	77	44	396
Southern corroboree frog	78	85	153	237	315	79	45	415
Sooty owl	81	86	124	434	511	73	36	243
Smoky mouse	82	87	133	371	478	71	40	273
Alpine she-oak skink	83	87	156	236	308	84	39	415

3.7   Species occupancy modelled under climate change

The _Saving our Species_ program includes the modelling of projected changes in habitat suitability, occupancy and species persistence expected under projected NARCliM simulations for landscape managed threatened species.

While currently in progress, this work will deliver products that will aid in understanding and addressing the long-term needs of landscape managed species (see link above) occurring in the Alpine region of New South Wales. Outputs will highlight areas predicted to currently be or become important for one or more species and help direct management towards areas most likely to benefit the greatest number of species, or towards areas that reduce the greatest extinction risks.

Draft species occupancy models for the eastern pygmy possum showing combinations of three RCMs and four GCMs for 2020 to 2039 and 2060 to 2079 are shown in Figure 12 to Figure 15. The 1990 to 2009 baseline map provides a comparison. The modified scenario (Figure 12 and Figure 13) simulates current and future occupancy given extant vegetation in its current condition, while the pristine scenario (Figure 14 and Figure 15) simulates potential occupancy as if no loss of habitat condition has occurred.
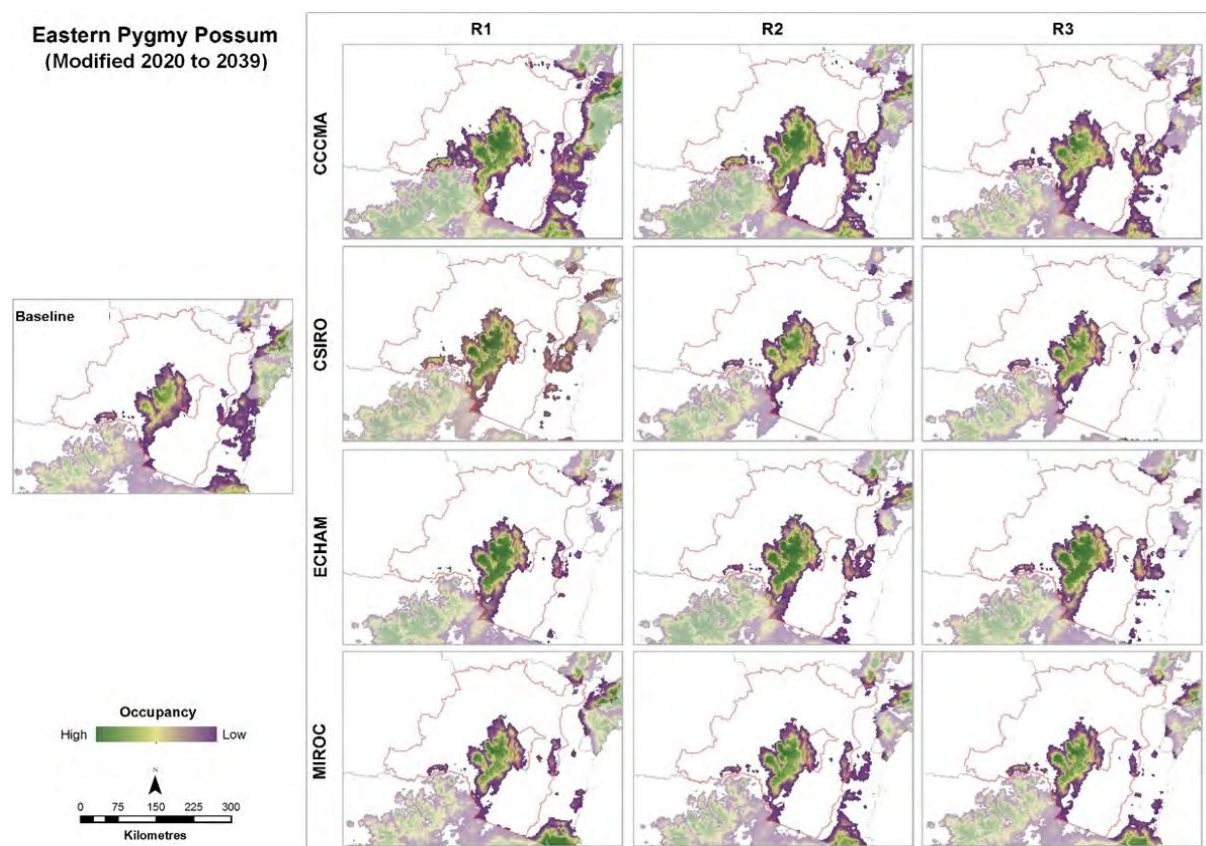

Figure 12   **Eastern pygmy possum occupancy modelled using modified (current) habitat for all NARCliM models (CCCMA3.1, CSIRO-Mk3.0, ECHAM5, MIROC3.2) for 2020 to 2039**

These early results project reductions in occupancy of eastern pygmy possum on the east coast in 2060 to 2079 when compared to the baseline and 2020 to 2039; however, the Alpine region is predicted to support higher levels of occupancy under all future scenarios. This model does not consider extreme events such as heatwaves and fire that could directly lead to high mortality, or indirectly through impacts on food resources.
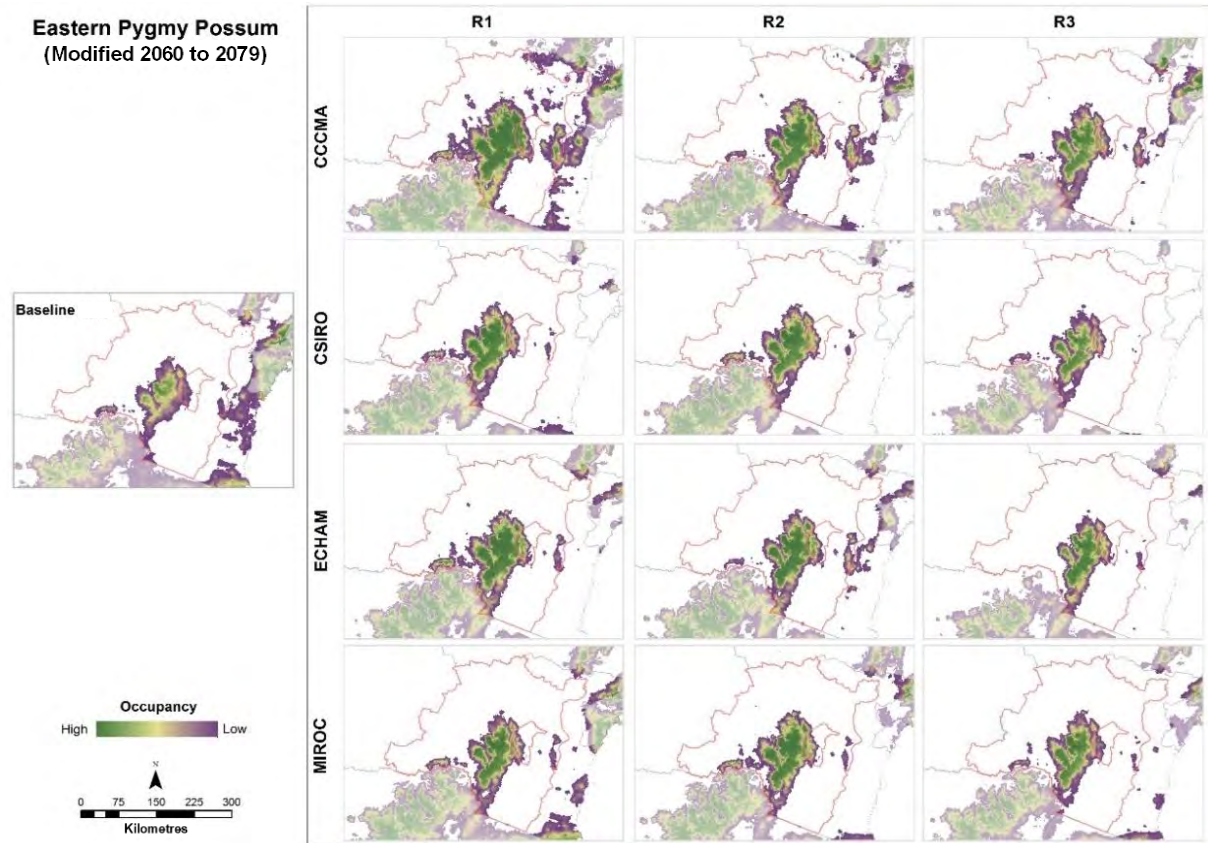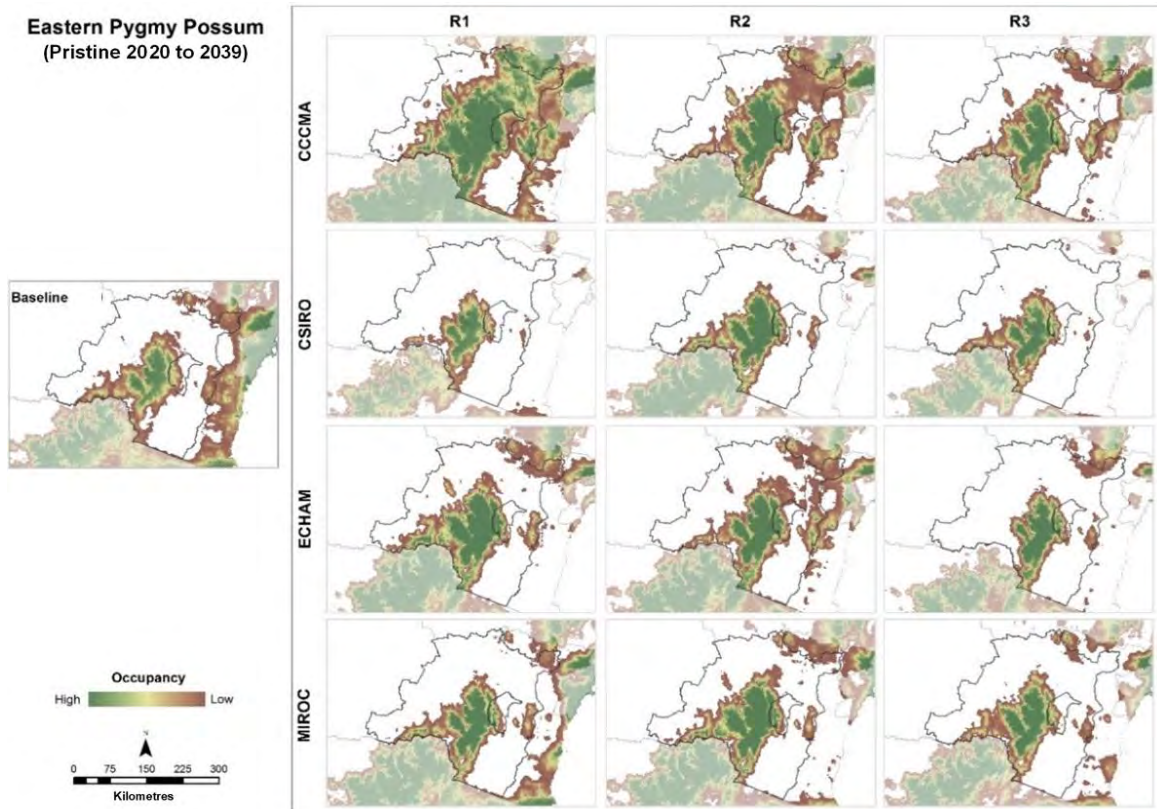
Figure 13 **Eastern pygmy possum occupancy modelled using modified (current) habitat for all NARCliM models (CCCMA3.1, CSIRO-Mk3.0, ECHAM5, MIROC3.2) for 2060 to 2079**

The comparison of modified and pristine scenarios allows areas to be identified that would likely support species populations now and into the future, if habitat condition had not been degraded. These are areas where environmental conditions are projected to be suitable for the species at some stage but where habitat has been fragmented or degraded beyond a threshold at which it's capable of supporting viable populations. These potential habitat areas highlighted by the pristine mapping (Figure 14 and Figure 15), are places where links between isolated existing habitat would also be beneficial in supporting persistence.

Figure 14 **Eastern pygmy possum occupancy modelled using unmodified (pristine) habitat for all NARCliM models (CCCMA3.1, CSIRO-Mk3.0, ECHAM5, MIROC3.2) for 2020 to 2039**
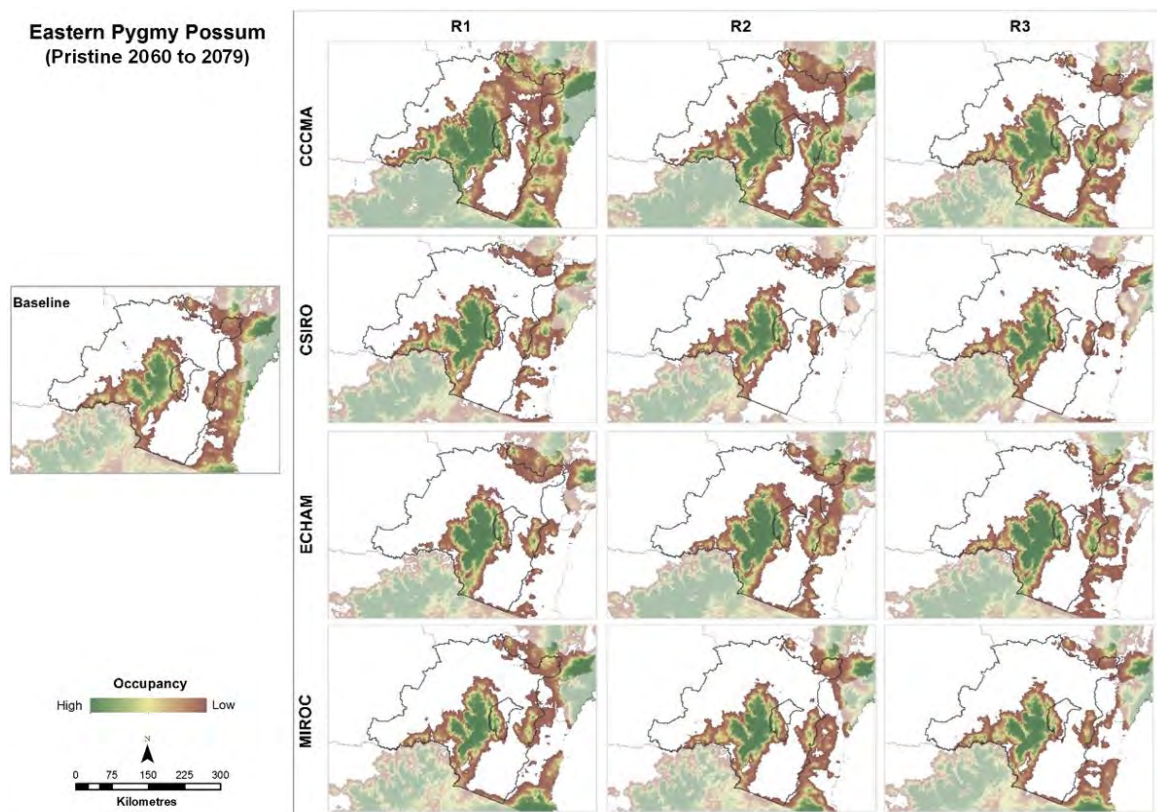
Figure 15 **Eastern pygmy possum occupancy modelled using unmodified (pristine) habitat for all NARCliM models (CCCMA3.1, CSIRO-Mk3.0, ECHAM5, MIROC3.2) for 2060 to 2079**

4.   Discussion

Ecosystem change is expected and is a normal part of the functioning of ecosystems (Likens 1992). These changes are rarely simple or linear in nature because responses to drivers of change are mediated through a range of interactions and feedbacks between biotic and abiotic components and processes (Pickett & White 1985; Sutherland et al. 2013). Ecosystems are characterised by self-organisation, hysteresis, non-linear dynamics and the potential for multiple stable states (Holling & Gunderson 2002; Walker & Salt 2012). While projected climate model simulations are somewhat uncertain, from the NARCliM climate projections available for New South Wales we can reasonably expect average and extreme temperatures and heatwaves will continue to increase in the Alpine region of the state, forcing ecosystems to fluctuate beyond their natural self-supporting states.

The BIAP projected a decline in overall biodiversity across New South Wales in the near future, with continuing losses into the far future. This decline results from the modelled geographic shifts of bioclimatic envelopes and reduced suitability of habitats for existing species and ecosystems (Drielsma et al. 2015; OEH 2016; Drielsma et al. 2017). Envelope shifts vary, sometimes significantly, across the 12 NARCliM climate simulations BIAP assessed. Despite this variability, the BIAP work found that across different projection scenarios, NSW-wide biodiversity loss arising directly from climate change up to the 2060 to 2079 period could be comparable to the loss that has already arisen from land clearing and degradation post-European settlement (Drielsma et al. 2015).

The BIAP analysis found that the NARCliM simulations predominantly suggest an additional loss of biodiversity of around 8% by 2060 to 2079 resulting directly from bioclimatic shifts (OEH 2016). For 2060 to 2079, it is projected that some areas of New South Wales will be 30–60% less bioclimatically suitable for the species they currently support. Consequently, for populations to persist, species will need to either migrate or adapt, or otherwise rely on intervention (Aitken et at. 2008; Nogués-Bravo et al. 2018). The ability to persist depends on the viability of the existing populations, ongoing availability of suitable habitat and the capacity of landscapes to support change (Drielsma et al. 2015; OEH 2016; Drielsma et al. 2017).

Alpine vegetation communities are expected to experience between a 21% to 70% change in their habitat's bioclimatic suitability by the 2060 to 2079 period. The greatest impacts within this timeframe are expected to occur in the highly modified central parts of the broader study area, between Wagga Wagga and Griffith. Bioclimatic suitability in alpine areas is expected to change at a slower rate across the broader study area. Bioclimatic envelope shifts are predicted to be multi-directional, with shifts in the Alpine region and surrounding areas predominantly towards higher altitudes. In the western part of the study area between Wagga Wagga and Griffith, the shifts are mostly southwards, accompanied with more rapid and higher degrees of change (see Figure 6).

The 12 NARCliM GCM/RCM simulations show projected impacts to the distribution of BCC envelopes in the Alpine region differently and to varying extents; however, all project a decline in biodiversity resulting directly from changing climatic conditions (see Figure 20 to Figure 23). As dissimilarity increases (red tones), greater changes in species composition are expected to result. For 2020 to 2039 and 2060 to 2079, the most dramatic changes occur under the CCCMA3.1 (R1 to R3) hot/wet scenario (Figure 20). It is uncertain which, if any, of these models most accurately represents the future, but given the range of scenarios they cover and their general similarity in degree of impact, the importance of immediate and ongoing conservation actions is clear.

All 12 NARCliM GCM/RCM combinations assessed under BIAP show changes in every vegetation class across the full study region. The areas currently occupied by all 13 vegetation classes selected for reporting experience large changes in compositional suitability between the baseline and far future periods (see Figure 9). Vegetation classes as

they're currently known are unlikely to support all the same species they're currently associated with, and as future vegetation types, may be quite compositionally dissimilar to what they are now. They may also occupy different spaces in the landscape, either by contraction, expansion, or latitudinal or altitudinal shifts (Wearne & Morgan 2001; Howden et al. 2003).

Additional to the impacts presented here, many weeds in the Alpine region are listed as Key Threatening Processes (KTPs). Pickering and Hill (2007) identified eight common weeds in and around the Snowy Mountains, including *Acetosella vulgaris, Hypocharies radicata, Trifolium repens, Taraxacum officinale, Agrostis capillaris, Dactylis glomerat, Anthoxanthum odoratum* and *Achillea millefolium* that are unlikely to be eradicated and may even become more abundant under climate change. South-eastern and south-western edges of KNP and surrounding areas are predicted to have more weed invasion with future climate change. Thus, management strategies must focus on reducing the current impacts to biological assets in these areas, as they are also likely to experience greater biodiversity change than other areas of the Alpine region.

Other species interactions are also expected to be negatively influenced by climate change. There may be increased predation by foxes and cats associated with warmer temperatures and decreasing snow cover (Hughes 2011). The impact of other feral animals, including pigs and horses may also increase with temperature as new areas become more environmentally suited to their habitat requirements. The management strategies currently in place for various threatened species, such as those under the nine SoS management streams, (see NSW SoS website) will need to be reviewed and adapted to reflect such changes as they unfold.

4.1 Key findings

The key findings of the study report that vegetation classes in the Alpine region are predicted to be significantly impacted by climate change. Vegetation classes in the Alpine region found to be most at risk from climate change are Montane Lakes, Alpine Herbfields, Wet Sclerophyll Forests (including Escarpment and Montane) and Dry Sclerophyll Forests, Grassy Woodlands, Montane Bogs and Fens, and Subalpine Woodlands. These vegetation types are those most likely to need direct intervention to ensure their persistence through near and far climate futures.

Large changes in species composition are predicted for vegetation communities between the baseline and far future projection periods; for example, by 2060 to 2079, Alpine Herbfields, Montane Bogs and Fens, Escarpment Wet Sclerophyll Forests, Montane and Southern Tableland Sclerophyll Forests are expected to decrease in area. It is predicted the geographic areas these communities currently occupy will transition to environmental conditions more suited to Subalpine Woodlands and Dry Sclerophyll Forests, which are predicted to expand accordingly.

Key flora species are predicted to be impacted by future changes in climate, including plants currently listed as critically endangered, including the black-hooded sun orchid (*Thelymitra atronitida*), Kelton's leek orchid (*Prasophyllum keltonii*) and *Prasophyllum bagoense*. These critically endangered species will be under increasing pressure as climate change proceeds.

Other threatened flora species predicted to be impacted by future climate change are: pale pomaderris, suggan buggan mallee, feldmark grass, anemone buttercup, austral pillwort, mauve burr-daisy, slender greenhood, Max Mueller's burr-daisy, shining cudweed, leafy anchor plant, Monaro golden daisy, slender greenhood, Kiandra leek orchid. These threatened flora species may need extra management interventions in the near future for them to maintain viable populations.

Threatened fauna species that are predicted to be impacted most from future climate change include southern myotis, hooded robin (south-eastern form), spotted-tailed quoll, sooty owl,

southern bell frog, glossy black cockatoo, white-fronted chat, brush-tailed rock-wallaby, dusky woodswallow, booroolong frog, eastern pygmy possum, mountain pygmy possum, southern and northern corroboree frog, white-bellied sea eagle, broad-toothed rat, smoky mouse, Australian painted snipe, and turquoise parrot. Thus, these threatened species may need to be managed in new ways if they are to be preserved.

Subalpine Woodlands, Alpine Heaths and Herbfields, and Alpine Bogs and Fens are habitat for several species of frogs listed as critically endangered. These vegetation classes also provide habitat for the endangered alpine she-oak skink (*Cyclodomorphus praealtus*) and the Guthega skink (*Liopholis guthega*). It is predicted that the southern corroboree frog (*Pseudophryne corroboree*) and alpine tree frog (*Litoria verreauxii alpina*) will also be severely impacted.

4.2   Limitations and further research

Our understanding of how biodiversity will respond to future climate change is still developing. Uncertainty and future improvements in the climatic models will affect the results we present here; for example, changes in rainfall cannot be reliably predicted. Fires are likely to be a major agent of change, but fire events and their severity cannot accurately be predicted. New climate projections will continue to move the baseline forward as actual events supersede prediction. Rigorous long-term monitoring and research into the magnitude and velocity of change will allow us to better understand the biodiversity impacts in areas such as the Alpine region (Biggs et al. 2009; Lindenmayer & Likens 2010). Improved understanding of environmental trends together with ongoing physio-ecological observation will help direct efforts to restore and maintain overall functioning of alpine ecosystems. A range of mitigation and adaptation strategies are needed now and into the future to ensure that as new challenges become apparent, they can be addressed.

This study does not consider further degradation or modification of the landscape, or similarly, positive management actions, including ecological restoration that may be undertaken. Rather, vegetation condition is modelled as of 2012 and kept static to allow the impacts resulting directly from climate change to be assessed. Biodiversity is likely to face compounding pressures as influencing anthropogenic factors interact with emerging impacts resulting from climate change, such as fire, severe storms and erosion. As such, other factors that are likely to influence the persistence of biodiversity need to be taken into consideration, along with the results of this study. Collectively, impacts are likely to be much greater than those reported here, and ongoing work is needed to monitor changes and trends in habitat status, and to understand how best to manage biodiversity as emerging pressures arise.

5.   Conclusion

This study assessed broad-scale impacts of climate change on alpine biodiversity in the context of the full study region, and for different vegetation classes and individual threatened flora and fauna. These findings add to existing research available for supporting effective monitoring and management of alpine biodiversity under climate change. In accordance with other literature, this study found that ecosystems in the Alpine region are predicted to be highly vulnerable to the impacts of climate change, as many species are endemic and depend on cold temperatures and adequate snow cover for their habitats. These habitats exist at the edge of environmental gradients that are likely to contract as climate changes, without new areas of environmentally suitable conditions emerging. However, this study finds alpine areas to be somewhat buffered from immediate impacts as the rate of change is expected to be slower than that in other parts of New South Wales, such as the western and central parts of the full study region. The relative intactness of alpine areas will also provide some opportunities for species to migrate in response to climate change, utilising higher altitude habitats where these exist. Although the pace of change in the higher altitude areas is predicted to be slower than in other parts of the state, the consequences are also expected to be greater, as ultimately, there is nowhere for biodiversity to migrate beyond mountain tops as temperatures increase. This will present unique challenges to the task of conserving alpine biodiversity.

As conditions are predominantly expected to become warmer and drier, the montane lakes, bogs and fens of the high country will be under increasing threat just from changes in climatic conditions alone. The same conditions are likely to place grassy woodlands and dry sclerophyll forests under greater threat from increasing severity and occurrence of bushfires. It is important these habitats are managed now with future conditions in mind as their maintenance will influence their utility as species move and adapt, or whether invasive colonisations occur, further altering their composition and structure, and consequently their capacity to persist. Ongoing monitoring of how ecosystems respond to change is needed to understand and address such challenges as they arise. How successful these responses are will depend on the adaptive capacity of ecosystems with some inherently less able to cope due to historic depletion, shrinking or rapidly changing climate niches, therefore more susceptible to transformation, whereas others, whether through greater intactness or tolerance, will be better equipped to absorb these impacts. Areas where habitats have suffered most to date from human modification, such as through the central part of the full study region, are predicted to be the same areas that experience the quickest and most severe effects of climate change.

Although the Alpine region is likely to be buffered from the most severe effects within the timeframe covered by this study, it is important to acknowledge that impacts will continue to unfold beyond this period, some of which may be managed or averted, while others will represent real and irreversible biodiversity loss, further reinforcing the need for immediate, ongoing and adaptive management, to ensure the best outcome we can for the unique, diverse and important biodiversity of the Alpine region.

6.   References

Aitken SN, Yeaman S, Holliday JA, Wang T and Curtis-McLane S 2008, Adaptation, migration or extirpation: climate change outcomes for tree populations, *Evolutionary applications*, vol.1, no.1, pp.95–111.

Biggs R, Carpenter SR and Brock WA 2009, Turning back from the brink: detecting an impending regime shift in time to avert it, *Proceedings of the National Academy of Sciences*, vol.106, pp.826–831.

Boulanger JP, Martinez F and Segura EC 2007, Projection of future climate change conditions using IPCC simulations, neural networks and bayesian statistics, Part 2: precipitation mean state and seasonal cycle in South America, *Climate Dynamics*, vol.28, pp.255–271.

Buytaert W, Celleri R and Timbe L 2009, Predicting climate change impacts on water resources in the Tropical Andes: The effects of GCM uncertainty, *Geophysical Research Letters*, vol.36.

Buytaert W, Cuesta-Camacho F and Tobón C 2011, Potential impacts of climate change on the environmental services of humid tropical Alpine regions, *Global Ecology and Biogeography*, vol.20, no.1, pp.19–33.

Chapin FSI, Kofinas GP and Folke C (eds) 2009, *Principles of ecosystem stewardship: resilience-based natural resource management in a changing world*, Springer, Berlin.

Crabb P 2003, *Managing the Australian Alps: A History of Cooperative Management of the Australian Alps National Parks*, Australian Alps Liaison Committee and Australian National University, Canberra.

Dollar ESJ, James CS, Rogers KH and Thoms MC 2007, A framework for interdisciplinary understanding of rivers as ecosystems, *Geomorphology*, vol.89, pp.147–162.

Drielsma MJ and Ferrier S 2009, Rapid evaluation of metapopulation persistence in highly variegated landscapes, *Biological Conservation*, vol.142, no.3, pp.529–540.

Drielsma MJ, Ferrier S and Manion G 2007a, A raster-based technique for analysing habitat configuration: the cost-benefit approach, *Ecological Modelling*, vol.202, nos3–4, pp.324–332.

Drielsma MJ, Manion G and Ferrier S 2007b, The spatial links tool: automated mapping of habitat linkages in variegated landscapes, *Ecological Modelling*, vol.200, no.3, pp.403–411.

Drielsma MJ, Love J, Manion G and Barrett TW 2010, *Great Eastern Ranges vegetation condition modelling project report, spatial analysis of conservation priorities in the Great Eastern Range*, NSW Department of Environment, Climate Change and Water, Armidale NSW.

Drielsma MJ, Howling G and Love J 2012, NSW native vegetation management benefits analyses – technical report, Office of Environment and Heritage (NSW), Sydney, NSW, www.environment.nsw.gov.au/resources/biodiversity/120905nvmtecrep.pdf.

Drielsma MJ, Ferrier S, Howling G, Manion G, Taylor S and Love J 2014, The biodiversity forecaster: answering the 'how much', 'what' and 'where' of planning for biodiversity persistence, *Ecological Modelling*, vol.274, pp.80–91, www.sciencedirect.com/science/article/pii/s0304380013005760.

Drielsma MJ, Manion G, Love J, Williams KJ, Harwood TD and Saremi H 2015, *3C modelling for biodiversity under future climate*, Office of Environment and Heritage, Sydney NSW.

Drielsma MJ, Love J, Williams, KJ, Manion G, Saremi H, Harwood T and Robb J 2017, Bridging the gap between climate science and regional-scale biodiversity conservation in south-eastern Australia, *Ecological Modelling*, vol.360, pp.343–362.

Evans JP, Ekstrom M and Ji F 2012, Evaluating the performance of a WRF physics ensemble over South-East Australia, *Climate Dynamics*, vol.39, no.6, pp.1241–1258.

Evans JP, Ji F, Abramowitz G, Ekstrom M 2013a, Optimally choosing small ensemble members to produce robust climate simulations, *Environmental Research Letters*, vol.8.

Evans JP, Fita L, Argüeso D and Liu Y 2013b, Initial NARCliM evaluation, in Piantadosi J, Anderssen RS and Boland J (eds), *MODSIM2013, 20th International Congress on Modelling and Simulation*, Modelling and Simulation Society of Australia and New Zealand, December 2013, pp.2765–2771.

Evans J, Ji F, Lee C, Smith P, Argüeso D and Fita L 2014, Design of a regional climate modelling projection ensemble experiment–NARCliM, *Geoscientific Model Development,* vol.7, pp.621–629.

Fita L, Evans JP, Argüeso D, King AD and Liu Y 2016, Evaluation of the regional climate response to large-scale modes in the historical NARCliM simulations, *Climate Dynamics*, pp.1–15, doi: 10.1007/s00382-016-3484-x.

Forman RTT and Godron M 1986, *Landscape ecology*, Wiley and Sons, New York.

Hennessy K, Fitzharris B, Bates BC, Harvey N, Howden SM, Hughes l, Salinger J and Warrick R 2007, 'Australia and New Zealand', in ML Parry, OF Canziani, JP Palutikof, PJVD Linden and CE Hanson (eds), *Climate change 2007: impacts, adaptation and vulnerability. contribution of working group ii to the fourth assessment report of the intergovernmental panel on climate* change, Cambridge University Press, Cambridge, pp.507–40.

Holling CS and Gunderson LH 2002, 'Resilience and adaptive cycles', in L Gunderson and CS Holling (eds), *Panarchy: understanding transformations in human and natural systems*, Island Press Washington DC, pp.25–62.

Howden M, Hughes L, Dunlop M, Zethoven I, Hilbert D and Chilcott C 2003, *Climate Change Impacts on Biodiversity in Australia*, Outcomes of a workshop sponsored by the Biological Diversity Advisory Committee, Commonwealth of Australia, Canberra.

Hughes L 2011, Climate change and Australia: key vulnerable regions, *Regional Environmental Change*, vol.11, no.1, pp.189–195.

ISC, Independent Scientific Committee 2004, *An Assessment of Kosciuszko National Park Values*, NSW National Parks and Wildlife Service, Sydney.

IPCC 2000, *Special Report on Emissions Scenarios: A Special Report of Working Group III of the Intergovernmental Panel on Climate Change*, published for the Intergovernmental Panel on Climate Change by Cambridge University Press, Cambridge, UK.

IPCC 2007, *Climate change 2007: Impacts, adaptation and vulnerability*, Cambridge University press, Cambridge, UK.

Ji F, Ekstrom M, Evans JP and Teng J 2014, Evaluating rainfall patterns using physics scheme ensembles from a regional atmospheric model, *Theoretical and Applied Climatology*, vol.115, pp.297–304.

Ji F, Evans JP, Teng J, Scorgie Y, Argüeso D and Di Luca A 2016, Evaluation of long-term precipitation and temperature WRF simulations for southeast Australia, *Climate Research*, vol.67, pp.99–115, DOI 10.3354/cr01366.

Keith DA 2002, *A compilation map of native vegetation for New South Wales*, NSW National Parks and Wildlife Service, Hurstville.

Keith DA and Simpson CC 2017, *Vegetation formations and classes of NSW* (Version3.03-200MRASTER)- VIS_ID3848, portal.data.nsw.gov.au/arcgis/home/item.html?id=3c29d31b3243430db87ae66aefddb125.

Likens GE 1992, *The ecosystem approach: its use and abuse*, Ecology Institute, Oldendorf/Luhe, Germany.

Lindenmayer DB and Likens GE 2010, *Effective ecological monitoring*, CSIRO Publishing.

Love J, Saremi H, Robb J, and Moerkerken L 2017, *Mapping Habitat Connectivity in the Riverina Local Land Service Region – Technical Report*, NSW Office of Environment and Heritage, Sydney and NSW Riverina Local Land Service, Wagga Wagga.

Love J, Taylor S, Drielsma MJ, Rehwinkel R and Moyle K 2015, *Southern Rivers NRM Stream 1 Habitat and Connectivity Modelling Project – Technical Report*, NSW Office of Environment and Heritage, Sydney and NSW South East Local Land Service.

Lucas C, Hennessy KJ and Bathols JM 2007, *Bushfire weather in southeast Australia recent trends and projected climate change impacts*, CSIRO, Bureau of Meteorology and Bushfire CRC Report for the Climate Institute, Canberra.

Millennium Ecosystem Assessment 2005, *Ecosystems and human well-being: wetlands and water synthesis*, World Resources Institute, Washington, DC.

Morrison C and Pickering CM 2013, Limits to climate change adaptation: case study of the Australian Alps, *Geographical Research*, vol.51, no.1, pp.11–25

Nogués-Bravo D, Rodríguez-Sánchez F, Orsini L, de Boer E, Jansson R, Morlon H, Fordham DA and Jackson ST 2018, Cracking the Code of Biodiversity Responses to Past Climate Change, *Trends in Ecology and Evolution*, vol.33, no.10, pp.765–776.

OEH 2016, *Biodiversity impacts and adaptation project (final report) – NSW and ACT regional climate modelling project*, NSW Office of Environment and Heritage, Armidale NSW.

OEH and UNE unpub., 'Saving Our Species: Landscape-managed threatened species pilot modelling project – Final report', NSW Office of Environment and Heritage and University of New England, Armidale NSW.

Parsons M and Thoms MC 2007, Hierarchical patterns of physical-biological associations in river ecosystems, *Geomorphology*, vol.89, pp.127–146.

Pereira HM, Leadley PW, Proença V, Alkemade R, Scharlemann JP, Fernandez-Manjarrés JF, ... and Chini L 2010, Scenarios for global biodiversity in the 21st century, *Science*, vol.330(6010), pp.1496–1501.

Pickett S and Cadenasso ML 1995, Landscape ecology: spatial heterogeneity in ecological systems, *Science*, vol.269, pp.331–334.

Pickering CM and Hill W 2007, Roadside weeds of the snowy mountains, Australia, *Mountain Research and Development*, vol.27, pp.359–367.

Pickering C, Good R and Green K 2004, *Potential effects of global warming on the biota of the Australian Alps*, Australian Greenhouse Office, Canberra ACT.

Pickett STA and White PS (eds) 1985, *The ecology of natural disturbances and patch dynamics*, Academic Press, New York.

Skamarock WC, Klemp JB, Dudhia J, Gill DO, Barker DM, Duda MG, Huang XY, Wang W and Powers JG 2008, *A description of the advanced research WRF Version 3,* NCAR Technical Note, National Center for Atmospheric Research, Boulder Colorado, USA.

Sutherland WJ, Freckleton RP, Godfray HCJ, Beissinger SR, Benton T, Cameron DD, Carmel Y, Coomes DA, Coulson T, Emmerson MC, Hail RS, Hays GC, HODGSON DJ, Hutchings MJ, Johnson D, Jones JPG, Keeling MJ, Kokko H, Kunin WE, Lambin X, Lewis OT, Malhi Y, Mieszkowska N, Milner-Gulland EJ, Norris K, Phillimore AB, Purves DW, Reid JM, Reuman DC, Thompson K, Travis JMJ, Turnbull LA, Wardle DA and Wiegand T 2013, Identification of 100 fundamental ecological questions, *Journal of Ecology*, vol.101, pp.58–67.

Thapa R, Thoms M and Parsons M 2016, An adaptive cycle hypothesis of semi-arid floodplain vegetation productivity in the dry and wet resource states, *Ecohydrology*, vol.9, pp.39–51.

Turner MG 2005, Landscape ecology: what is the state of the science?, *Annual Review of Ecology, Evolution, and Systematics*, vol.36, pp.319–344.

VanDerWal J, Murphy HT, Kutt AS, Perkins GC, Bateman BL, Perry JJ and Reside AE 2013, Focus on poleward shifts in species' distribution underestimates the fingerprint of climate change, *Nature Climate Change*, vol.3, pp.239–243.

Walker B and Salt D 2012, *Resilience practice: building capacity to absorb disturbance and maintain function*, Island Press, Washington DC.

Wearne LJ and Morgan JW 2001, Recent Forest Encroachment into Subalpine Grasslands near Mount Hotham, Victoria, Australia, *Arctic, Antarctic, and Alpine Research*, vol.33, no.3, pp.369–377, DOI: 10.1080/15230430.2001.12003441.

Whalley R, Price J, Macdonald M and Berney P 2011, Drivers of change in the social-ecological systems of the Gwydir wetlands and Macquarie Marshes in northern New South Wales, Australia, *The Rangeland Journal*, vol.33, pp.109–119.

Wiens JA 1989, Spatial scaling in ecology, *Functional Ecology*, vol.3, pp.385–397.

Wolf EC, Cooper DJ, and Hobbs NT 2007, Hydrologic regime and herbivory stabilize an alternative state in Yellowstone National Park, *Ecological Applications*, vol.17, pp.1572–1587.

Worboys GL, Good RB and Spate A 2010, *Caring for our Australian Alps catchments, A climate change action strategy for the Australian Alps to conserve the natural condition of the catchments and to help minimise threats to high quality water yields*, Australian Alps Liaison Committee and Australian Department of Climate Change, Canberra.

Wu J 1999, Hierarchy and scaling: extrapolating information along a scaling ladder, *Canadian Journal of Remote Sensing*, vol.25, pp.367–380.

Appendix A Spatial data sources

Table 8   **Spatial data sources used as inputs to the alpine biodiversity impacts analysis**

Data source	Type	Figure	Reference	Retrieved from	Retrieval date
StudyAreaBND	Vector	Figure 1	NA	OEH Corporate (supplied)	29/05/2017
Southern Ranges NPWS Region Boundary	Vector	Figure 1	NA	OEH Corporate (supplied)	29/05/2017
Kosciuszko National Park	Vector	Figure 1	NA	OEH Corporate (supplied)	29/05/2017
BioClimatic_Class (BCC) envelopes	Grid	Figure 2, 3, 6	Drielsma et al. 2017	NARCLiM\9SecondAnalysis\Data\GDM\ClassGrids\ESRI\	6/07/2017
Keith vegetation classes	Grid	Figure 4, 5	Keith, D. 2002	Vegetation\VegClassification\ VegNSWMap_Keith_v3_E3848_VIS	18/09/2017
GDM_NARCliM climate models mean dissimilarity	Grid	Figure 8, 9	Drielsma et al. 2017	NARCLiM\9SecondAnalysis\Data\GDM\DissimilarityGrids\Calcs\dis_mean30	30/08/2017
Eastern pygmy possum occupancy	Grid	Figure 12–15	OEH unpub.	Currently unpublished	Currently unpublished
Statewide vegetation condition	Grid	Figure 16	Drielsma et al. 2017	3C\Products\DerivedProductsData\VegetationCondition2014	8/06/2017
Effective habitat area	Grid	Figure 17	Drielsma et al. 2017	3C\Products\DerivedProductsData\3c_eha	1/06/2017
Link benefits maps	Grid	Figure 18	Drielsma et al. 2015	3C\Products\DerivedProductsData\	20/09/2017
New3cMP	Grid	Figure 19	Drielsma et al. 2015	3C\Products\DerivedProductsData\	13/10/2017
GDM_NARCliM climate models	Grid	Figure 20–23	Drielsma et al. 2017	NARCLiM\9SecondAnalysis\Data\GDM\DissimilarityGrids\	6/07/2017
Conservation manage benefits	Grid	Figure 24	Drielsma et al. 2017	NARCLiM\9SecondAnalysis\3C_NARv2\ia_c	30/08/2017
Revegetation benefits	Grid	Figure 25	Drielsma et al. 2017	NARCLiM\9SecondAnalysis\3C_NARv2\ia_r	22/08/2017
Relative change benefits	Grid	Figure 26	Drielsma et al. 2017	3C\Products\DerivedProductsData\	13/07/2017
Threatened fauna	Vector	NA	NA	OEH Corporate Corporate\Themes\Biodiversity\Fauna\Fauna.gdb	5/09/2017
Threatened flora	Vector	NA	NA	OEH Corporate Corporate\Themes\Biodiversity\Flora\Flora.gdb	11/09/2017

Appendix B Spatial input details

The following sections provide additional details and statistics for each of the spatial products used to develop reported measures.

B1. Current vegetation condition

Vegetation condition modelling provides continuous condition values ranging from zero (complete removal/alteration of native vegetation) to 95 (near pristine state, see Figure 16). The model used assumes condition is static (as of 2012) and does not account for future changes in management. Where the current condition layer is being used in analysis the actual results may be worse than modelled, unless land management practices undergo positive change in the future. This study used the vegetation condition model derived for the whole of New South Wales as part of BIAP (Drielsma et al. 2012, OEH 2016). Vegetation type modelling, remotely sensed foliage projective cover (FPC), land use, tenure and expert derived soil resilience were used as surrogates for estimating the current condition of native vegetation. Land use, tenure and soil resilience were used to inform the model about changes in condition resulting from different management regimes.

Table 9   **Vegetation condition statistics for the 13 selected vegetation classes with the mean values used for reporting shown in bold**

		Vegetation condition			
Vegetation class	**Area (ha)**	**Min.**	**Max.**	**Mean**	**Std dev.**
Alpine Bogs and Fens	40,431	32	95	**79**	11.55
Alpine Fjaeldmarks	175	61	95	**86**	9.61
Alpine Heaths	71,781	37	95	**77**	9.40
Alpine Herbfields	39,113	13	95	**74**	10.53
Montane Bogs and Fens	12,625	9	92	**68**	14.52
Montane Lakes	2,906	29	81	**50**	8.43
Montane Wet Sclerophyll Forests	78,119	14	95	**80**	7.75
Southern Escarpment Wet Sclerophyll Forests	195,275	9	95	**81**	9.68
Southern Montane Heaths	8,281	13	92	**77**	11.23
Southern Tableland Dry Sclerophyll Forests	692,644	6	95	**71**	14.58
Southern Tableland Grassy Woodlands	105,231	4	95	**63**	17.65
Southern Tableland Wet Sclerophyll Forests	197,288	6	95	**77**	12.01
Subalpine Woodlands	366,619	7	95	**75**	11.01
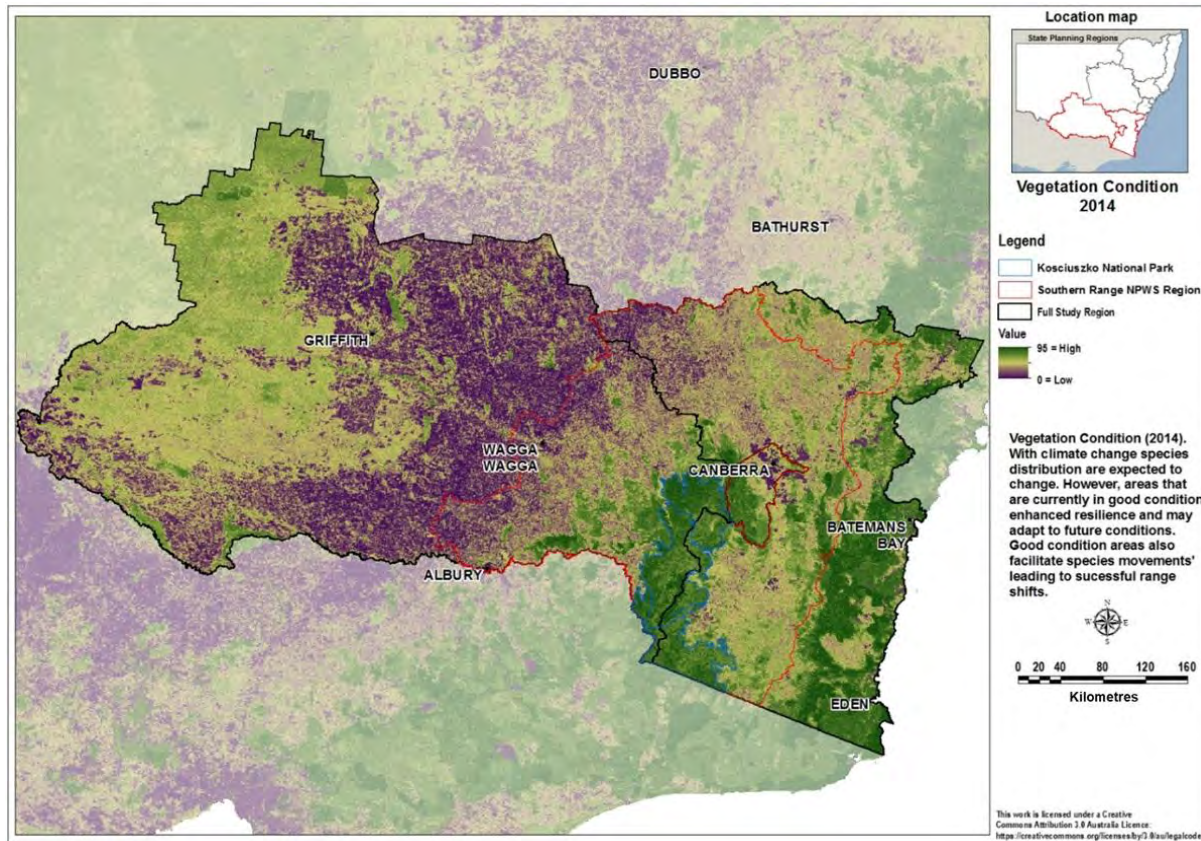
Figure 16   **Vegetation condition modelled for the NARCliM domain and shown for the full study region**

Condition values range from low (purple) to high (dark green).

B2. Effective habitat area

Effective habitat area (EHA) is a measure of habitat's spatial context (Figure 17), integrating ecological condition at each location (grid cell) with measures of its connectivity to, and the condition of, surrounding habitat. Maximum values are achieved in high condition habitat within large intact patches. Effective habitat area values are reduced through poorer condition at or within a five-kilometre radius of the site, or where degraded habitat reduces connectivity to neighbouring high condition areas.

Table 10   **Effective habitat area statistics for the 13 selected vegetation classes with the mean values used for reporting shown in bold**

Vegetation class	Area (ha)	Effective habitat area			
		Min.	Max.	Mean	Std dev.
Alpine Bogs and Fens	40,431	55	94	**85**	5.63
Alpine Fjaeldmarks	175	81	94	**90**	3.20
Alpine Heaths	71,781	66	94	**84**	3.76
Alpine Herbfields	39,113	51	94	**83**	4.92
Montane Bogs and Fens	12,625	39	92	**77**	8.51
Montane Lakes	2,906	53	89	**63**	4.01
Montane Wet Sclerophyll Forests	78,119	45	93	**86**	3.62
Southern Escarpment Wet Sclerophyll Forests	195,275	41	93	**86**	5.16
Southern Montane Heaths	8,281	44	92	**84**	6.53
Southern Tableland Dry Sclerophyll Forests	692,644	29	93	**78**	8.88
Southern Tableland Grassy Woodlands	105,231	28	91	**72**	10.27
Southern Tableland Wet Sclerophyll Forests	197,288	34	93	**83**	7.21
Subalpine Woodlands	366,619	38	93	**82**	6.24
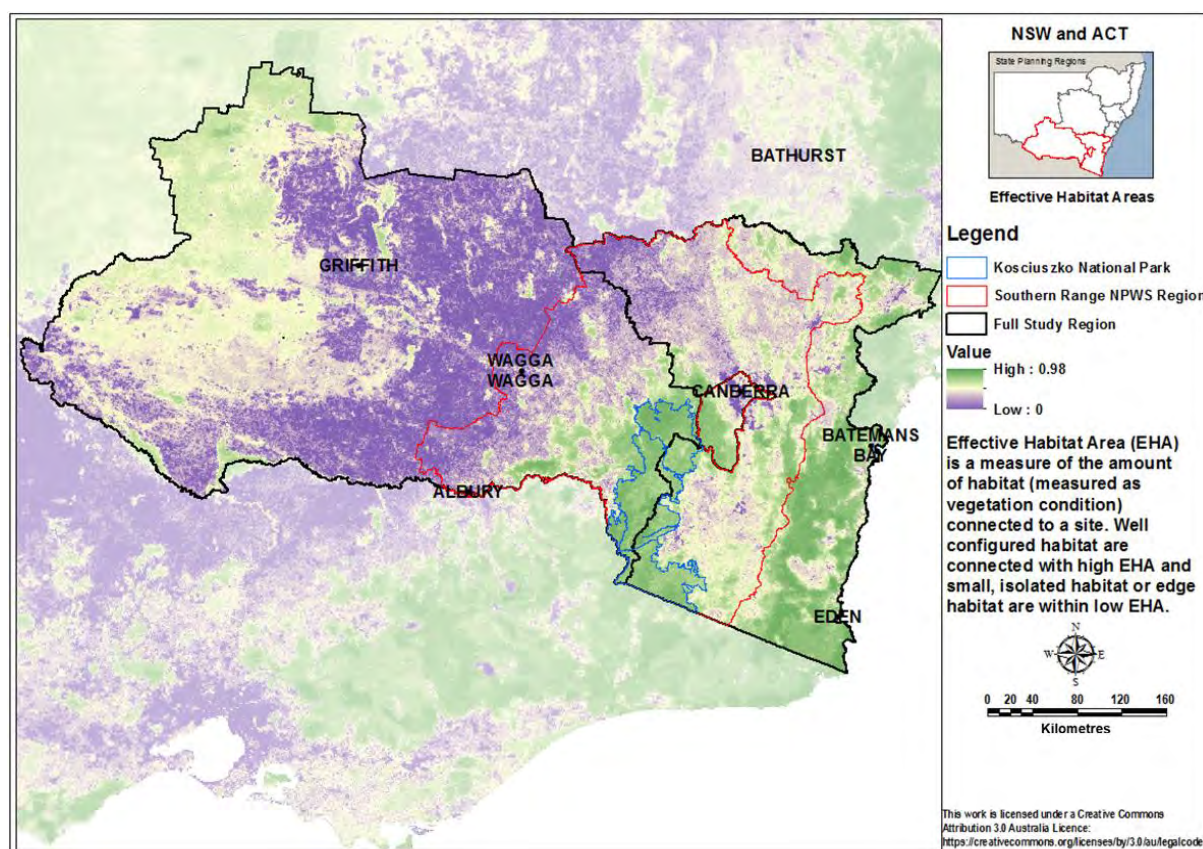
Figure 17   **Effective habitat area for the full study region**

Effective habitat area values range from low (0, purple) to high (98, dark green).

B3. Habitat connectivity

The links habitat connectivity map shows where the placement and structure of habitat is most likely to facilitate the movement of biodiversity through the landscape. Connectivity is modelled across a wide range of ecological scales to provide an unbiased evaluation of habitat connectivity independent of specific taxa, movement processes or timeframes. In this case, connectivity between habitat has been measured across spatial scales ranging from a few hundred metres to hundreds of kilometres.

Areas with higher connectivity are more likely to support propagation, migration or colonisation as species shift in response to changes in habitat suitability resulting from climate change. In contrast, lower connectivity areas are more likely to impede ecological movement as species and ecosystems respond to change. Areas having higher connectivity do not directly imply they have higher habitat condition. These areas can also include degraded locations that may not be colonised but will allow biodiversity to move through them to more suitable habitat due to their relative locality. Restoring or improving lost and degraded habitat in such areas is likely to help facilitate successful responses to climate change. Further loss of intact habitats that also provide connectivity should be avoided to prevent further impeding the capacity to respond.

Links habitat connectivity mapping (Figure 18) highlights areas where it is important to maintain or improve habitat connectivity to allow biodiversity to remain viable across the region.

Table 11   **Habitat connectivity statistics for the 13 selected vegetation classes with the mean values used for reporting shown in bold**

Vegetation class	Area (ha)	Habitat connectivity			
		Min.	Max.	Mean	Std dev.
Alpine Bogs and Fens	40,431	91	201	**153**	18.29
Alpine Fjaeldmarks	175	122	177	**150**	15.53
Alpine Heaths	71,781	107	199	**147**	15.00
Alpine Herbfields	39,113	94	193	**145**	13.71
Montane Bogs and Fens	12,625	58	205	**128**	24.60
Montane Lakes	2,906	62	156	**95**	15.11
Montane Wet Sclerophyll Forests	78,119	72	208	**140**	13.15
Southern Escarpment Wet Sclerophyll Forests	195,275	72	211	**150**	17.60
Southern Montane Heaths	8,281	70	193	**144**	16.14
Southern Tableland Dry Sclerophyll Forests	692,644	34	229	**128**	25.97
Southern Tableland Grassy Woodlands	105,231	24	184	**111**	27.06
Southern Tableland Wet Sclerophyll Forests	197,288	59	210	**139**	19.96
Subalpine Woodlands	366,619	58	218	**141**	18.83
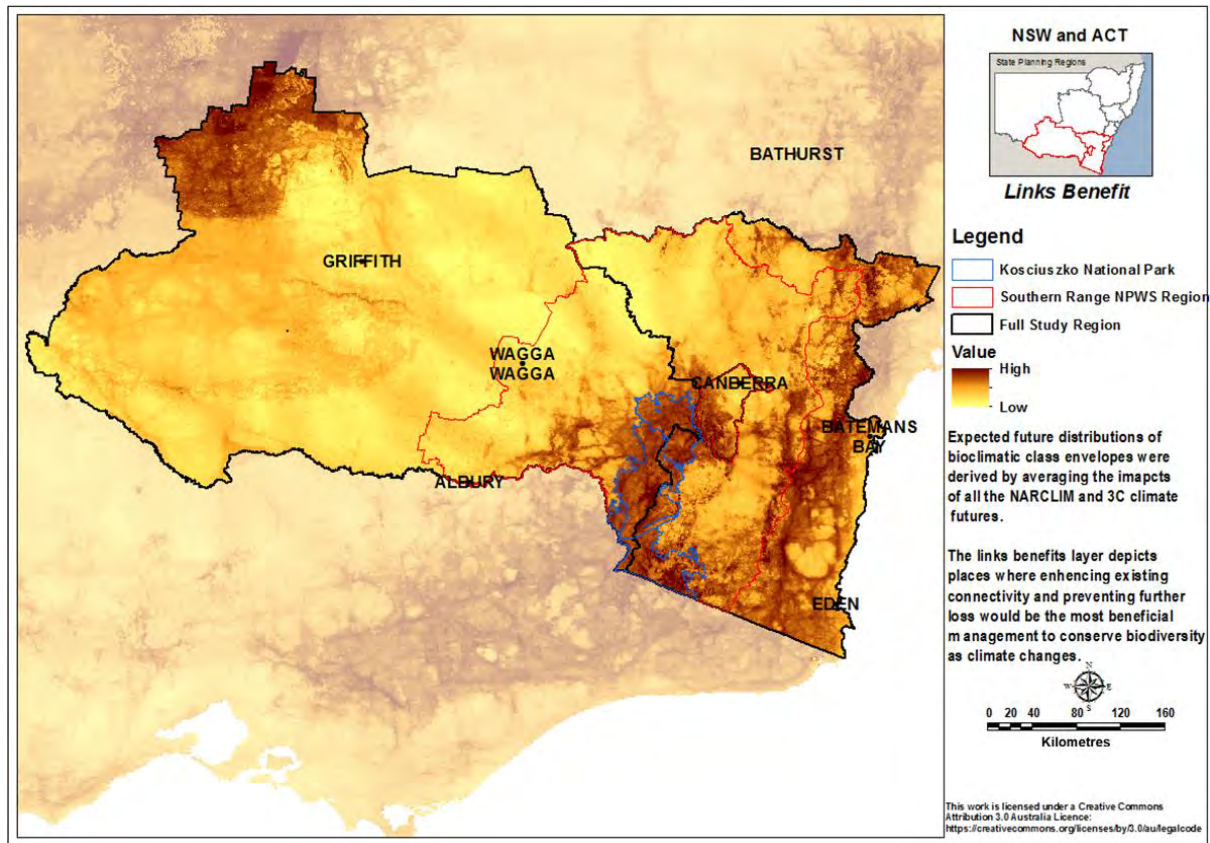
Figure 18   **Links habitat connectivity map depicting places where enhancing existing connectivity and preventing future loss will most benefit biodiversity conservation**

B4. Climate ready metapopulation analysis

Climate ready metapopulation analysis (3CMP) performed as a prototype under the 3C project (Drielsma et al. 2015) shows areas that will be able to support ecosystem diversity under predicted future climate change scenarios (Figure 19). Areas shaded green are either 1) relatively stable through climate change, supporting depleted (cleared or degraded) ecosystems; or 2) by their connectivity can passively transition between depleted ecosystems. Maintaining appropriate connectivity is an increasingly important component of effective conservation strategies, as species adapt to the impacts of climate change. The ability to move across the landscape to more suitable habitat as environmental conditions change will be vital to the persistence of many species.

3CMP is broadly based on the REMP methodology (Drielsma & Ferrier 2009). Consistent with that approach, occupancy is mapped across the region subject to the suitability, amount, quality and spatial pattern of habitat. In the context of climate change modelling, the 3CMP model is an early attempt at this style of modelling and was only performed using the MPI (RCP8.5) climate future from 2000 to 2050. The results at this stage are preliminary; therefore, these results have been given less focus here when reporting.
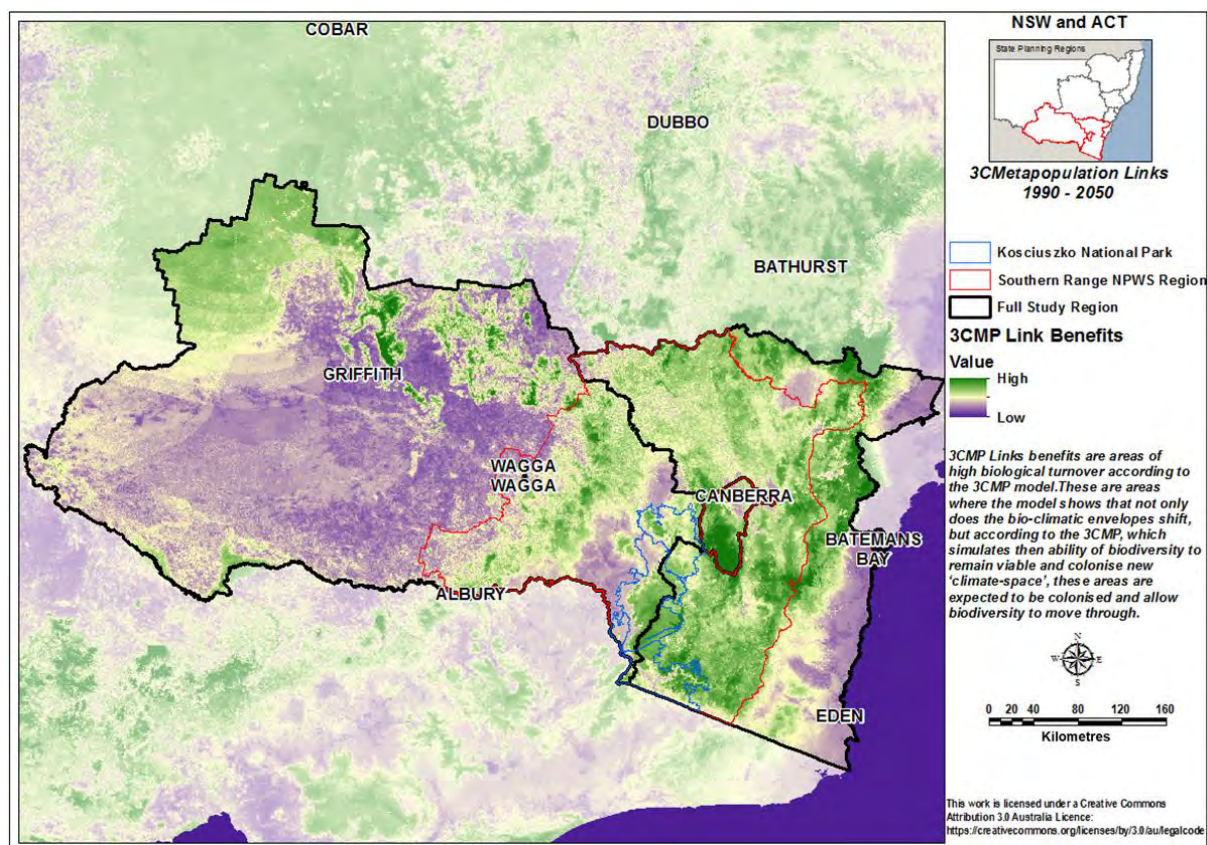
Figure 19 **3C metapopulation links, showing areas of expected migration, colonisation and temporal compositional turnover**

Greener areas support ecosystem diversity through expected future climate and are either stable through climate change or by virtue of their connectivity are able to passively transition to alternative ecosystems.

B5. Climate impacts – dissimilarity with baseline biodiversity

As climatic conditions change, species unable to tolerate or adapt to prevailing conditions are less likely to persist in situ and will more frequently be replaced by those better equipped and more able to colonise under future conditions, whether native or exotic. Species that can tolerate changing conditions will persist in situ for longer, forming the basis of novel emerging communities.

Future climate projections were used to estimate the dissimilarity in species composition between current and future climate projections at each location (grid cell). This provides a measure of how unsuitable each location will become for the composition of species it currently supports and how dissimilar the composition of species best suited to future conditions is, to that which currently occurs.

The dissimilarity in species composition was averaged for each location (grid cell) across each of the individual NARCliM GCM/RCMs (Figure 20 to Figure 23) using a multi-model mean for 2020 to 2039 relative to 1990 to 1990, and 2060 to 2079 relative to 1990 to 2009. Potential values can range from 0, indicating no compositional change (no dissimilarity), to 1 where no species are expected to be shared between the two time periods. These values have been multiplied by 1000 for reporting.
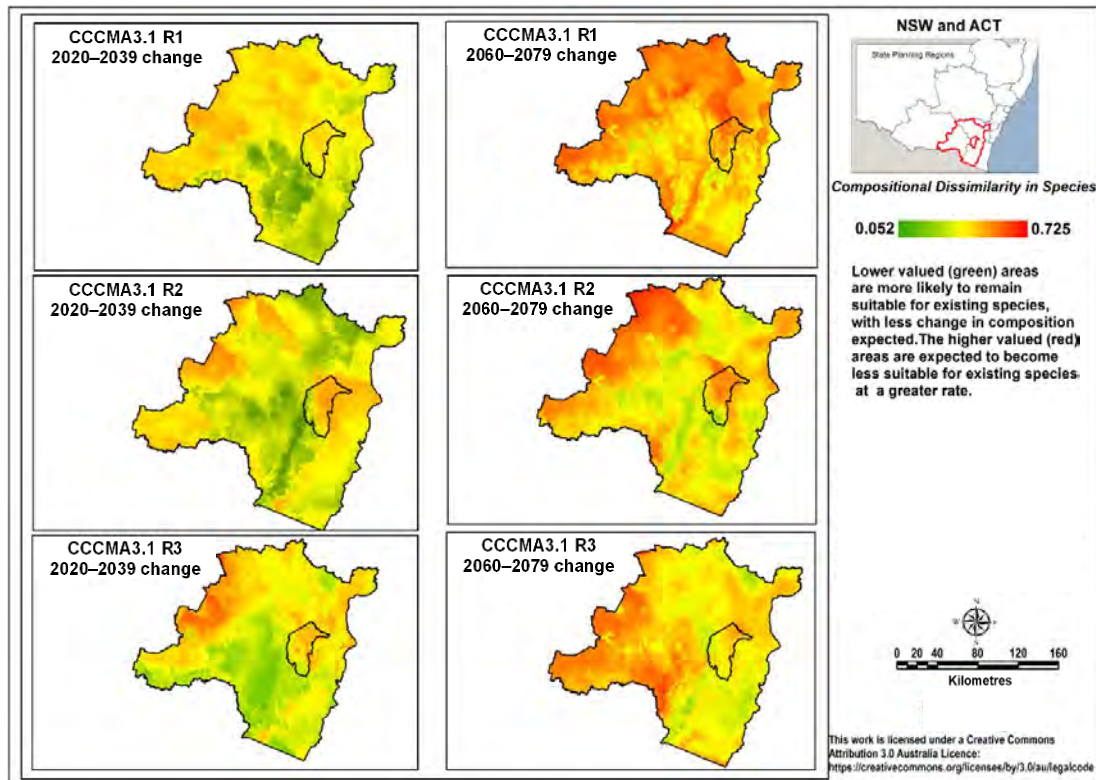
Figure 20 Compositional dissimilarity between transformed environmental variables for 2020 to 2039 relative to 1990 to 2009 (left column), and 2060 to 2079 relative to 1990 to 2009 (right column), at each location (grid cell) for the NARCliM CCCMA3.1 GCM and R1 (top), R2 (middle) and R3 (bottom) RCMs
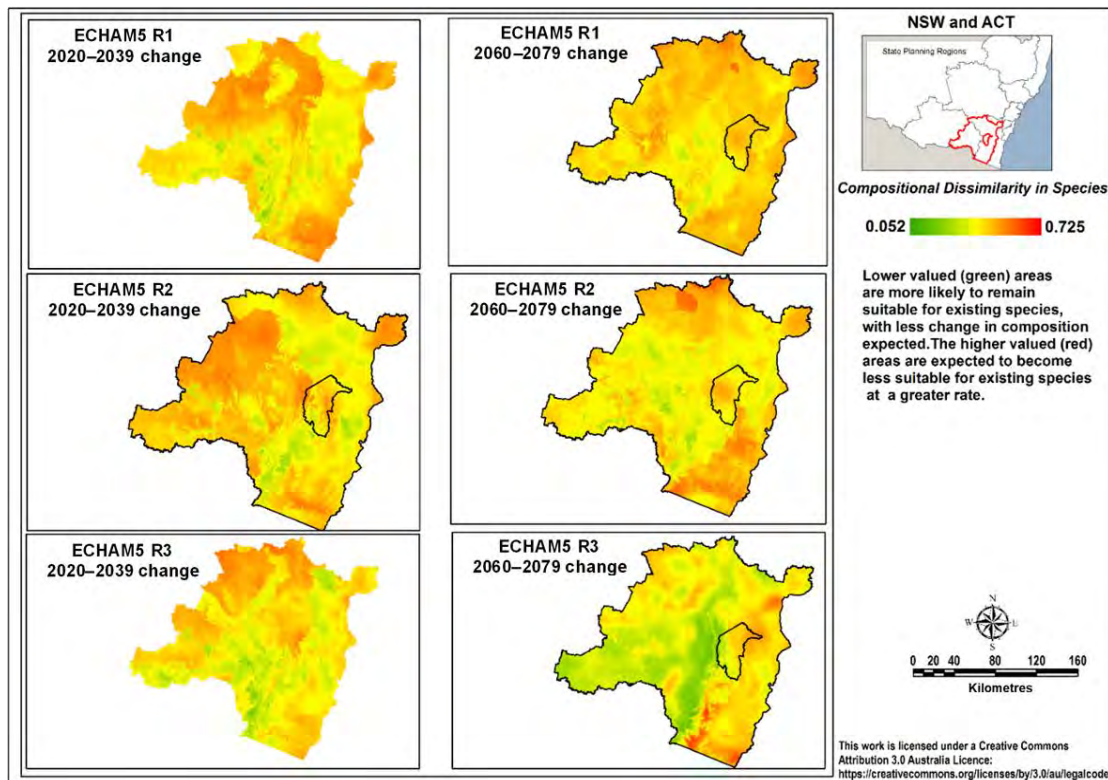
Figure 21 Compositional dissimilarity between transformed environmental variables for 2020 to 2039 relative to 1990 to 2009 (left column), and 2060 to 2079 relative to 1990 to 2009 (right column), at each location (grid cell) for the NARCliM ECHAM5 GCM and R1 (top), R2 (middle) and R3 (bottom) RCMs
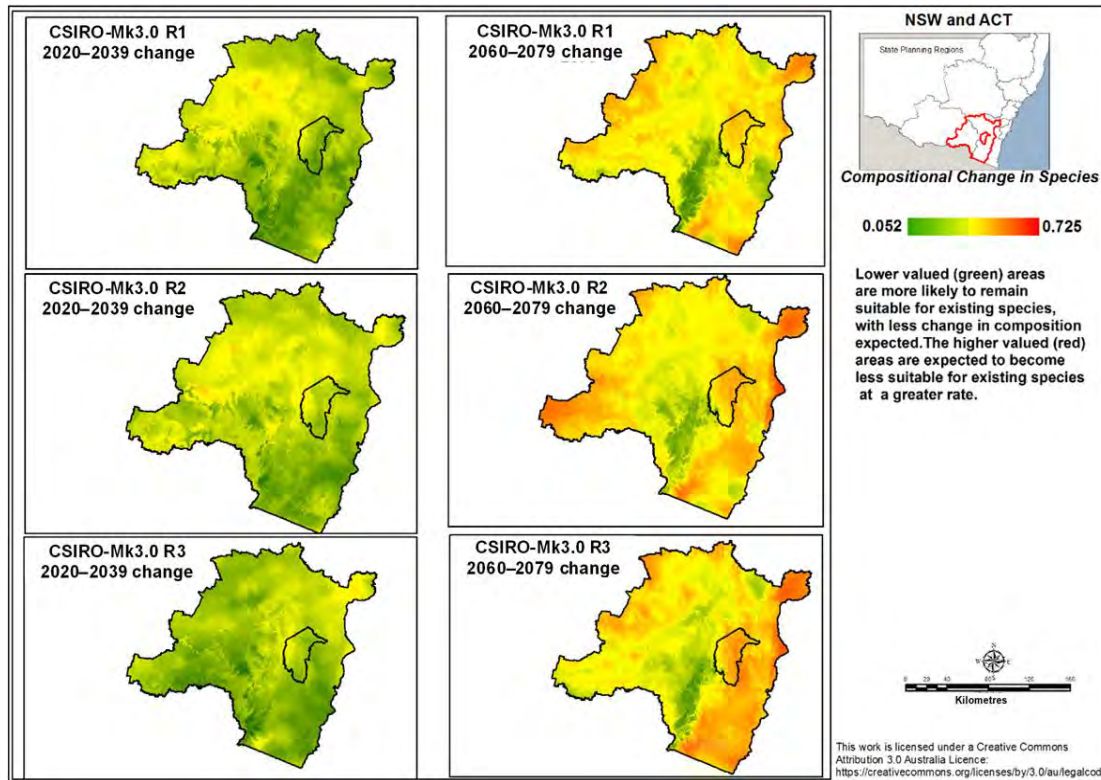
Figure 22 Compositional dissimilarity between transformed environmental variables for 2020 to 2039 relative to 1990 to 2009 (left column), and 2060 to 2079 relative to 1990 to 2009 (right column), at each location (grid cell) for the NARCliM CSIRO-Mk3.0 GCM and R1 (top), R2 (middle) and R3 (bottom) RCMs
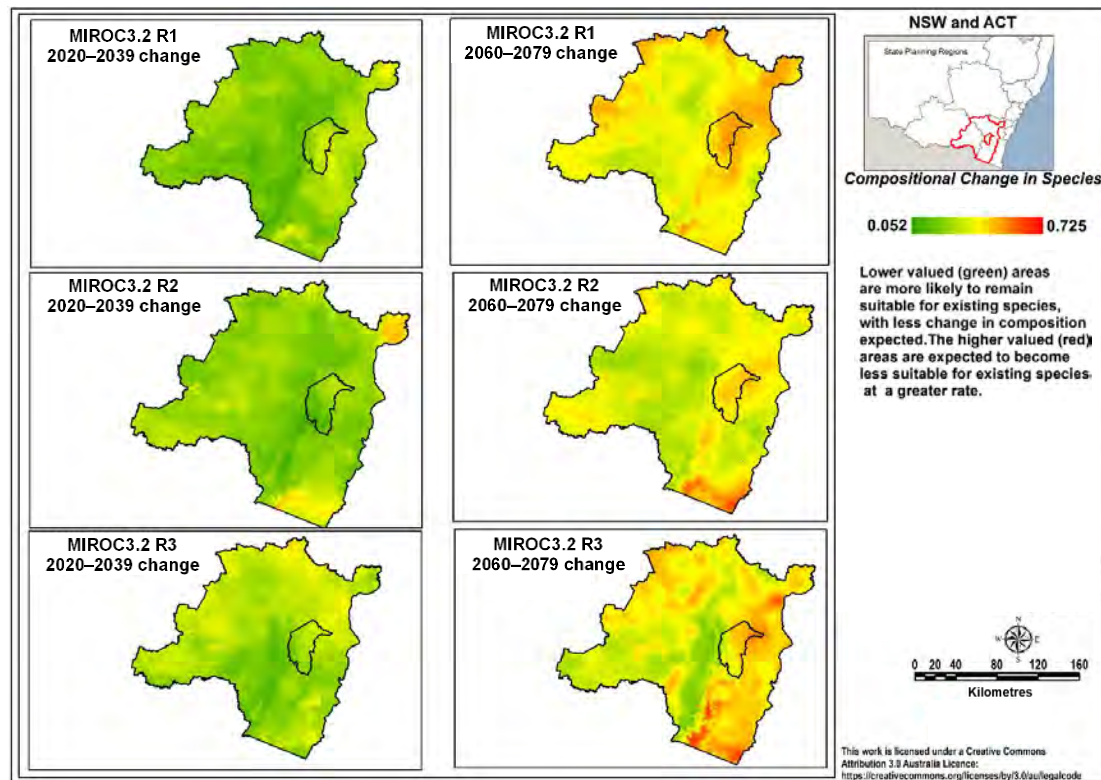
Figure 23 Compositional dissimilarity between transformed environmental variables for 2020 to 2039 relative to 1990 to 2009 (left column), and 2060 to 2079 relative to 1990 to 2009 (right column), at each location (grid cell) for the NARCliM MIROC3.2 GCM and R1 (top), R2 (middle) and R3 (bottom) RCMs

B6. Conservation manage benefits

Conservation manage benefits (Drielsma et al. 2014) measure the benefit to regional biodiversity persistence that occurs if existing intact habitat is retained at each location (grid cell), proportional to the avoided loss that would result from its removal. These benefits consider the representativeness and condition of habitat at each location (grid cell) and how well connected it is to other surrounding habitat (up to a 5 km radius).

Conservation manage benefits are most relevant to conservation efforts aimed at retaining relatively intact well-connected examples of habitat types that are not well represented in the contemporary landscape. These are often habitat types that have been largely cleared or degraded through past management; therefore, retain a lower proportion of their original extent and condition. Conservation manage benefits are designed to inform management actions such as reserve establishment and private land conservation that promote the maintenance of intact and well-connected habitats to protect remaining diversity.

Conservation manage benefit values for this study are scaled between 0 (low), where habitat has been completely degraded, to a maximum possible value of 255 (high), where less-well represented habitat types remain intact and well connected with surrounding habitat (Figure 24).

Table 12   Conservation manage benefits (1990 to 2009 to 2060 to 2079) statistics for the 13 selected vegetation classes with the mean values used for reporting shown in bold

Vegetation class	Area (ha)	Conservation manage benefits			
		Min.	Max.	Mean	Std dev.
Alpine Bogs and Fens	40,431	39	111	**81**	11.51
Alpine Fjaeldmarks	175	64	98	**87**	8.77
Alpine Heaths	71,781	42	111	**77**	8.90
Alpine Herbfields	39,113	23	108	**77**	10.49
Montane Bogs and Fens	12,625	16	127	**79**	16.20
Montane Lakes	2,906	48	103	**73**	10.25
Montane Wet Sclerophyll Forests	78,119	15	120	**80**	9.60
Southern Escarpment Wet Sclerophyll Forests	195,275	14	154	**82**	16.83
Southern Montane Heaths	8,281	21	129	**87**	13.69
Southern Tableland Dry Sclerophyll Forests	692,644	9	158	**93**	19.29
Southern Tableland Grassy Woodlands	105,231	12	159	**85**	23.10
Southern Tableland Wet Sclerophyll Forests	197,288	9	152	**87**	16.73
Subalpine Woodlands	366,619	13	130	**83**	12.92
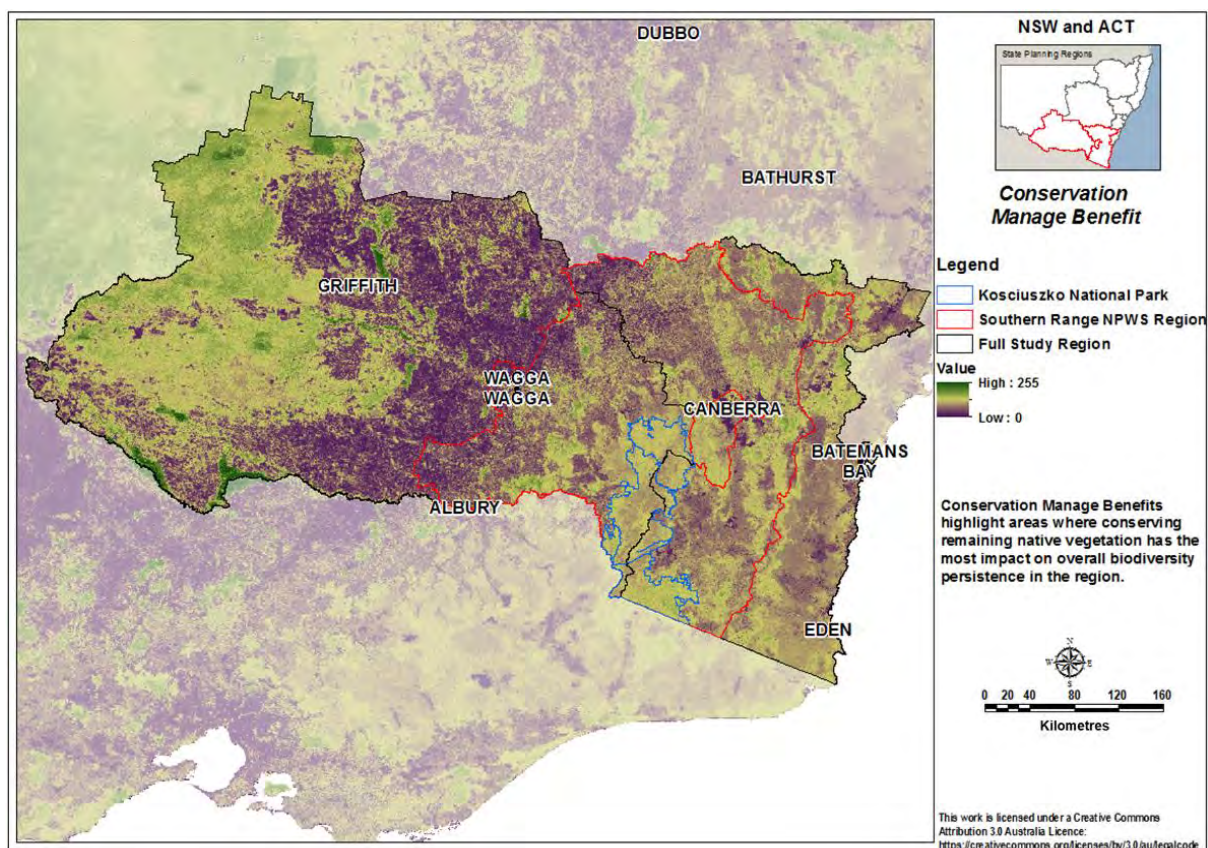
Figure 24　　Conservation manage benefits highlight areas where conserving remaining native vegetation has the most impact on overall biodiversity persistence in the region

B7. Revegetation benefits

Revegetation benefits identify degraded areas where replanting or the natural regeneration of species previously occurring (or expected to occur under future climate) will have the greatest positive influence on regional biodiversity persistence by increasing the representativeness of species and restoring lost neighbouring connectivity (Drielsma et al. 2014). Revegetation benefits are derived by simulating changes in habitat condition at each location (grid cell) from its current state to a pristine state, then measuring the effect on regional biodiversity persistence. Revegetation benefits aim to direct restoration and revegetation efforts towards degraded areas where important habitat types have been lost (or could persist under future climate) but where good context through proximity and connectivity to other intact habitats remain.

The revegetation benefits map (Figure 25) identifies areas where restoring lost or degraded habitat will have the greatest contribution to biodiversity persistence averaged across the 12 NARCliM GCM/RCM combinations for the 1990 to 2009 baseline and two future periods. Revegetation benefit values occurring in the full study region range between 0 (low) and 245 (high, out of a possible 255) (Figure 25 and Table 13).

Benefits have been averaged across current and all future climate scenarios to account for the uncertainty associated with future climate and highlight areas that are of high value across the potential range of climate outcomes. Irrespective of how climate may change, these are the areas where the greatest benefits from investment in revegetation or restoration is most certain.

Table 13 **Revegetation benefits statistics for the 13 selected vegetation classes with the mean values used for reporting shown in bold**

Results are averaged across the three NARCliM periods (1990 to 2009, 2020 to 2039, and 2060 to 2079) for all 12 GCM/RCM combinations.

Vegetation class	Area (ha)	Revegetation manage benefits			
		Min.	Max.	Mean	Std dev.
Alpine Bogs and Fens	40,431	10	124	**43**	17.99
Alpine Fjaeldmarks	175	10	45	**25**	8.72
Alpine Heaths	71,781	10	109	**46**	11.19
Alpine Herbfields	39,113	10	102	**56**	17.10
Montane Bogs and Fens	12,625	27	133	**76**	22.82
Montane Lakes	2,906	26	153	**124**	9.35
Montane Wet Sclerophyll Forests	78,119	17	110	**46**	11.05
Southern Escarpment Wet Sclerophyll Forests	195,275	15	125	**47**	18.04
Southern Montane Heaths	8,281	19	145	**58**	22.67
Southern Tableland Dry Sclerophyll Forests	692,644	21	170	**78**	28.06
Southern Tableland Grassy Woodlands	105,231	27	169	**92**	27.72
Southern Tableland Wet Sclerophyll Forests	197,288	16	150	**57**	23.19
Subalpine Woodlands	366,619	16	166	**59**	19.52
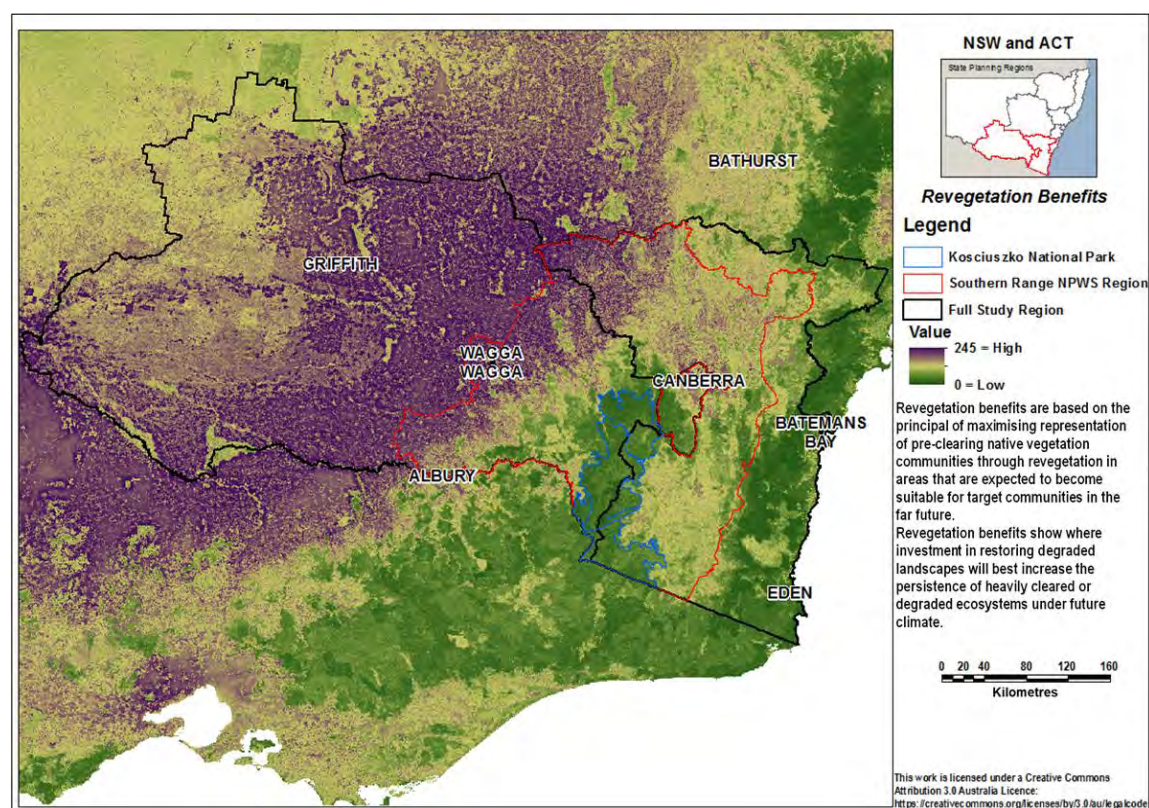
Figure 25 **Revegetation benefits show where investment in restoring degraded landscapes will best increase the persistence of degraded ecosystems under future climate**

Results are averaged across the three NARCliM periods (1990 to 2009, 2020 to 2039, and 2060 to 2079) for all 12 GCM/RCM combinations.B8. Relative change in benefits

The relative change in biodiversity benefits between 2000 and 2050 provides a perspective on how climate change is expected to influence the way in which habitat at each location (grid cell) is best managed across the region (Figure 26). This relative change in biodiversity benefit values shows how actual conservation and revegetation benefit values, which are intended to inform investment decisions (Figure 24 and Figure 25), change over time.

Benefit values only increase, not decrease, across the full study region, indicating increasing pressure on biodiversity from climate change; therefore, an increasing need to undertake management actions that benefit biodiversity persistence. Important alpine habitats, with biodiversity benefits already in the upper range, are increasing disproportionally in relation to habitats in lower slopes and the plains to the west. This highlights an increasing role for alpine areas in biodiversity conservation. As BCCs shift altitudinally in response to increasing temperatures, these areas will need to accommodate retreating climate refugees from other areas, while also remaining the last refuge of species already dependant on alpine environments.

Table 14 **Change in biodiversity benefits from 2000 to 2050 for the 13 selected vegetation classes with the mean values used for reporting shown in bold**

Vegetation class	Area (ha)	Relative change in benefits			
		Min.	Max.	Mean	Std dev.
Alpine Bogs and Fens	40,431	235	435	**409**	24.50
Alpine Fjaeldmarks	175	395	414	**405**	5.34
Alpine Heaths	71,781	253	435	**407**	21.22
Alpine Herbfields	39,113	303	434	**384**	33.42
Montane Bogs and Fens	12,625	165	401	**281**	46.66
Montane Lakes	2,906	193	409	**249**	21.19
Montane Wet Sclerophyll Forests	78,119	190	427	**348**	34.10
Southern Escarpment Wet Sclerophyll Forests	195,275	151	401	**297**	38.79
Southern Montane Heaths	8,281	192	370	**279**	41.93
Southern Tableland Dry Sclerophyll Forests	692,644	136	398	**248**	43.33
Southern Tableland Grassy Woodlands	105,231	124	367	**226**	39.30
Southern Tableland Wet Sclerophyll Forests	197,288	134	401	**280**	51.20
Subalpine Woodlands	366,619	170	435	**333**	48.96
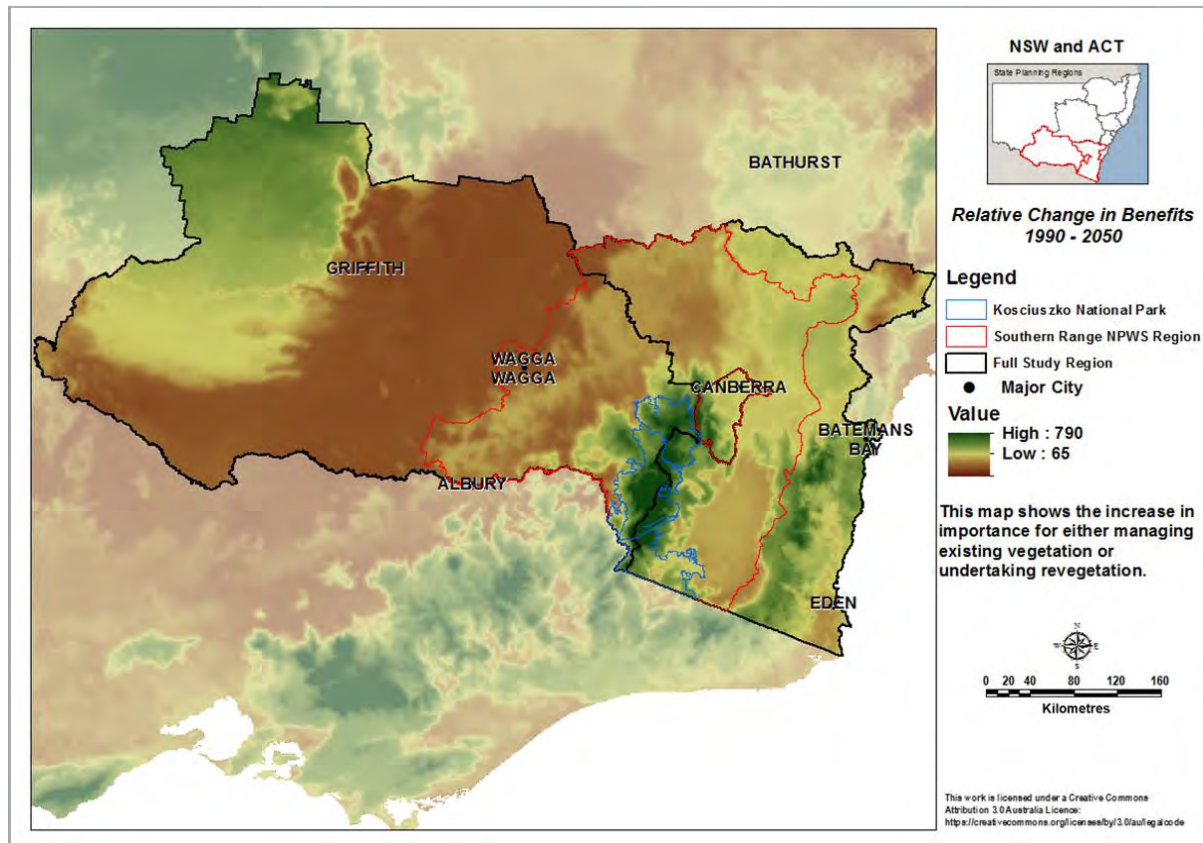
Figure 26   **Relative change in benefits shows the increase in importance for either managing existing vegetation or undertaking revegetation by 2050**

DEPARTMENT OF PLANNING, INDUSTRY & ENVIRONMENT

Climate change impacts in the NSW and ACT Alpine region

Impacts on crop suitability

Cover photo: Winter landscape in Kosciuszko National Park. John Spencer/DPIE

Find out more about your environment at:

www.environment.nsw.gov.au

Contents

List of figures

List of shortened forms

ACT	Australian Capital Territory
APSIM	Agricultural Production Systems SIMulator
ANN	Annual
AWAP	Australian Water Availability Project
CAP	Catchment Action Plan
CC	CCCMA3.1
CGS	cropping growing season
CS	CSIRO-MK3.0
CMIP	Coupled Model Intercomparison Project
DD	deep drainage
DPIE	Department of Planning, Industry and Environment
EC	ECHAM5
EP	plant evaporation
ES	water evaporation
FTH	flowering to harvesting
GCM	Global Climate Model
MBE	mean bias error
MI	MIROC3.2
mm	millimetre
MM	Murray-Murrumbidgee state planning region
MRC	Murray–Riverina cropping region
NARCliM	NSW/ACT Regional Climate Modelling project
NSW	New South Wales
OEH	Office of Environment and Heritage
PAWC	plant available water capacity
PPD	Patched Point Data
PS	pre-sowing
RO	runoff

RCM	Regional Climate Model
SBC	secondary bias correction
SET	South East and Tablelands
SILO	Scientific Information for Land Owners climate database
SoilN	soil nitrogen
SoilWat	soil water
SRES	Special Report on Emissions Scenarios
STF	sowing to flowering
UNSW	University of New South Wales
WRF	Weather Research and Forecasting

Summary of findings

Impacts on crop suitability in the NSW and ACT Alpine region

1. This study investigated the impacts of climate change on four crops (wheat, barley, canola and lupin) across the Murray–Riverina cropping (MRC) region.

2. Results suggest that bias correction of simulated temperature and rainfall effectively removed biases in the climate models at an annual time scale; however, it did not remove biases at finer temporal scales such as the cropping season.

3. Results suggest that mean crop yield will slightly increase in the near future (2020 to 2039) and substantially increase in the far future (2060 to 2079) when compared to a baseline period (1990 to 2009).

4. The ensemble mean yield of 12 Global Climate Model/Regional Climate Model simulations for the four crops across the MRC region is projected to increase by 2–9% and 8–20% for the 2020 to 2039 and 2060 to 2079 periods, respectively, relative to 1990 to 2009.

5. The biases in climate variables could explain 72–76% of the variance in the crop yield biases and 80–87% of the variance in the crop phenological biases.

6. Small changes in seasonal radiation are projected for the near and far future periods. The ensemble means for projected change in growing season radiation were –0.13% in 2020 to 2039 and +0.22% in 2060 to 2079, relative to 1990 to 2009.

7. Strong seasonal warming trends are projected for the near and far future periods. Maximum temperature for the growing season was projected to moderately increase, 0.5°C in 2020 to 2039 and 1.7°C in 2060 to 2079, relative to 1990 to 2009.

1. Introduction

1.1 Background

The New South Wales (NSW) and Australian Capital Territory (ACT) Alpine region is located in the south-eastern corner of mainland Australia and is the highest mountain range in Australia. Though it comprises only about 0.16% of Australia in size, it is an important region for ecosystems, biodiversity, energy generation and winter tourism. It forms the southern end of the Great Dividing Range, covering a total area of 1.64 million hectares that extend over 500 kilometres. The highest peak, Mount Kosciuszko, rises to an altitude of 2228 metres.

This report is part of a larger project delivered by the NSW Department of Planning, Industry and Environment (DPIE) on the various impacts from climate change on the NSW and ACT Alpine region, hereafter referred to as the Alpine region. The full study region covers the Murray-Murrumbidgee region (MM), South East and Tablelands (SET) and the ACT, bordering the Victorian border in the south (Figure 1).

Within this study region, we analysed the Murray–Riverina cropping (MRC) region, which is located in southern New South Wales (Figure 2) and covers an area of 125,551 km^2 or 16% of the state, and around 35% of the NSW cropping area (Liu et al. 2014). There are 370 SILO (Scientific Information for Land Owners climate database) Patched Point Data (PPD) sites, which are relatively evenly distributed in the region (Figure 2). The region is characterised by a semi-arid climate with an average daily radiation of 18.0 megajoules per square metre, average annual minimum temperature of 9.3°C, maximum temperature of 22°C and annual rainfall of 495 millimetres over the entire region, with the 10th percentile of site rainfall being 312 millimetres and the 90th percentile being 677 millimetres.
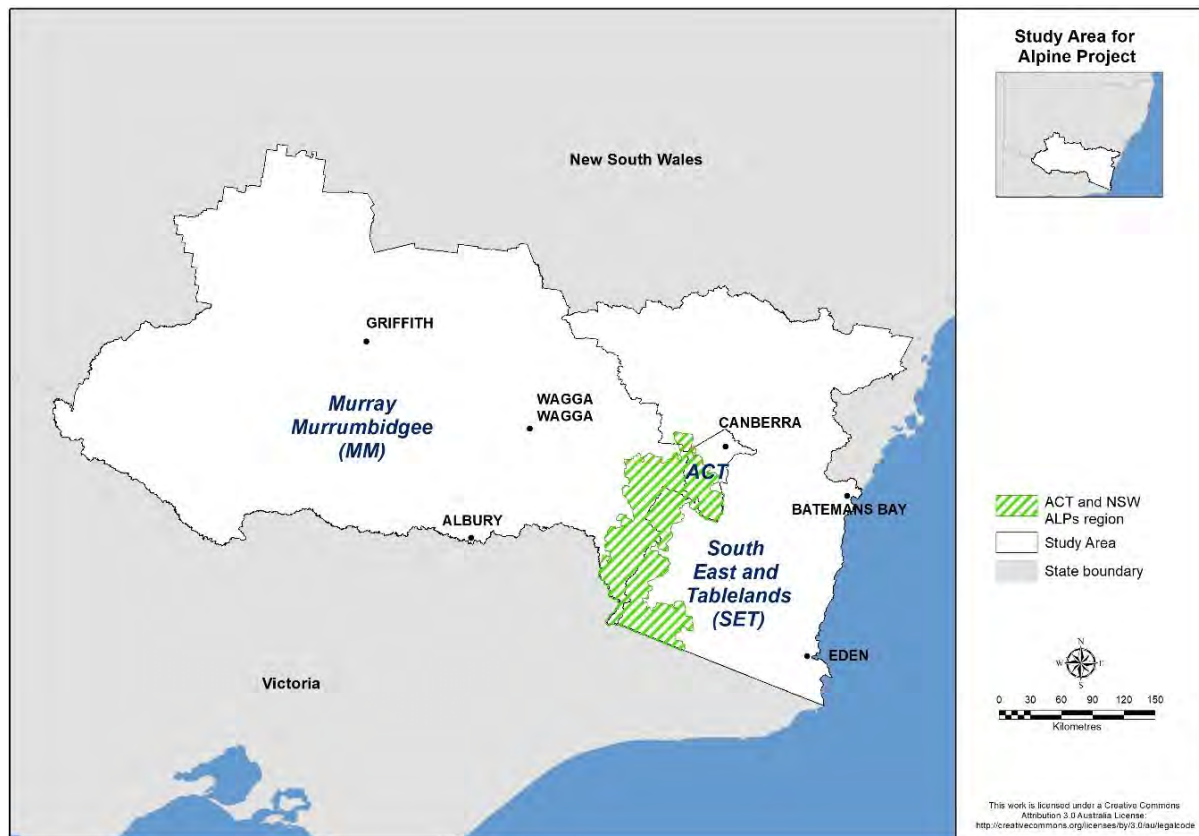
Figure 1 **The study area for the Alpine project, including the NSW and ACT Alpine region, Murray-Murrumbidgee region and South East and Tablelands**
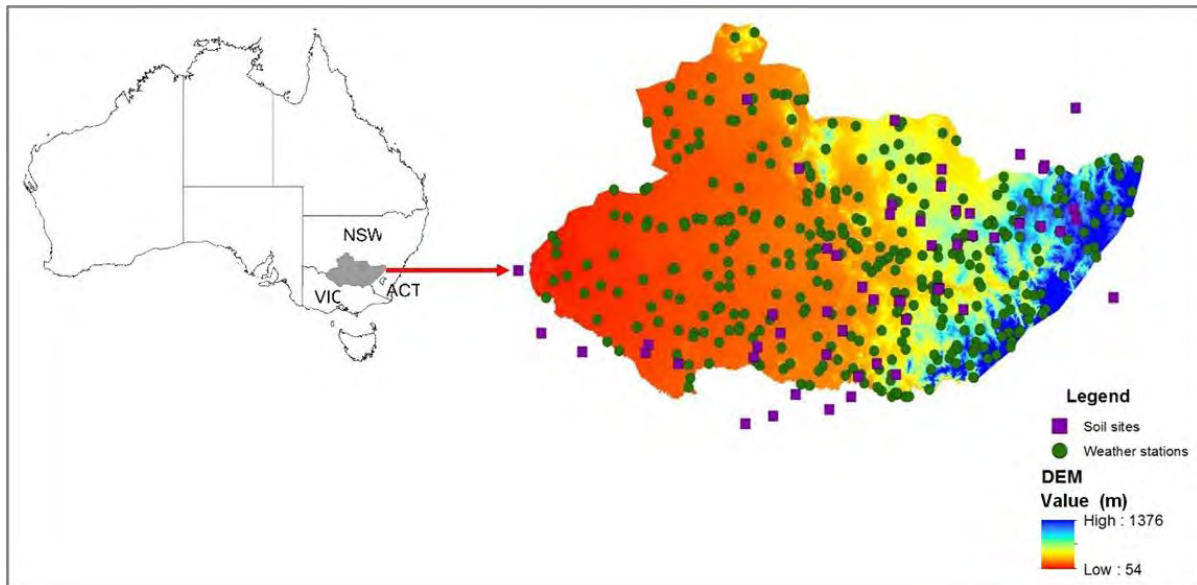
Figure 2   **The Murray–Riverina cropping area and the distribution of weather stations (green dots) used in this study**

The purple rectangles indicate soil sites used for the APSIM simulation, which also includes 13 soil sites outside the study area.

1.2   Objectives

Climate change has direct impacts on crop productivity, presenting challenges to food security worldwide (Ziska et al. 2012; Wheeler & Von Braun 2013; Tai et al. 2014; Lychuk et al. 2017). It has been estimated that climate change could decrease global wheat production by 37–52 and 54–103 megatonnes per year in the 2050s and 2090s, respectively (Balkovič et al. 2014). The Murray–Riverina region is an important NSW cropping region and it is anticipated that future climate change will impact significantly on the performance and profitability of farms. Understanding the regional impacts of climate change on crop yields is an essential step towards the development of key adaptive strategies to adapt to unavoidable climate change and mitigate the negative impacts on food security.

The downscaled 10 kilometre climate projections from the NARCliM project (Evans et al. 2014) have become available for the 1990 to 2009 baseline period, and the 2020 to 2039 and 2060 to 2079 periods. The improvement in simulation of wheat yields with increasing climate model resolution is largely due to an improvement in the simulation of growing season rainfall (Macadam et al. 2014), and a further study (Macadam et al. 2016) showed that downscaling to 10 kilometres, compared with 50 kilometres, was only beneficial when bias-corrected data were used. However, the bias-corrected NARCliM data has not been applied to the agricultural sector.

In this study, we used NARCliM simulations to drive a crop simulation model, the APSIM (Agricultural Production Systems SIMulator) model, to assess impacts of climate change on yields for four crops (wheat, barley, canola and lupin) and adaptation options related to nitrogen fertiliser application and stubble management. The objectives of the study were to:

- quantify the magnitude of climate change impacts on four crops
- assess whether adaptation options can mitigate the negative impacts of climate change.

Since this study is the first to generate crop yield projections from the NARCliM climate projections, meeting these objectives involved developing approaches to:

- assess the uncertainties in both NARCliM projections and the APSIM simulated outputs; these are critical for projection of wheat cropping modelling
- handle differences between the climate model output and the observed climate appropriately.

1.3   Outputs

Output	Details	Key users
Report	Crop suitability	Researchers
Maps	Maps of the annual and seasonal crop indices	Councils, NSW Rural Fire Service

2.   Method

2.1   Source of data

Historical observed climate data

There are 370 climate observation sites with SILO PPD, which are relatively evenly distributed in the region (Figure 2). The site-specific observed climate variables (daily radiation, rainfall, minimum and maximum temperatures) for the 20-year 1990 to 2009 baseline period were downloaded from the SILO-patched point dataset. This period is chosen in order to compare the observational data with NARCliM baseline simulations.

NARCliM simulated climate data

NARCliM, simulations from four Coupled Model Intercomparison Project phase 3 (CMIP3) Global Climate Models (GCMs) were used to drive three Regional Climate Models (RCMs) to form a 12-member GCM/RCM ensemble (Evans et al. 2014). The four GCMs selected in NARCliM were CCCMA3.1, CSIRO-MK3.0, ECHAM5 and MIROC3.2, hereafter abbreviated to CC, CS, EC and MI, respectively. The GCM names are further followed by R1, R2 and R3, which denote the names of the three RCMs. For the future projections the Special Report on Emissions Scenarios (SRES) business-as-usual A2 scenario was used (IPCC 2000). The three selected RCMs are three physics scheme combinations of the Weather Research and Forecasting model (WRF). Each simulation consists of three 20-year runs for a baseline period (1990 to 2009) and near and far future periods (2020 to 2039 and 2060 to 2079). The four GCMs were chosen based on a number of criteria: i) adequate performance when simulating historic climate; ii) most independent; iii) cover the largest range of plausible future precipitation and temperature changes for Australia. The three RCMs correspond to three different physics scheme combinations of the WRF V3.3 model (Skamarock et al. 2008), which were also chosen for adequate skill and error independence, following a comprehensive analysis of 36 different combinations of physics parameterisations over eight significant East Coast Lows (ECLs) (Evans et al. 2012; Ji et al. 2014). For the selected three RCMs, the WRF Double Moment 5-class (WDM5) microphysics scheme and NOAH land surface scheme are used in all cases. Refer to Evans et al. (2014) for more details on each physics scheme.

We acknowledge that the results are model dependent (as all model studies are) but through the use of this carefully selected ensemble we have attempted to minimise this dependence. By using this model selection process, we have shown that it is possible to create relatively small ensembles that are able to reproduce the ensemble mean and variance from the large parent ensemble (i.e. the many GCMs) as well as minimise the overall error (Evans et al. 2013a).

Some initial evaluation of NARCliM simulations shows that they have strong skill in simulating the precipitation and temperature of Australia, with a small cold bias and overestimation of precipitation on the Great Dividing Range (Evans et al. 2013b; Ji et al. 2016). The differing

responses of the different RCMs confirm the utility of considering model independence when choosing the RCMs. The RCM response to large-scale modes of variability also agrees well with observations (Fita et al. 2016). Through these evaluations we found that while there is a spread in model predictions, all models perform adequately with no single model performing the best for all variables and metrics. The use of the full ensemble provides a measure of robustness such that any result that is common through all models in the ensemble is considered to have higher confidence.

Soil data

There are 56 soil types registered in the APSoil database that are located in the region (Figure 2) and these were used to run APSIM. The most frequently occurring soil textures for the region were sandy clay and sandy loam above a clay layer, while the soil types range from sodosols (grey) to kandosols (red).

2.2   Simulation setup

Four winter crops, wheat (*Tritcum aestivum*), barley (*Hordeum vulgare*), canola (*Brassica napus*) and lupin (*Lupinus angustifolious*) were considered in the study.

We considered three levels of crop residue incorporation (0, 50% and 100%, denoted as RI0, RI50 and RI100, respectively). Crop residue incorporation is a farm management that incorporates harvested crop residue into soils by tillages. The procedure for executing crop RI were similar to those of Liu et al. (2014) and Liu et al. (2017). Under the APSIM Manager, we defined a variable to record the amount of crop residue at harvest time and calculated the appropriate amount of crop residue incorporated into the top 100 millimetres of soil for each treatment. Crop residue incorporation was executed two weeks after harvesting by disc tillage. The actual amount of crop residue incorporated by a single tillage depends on the amount of crop residue harvested. In this study, we implemented one additional tillage for RI50 and two additional tillages for RI100 to reflect actual residue incorporation.

The second option for farm management in the simulation was nitrogen fertiliser application; N-application hereafter. There were 12 levels of N-application, denoted as N1, N2, …, N12. The base N-application levels for wheat, barley, canola and lupin are 55, 65, 80 and 50 kilograms per hectare, respectively, which is denoted as N_{BS}. The amount of N applied for each treatment was calculated as

$$N_I = N_{BS}\left[1 + (I - 3) \times 0.4\right]. \qquad\qquad I = 1, 2, 3, …, 12 \qquad\qquad (1)$$

which gives the change N-rate of –80%, –40%, 0%, +40%, +80%, +120%, +160%, +200%, +240%, +280% and +320% over the base N-application. With the combination of all treatments (3 RI x 12 N-application = 36 treatments), future climate datasets (12 NARCliM x 3 time periods = 36 datasets), four crops and 370 sites, together with SILO baseline simulations, we have a total of 1,971,360 20-year simulations.

The APSIM has been widely validated for cropping system simulations under different environments worldwide, including this study region (Keating et al. 2003; Liu et al. 2016; O'Leary et al. 2016; Turpin et al. 2003). The APSIM version 7.7 (Holzworth et al. 2014) was used to evaluate the impact of climate change, crop RI and N-applications on the four broadacre crops for the MRC region in this study. The key APSIM modules that were used to represent the crops (wheat, barley, canola and lupin), were soil moisture (SoilWat/SWIM3), soil nitrogen (SoilN), surface organic matter (SurfaceOM) and crop management actions (Manager). Detailed descriptions of SWIM3, SurfaceOM and SoilN are also available elsewhere (Probert et al. 1998; Huth et al. 2014; Liu et al. 2014; Dietzel et al. 2015).

As large spatial variation in soil and climate including temperature, radiation and rainfall occurred across the MRC region, we developed a suitable sowing rule. To set a sowing rule that suited all soils and rainfall zones across the region, we considered the sowing as a

function of soil water content, plant available water capacity (PAWC), recent rainfall and day of year. The relationship between the recent cumulative four-day rainfall and soil water content is illustrated in Figure 3, using different sowing days of year and PAWC. To assess the application of nitrogen across the region and climate effect on the cropping system without carrying over the cumulative effects, we reset the soil water and nitrogen to their respective initial levels on 1 February of each year. Without resetting, the residual N applied from previous years can affect crop growth for the current year and interact with climate and farming management.
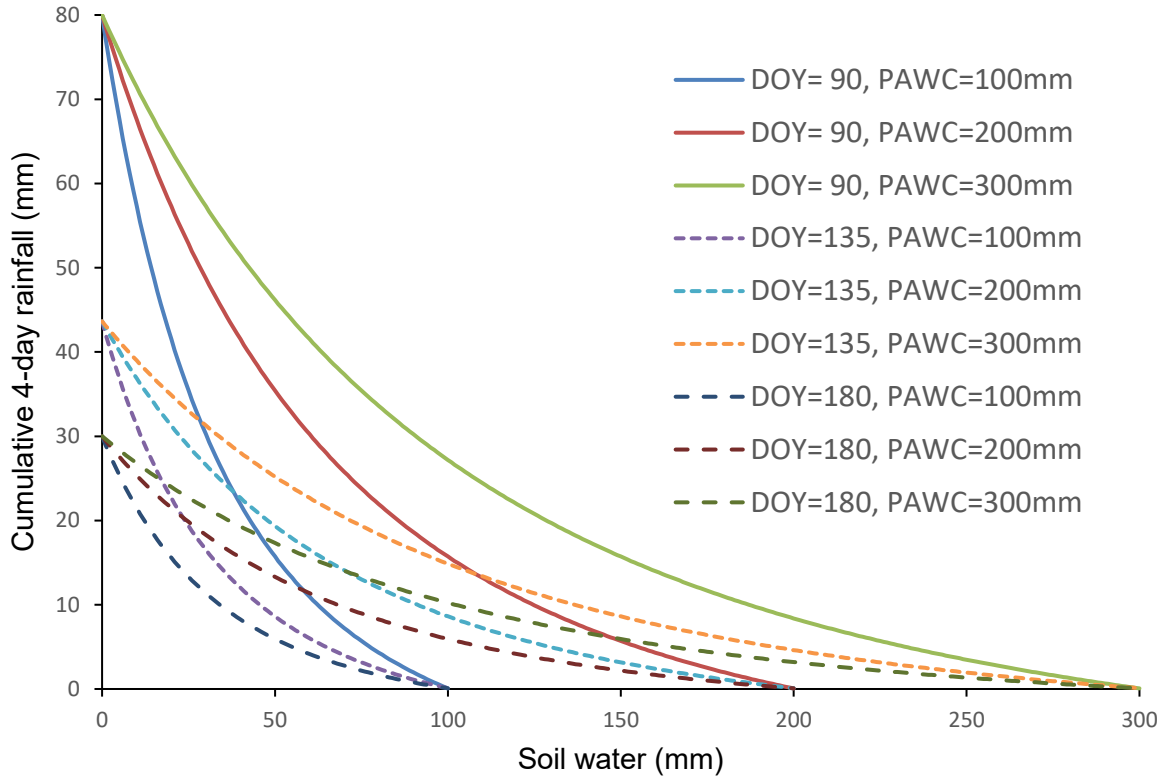
Figure 3   **The relationship between the amount of cumulative four-day rainfall (mm) required for meeting the soil criteria and the soil water content at different days of year (DOY)**
Sowing and soil types are characterised by plant available water capacity (PAWC).

Here, we used an innovative approach to determine sowing dates based on soil water content and cumulative rainfall. This approach allows crops to be sown in dry soils when there is a large amount of precipitation or sown in wet soils requiring no rainfall or a small amount of recent rainfall. In this way, the sowing rule suits a wide range of conditions for the study area.

2.3   Bias and secondary bias correction

We defined the biases in NARCliM climate variables as the differences between the RCM-simulated values (X_M) and their respective observed values (X_O). Similarly, the biases in APSIM outputs are the differences between the APSIM simulated outputs forced (i.e. applied) by RCMs (X_M) and those forced by observed climate (X_O). We defined mean bias error (MBE) as the differences in the mean over the 20-year period either in absolute terms (i.e. temperature in °C, runoff in mm) or in relative terms (i.e. rainfall, %) using the formula

$$MBE = \overline{X}_M - \overline{X}_O \ \text{ or } \ MBE(\%) = 100 \times \frac{\overline{X}_M - \overline{X}_O}{\overline{X}_O} \tag{2}$$

where $\overline{X}_M$ is the 20-year mean of NARCliM climate variables or the APSIM outputs forced by NARCliM climate, and $\overline{X}_O$ is the observed climate or the APSIM outputs forced by observations.

The bias correction applied in NARCliM resulted in more realistic daily temperature and rainfall than non bias-corrected outputs in many ways; however, no bias correction can fully eliminate all biases in climate model outputs (Piani et al. 2010). Due to this and the lack of bias-corrected solar radiation data available for the NARCliM simulations, we assessed both the remaining biases in the climate data and biases in APSIM outputs. We also removed the biases in APSIM simulated outputs, such as crop yield, by a 'secondary bias correction' (SBC) (Yang et al. 2016). We used the method proposed by Haerter et al. (2011) that can correct both the mean bias and biases in year-to-year variation as

$$ X = \overline{X}_{O,bl} + \frac{S_{O,bl}}{S_{M,bl}}\left(X_M - \overline{X}_{M,bl}\right) $$

(3)

where the subscript *bl* denotes the baseline and *S* is the standard deviation. The data before SBC are hereafter denoted as NonSBC and after SBC as SBCMnSD.

2.4 Quality control

Input NARCliM data have passed a series of quality assurance/quality control checks. The APSIM model and methods used in this study have been widely used in other climate change impact studies. The SILO data and APSIM soil database are well-established.

This report has been reviewed by internal and external reviewers and followed the procedures set out in DPIE's Scientific Rigour Position Statement (OEH 2013). Two scientific papers have been published in academic journals: 'Propagation of biases in regional climate model simulations to biophysical modelling can complicate assessments of climate change impact in agricultural systems' has been published in the _International Journal of Climatology_ (Liu et al. 2019) and 'Modelling and evaluating the impacts of climate change on three major crops in south-eastern Australia using regional climate model simulations' has been published in _Theoretical and Applied Climatology_ (Wang et al. 2019).

Meetings were organised with external experts to evaluate the methodology and review the results of this study. The first meeting was held on 14 August 2017 at the University of New South Wales (UNSW) to elicit expert feedback on methodology and initial results. Project leader (Dr De Li Liu) introduced the method and presented the initial results to Professor Jason Evans (UNSW), Dr Nicholas Herold (UNSW), Dr Kathleen Beyer (NSW DPIE), Dr Fei Ji (NSW DPIE) and Dr Ian Macadam (NSW DPIE), who represent a broad range of expertise in regional climate modelling and its usage in assessing climate change impacts.

The second meeting was held on 12 December 2017 at UNSW to elicit further expert feedback on results. Project leader (Dr De Li Liu) presented the results of the analysis to Professor Jason Evans (UNSW), Anthony Coward (NSW DPIE), Dr Kathleen Beyer (NSW DPIE), Dr Cathy Waters (NSW DPI), Dr Fei Ji (NSW DPIE) and Dr Ian Macadam (NSW DPIE), who represent a broad range of expertise in regional climate modelling and climate change impacts.

2.5 Data storage and access

All output data were converted to raster format (ArcGIS ESRI grid) and supplied to the MCAS-S (Multi-Criteria Analysis Shell for Spatial Decision Support) datapacks for distribution and storage. All input data to the model and by-products are stored on hard disk drives. All data are in the NARCliM coordinate system. The extent of the datasets includes the MM region, ACT and SET with the boundary at top: –32.671254, left: 143.317445, right: 150.745676, and bottom: –37.505077.

3. Results

The observed and NARCliM simulated climate variables for the crop-growing season (from sowing to harvesting) are analysed for the baseline period (1990 to 2009), and a near future and far future period (2020 to 2039 and 2060 to 2079 respectively). The climate variables include radiation, rainfall, maximum and minimum temperature, which are required as input to APSIM. The biases for NARCliM simulated climate variables are expressed as mean bias errors (MBE) shown in box plots. Here, the biases were calculated for three stages of crop growth: pre-sowing (PS) from 1 February to sowing; sowing to flowering (STF); flowering to harvesting (FTH), as well as for the whole year. The PS is included in this analysis as our sowing rule is based on soil water at the sowing time.

To simplify the presentations, four treatments that include two contrasting residue incorporations (0% and 100%) and two N-applications (55 kg ha^{-1} and 165 kg ha^{-1}) were selected to illustrate the biases in soil water balance, crop phenology and crop yield. As biases were similar for each crop, we report bias results for a wheat cropping system only.

With the substantial biases in NARCliM simulated variables and the subsequent biases in APSIM outputs, biases in crop yield were removed prior to the impact assessment. This was followed by secondary bias correction and impact assessments for the four crops.

3.1 NARCliM simulated climate for cropping growing season for the baseline period

NARCliM simulated climate variables (radiation, rainfall, maximum temperature and minimum temperature) for the cropping growing season (CGS) were extracted and 20-year mean values for the baseline period were also calculated, which were compared with observations (SILO) for the same time period.

The spatial distributions of simulated radiation for the 12 NARCliM ensemble members and SILO are shown in Figure 4. All simulations overestimated radiation for CGS when compared with SILO, especially for the four R3 simulations. Over the region, the averaged difference between both R1 and R2 simulations and SILO observations ranged from +1.3 to +2.1 megajoules per square metre per day, and the difference between R3 simulations and observations ranged from +2.7 to +3.9 megajoules per square metre per day. However, the spatial distributions of observed SILO radiation were captured well by R1 and R2 simulations, i.e. higher values in the western region and lower values in the eastern region.

The patterns of bias-corrected RCM simulated CGS rainfall matched well with observations for all simulations (Figure 5); however, the three CC-driven simulations slightly overestimated observed rainfall, while other simulations produced much smaller amounts of CGS rainfall across the region.

The patterns of observed maximum and minimum temperatures for CGS are also well captured by all simulations (Figure 6 and Figure 7). The CC-forced and CS-forced simulations only overestimated maximum temperature by between 0.1 and 0.3°C, while the EC-forced and MI-forced simulations overestimated maximum temperature from 0.3 to 0.6°C. In contrast, most simulations underestimated minimum temperature for CGS except for the MI-R3 simulation, which slightly overestimated minimum temperature by about 0.1°C. The magnitude of overall overestimations in maximum temperature was approximately the same as overall underestimations in minimum temperature (Figure 6 and Figure 7).

The biases in climate variables are expected to affect the simulated results of crop models. In a semi-arid environment such as the Murray–Riverina cropping region, rainfall biases can significantly affect crop growth and crop yield.
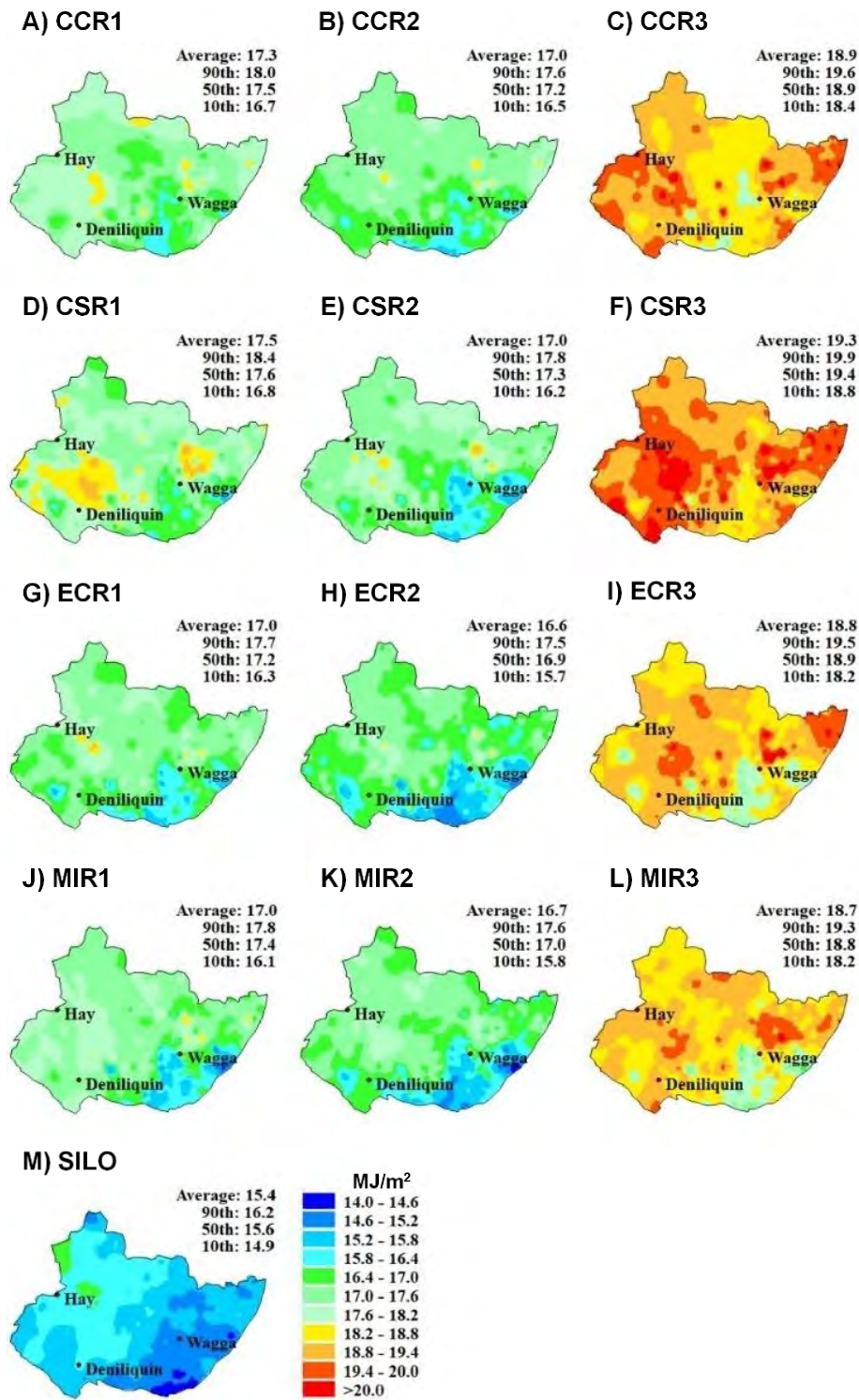
Figure 4 **Comparison of the 12 NARCliM RCMs simulated mean daily CGS radiation (MJ/m²) (A–L), with SILO data (M), across the Murray–Riverina cropping region, for the 1990 to 2009 baseline period**

Here and in the following three figures, the four GCMs: CCCMA3.1, CSIRO-Mk3.0, ECHAM5 and MIROC3.2, are abbreviated to CC, CS, EC and MI, respectively, followed by R1, R2 and R3, which denote the RCMs.
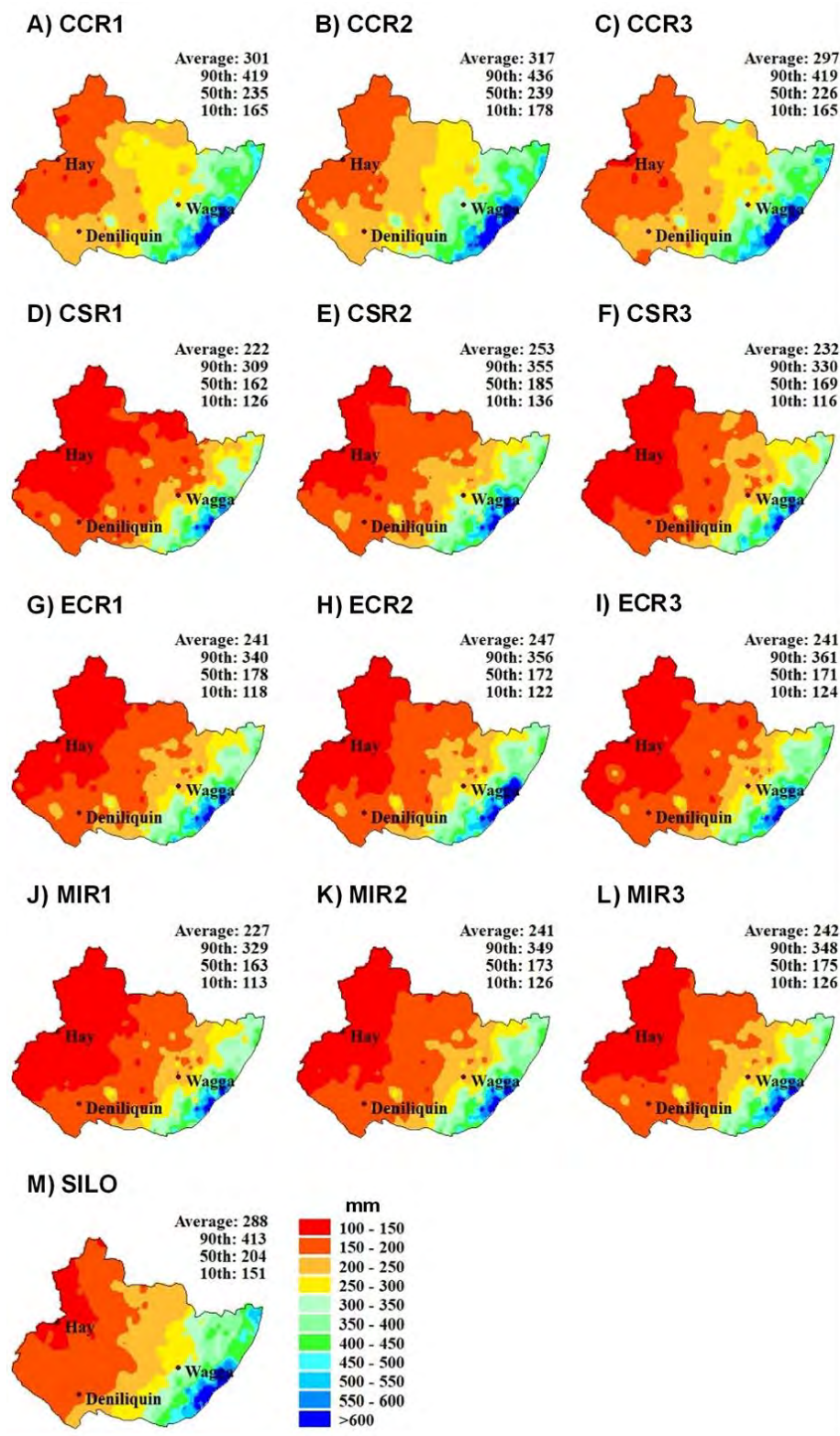
Figure 5   Comparison of the 12 NARCliM RCMs simulated total CGS rainfall (mm) (A–L), with SILO data (M), across the Murray–Riverina cropping region, for the 1990 to 2009 baseline period
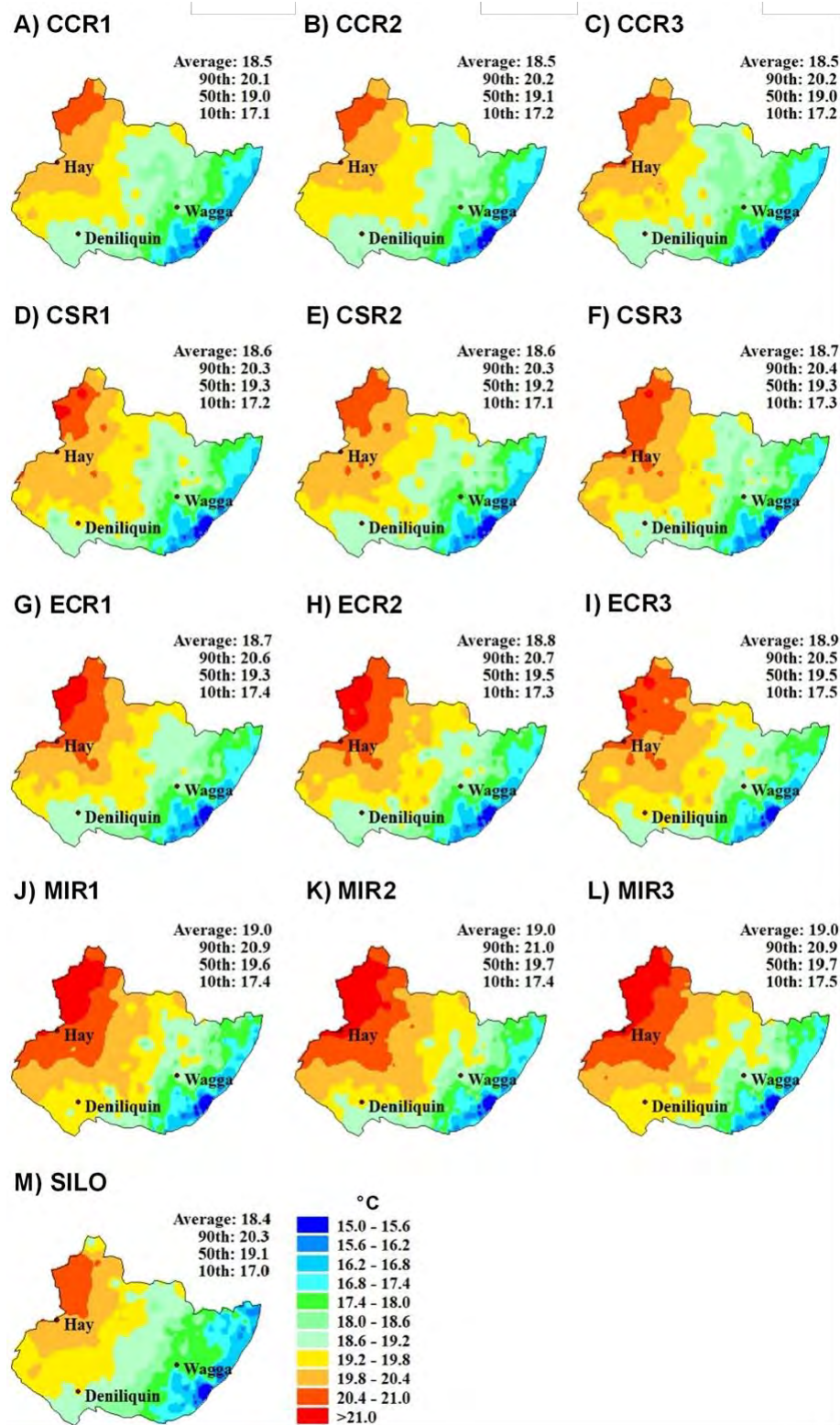
Figure 6   Comparison of the 12 NARCliM RCMs simulated mean CGS maximum temperature (°C) (A–L), with SILO data (M), across the Murray–Riverina cropping region, for the 1990 to 2009 baseline period
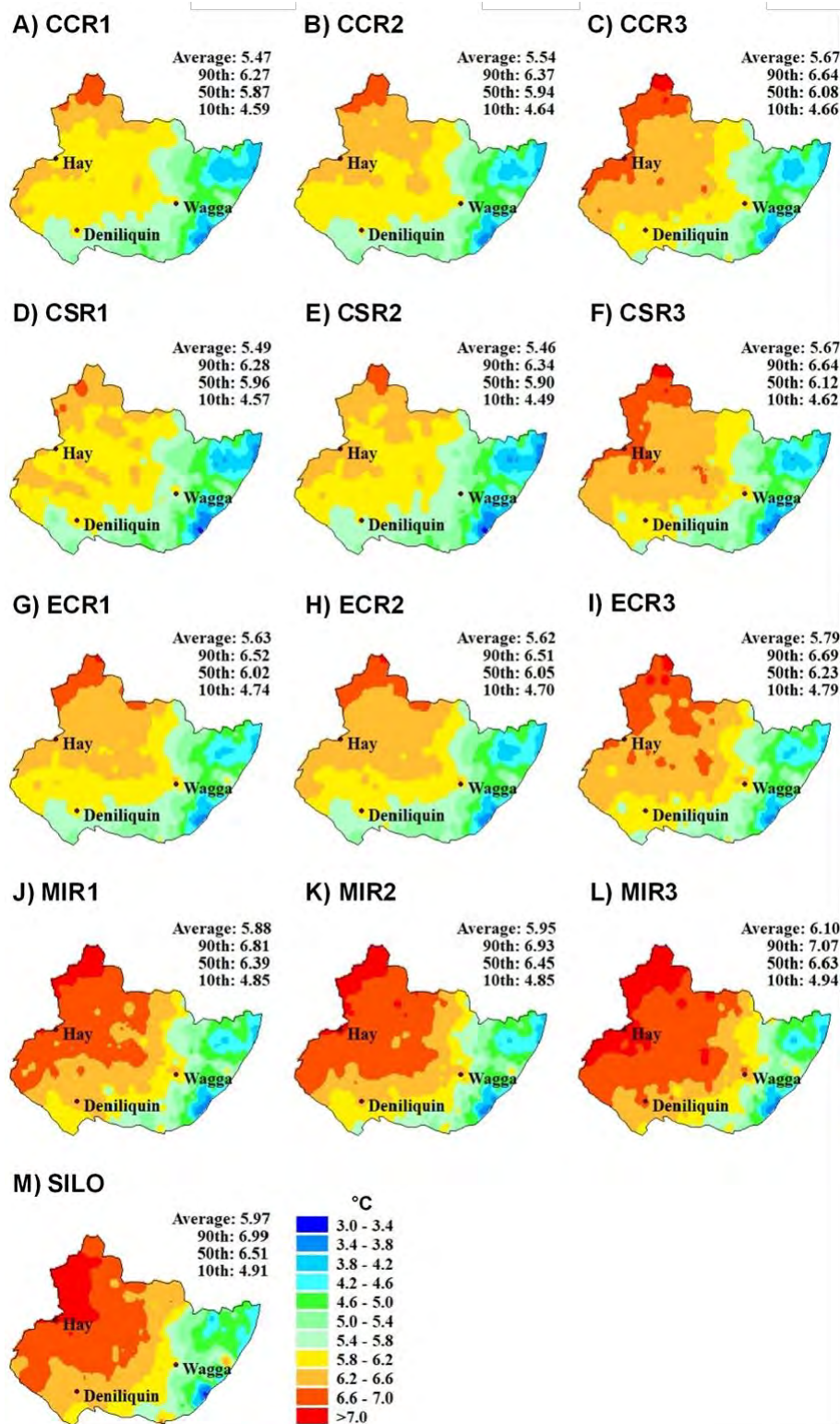
Figure 7 **Comparison of the 12 NARCliM RCMs simulated mean CGS minimum temperature (°C) (A–L), with SILO data (M), across the Murray–Riverina cropping region, for the 1990 to 2009 baseline period**

3.2   Future climate projections

We used box plots to summarise the changes across the 12 RCM combinations. Figure 8 shows the distribution of changes in mean radiation, maximum, minimum and mean temperature, and rainfall, for the growing season and non-growing season for each simulation over 370 sites in 2020 to 2039 and 2060 to 2079. Changes are relative to the 1990 to 2009 baseline period. In the text, 1990 to 2009, 2020 to 2039 and 2060 to 2079 are abbreviated to 2000s, 2030s and 2070s respectively. Changes in intra-seasonal variance (intra-SD) for the climate variables are also calculated.

Small changes in seasonal radiation are projected for the near and far future periods for each simulation (Figure 8A); for example, the ensemble means for projected change in growing season radiation were –0.13% in the 2030s and +0.22% in the 2070s relative to the 2000s over the region. Similarly, non-growing season radiation was projected to decrease (–0.53%) in 2020 to 2039 and –0.51% in 2060 to 2079 (Figure 8A)

For the two future time periods, a strong seasonal warming trend was observed for all RCM simulations (Figure 8B); in particular, maximum temperature for the growing season was projected to moderately increase (+0.5°C and +1.7°C) across all 12 simulations in 2020 to 2039 and 2060 to 2079, respectively. Increases in maximum temperature for the non-growing season are projected to increase +0.7°C and +2.2°C for 2030s and 2070s, respectively (Figure 8B). A similar warming trend was found in minimum temperature with a larger increase from December to March (Figure 8C).

Overall, the changes in mean temperature were similar to those for the minimum and maximum temperature (Figure 8D). Decreasing growing season rainfall was observed for some of the 12 simulations (e.g. CS-R1, CS-R2, and CS-R3) (Figure 8E) and, on average across all simulations, growing seasonal rainfall was projected to decrease (–3.8% and –2.4% for 2020 to 2039 and 2060 to 2079 respectively). It may be worthwhile to note that the increased rainfall occurred in the non-growing season (+5.8% and +13% for 2030s and 2070s, respectively). While this may have no immediate benefit to crop yields, this rainfall may provide useful levels of soil moisture to aid crop establishment.

The variance of future growing season radiation changed little, relative to the 1990 to 2009 baseline period (Figure 8F); however, the change in the variance of non-growing season radiation varied greatly among RCMs for both future time periods. Almost all RCMs projected increased intra-seasonal variances of temperature (Figure 8G, H and I). In contrast, there was a large difference in change of intra-seasonal rainfall variability for the RCMs (Figure 8J).
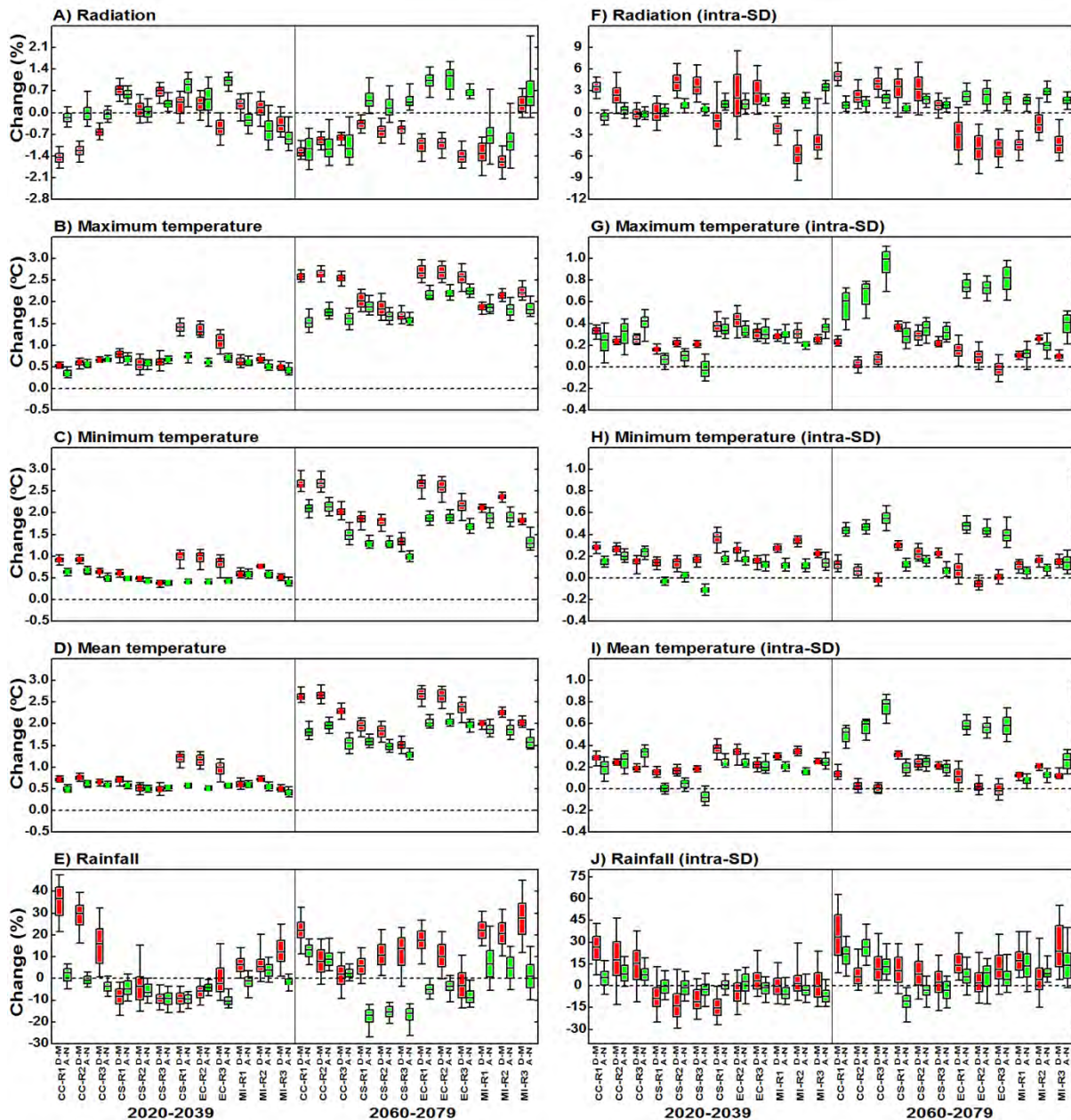
Figure 8 **Projected changes in mean radiation (%), maximum, minimum and mean temperature (°C), and rainfall (%) in the growing season (green = April through November (A–N)) and non-growing season (red = December through March (D–M)) (A–E), and intra-seasonal standard deviations (intra-SD) of same (F–J)**

Box plots show the distribution of mean changes and intra-SD in the period 2020 to 2039 and 2060 to 2079 relative to 1990 to 2009 for each of the 12 RCMs across the MRC region. Box plots show the 10, 25, 50, 75, and 90 percentiles, calculated from the 370 sites.

3.3 Biases for NARCliM simulated climate variables

Biases in climate variables for each of the 12 RCM simulations were calculated by comparing NARCliM simulated climate with SILO observed climate for the 1990 to 2009 baseline period. Figure 9 shows the mean bias error (MBE) for the climate variables (radiation, minimum, maximum and mean temperature, rainfall) and their intra-SD, as well as rainfall probability and rain intensity. As intra-SD measures the variability of daily sequences,

a negative or positive intra-SD bias means the daily sequence of RCMs exhibits a larger or smaller daily variation than observed daily sequences, respectively.

It is important to quantify intra-SD because crop development and growth are sensitive to range of diurnal temperature variation, which is quantified by daily minimum and maximum temperature, and also because rainfall distribution in the season can greatly affect crop growth. As a crop has different sensitivities to bias in different crop stages, we calculated the bias for annual and three cropping periods: pre-sowing (PS) from 1 February to sowing, sowing to flowering (STF), and flowering to harvesting (FTH).

Small annual biases in both magnitude and the variations over the 370 sites were found across all RCMs for all variables, except for both mean and intra-SD of radiation (Figure 9A&B). This largely reflects large biases in radiation that are due to no observed radiation for bias correction of simulated radiation. In addition, the annual biases in intra-SD of rainfall and rain intensity were also quite large, with significantly lower values when compared to observations for all RCMs (Figure 9K and 9L).

In the three cropping periods (PS, STF and FTH), almost all RCM simulations overestimated radiation (Figure 9A). Radiation MBE exhibited an increased trend of MBEs from PS to FTH. Biases for R3 simulations were larger than those for R1 and R2 simulations; however, the intra-SD of bias in radiation for the STF period had negative MBEs, largely positive (Figure 9G) before flowering (PS & STF), indicating that the daily sequences of the NARCliM simulated radiation didn't match the SILO-radiations. It is worth noting that NARCliM simulated radiation was not bias-corrected, but a large proportion of radiation in SILO was calculated (i.e. not actual observed).

Unlike the consistent biases in radiation, the temperature MBE varied considerably between RCMs and growing periods (Figure 9B–D). The most distinct feature was that the bias had a reciprocal low–high pattern between periods, i.e. one higher companied with another lower, suggesting some different biases in different seasons. For example, downscaling of some GCMs (CC-, CS- and EC) produced higher minimum temperature (T_{min}) in the PS period, but lower in another two phenological stages (STF and FTH) (Figure 9C).

In comparison between climate variables, RCMs gave a higher maximum temperature (T_{max}) in one period and often showed a lower T_{min} for the same period. For example, CC-R1 had a median MBE of +0.7°C for T_{max} in the period of FTH (Figure 9B), but –0.5°C for T_{min} in that period (Figure 9C). However, the magnitude of MBEs was not the same for T_{min} and T_{max}; the MBEs for daily mean temperature (T_{mean}) were still large and maintained a similar pattern to T_{max} or T_{min}. Generally, more negative T_{mean} MBEs for the STF period were found for CC-, CS- and EC-forced RCMs, but more positive T_{mean} MBEs were found for MI-forced RCMs for this important phenological period (Figure 9D). This may lead to biases in the phenological development as temperature is a primary factor controlling crop phenology. The intra-SD MBEs for temperatures varied considerably, suggesting a mismatched distribution of NARCliM simulated daily temperature sequences with observations (Figure 9H–J).

The rainfall simulated by the CC-forced RCMs had lower bias than other RCM simulations, showing a narrow MBE interquartile from –10% to +30% (Figure 9E). A second group of RCM simulations forced by the CS and EC GCMs, produced significantly higher rainfall than observed in the PS period, but lower rainfall for the crop growing periods (STF and FTH), exhibiting a wide MBE interquartile from –40% to +50% across RCMs. The third group of simulations forced by the MI GCM gave over 90% of sites with positive MBEs in the PS period and negative MBEs in the STF period. Generally, a similar seasonal bias pattern, i.e. a positive MBE in one period companied with a negative in another period, was found in rainfall bias, suggesting imperfect matching between seasonal bias-corrected NARCliM rainfall and observation. The intra-SD MBE for rainfall in the growing season was mostly negative, suggesting smaller variations in daily rainfall than observations (Figure 9K).

In the semi-arid environment of our study area, rainfall characters such as the frequency of rainfall events and rain intensity are important because they can alter rainfall water partitioning in soil water balance and availability of moisture for crop growth. Thus, in addition to analysis of rainfall MBE, we further explored the rain-event characters. Figure 9F and 9L exhibit an obvious contrasting pattern between rainfall probability and rainfall intensity, demonstrating that RCMs tended to produce a higher rainfall probability (Figure 9F) and lower rainfall intensity than observations (Figure 9L). This indicates that all RCMs simulated more frequent but less intensive rainfall when compared with SILO data.
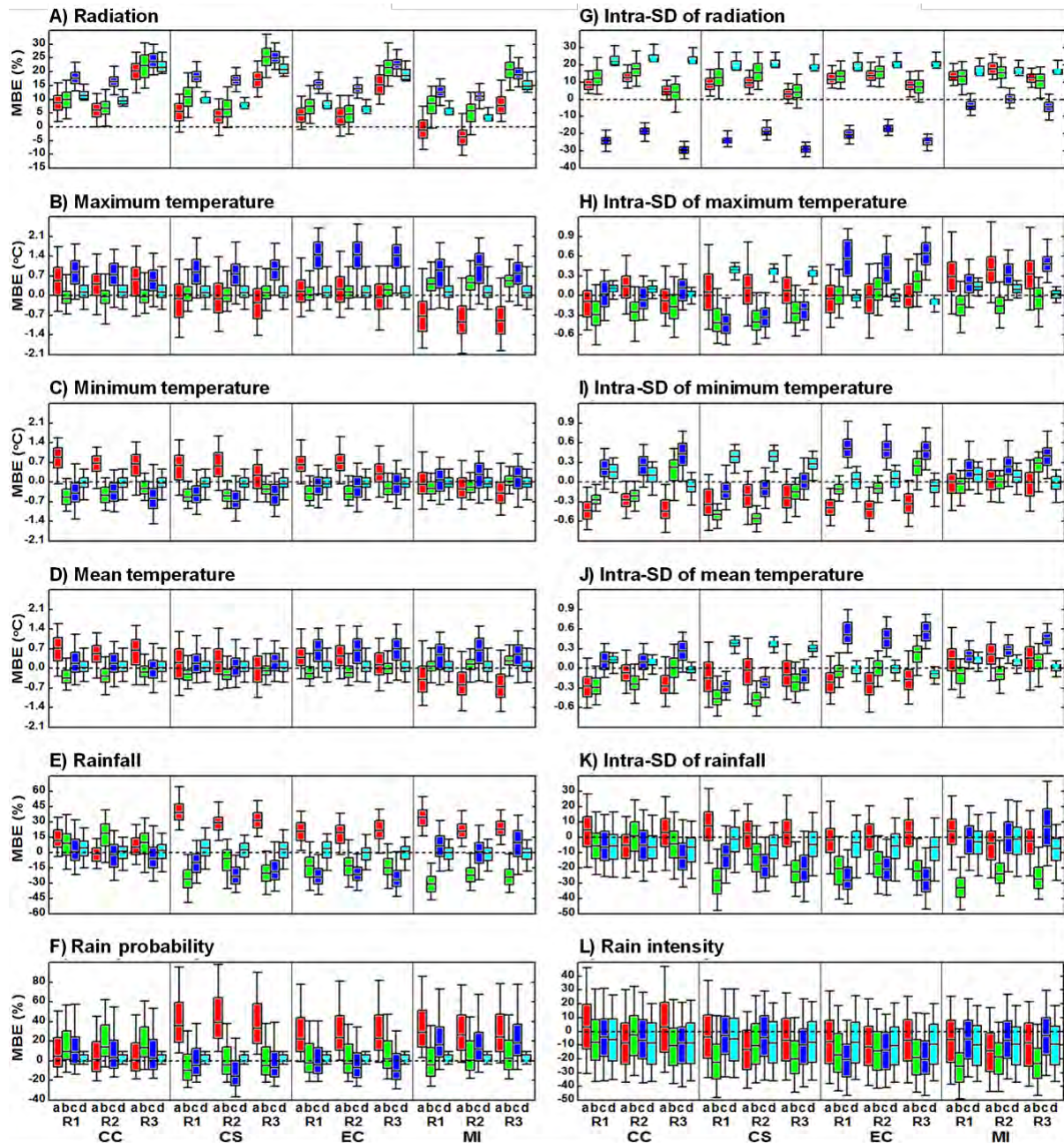
Figure 9   **Mean bias error (MBE) in NARCliM simulated climate variables radiation (%), maximum, minimum & mean temperature (°C), and rainfall (%) (A–E), and their intra-SD (G–K), along with MBEs in rain probability (%) (F) and rain intensity (%) (L), for PS (red, a), STF (light green, b), FTH (dark blue, c) and annual (cyan, d)**

Box plots show the 10, 25, 50, 75 and 90 percentiles, calculated from the 370 sites.

Biases for APSIM simulations forced by NARCliM data

It is important to understand the consequences of RCM biases for the APSIM outputs. Here we do not assess the uncertainty of APSIM simulations, but we use the same settings of APSIM for observed climate and RCM simulated climate. The underlying hypothesis is that if the climate variables simulated by RCMs were realistic and perfectly matched the observed climate, the outputs of a biophysical model forced by the observed and RCMs projected climate should be identical. The differences in APSIM outputs between RCM simulated climate and observed climate is considered as the biases that are derived from the differences between the two climates. We compared the biases in a wide range of APSIM outputs through the difference between the outputs forced by RCMs simulated climate and observed climate (SILO).

Biases in APSIM simulated soil water balance, crop phenology and production are shown in Figure 10. Most RCMs resulted in a positive MBE in soil water at sowing (SWS) at most sites, due to their produced higher pre-sowing rainfall; however, biases in runoff (RO) (Figure 10B) and deep drainage (DD) (Figure 10C) were negative at the majority of sites. Similarly, biases in soil water evaporation (ES) were positive at all sites. In addition, across around 75% of sites, plant transpiration (EP) biases were higher when APSIM simulation were forced by the CC-forced RCMs and lower than observations for the remaining nine RCM simulations (Figure 10E). These results were highly correlated with the biases in the rainfall simulations; for example, the CC-forced RCMs that produced positive EP are the RCMs that had positive rainfall biases, while the other three GCM-forced RCMs resulted in negative EP MBE largely due to their negative rainfall biases. Moreover, because plant N uptake follows water uptake, the biases in APSIM simulated N uses (NU) exhibited a similar pattern to EP biases (Figure 10F).

Importantly, there is a clear interaction between biases in APSIM outputs and farming management practice; for example, the crop residue incorporation (RI) considerably reduced the range of the SWS bias (Figure 10A), deep drainage bias (Figure 10C) and plant transpiration bias (Figure 10E) at RI0 but increased the magnitude of the negative RO MBE in RI100 (Figure 10B). Similarly, a larger bias in EP and NU were simulated at a higher N-application than lower N-application (Figure 10E & 10F). The study reveals that farm management practice may interact with the climate biases and consequently interact with biophysical modelled outputs such as biomass and crop yields.

For MI-RCMs, approximately 75% of sites had a sowing date (SD) later than that resulting from observed climate, while other GCM-based RCMs exhibited more negative SD biases (Figure 10G). The numbers of days from sowing to flowering (DTF) and crop duration (CD) simulated by APSIM forced by CC-, CS- and EC-RCMs were longer (positive MBE) at most sites but those forced by MI-based RCMs were shorter (negative MBE), relative to that forced by observed climate (Figure 10H & 10J). It is not surprising that the differences in crop phenological biases were consistent with the biases in NARCliM simulated temperature, i.e. the MI-RCMs that produced a faster development (negative positive DTF and CD MBE) in crop development are the RCMs that had positive T_{mean} biases in this phenological period (Figure 9D).

Similarly, the three CC-RCMs showed positive biomass bias in more than 75% of sites, largely resulting from the positive rainfall MBEs; however, the positive biomass biases forced by CC-RCMs are not large for wheat yield, due to the difference in the rainfall biases from the positive rainfall biases in the STF period to the negative rainfall biases in the FTH period produced by these RCMs (Figure 9E). Simplistically, the crop used CO_2 and water to form photosynthetic product (biomass). The nine RCM (CS, EC & MI) forced simulations exhibited negative biases in both wheat biomass and wheat yield in most sites, corresponding to the pattern of the biases in rainfall and ultimately plant transpiration (Figure 10).
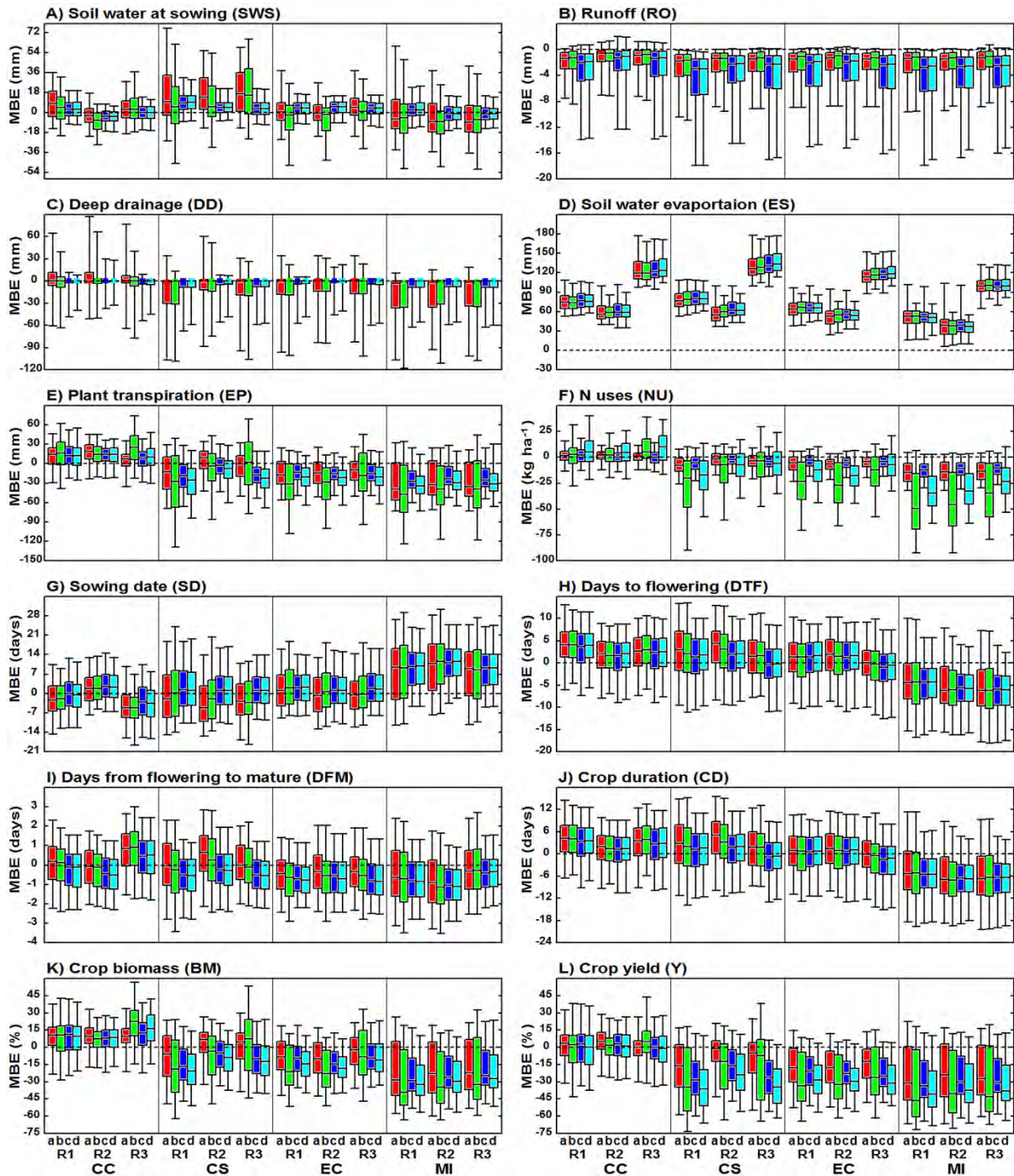
Figure 10 Biases in APSIM simulated soil variables (A–E), N-uses (F) and plant variables (G–L) under the four management treatments (a, red: 0% residue incorporation (RI) by 50 kgN ha^{-1}; b, green: 0% of RI by 165 kgN ha^{-1}; c, blue: 1000% of RI by 50 kgN ha^{-1}; d, cyan: 100% of RI by 165 kgN ha^{-1})

Box plots show the 10, 25, 50, 75 and 90 percentiles, calculated from the 370 sites.

Secondary bias correction

We used a simple secondary bias correction (SBC) method to correct the biases in RCM-driven crop yields (Yang et al. 2014). The distributions of rainfed crop yield for the 1990 to 2009 baseline period are shown in Figure 11. For all cases, using NonSBC outputs produced a high skewness of yield distributions relative to those forced by SILO observations when simulated wheat yield was lower than approximately 2200 kilograms per

hectare; however, when projected yields were more than 3000 kilograms per hectare, a low skewness of yield distribution was shown (Figure 11a&b). Similar results were found for canola and lupin crops (Figure 11c–f). Applying the simple SBC resulted in yield distributions largely consistent with those forced by historical observations (Figure 11b,d&f).
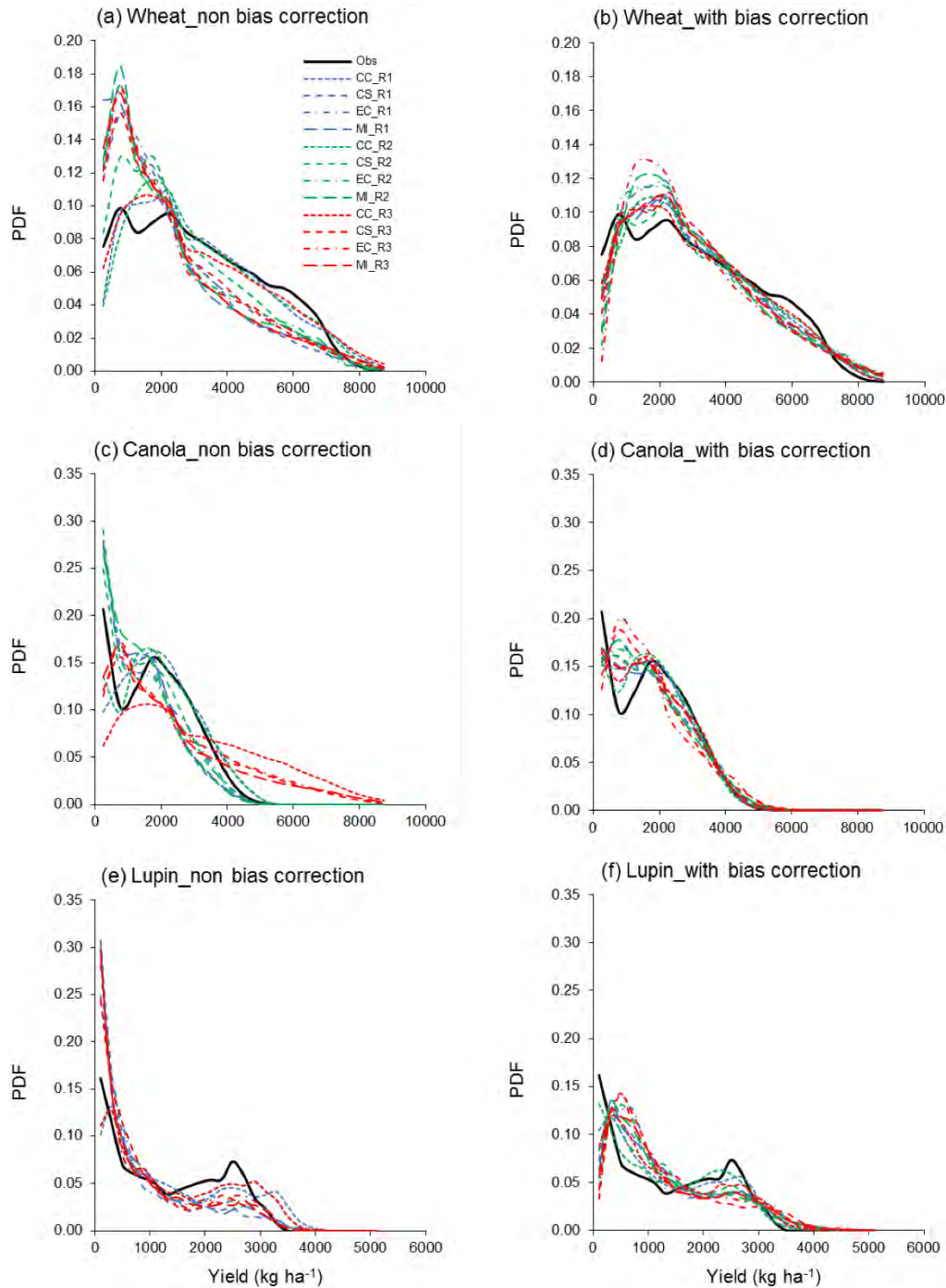
Figure 11 **Probability distribution functions of APSIM-simulated yields for the 1990 to 2009 baseline period, driven by historical observed climate data (black line) and 12 RCMs climate data with NonSBC (a,c,e) and SBCMnSD (b,d,f) values**

SBC yield largely eliminated the distributional discrepancies against the yield driven by observed climate.

Impact of climate change on crops

The bias-corrected yields were to assess future climate change impacts on crop yield for the 2020 to 2039 and 2060 to 2079 projection periods. To simplify the presentation of results, only four N-applications (N1, N3, N6 and N9) are illustrated here. The change in future simulated crop yields varied across the sites. Overall, the ensemble mean of yield for four crops across the MRC region (A2 emissions scenario) was projected to increase for both future time periods compared to the reference period (Figure 12 to Figure 15). The magnitude of increase in crop yields was larger in the far future as a result of the high carbon dioxide (CO_2) concentration compensating some negative effects of climate change. Crop responses to elevated CO_2 is through increase in efficiency of radiation and water use.

Figure 12 shows the mean changes in wheat yield for the 12 RCM ensemble at RI0 and RI100 and different N-applications in the 2030s and 2070s over the study area. The results show more significant increases in wheat yield for the 2070s in the western region than the eastern region (Figure 12). When residue was completely removed, and nitrogen application was at a very low level (N1), wheat yield was projected to increase by +2.6% and +10.5% in the 2030s and 2070s, respectively (Figure 12). Such increases likely resulted from the elevated CO_2 concentration that over-performed the low N-application in the current environment; however, the change in yield increased with increasing rate of nitrogen application in most cases, particularly when 100% residue incorporation was considered (Figure 12). This is likely due to RI increasing soil porosity and soil water availability for crop uses, and the interaction of high N and evaluated CO_2 concentration. The largest increase of +24.9 % for wheat yield was projected in the 2070s with high amounts of N and 100% RI (Figure 12).

Figure 13 shows the changes in barley yield of the RCM ensemble mean at RI0 and RI100 and different N-applications in the 2030s and 2070s over the study area. Similarly, results showed more significant increases in barley yield in the 2070s in the western portion of the area than those in east (Figure 13). There was a strong N response to the future yield increase. When residue was completely removed, barley yield was projected to increase by +0.8% at N1 to +8.5% at N9 in the 2030s and by +3.2% at N1 to +19.8% in the 2070s (Figure 13). It is interesting to note the significant effect of residue incorporation and also its interaction with N-application. With N-applications of N1, N3, N6 and N9, the difference in barley yield change was +2.6% (from 0.8–3.4%), +3.1% (1.99–5.04%), +1.0% (4.9–5.9%) and –2.2% (8.5–6.3%) from complete residue removal to 100% RI, respectively for the 2030s. However, in the far future higher yield changes are expected +9.7%, +15.3%, +9.6% and +2.9% for N1, N3, N6 and N9, respectively. Again, the effectiveness of N interaction with RI is likely the interaction of elevated CO_2 concentrations.

For canola, there was strong agreement among all the treatments with respect to pronounced projected increases in yield (Figure 14). The simulated canola yield increased due to increased CO_2 concentrations in the A2 emissions scenario. N-application and RI had limited contributions to yield increase in each time period; for example, canola yields only increased from +34.7% to +39.4% for the 2070s when N was increased from 16 kilograms per hectare (N1) to 272 kilograms per hectare (N9) at 100% RI (Figure 14D & P).

In addition, it is not surprising that simulated lupin yield had no response to nitrogen increase due to its nature of N fixation, although average yield was expected to increase by +4.6% to +29.9% across the study area (Figure 15).
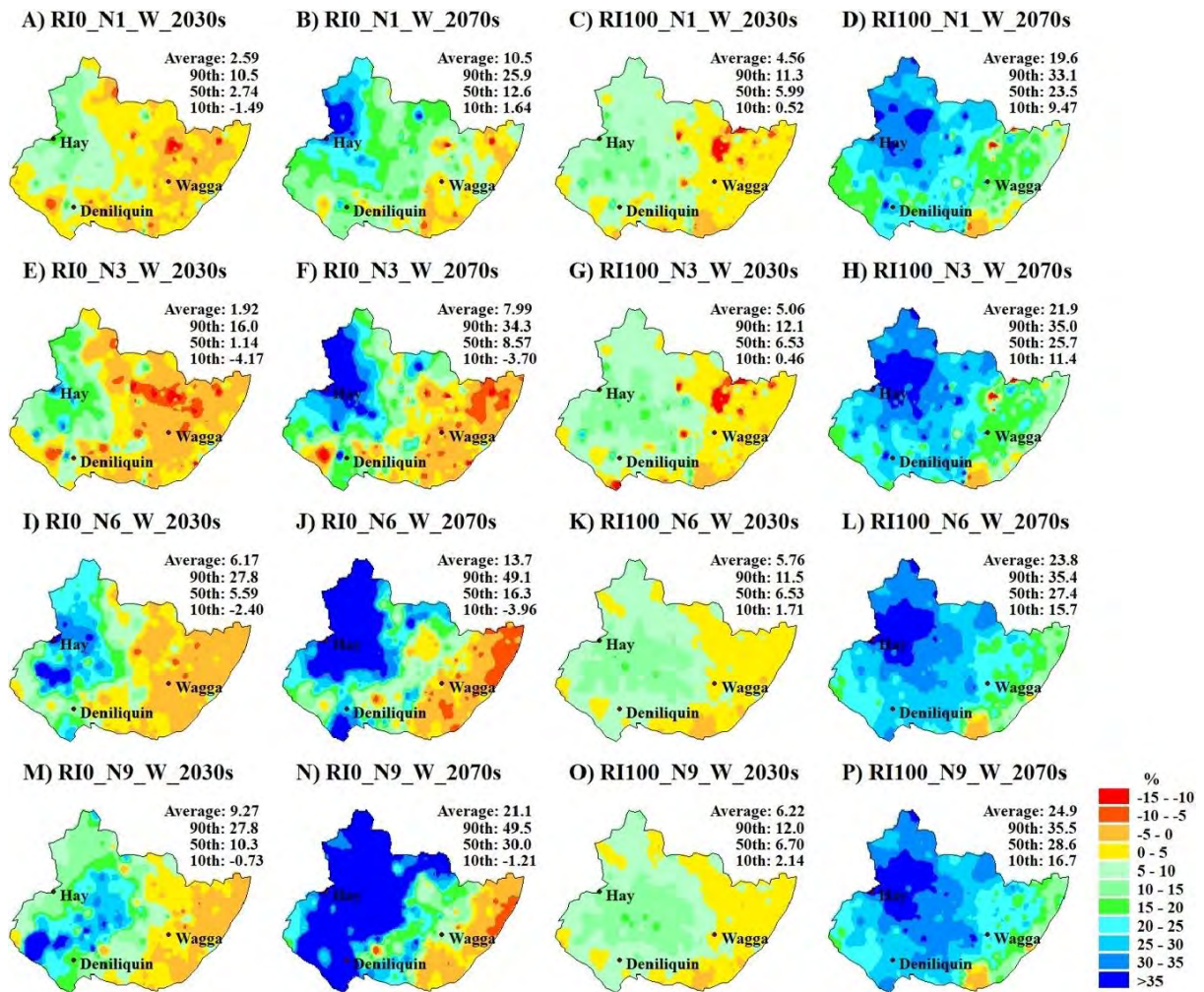
Figure 12   Impact of climate change on wheat (W) at two contrasting residue incorporations (RI0: 0%; RI100: 100%) and for N-application (N1, N2, N6 and N9) in the 2030s and 2070s over the Murray–Riverina cropping region

Here and in the following three figures, 2030s and 2070s refers to the 2020 to 2039 and 2060 to 2079 periods, respectively.
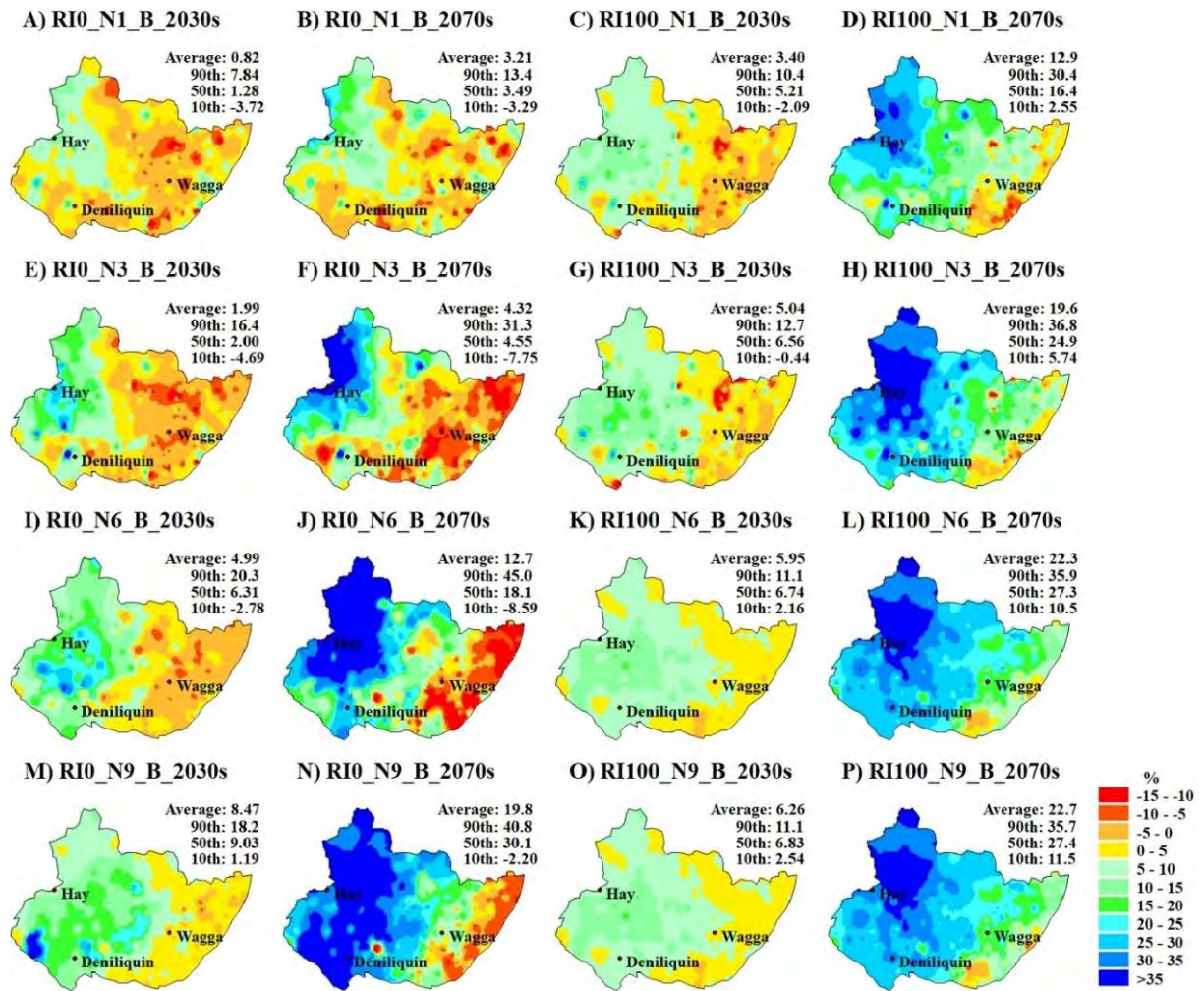
Figure 13 **Impact of climate change on barley at two contrasting residue incorporations (RI0: 0%; RI100: 100%) and for N-application (N1, N2, N6 and N9) in the 2030s and 2070s over the Murray–Riverina cropping region**
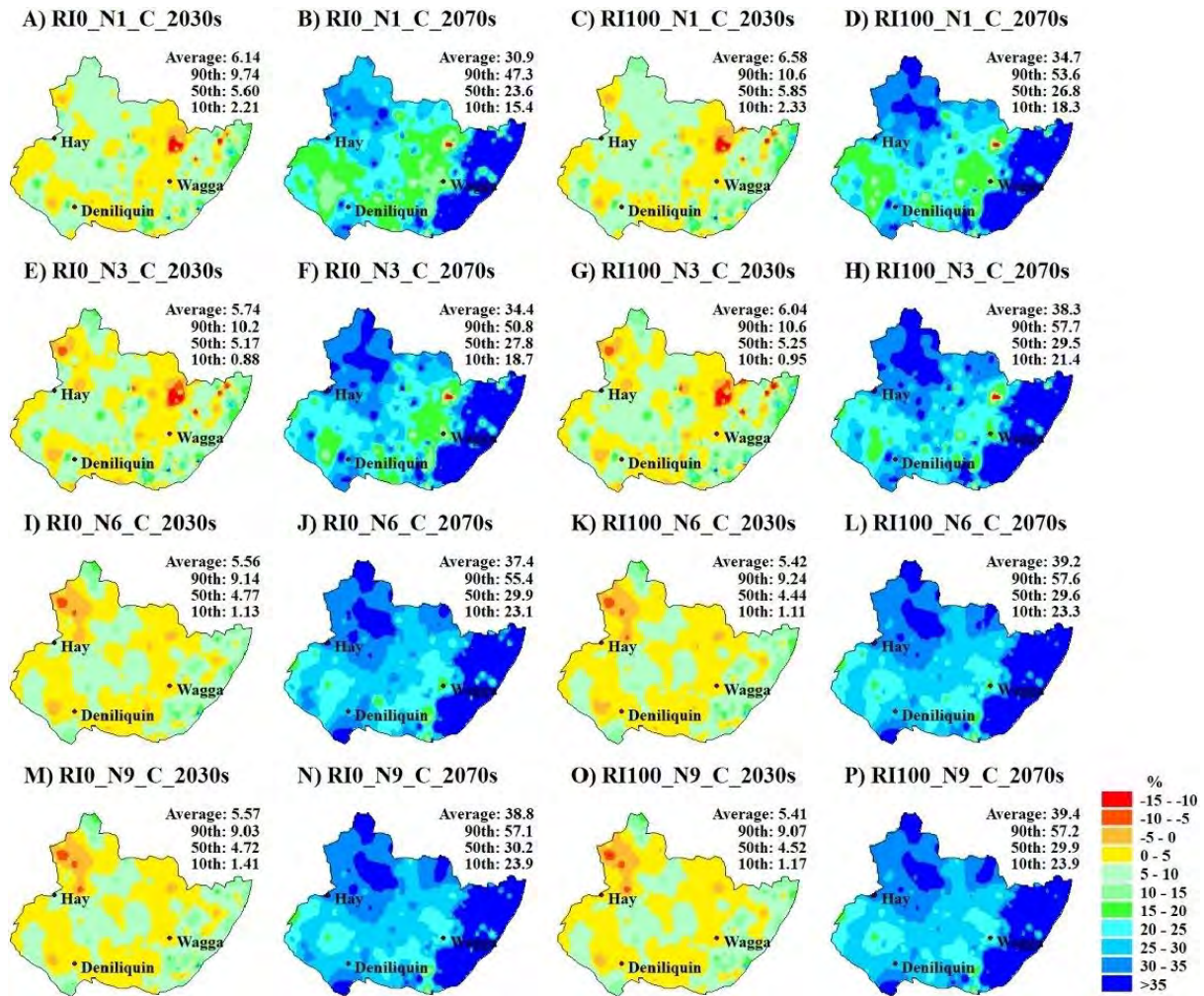
Figure 14   **Impact of climate change on canola at two contrasting residue incorporations (RI0: 0%; RI100: 100%) and for N-application (N1, N2, N6 and N9) in the 2030s and 2070s over the Murray–Riverina cropping region**
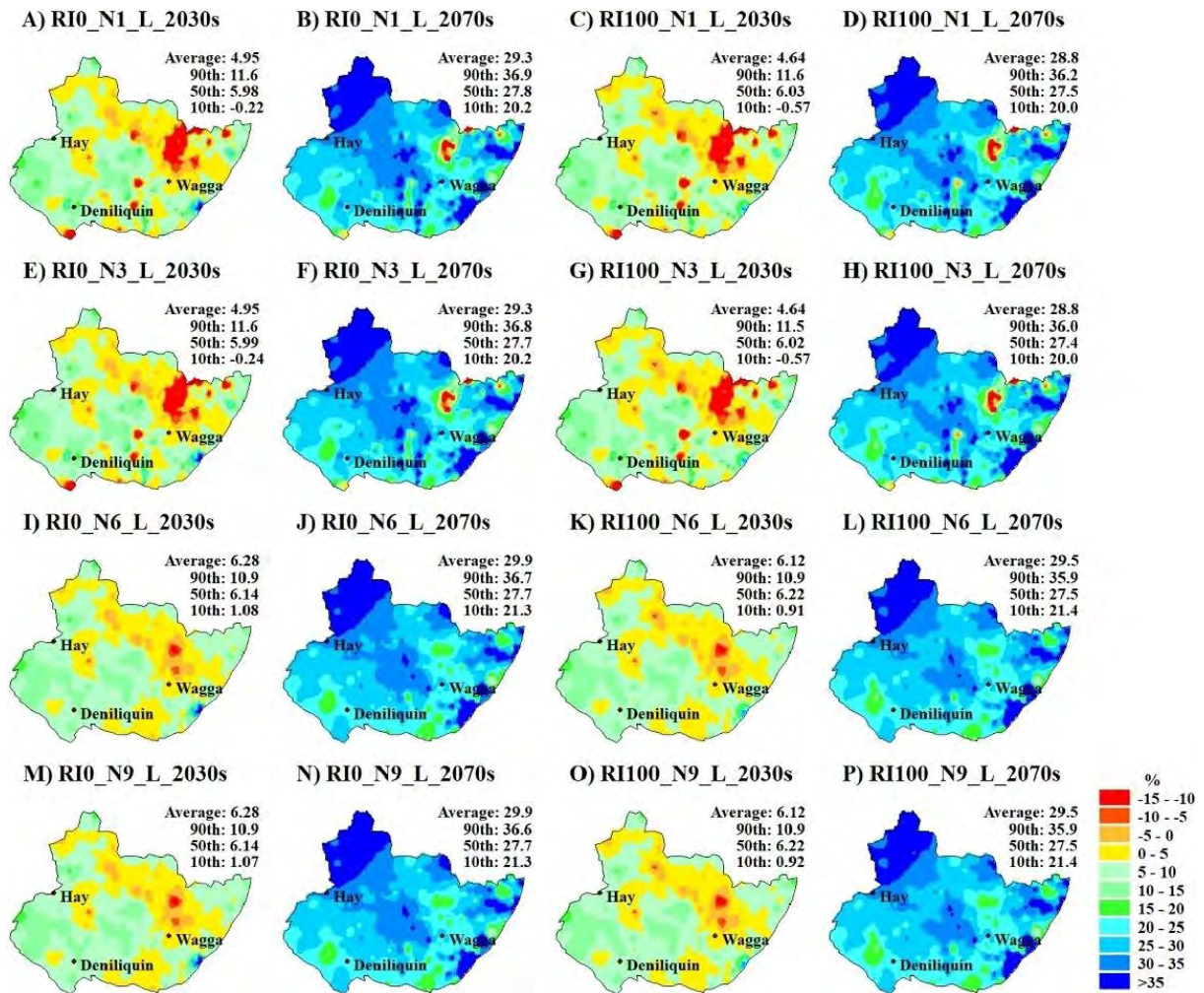
Figure 15 Impact of climate change on lupin at two contrasting residue incorporations (RI0: 0%; RI100: 100%) and for N-application (N1, N2, N6 and N9) in the 2030s and 2070s over the Murray–Riverina cropping region

4. Discussion

4.1 Key findings

NARCliM simulated climate

Although the bias correction (BC) of NARCliM simulated temperature and rainfall effectively removed bias at an annual time scale (Evans et al. 2017), it did not remove biases at finer temporal scales such as cropping season. We show that a positive bias in one phenological period for a given variable such as temperature or rainfall was often associated with a negative bias in a different period. Therefore, we suggest that BC should be done at finer temporal scales, i.e. seasonally or monthly, which could be useful for simulation of crop growth.

APSIM modelling responses to RCM biases

The biases in climate variables could explain 72–76% of the variance in the crop yield biases and 80–87% of the variance in the crop phenological biases. The climate biases were the cause of biases in the biophysical modelling outputs. Figure 16 shows the trajectories of the biases in crop yields through a schematic representation of bias source in APSIM crop yield. This tracks the sequence of climate biases and soil water balance biases that leads to less water available to the crop.

The results indicate the climate biases can interact with the projected climate change, which can result in confounding contributions to biophysical modelling outputs that increase uncertainties about effects of climate change and farm management factors. For example, simulated lower rainfall intensity associated with higher rainfall probability than observed climate, can be found in the largest proportion of sites. Low intensity, frequent rainfall makes the soil surface wetter and results in greater soil water distribution in shallow layers. This characteristic rainfall pattern can reduce water availability for plant use because a wetter soil surface can contribute more soil water evaporation, resulting in less water available for plant uptake. Our results showed that the responses of the wheat cropping system to this type of rainfall are typically positive biases in soil evaporation across almost all sites, which consequently lead to less water available for plant transpiration and ultimately lower yield. In addition, we found that the majority of sites had negative biases in both runoff and deep drainage. This highlighted that rainfall characteristics were as important as the total amount of rainfall in agricultural systems. Improved downscaling outputs are prerequisites for realistically assessing climate change impacts in agricultural systems.

Functions of secondary bias correction

Applying a simple SBC resulted in yield distributions largely consistent with those forced by historical observations. Importantly, the bias correction can effectively remove the uncertainties. The simple SBC method applied on the modelled yield outputs could result in RCM-driven crop yields being consistent with the PDF of observation-driven crop yields. After the SBC was applied to correct some of the biases in APSIM simulated yield, the parameters associated with the impact assessment became more meaningful, i.e. regaining positive atmospheric CO_2 effect on future crop production and diminishing the false collinearity between changes in climate variables and farm management practices.

However, SBC used in the study corrects the mean and variance under the assumption that the APSIM responses of climate biases in the baseline period are the same as in the future periods. As crop models are implemented with many linear and non-linear functions, the response of crop models to climate biases may interact with the changes in environmental conditions such as elevated future atmospheric CO_2. Such possible interacting responses of climate biases cannot be corrected by SBC. Thus, preference should be given to using improved climate projections that can result in small biases in biophysical modelled outputs.
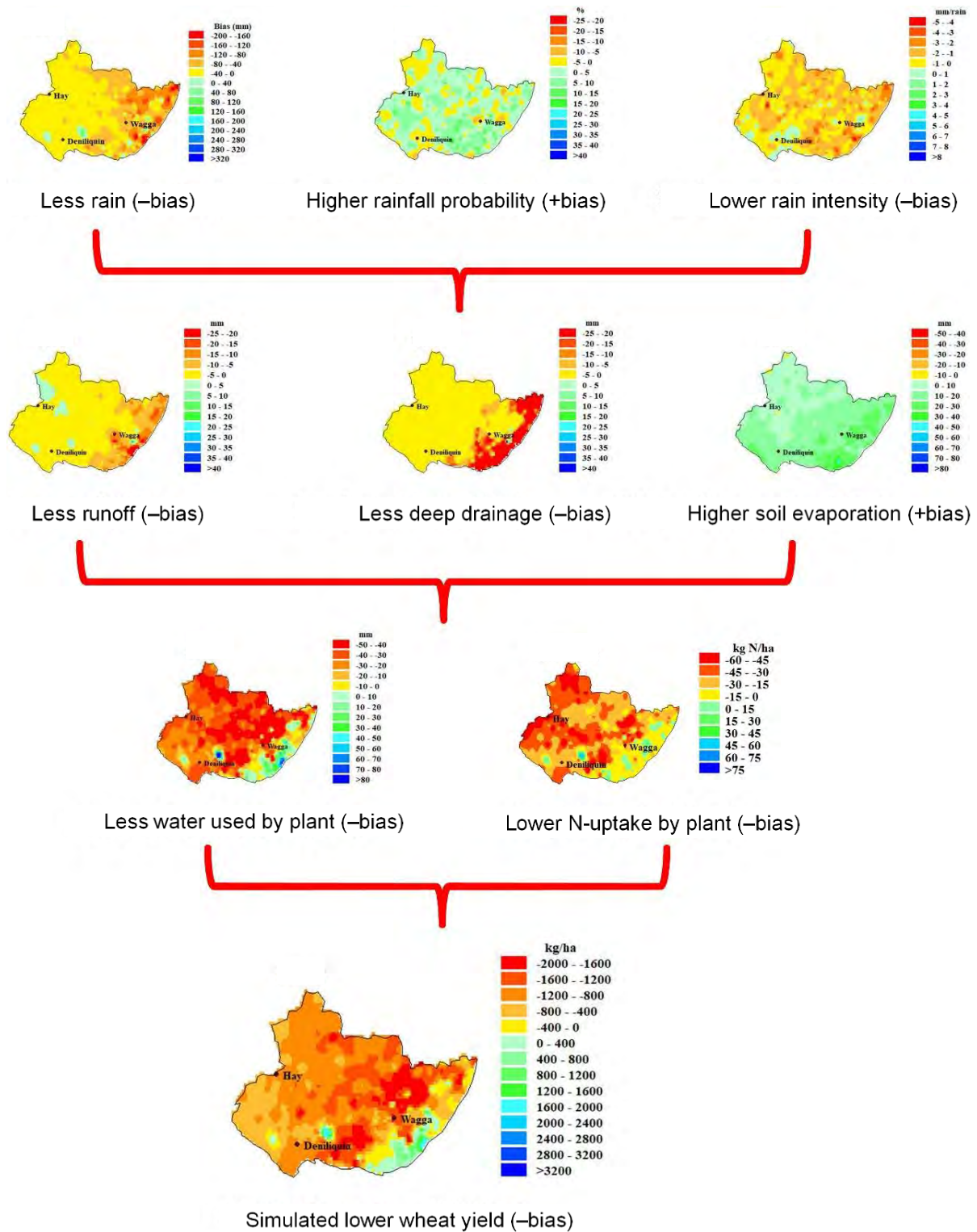
Figure 16 Schematic representation of the cause of biases in APSIM crop yield that track back to the subsequence of climate biases on soil water balance biases that lead to less plant water uptake, using the GCM MIROC3.2 as an example

Impacts of climate change on major crops in the MRC region

The bias-corrected yields were used to assess future changes in crop yields for the 2030s and 2070s. The simulated change in future crop yields varied across the study area. Overall, the ensemble mean yield for four crops across the Murray–Riverina cropping region corresponding to the A2 emissions scenario was projected to increase for both future time periods compared to the reference period. The magnitude of increase in crop yields was significant in the far future as a result of the higher CO_2 concentration compensating for some negative effects of climate change, such as shortening development due to increased temperature.

4.2　Limitations and further research

Uncertainties in the study include uncertainty of the GCMs and CO_2 emissions scenarios, the dynamical downscaling procedure and the bias correction of climate data based on an annual scale that resulted in retention of biases on a seasonal scale. Further, biophysical models contribute to uncertainties in the assessments. Therefore, care is needed in assessing each source of uncertainty and possible elimination of such biases is warranted.

5.　Conclusion

This study provided a comprehensive assessment of biases in NARCliM simulations at different cropping growth stages. Substantial biases were identified in NARCliM simulated climate for crop growing season, largely due to the NARCliM bias correction not accounting for different biases in different seasons. The biases in rainfall characteristics were generally positive in rainfall probability and negative in rainfall intensity, which resulted in APSIM simulated negative biases for most of the study area in runoff and deep drainage and positive biases in soil evaporation (due to wetter soil surface as a consequence of small and frequent rains). Consequently, biases in soil water balance and water availability resulted in less plant transpiration and less N uptake. Ultimately, those biases together with biases in crop phenology led to biases in crop yields.

The APSIM simulated crop yields exhibited a skewed distribution towards low yield, largely due to negative yield biases. Simple secondary bias correction (SBC) was able to produce yield distributions largely consistent with those forced by observed climate data. Impacts of climate change on crop yields were assessed for wheat, barley, canola and lupin and the SBC of crop yields were considered. The ensemble mean yield for the four crops across the MRC region corresponding to the A2 emissions scenario was projected to increase by +2–9% and +8–20% for the 2020 to 2039 and 2060 to 2079 periods respectively, compared to the 1990 to 2009 baseline period. A larger increase in the far future was a result of the higher CO_2 concentration compensating for negative effects. Positive effects on crops at the elevated CO_2 concentrations can be further increased under farm management options, particularly for cereal crops. For example, the rate of yield increased with increased N-application and residue incorporation, which benefited from the interaction between elevated CO_2 and crop higher N level, and from increased soil porosity and reduced soil water evaporation. Therefore, these farm management options can be used as effective adaptation options for cropping systems under future climate conditions.

The study implied that the current bias correction of NARCliM climate data did not result in adequate climate projections that can be used directly for assessment of climate change impacts on agriculture. This could be improved through refinement of the correction method to take into account different biases in different seasons of the year.

6. References

Balkovič J, van der Velde M, Skalsky R, Xiong W, Folberth C, Khabarov N, Smirnov A, Mueller ND, et al. 2014, Global wheat production potentials and management flexibility under the representative concentration pathways, *Global and Planetary Change*, vol.122, pp.107–121.

Dietzel R, Liebman M, Ewing R, Helmers M, Horton R, Jarchow M and Archontoulis S 2015, How efficiently do corn-and soybean-based cropping systems use water? A systems modeling analysis, *Global change biology*, vol.22, no.2, pp.666–681.

Evans JP, Ekstrom M and Ji F 2012, Evaluating the performance of a WRF physics ensemble over South-East Australia, *Climate Dynamics*, vol.39, no.6, pp.1241–1258.

Evans JP, Ji F, Abramowitz G, Ekstrom M 2013a, Optimally choosing small ensemble members to produce robust climate simulations, *Environmental Research Letters*, vol.8.

Evans JP, Fita L, Argüeso D and Liu Y 2013b, Initial NARCliM evaluation, in Piantadosi J, Anderssen RS and Boland J (eds), *MODSIM2013, 20th International Congress on Modelling and Simulation*, Modelling and Simulation Society of Australia and New Zealand, December 2013, pp.2765–2771.

Evans J, Ji F, Lee C, Smith P, Argüeso D and Fita L 2014, Design of a regional climate modelling projection ensemble experiment–NARCliM, *Geoscientific Model Development,* vol.7, pp.621–629.

Evans JP, Argueso D, Olson R and Di Luca A 2017, Bias-corrected regional climate projections of extreme rainfall in south-east Australia, *Theoretical and Applied Climatology*, vol.130, nos3–4, pp.1085–1098.

Fita L, Evans JP, Argüeso D, King AD and Liu Y 2016, Evaluation of the regional climate response to large-scale modes in the historical NARCliM simulations, *Climate Dynamics*, pp.1–15, doi: 10.1007/s00382-016-3484-x.

Haerter J, Hagemann S, Moseley C and Piani C 2011, Climate model bias correction and the role of timescales, *Hydrology and Earth System Sciences*, vol.15, no.3, pp.1065–1079.

Holzworth DP, Huth NI, Devoil PG, Zurcher EJ, Herrmann NI, Mclean G, Chenu K, Van Oosterom EJ, Snow V, Murphy C, Moore AD, Brown H, Whish JPM, Verrall S, Fainges J, Bell LW, Peake AS, Poulton PL, Hochman Z, Thorburn PJ et al. 2014, APSIM – Evolution towards a new generation of agricultural systems simulation, *Environmental Modelling and Software*, vol.62(C), pp.327–350.

Huth NI, Banabas M, Nelson PN and Webb M 2014, Development of an oil palm cropping systems model: Lessons learned and future directions, *Environmental Modelling and Software*, vol.62, pp.411–419.

IPCC 2000, *Special Report on Emissions Scenarios: A Special Report of Working Group III of the Intergovernmental Panel on Climate Change*, published for the Intergovernmental Panel on Climate Change by Cambridge University Press, Cambridge, UK.

Ji F, Ekstrom M, Evans JP and Teng J 2014, Evaluating rainfall patterns using physics scheme ensembles from a regional atmospheric model, *Theoretical and Applied Climatology*, vol.115, pp.297–304.

Ji F, Evans JP, Teng J, Scorgie Y, Argüeso D and Di Luca A 2016, Evaluation of long-term precipitation and temperature WRF simulations for southeast Australia, *Climate Research*, vol.67, pp.99–115.

Keating BA et al. 2003, An overview of APSIM, a model designed for farming systems simulation, *European Journal of Agronomy*, vol.18, no.3, pp.267–288.

Liu DL, Anwar MR, O'Leary G and Conyers MK 2014, Managing wheat stubble as an effective approach to sequester soil carbon in a semi-arid environment: Spatial modelling, *Geoderma*, vol.214–215, pp.50–61.

Liu DL, O'Leary GJ, Ma Y, Cowie A, Li FY, McCaskill M, Conyers M, Dalal R, Robertson F and Dougherty W 2016, Modelling soil organic carbon 2: Changes under a range of cropping and grazing farming systems in eastern Australia, *Geoderma*, vol.265, pp.164–175.

Liu DL, Zeleke KT, Wang B, Macadam I, Scott F and Martin RJ 2017, Crop residue incorporation can mitigate negative climate change impacts on crop yield and improve water use efficiency in a semiarid environment, *European Journal of Agronomy*, vol.85, pp.51–68.

Liu DL, Wang B, Evans J, Ji F, Waters C, Macadam I, Yang X and Beyer K 2019, Propagation of climate model biases to biophysical modelling can complicate assessments of climate change impact in agricultural systems, *International Journal of Climatology*, vol.39, pp.424–444, https://doi.org/10.1002/joc.5820.

Lychuk TE, Hill RL, Izaurralde RC, Momen B and Thomson AM 2017, Evaluation of climate change impacts and effectiveness of adaptation options on crop yield in the Southeastern United States, *Field Crops Research*, vol.214(Supplement C), pp.228–238.

Macadam I, Pitman AJ, Whetton PH, Liu DL and Evans JP 2014, The use of uncorrected regional climate model output to force impact models: a case study for wheat simulations, *Climate Research*, vol.61, no.3, pp.215–229.

Macadam I, Argüeso D, Evans JP, Liu DL and Pitman AJ 2016, The effect of bias correction and climate model resolution on wheat simulations forced with a regional climate model ensemble, *International Journal of Climatology*, vol.36, no.14, pp.4577–4591.

OEH 2013, *Scientific Rigour Position Statement*, NSW Office of Environment and Heritage, www.environment.nsw.gov.au/-/media/OEH/Corporate-Site/Documents/Research/Our-science-and-research/oeh-scientific-rigour-position-statement-2013.pdf.

O'Leary GJ, Liu DL, Ma Y, Li FY, McCaskill M, Conyers M, Dalal R, Reeves S, Page K, Dang YP and Robertson F 2016, Modelling soil organic carbon 1: Performance of APSIM crop and pasture modules against long-term experimental data, *Geoderma*, vol.264(Part A), pp.227–237.

Piani C, Haerter J and Coppola E 2010, Statistical bias correction for daily precipitation in regional climate models over Europe, *Theoretical and Applied Climatology*, vol.99, nos1–2, pp.187–192.

Probert M, Dimes J, Keating B, Dalal R and Strong W 1998, APSIM's water and nitrogen modules and simulation of the dynamics of water and nitrogen in fallow systems, *Agricultural systems*, vol.56, no.1, pp.1–28.

Skamarock WC, Klemp JB, Dudhia J, Gill DO, Barker DM, Duda MG, Huang XY, Wang W and Powers JG 2008, *A description of the advanced research WRF Version 3,* NCAR Technical Note, National Center for Atmospheric Research, Boulder Colorado, USA.

Tai AP, Martin MV and Heald CL 2014, Threat to future global food security from climate change and ozone air pollution, *Nature Climate Change*, vol.4, no.9, pp.817–821.

Turpin JE, Robertson M, Haire C, Bellotti W, Moore A and Rose I 2003, Simulating fababean development, growth, and yield in Australia, *Crop and Pasture Science,* vol.54, no.1, pp.39–52.

Wang B, Evans J, Ji F, Waters C, Macadam I, Feng P and Beyer K 2019, Modelling and evaluating the impacts of climate change on three major crops in south-eastern Australia using regional climate model simulations, *Theoretical and Applied Climatology*, vol. 136, nos1–2, pp. 509–526, 10.1007/s00704-019-02843-7.

Wheeler T and Von Braun J 2013, Climate change impacts on global food security, *Science*, vol.341(6145), pp.508–513.

Yang Y, Liu DL, Anwar MR, Zuo H and Yang Y 2014, Impact of future climate change on wheat production in relation to plant-available water capacity in a semiarid environment, *Theoretical and Applied Climatology*, vol.115, nos3–4, pp.391–410.

Yang Y, Liu DL, Anwar MR, O'Leary G, Macadam I and Yang Y 2016, Water use efficiency and crop water balance of rainfed wheat in a semi-arid environment: sensitivity of future changes to projected climate changes and soil type, *Theoretical and Applied Climatology*, vol.123, pp.565–579.

Ziska LH, Bunce JA, Shimono H, Gealy DR, Baker JT, Newton PCD, Reynolds MP, Jagadish KSV, Zhu C, Howden M and Wilson LT 2012, Food security and climate change: on the potential to adapt global crop production by active selection to rising atmospheric carbon dioxide, *Proceedings of the Royal Society of London Proceedings B*, 279(1745), pp.4097–4105.

DEPARTMENT OF PLANNING, INDUSTRY & ENVIRONMENT

Climate change impacts in the NSW and ACT Alpine region

Impacts on fire weather

Cover photo: Winter landscape in Kosciuszko National Park. John Spencer/DPIE

Find out more about your environment at:

www.environment.nsw.gov.au

Contents

List of tables

List of figures

List of shortened forms

ACT	Australian Capital Territory
CMIP	Coupled Model Intercomparison Project
DJF	December January February
DPIE	Department of Planning, Industry and Environment
ECL	East Coast Low
FFDI	Forest Fire Danger Index
FDR	Fire Danger Rating
GCM	Global Climate Model
JJA	June July August
KBDI	Keetch-Byram Drought Index
MAM	March April May
MCAS-S	Multi-Criteria Analysis Shell for Spatial Decision Support
mm	millimetre
MM	Murray-Murrumbidgee state planning region
NARCliM	NSW/ACT Regional Climate Modelling project
NSW	New South Wales
RCM	Regional Climate Model
SET	South East and Tablelands state planning region
SON	September October November
SRES	Special Report on Emissions Scenarios
UNSW	The University of New South Wales
WRF	Weather Research and Forecasting
WDM5	WRF Double Moment 5-class

Summary of findings

Impacts on fire weather in the NSW and ACT Alpine region

1. Clear seasonal variation in the Forest Fire Danger Index (FFDI) is observed in the central and western Murray-Murrumbidgee (MM) state planning region, likely due to the large season variations in temperature.

2. In the near future (2020 to 2039), a less than 5% decrease in FFDI is projected for the southern MM region and South East and Tableland (SET) region. A 5–10% decrease is projected for remaining parts of the study area, apart from the Alpine region.

3. These decreases are likely due to predicted increases of 10% in precipitation. While temperature is projected to increase by 0.5–1°C, wind speed is projected to decrease by 2–4%.

4. In the Alpine region in the near future, a small increase (5%) is projected in the annual FFDI, mostly due to the predicted decrease in precipitation. Strong seasonal variation in the FFDI is seen in this region however, with an up to 30% increase in FFDI projected for winter and spring.

5. Other than the Alpine and southern SET regions, a decrease of up to 15% in FFDI is projected for most regions in the far future (2060 to 2079).

6. In the far future a greater than 30% increase in FFDI is projected for the Alpine region in winter and spring, with an annual increase of 5–10% predicted across all seasons.

7. In the near future, a small increase in the number of extreme fire days (0.5–1.5 days a year) is projected for the central and western MM region.

8. In the far future, an increase of 2–3, 1–2 and 0.5 extreme fire weather days is projected for the western MM, central MM and northern SET regions, respectively.

9. The Alpine and southern SET regions show little change in the number of extreme fire days in either the near or far future projections.

1.   Introduction

1.1   Background

The New South Wales (NSW) and Australian Capital Territory (ACT) Alpine region is located in the south-eastern corner of mainland Australia and is the highest mountain range in Australia. Though it comprises only about 0.16% of Australia in size, it is an important region for ecosystems, biodiversity, energy generation and winter tourism. It forms the southern end of the Great Dividing Range, covering a total area of 1.64 million hectares that extend over 500 kilometres. The highest peak, Mount Kosciuszko, rises to an altitude of 2228 metres.

This report is part of a larger project delivered by the NSW Department of Planning, Industry and Environment on the various impacts from climate change on the NSW and ACT Alpine region, hereafter referred to as the Alpine region. The full study region covers the Murray-Murrumbidgee region (MM), South East and Tablelands (SET) and the ACT, bordering the Victorian border in the south (Figure 1).

The Alpine region is vulnerable to climate change. Observations have shown substantial changes in precipitation and temperature for this area (Di Luca et al. 2018), which have already impacted biodiversity and ecosystems (Hughes 2011). In 2014, the NSW/ACT Regional Climate Modelling (NARCliM) project was delivered. Climate snapshots for each of the 11 NSW planning regions and the ACT were developed to demonstrate observed and projected climate change; however, the snapshots only show changes for some variables and focus on each planning region.

Figure 1   **The study area for the Alpine project, including the NSW and ACT Alpine region, Murray-Murrumbidgee region and South East and Tablelands**

1.2   Objectives

While bushfires are a natural phenomenon in Australia, they can cause dramatic damage and loss. The risk of bushfire in any given region depends on four 'switches' that must all be present for a bushfire to occur (Bradstock 2010):

1. There needs to be enough vegetation (fuel).
2. The fuel must be dry enough to burn.
3. The weather must be favourable for fire to spread.
4. There must be an ignition source.

Fuel load in Australia is projected to increase substantially by the late 21st century (Clarke 2015a). More days with extremely dry fuel in eucalypt forests are expected when a warmer and drier climate is projected (Matthews et al. 2011). Clarke (2015b) reviewed the state of knowledge about how climate change will impact bushfire risk in New South Wales. This study considers the full range of national and international research on the four 'switches'.

Bushfires can be calculated from meteorological variables obtained directly from global and regional climate models. Fire weather has been heavily studied in Australia, with many studies investigating changes in the Forest Fire Danger Index (FFDI) (e.g. Beer & Williams 1995; Williams et al. 2001; Cary 2002; Lucas et al. 2007; Bradstock et al. 2009; Clarke et al. 2011; Fox-Hughes et al. 2014). Clarke et al. (2013) examined historical trends in FFDI. They found that the observational record of FFDI in Australia is marked by clear inter-annual variability with a large degree of spatial coherence, suggesting common drivers in its evolution.

The natural ignition source is lightning. The impact of climate change on lightning has been assessed directly by modelling the drivers of lightning (Price & Rind 1994; Goldammer & Price 1998) and indirectly by linking lightning with other weather patterns (Krawchuk et al. 2009; Penman et al. 2013).

In this study, we focus on bushfire weather. In Australia, fire weather risk is quantified using the Forest Fire Danger Index (FFDI) (Luke & McArthur 1978):

$$FFDI = 2 \times \exp\big(0.987 \times \ln(DF) + 0.0338T + 0.0234V - 0.0345RH - 0.45\big)$$

where DF = drought factor, T = air temperature (°C), V = 3pm wind speed in km/h and RH = 3pm relative humidity (%). The drought factor is calculated using the Griffiths (1999) formulation and uses the Keetch-Byram Drought Index (KBDI; Keetch & Byram 1968) to estimate the soil moisture deficit. The Mount Soil Dryness Index (Mount 1972) is a possible alternative to KBDI, but it is not well-suited to inland areas of Australia (Finkele et al. 2006).

The Fire Danger Rating (FDR) system is often used by fire agencies to reflect the behaviour of a fire and the difficulty of controlling a particular fire (Table 1).

The FFDI estimates (derived from the weather observation) are available for 17 meteorological stations across New South Wales and the Australian Capital Territory (Table 2). While these stations are spread fairly evenly across the state, there are few stations in the study area. The mean annual FFDI estimated for the 1990 to 2009 baseline period ranges from 3.3 in Coffs Harbour to 21.2 in Tibooburra. The highest mean FFDI occurs in summer and spring and the lowest is usually in winter.

Table 1   **Categories of the Fire Danger Rating system and the expected fire behaviour for standardised fuel**

(i.e. dry sclerophyll forest with an available fuel load of 12 tonnes/hectare on flat ground) (Vercoe 2003)

Fire Danger Rating	FFDI range	Difficulty of suppression
Low	0 to 5	Fire easily suppressed with hand tools.
Moderate	5 to 12	Fire usually suppressed with hand tools and easily suppressed with bulldozers. Generally, the upper limit for prescribed burning.
High	12 to 25	Fire generally controlled with bulldozers working along the flanks to pinch the head out under favourable conditions. Back burning may fail due to spotting.
Very high	25 to 50	Initial attack generally fails but may succeed in some circumstances. Back burning will fail due to spotting. Burning out should be avoided.
Extreme	50+	Fire suppression virtually impossible on any part of the fire line due to the potential for extreme and sudden changes in fire behaviour. Any suppression actions such as burning out will only increase fire behaviour and the area burnt.

Table 2   **Mean annual and seasonal Forest Fire Danger Indices for the 1990 to 2009 baseline period for 17 meteorological stations within NSW and the ACT**

Station	Annual	Summer	Autumn	Winter	Spring
Bourke	16.3	24.4	13.9	8.0	19.4
Broken Hill	12.1	17.7	10.3	6.0	14.8
Canberra	6.9	11.4	7.2	2.6	6.4
Casino	6.4	5.0	4.1	6.8	10.0
Cobar	14.0	21.5	11.9	6.3	16.3
Coffs Harbour	3.3	2.8	2.0	4.0	4.3
Dubbo	10.3	16.1	10.1	4.1	10.9
Hay	9.4	15.6	8.9	3.4	10.2
Lismore	4.9	4.1	3.1	5.3	7.1
Moree	12.1	13.8	11.9	7.5	15.3
Nowra	5.2	5.6	4.3	4.4	6.6
Richmond	7.1	8.3	5.2	5.4	9.8
Sydney Airport	5.5	6.1	4.1	4.5	7.4
Tibooburra	21.2	31.1	18.2	10.3	25.1
Wagga	10.0	19.4	10.0	2.2	8.6
Wilcannia	18.5	28.3	16.4	8.6	21.2
Williamtown	5.4	6.7	3.4	4.1	7.4

Extreme fire weather conditions are estimated to occur at least once a year at all stations with the exceptions of Lismore and Coffs Harbour. Extreme fire weather days are more likely to occur in the summer and spring months (Table 3). Tibooburra and Wilcannia record considerably more days with the FFDI above 50 each year compared to other stations (20 days per year and 12 days per year, respectively).

Table 3 **Mean annual and seasonal extreme fire weather days for the 1990 to 2009 baseline period (FFDI >50) for stations within NSW and the ACT**

Station	Annual	Summer	Autumn	Winter	Spring
Bourke	7.2	4.7	0.2	0.1	2.3
Broken Hill	2.2	0.7	0.2	0.1	1.3
Canberra	1.1	0.8	0.2	0.0	0.2
Casino	2.1	0.1	0.0	0.5	1.5
Cobar	5.3	3.4	0.2	0.0	1.8
Coffs Harbour	0.3	0.1	0.0	0.0	0.2
Dubbo	3.1	1.7	0.1	0.0	1.4
Hay	1	0.4	0.1	0.0	0.6
Lismore	0.3	0.0	0.0	0.1	0.3
Moree	3.3	1.6	0.2	0.0	1.5
Nowra	1.1	0.6	0.0	0.0	0.5
Richmond	1.8	1.0	0.1	0.0	0.7
Sydney Airport	1.4	0.6	0.1	0.1	0.7
Tibooburra	19.9	11.2	1.3	0.3	7.2
Wagga	5.2	3.7	0.2	0.0	1.3
Wilcannia	12.4	6.8	1.1	0.2	4.4
Williamtown	1.4	0.7	0.0	0.0	0.7

Observations have shown some changes in precipitation and temperature and NARCliM future climate projections indicate increases in temperature and decreases in precipitation for this region (Di Luca et al. 2018). Such changes will lead to changes in bushfire behaviour. In this study, we use NARCliM projections to assess whether bushfire weather for the Alpine region will change under future projected climate conditions.

The downscaled 10 kilometre climate projections from the NARCliM project (Evans et al. 2014) are available for a baseline period (1990 to 2009), and near future (2020 to 2039) and far future (2060 to 2079) periods. The NARCliM project produced more than 140 variables for 12 ensemble members, which were used to calculate FFDI (Clarke et al. 2016).

The objectives of this study were to (i) project the mean changes of FFDI across the alpine study area in New South Wales based on the NARCliM projections; and (ii) project changes in extreme FFDI days across the study area to assist the long-term climate change adaptation and regional planning in the Alpine region.

1.3   Outputs

Output	Details	Key users
Report	Future fire weather projection	Researchers
Data	FFDI for each of the 12 ensemble members Mean FFDI for three time periods Mean extreme FFDI days for three time periods	NSW National Parks & Wildlife Service NSW Rural Fire Service
Maps	Maps of the annual and seasonal FFDI	Councils, NSW Rural Fire Service

2.   Method

2.1   Source of data

NARCliM simulations from four Coupled Model Intercomparison Project phase 3 (CMIP3) Global Climate Models (GCMs) were used to drive three Regional Climate Models (RCMs) to form a 12-member GCM/RCM ensemble (Evans et al. 2014). The four selected GCMs are MIROC3.2, ECHAM5, CCCMA3.1 and CSIRO-MK3.0. For future projections, the Special Report on Emissions Scenarios (SRES) business-as-usual A2 scenario was used (IPCC 2000). The three selected RCMs are three physics scheme combinations of the Weather Research and Forecasting (WRF) model. Each simulation consists of three 20-year runs (1990 to 2009, 2020 to 2039, and 2060 to 2079). The four GCMs were chosen based on a number of criteria: i) adequate performance when simulating historic climate; ii) most independent; iii) cover the largest range of plausible future precipitation and temperature changes for Australia. The three RCMs correspond to three different physics scheme combinations of the WRF V3.3 model (Skamarock et al. 2008), which were also chosen for adequate skill and error independence, following a comprehensive analysis of 36 different combinations of physics parameterisations over eight significant East Coast Lows (ECLs) (Evans et al. 2012; Ji et al. 2014a). For the selected three RCMs, the WRF Double Moment 5-class (WDM5) microphysics scheme and NOAH land surface scheme are used in all cases. Refer to Evans et al. (2014) for more details on each physics scheme.

We acknowledge that the results are model dependent (as all model studies are) but through the use of this carefully selected ensemble we have attempted to minimise this dependence. By using this model selection process, we have shown that it is possible to create relatively small ensembles that are able to reproduce the ensemble mean and variance from the large parent ensemble (i.e. the many GCMs) as well as minimise the overall error (Evans et al. 2013a).

Some initial evaluation of NARCliM simulations shows that they have strong skill in simulating the precipitation and temperature of Australia, with a small cold bias and overestimation of precipitation on the Great Dividing Range (Evans et al. 2013b, Ji et al. 2016). The differing responses of the different RCMs confirm the utility of considering model independence when choosing the RCMs. The RCM response to large-scale modes of variability also agrees well with observations (Fita et al. 2016). Through these evaluations we found that while there is a spread in model predictions, all models perform adequately with no single model performing the best for all variables and metrics. The use of the full ensemble provides a measure of robustness such that any result that is common through all models in the ensemble is considered to have higher confidence.

In total, there were four same GCM driven simulations (average of three members) and three same RCM used simulations (average of four members). The analyses in this study are based on the ensemble mean of these simulations.

2.2   Quality control

FFDI is calculated using NARCliM outputs, which have been subjected to comprehensive data quality assurance/quality control (Ji et al. 2014b). The method for quantifying future climate projections is widely used. Annual climate projections are similar to those shown on the AdaptNSW Climate projections for your region webpage. Seasonal and monthly future projections use the same method but for finer timescale outputs.

The data have also been evaluated as conference and journal papers (Evans et al. 2013b; Ji et al. 2016; Fita et al. 2016). Similar climate projections from NARCliM have been published as technical reports (Olson et al. 2014; Di Luca et al. 2016) and peer reviewed scientific publications (Olson et al. 2016; Di Luca et al. 2018).

2.3   Data storage and access

All output data were converted to raster format (ArcGIS ESRI grid) and supplied to the MCAS-S (Multi-Criteria Analysis Shell for Spatial Decision Support) datapacks for distribution and storage. All input data to the model and by-products are stored on hard disk drives. All data are in the NARCliM coordinate system. The extent of the datasets includes the MM region, ACT and SET with the boundary at top: –32.671254, left: 143.317445, right: 150.745676, and bottom: –37.505077.

3.   Results

3.1   Forest Fire Danger Index

Mean FFDI for the 1990 to 2009 baseline period

The annual mean daily FFDI for the NARCliM baseline period (1990 to 2009) is shown in Figure 2. Generally, a moderate fire rating is simulated for the central and western MM and a low fire rating for the remaining areas. The smallest FFDI values are found in the Alpine region. The larger FFDI for the central and western MM is mostly due to the higher temperatures and lower precipitation. In contrast, the smallest FFDI values for the Alpine region are caused by the lower temperatures and wetter conditions (where annual precipitation is greater than 1800 mm).

There is a clear seasonal variation in the FFDI for the central and western MM, with the largest value in summer and the smallest value in winter (Figure 3). Relatively smaller seasonal variation is found for other regions, especially in the coastal region. In summer a high fire rating (greater than 12) is simulated for the central and western MM and a moderate fire rating (5–12) for most other areas. A low fire rating (less than 5) is simulated for almost the entire region in winter. The fire weather rating for the remaining two seasons is like that for the annual average.

As noted in the accompanying 'Projected climate' report, there is a larger seasonal variation in temperature for the central and western MM; however, the seasonal variations of rainfall and wind speed are relatively small. This implies that larger seasonal variation in the FFDI is mostly determined by the larger seasonal variation in temperature for those areas.
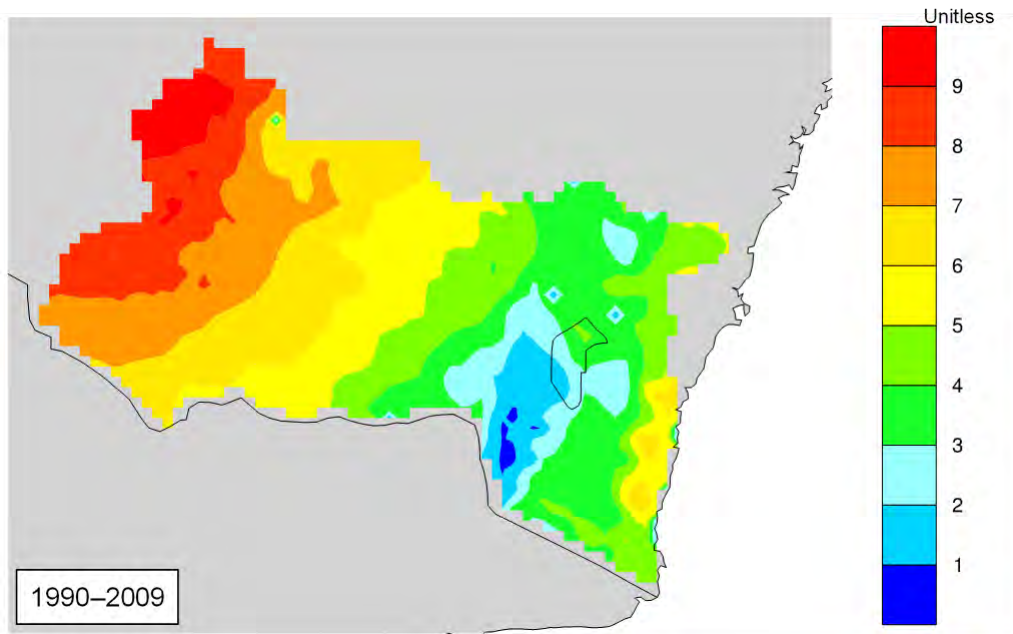
Figure 2   **Mean annual FFDI for the 1990 to 2009 baseline period**
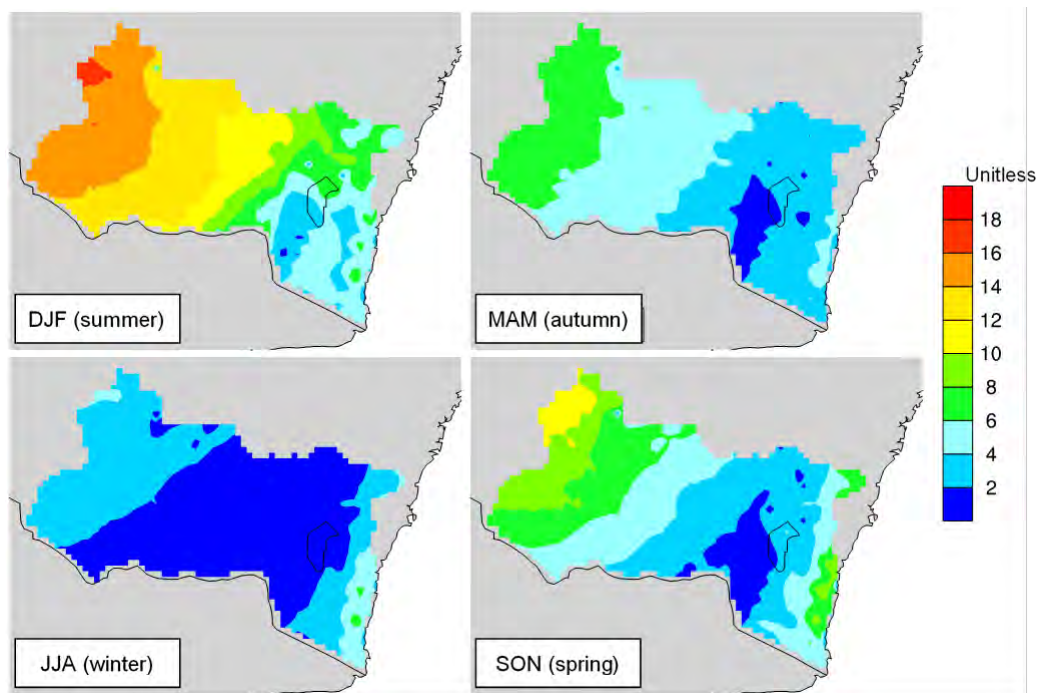
Figure 3   **Mean seasonal FFDI for the 1990 to 2009 baseline period**

Changes in mean FFDI for 2020 to 2039

Relative changes in the annual mean daily FFDI for the near future (2020 to 2039) are shown in Figure 4. A less than 5% increase in FFDI is projected for the Alpine region, but a decrease in the FFDI is projected for most of the study area. Larger decreases (above 10%) are projected for the northern SET and north-east MM. A less than 5% decrease is projected for the southern MM and south-western SET region. A 5–10% decrease is projected for the remaining regions.

An increase in daily FFDI for the Alpine region is mostly due to a decrease in precipitation. For the Alpine region, up to a 10% decrease in precipitation is projected for the near future, and temperature is projected to increase by 0.5–1°C. Wind speed on the other hand is projected to decrease by 2–4%. Similarly, a decrease in daily FFDI for other regions is also determined by increases in precipitation as there is little difference in projected change in temperature between the alpine and other regions.
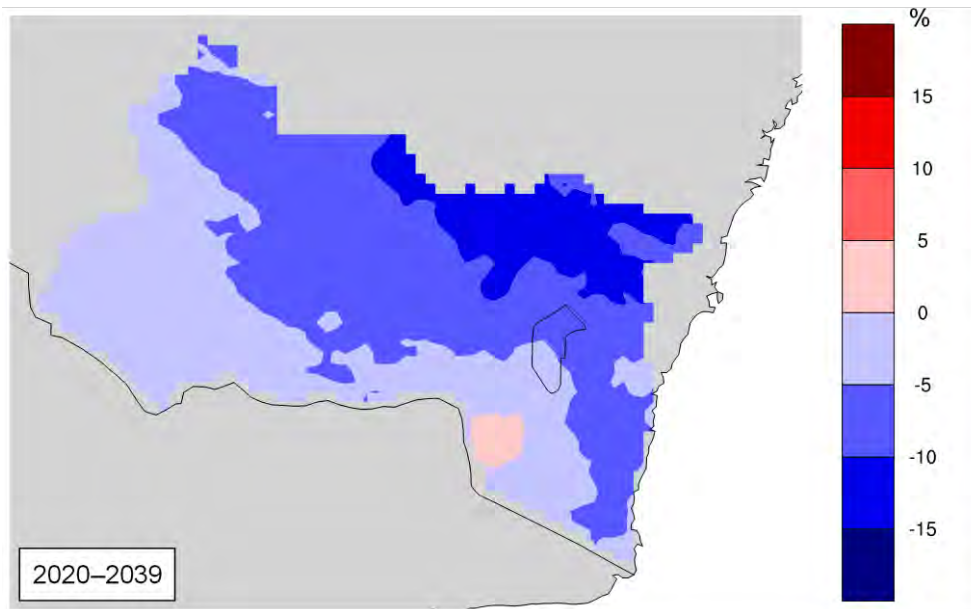
Figure 4   Changes in annual FFDI (%) for 2020 to 2039 relative to 1990 to 2009

An up to 30% increase in the FFDI is projected for the Alpine region in winter and spring (Figure 5). This is mainly due to a 10–20% decrease in rainfall for the region during the same period. Large increases in temperature in spring projected for the Alpine region may also contribute to the larger increase in FFDI for the same season. The FFDI in other regions is projected to decrease, particularly for the northern study area where an up to 20% decrease is projected for summer due to more precipitation for the region in future.
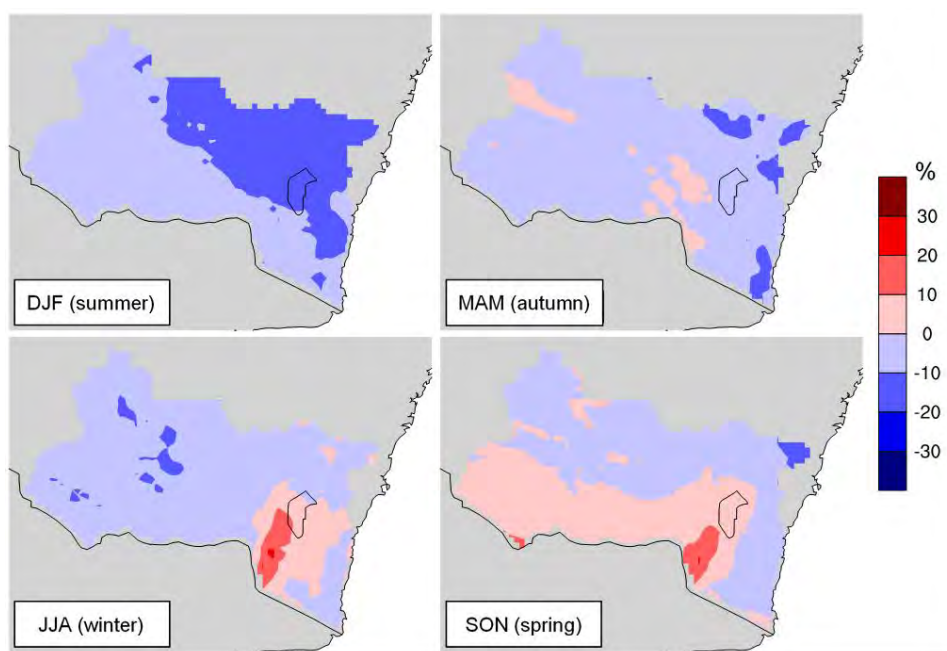
Figure 5   Changes in seasonal FFDI (%) for 2020 to 2039 relative to 1990 to 2009

Changes in mean FFDI for 2060 to 2079

A 5–10% increase in the FFDI is projected for the Alpine region in the far future (Figure 6), which is larger than the projected increase for the near future. The larger increase in FFDI is determined by an up to 10% decrease in precipitation, a large increase in the number of dry days and a large increase in maximum temperature.
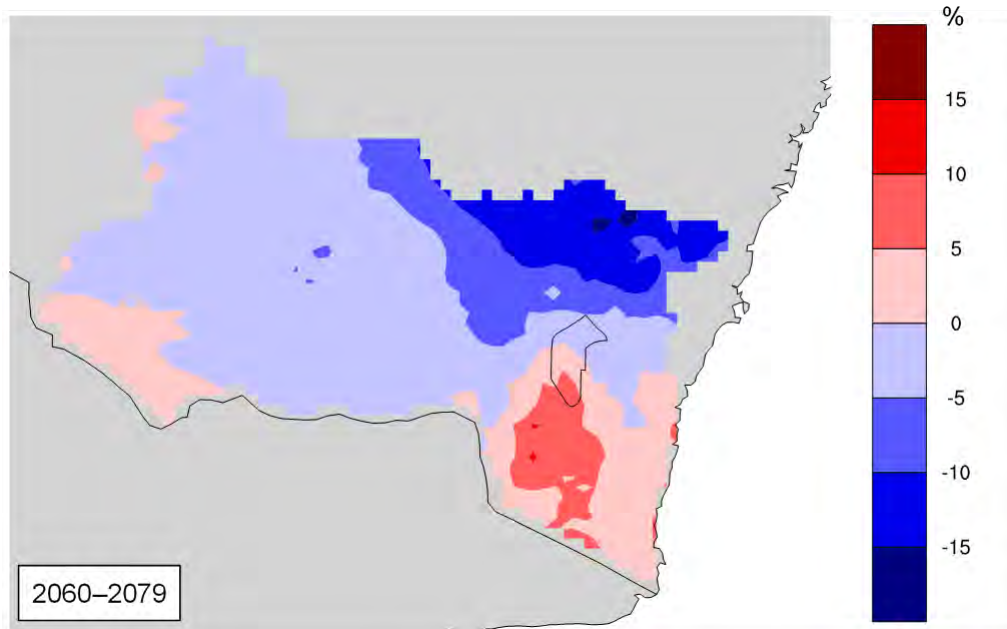
Figure 6   **Changes in annual FFDI (%) for 2060 to 2079 relative to 1990 to 2009**

Additionally, a greater than 30% increase in the FFDI is projected for the Alpine region in winter and spring (Figure 7). This is mostly caused by the larger decrease in precipitation during these seasons. Increases in temperature for the Alpine region may contribute to increases in FFDI.
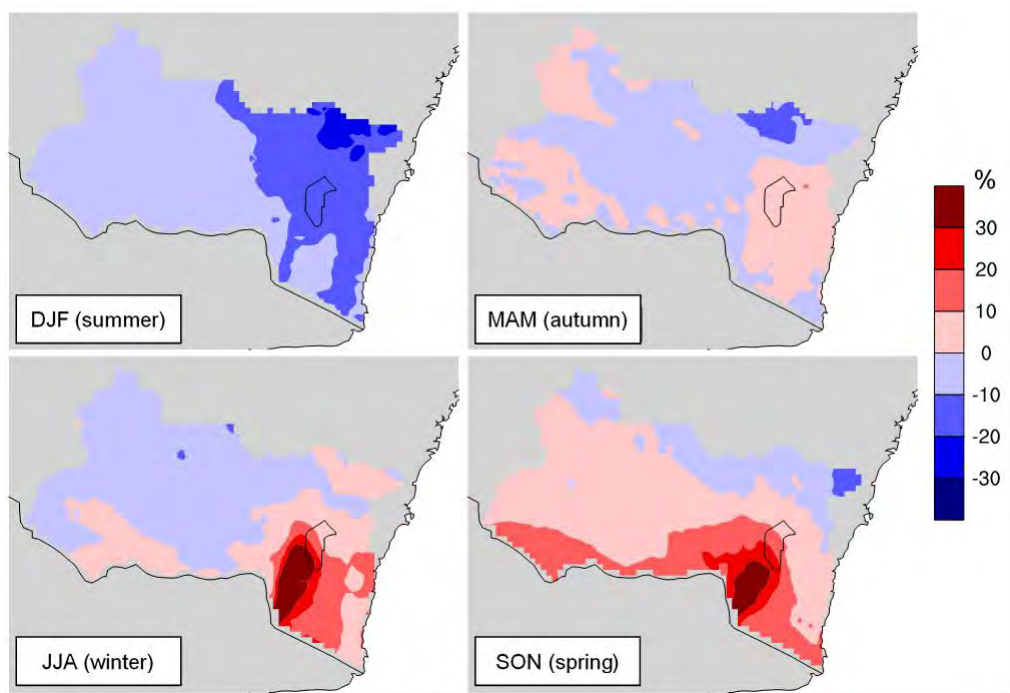
Figure 7   **Changes in seasonal FFDI (%) for 2060 to 2079 relative to 1990 to 2009**

3.2 Extreme fire weather days

Extreme fire weather days for the 1990 to 2009 baseline period

Extreme fire weather is defined by an FFDI greater than 50. For the 1990 to 2009 baseline period, there are almost no extreme fire weather days for the ACT and SET regions, 1–2 extreme fire weather days per year for the eastern MM, and 2–5 extreme fire weather days for central and western MM (Figure 8). Extreme fire weather in the central and western MM is due to high temperatures and low rainfall in these regions. In contrast, there is no extreme fire weather in other regions due to lower temperatures and higher rainfall.
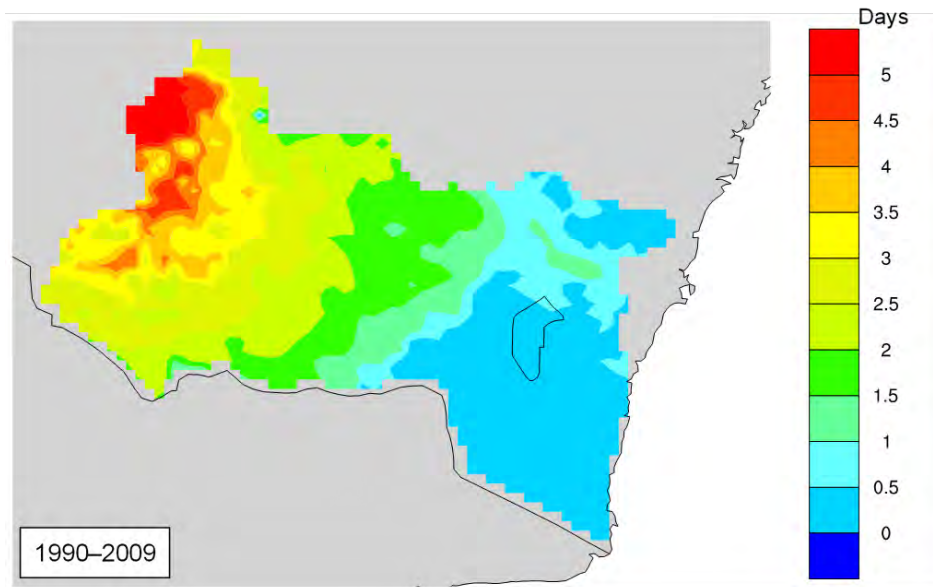
Figure 8   **Mean annual extreme FFDI days (days with FFDI >50) for the 1990 to 2009 baseline period**

Extreme fire weather days are mostly in summer for the MM, with few extreme fire weather days in spring, particularly for the western MM (Figure 9). There is no extreme fire weather in autumn and winter.
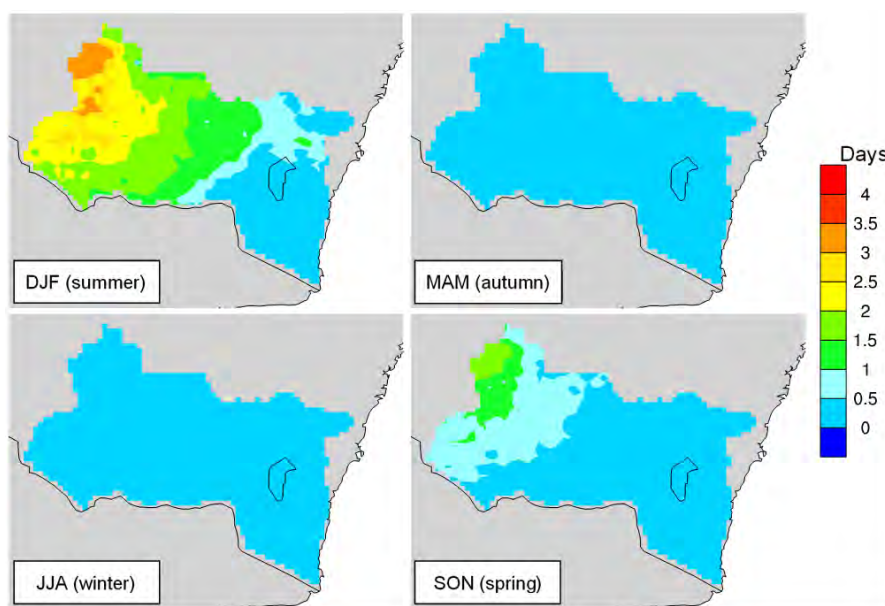
Figure 9   **Mean seasonal extreme FFDI days (days with FFDI >50) for the 1990 to 2009 baseline period**

Changes in the number of extreme fire weather days for 2020 to 2039

Changes in the number of extreme fire weather days for the near future projection period of 2020 to 2039 are relatively small (Figure 10). Little change is projected for SET, ACT and eastern MM. A small increase (0.5–1.5 days a year) is projected for the central and western MM. Increases in extreme fire weather days are mostly in spring and summer for the central and western MM, with minor changes for other regions and other seasons (Figure 11).
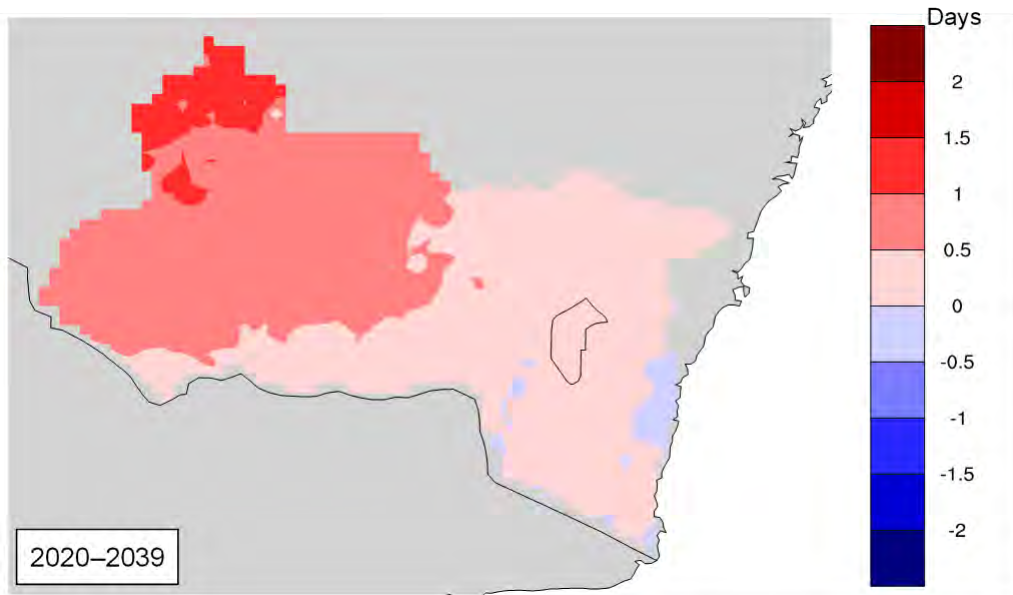
Figure 10   **Changes in annual extreme FFDI days (days with FFDI >50) for 2020 to 2039 relative to 1990 to 2009**
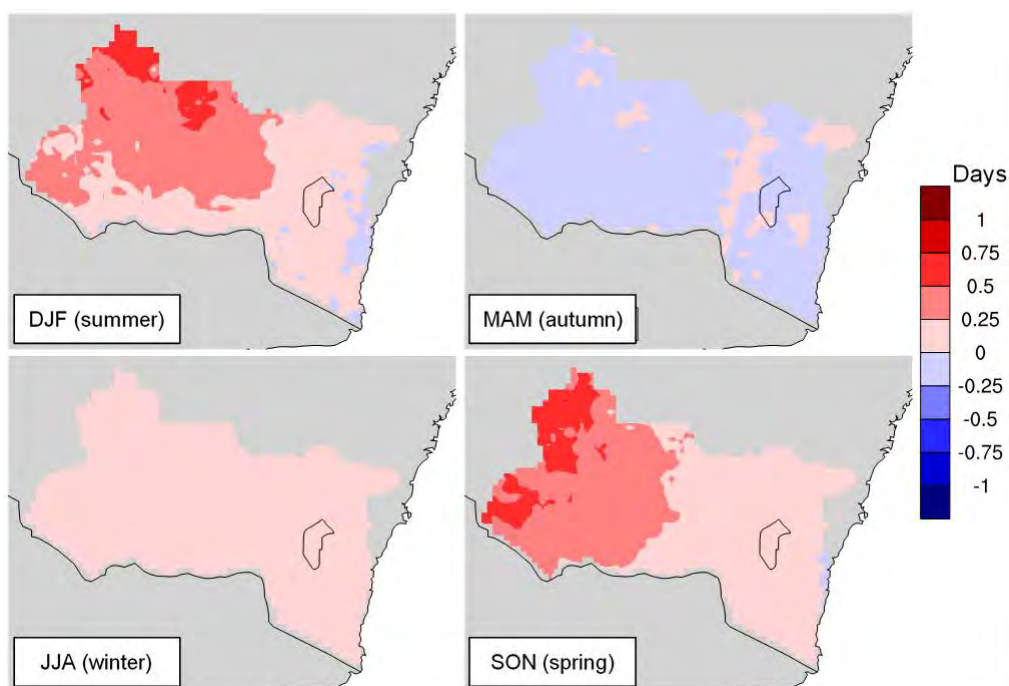
Figure 11   **Changes in seasonal extreme FFDI days (days with FFDI >50) for 2020 to 2039 relative to 1990 to 2009**

Changes in the number of extreme fire weather days for 2060 to 2079

Changes in annual extreme fire weather days for the far future (2060 to 2079) are larger than those for the near future (2020 to 2039). There is a projected increase of 2–3 days in extreme fire weather for the western MM, 1–2 days for the central MM, and a small increase for the northern SET region (more than 0.5 days a year) (Figure 12). There is little change for other regions, notably for the Alpine region. Increases in extreme fire weather days are mostly in spring and summer for the central and western MM, with little change for other regions and other seasons (Figure 13).
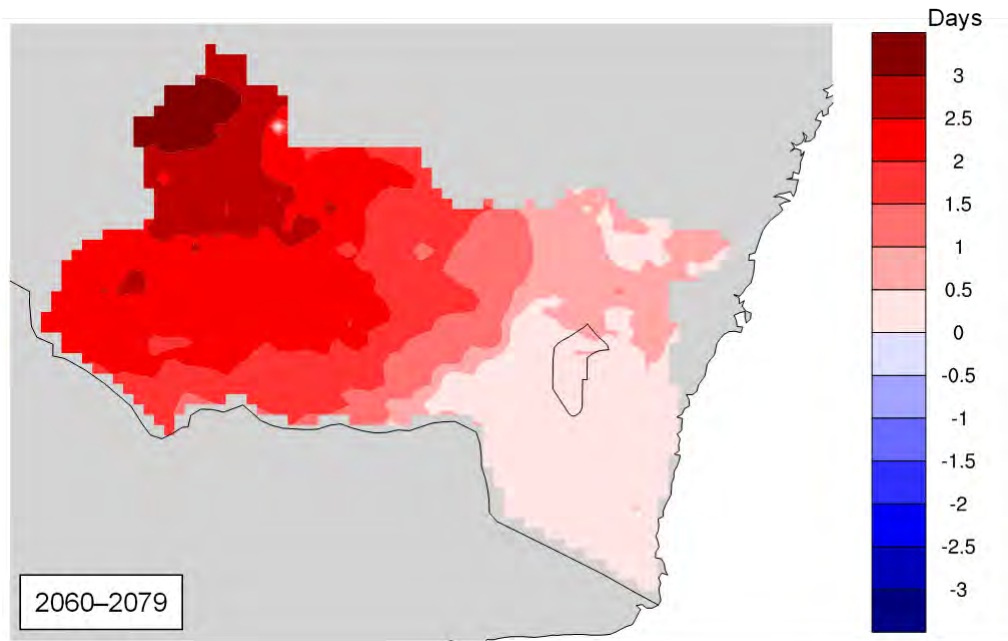
Figure 12 **Changes in annual extreme FFDI days (days with FFDI >50) for 2060 to 2079 relative to 1990 to 2009**
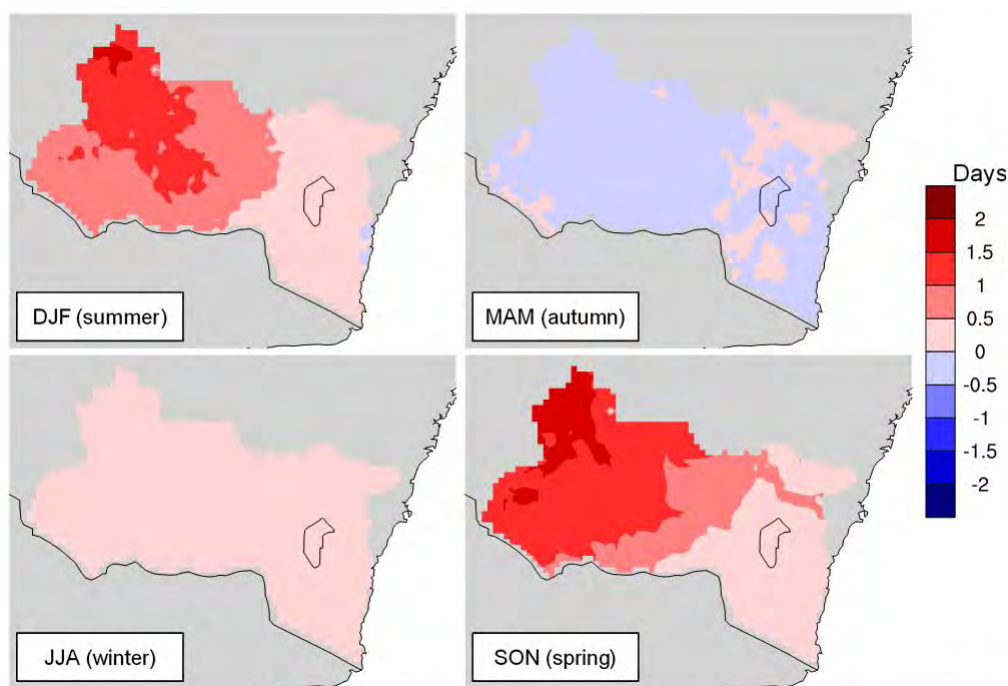
Figure 13 **Changes in seasonal extreme FFDI days (days with FFDI >50) for 2060 to 2079 relative to 1990 to 2009**

4.   Discussion

4.1   Key findings

The results of this report show changes in the FFDI that are projected for the Alpine region and surrounding areas. The overall key findings indicate:

- The annual mean FFDI is generally small for the study area with a moderate fire weather rating for the central and western MM and a small fire weather rating for other regions.

- The central and western MM shows clear seasonal variation in FFDI, generally having its highest fire rating in summer and spring. This is likely due to the large season variations in temperature.

- For the near future, decreases in the annual mean FFDI are projected for all regions except the Alpine region. These decreases are mostly projected for the summer months and are likely due to predicted increases in precipitation. While temperature is projected to increase in these areas, wind speed is projected to decrease.

- In the Alpine region in the near future, up to 30% increases in seasonal mean FFDI are projected in winter and spring.

- For the far future, a decrease of up to 15% in the annual mean FFDI is projected for most regions except for the Alpine and southern SET regions, where a more than 30% increase in mean seasonal FFDI is projected in winter and spring.

- Large decreases in mean FFDI are mostly projected for the north-east MM, ACT and SET regions in the far future.

- In the near future, a small increase in the number of extreme fire days (0.5–1.5 days a year) is projected for the central and western MM region.

- In the far future, an increase of 2–3, 1–2 and 0.5 extreme fire weather days is projected for the western MM, central MM and northern SET regions, respectively.

- The Alpine and southern SET regions show little change in the number of extreme fire days in either the near or far future projections.

4.2   Limitations and further research

NARCliM data were used in the study. NARCliM has its limitations, such as using an older generation CMIP ensemble (i.e. CMIP3), being at a relatively coarse resolution, having limited ensemble members and having only short time periods for analysis.

Results presented in the report are based on the multi-model mean. The same weight was used for each of the 12 GCM/RCM ensemble members. Four GCMs were selected to represent the CMIP3 ensemble. A selected GCM represents different numbers of GCMs in the CMIP3 ensemble. We should consider giving a different weight to each GCM according to the number of GCMs in the ensemble it represents. We should also consider the simulation performance to adjust the weight factor.

Given the short duration of the project, we did not look at the statistical significance and model agreement. This should be assessed in further research.

5. Conclusion

The daily FFDI derived from the NARCliM simulations are used to analyse the change in annual and seasonal means of daily FFDI, and extreme fire weather days (daily FFDI greater than 50). The multi-model mean is taken as the best estimation.

Small decreases in the FFDI are projected for most parts of the study area in both the near and far futures, likely due to predicted increases in precipitation in these regions. The Alpine region is the exception (and the southern SET region in the far future), where large increases in FFDI are projected for winter and spring, likely due to predicted decreases in precipitation during these seasons and possibly also due in part to increased temperatures.

Extreme fire weather days are mostly seen in the central and western MM in summer and spring. There are no extreme fire weather day in other regions and other seasons. For the near future, 0.5–1.5 days per year more extreme fire days are projected for the central and western MM and with significant change elsewhere. The increases are mostly in spring and summer. For the far future, 1–3 more extreme fire weather days are projected for the central and western MM, 0.5–1 more extreme fire weather day for the north-east MM and northern SET regions, and not much change in other regions. The increases are greatest during spring and summer.

6. References

Beer T and Williams A 1995, Estimating Australian forest fire danger under conditions of doubled carbon dioxide concentrations, *Climatic Change*, vol.29, pp.169–188.

Bradstock RA 2010, A biogeographic model of fire regimes in Australia: current and future implications, *Global Ecology and Biogeography*, vol.19, pp.145–158.

Bradstock RA, Cohn JS, Gill AM, Bedward M and Lucas C 2009, Prediction of the probability of large fires in the Sydney region of south-eastern Australia using fire weather, *International Journal of Wildland Fire*, vol.18, pp.932–943.

Cary GJ 2002, Importance of a changing climate for fire regimes in Australia, in RA Bradstock, JE Williams, and AM Gill (eds), *Flammable Australia: the fire regimes and biodiversity of a continent*, Cambridge University Press, Cambridge, pp.26–46.

Clarke H 2015a, 'The impact of climate change on bushfire weather conditions and fuel load', PhD Thesis, University of New South Wales, Sydney NSW.

Clarke H 2015b, *Climate change impacts on bushfire risk in NSW*, NSW Office of Environment and Heritage, Sydney NSW.

Clarke H, Lucas C and Smith P 2013, Changes in Australian fire weather between 1973 and 2010, *International Journal of Climatology*, vol.33, pp.931–944.

Clarke H, Pitman AJ, Kala J, Caroug C, Haverd V and Evans JP 2016, An investigation of future fuel load and fire weather in Australia, *Climatic Change*, vol.139, no.3–4, pp.591–605.

Clarke HC, Smith PL and Pitman AJ 2011, Regional signatures of future fire weather over Eastern Australia from Global Climate Models, *International Journal of Wildland Fire*, vol.20, pp.550–562.

Di Luca AJ, Evans P and Ji F 2016, *Australian Snowpack: NARCliM ensemble valuation, statistical correction and future projections*, NARCliM Technical Note 7, NARCliM Consortium, Sydney, Australia, 88 pp.

Di Luca AJ, Evans P and Ji F 2018, Australian snowpack in the NARCliM ensemble: evaluation, bias correction and future projections, *Climate Dynamics,* vol.51, no.1–2, pp.639–666.

Evans JP, Ekstrom M and Ji F 2012, Evaluating the performance of a WRF physics ensemble over South-East Australia, *Climate Dynamics*, vol.39, no.6, pp.1241–1258.

Evans JP, Ji F, Abramowitz G, Ekstrom M 2013a, Optimally choosing small ensemble members to produce robust climate simulations, *Environmental Research Letters*, vol.8.

Evans JP, Fita L, Argüeso D and Liu Y 2013b, Initial NARCliM evaluation, in Piantadosi J, Anderssen RS and Boland J (eds), *MODSIM2013, 20th International Congress on Modelling and Simulation*, Modelling and Simulation Society of Australia and New Zealand, December 2013, pp.2765–2771.

Evans J, Ji F, Lee C, Smith P, Argüeso D and Fita L 2014, Design of a regional climate modelling projection ensemble experiment–NARCliM, *Geoscientific Model Development,* vol.7, pp.621–629.

Finkele K, Mills GA, Beard G and Jones D 2006, National daily gridded soil moisture deficit and drought factors for use in prediction of Forest Fire Danger Index in Australia, *Australian Meteorological Magazine*, vol.55, no.3, pp.183–197.

Fita L, Evans JP, Argueso D, King AD and Liu Y 2016, Evaluation of the regional climate response to large-scale modes in the historical NARCliM simulations, *Climate Dynamics*, DOI 10.1007/s00382-016-3484-x.

Fox-Hughes P, Harris RMB, Lee G, Grose MR and Bindoff NL 2014, Future fire danger climatology for Tasmania, Australia, using a dynamically downscaled regional climate model, *International Journal of Wildland Fire*, vol.23, no.3, pp.309–321.

Goldammer JG and Price C 1998, Potential impacts of climate change on fire regimes in the tropics based on MAGICC and a GISS GCM-derived lightning model, *Climatic Change*, vol.39, pp.273–296.

Griffiths D 1999, Improved formula for the drought factor in McArthur's Forest fire danger meter, *Australian Forestry*, vol.62, no.2, pp.202–206.

Hughes L 2011, Climate change and Australia: key vulnerable regions, *Regional Environmental Change*, vol.11, no.1, pp.189–195.

IPCC 2000, Special Report on Emissions Scenarios: A Special Report of Working Group III of the Intergovernmental Panel on Climate Change, published for the Intergovernmental Panel on Climate Change by Cambridge University Press, Cambridge, UK.

Ji F, Ekstrom M, Evans JP and Teng J 2014a, Evaluating rainfall patterns using physics scheme ensembles from a regional atmospheric model, *Theoretical and Applied Climatology*, vol.115, pp.297–304.

Ji F, Evans JP, Argueso D and Di Luca A 2014b, *NARCliM Data Quality Assurance Report*, report compiled by the Office of Environment and Heritage and the University of NSW, Sydney NSW.

Ji F, Evans JP, Teng J, Scorgie Y, Argüeso D and Di Luca A 2016, Evaluation of long-term precipitation and temperature WRF simulations for southeast Australia, *Climate Research*, vol.67, pp.99–115.

Keetch JJ and Byram GM 1968, *A drought index for forest fire control*, Research Paper SE-38, US Department of Agriculture Forest Service, Ashville, NC, USA.

Krawchuk MA, Moritz MA, Parisien M, Van Dorn J and Hayhoe K 2009, Global pyrogeography: the current and future distribution of wildfire, *PLoS ONE*, vol.4, no.4, e5102.

Lucas C, Hennessy KJ and Bathols JM 2007, *Bushfire weather in southeast Australia recent trends and projected climate change impacts*, CSIRO, Bureau of Meteorology and Bushfire CRC Report for the Climate Institute, Canberra, Australia.

Luke R and McArthur A 1978, *Bushfires in Australia*, Australian Government Publishing Service, Canberra.

Matthews S, Nguyen K and McGregor J 2011, Modelling fuel moisture under climate change, *International Journal of Climate Change Strategies and Management*, vol.3, pp.6–15.

Mount AB 1972, *The derivation and testing of a soil dryness index using run-off data*, Bulletin No. 4, Tasmanian Forestry Commission, Hobart TAS.

Olson R, Evans JP, Argüeso D, and Di Luca A 2014, *NARCliM Climatological Atlas*, NARCliM Technical Note 4, NARCliM Consortium, Sydney, Australia, 423 pp.

Olson R, Evans JP, Di Luca A, and Argüeso D 2016, The NARCliM project: model agreement and significance of climate projections, *Climate Research*, vol.69, pp.209–227.

Penman TD, Bradstock RA and Price O 2013, Modelling the determinants of ignition in the Sydney Basin, Australia: implications for future management, *International Journal of Wildland Fire*, vol.22, pp.469–478.

Price C and Rind D 1994, Possible implications of global climate change on global lightning distributions and frequencies, *Journal of Geophysical Research*, vol.99, no.D5, pp.10823–10831.

Skamarock WC, Klemp JB, Dudhia J, Gill DO, Barker DM, Duda MG, Huang XY, Wang W and Powers JG 2008, *A description of the advanced research WRF Version 3,* NCAR Technical Note, National Center for Atmospheric Research, Boulder Colorado, USA.

Vercoe T 2003, *Whoever owns the fuel owns the fire – Fire management for forest growers*, AFG Special Liftout no. 65, *Australian Forest Grower*, vol.26, no.3.

Williams AAJ, Karoly DJ and Tapper N 2001, The sensitivity of Australian fire danger to climate change, *Climatic Change*, vol.49, pp.171–191.

DOCUMENT 18

DEPARTMENT OF PLANNING, INDUSTRY & ENVIRONMENT

Climate change impacts in the NSW and ACT Alpine region

Projected climate

environment.nsw.gov.au

Cover photo: Winter landscape in Kosciuszko National Park. John Spencer/DPIE

This report should be cited as:

Fei Ji 2019, *Climate change impacts in the NSW and ACT Alpine region: Projected climate*, NSW Department of Planning, Industry and Environment, Sydney, Australia.

Find out more about your environment at:

www.environment.nsw.gov.au

Contents

List of figures

List of shortened forms

ACT	Australian Capital Territory
AWAP	Australian Water Availability Project
CMIP	Coupled Model Intercomparison Project
DJF	December January February
DPIE	Department of Planning, Industry and Environment
ECL	East Coast Low
GCM	Global Climate Model
JJA	June July August
MAM	March April May
MCAS-S	Multi-Criteria Analysis Shell for Spatial Decision Support
mm	millimetre
MM	Murray-Murrumbidgee state planning region
NARCliM	NSW/ACT Regional Climate Modelling project
NetCDF	Network Common Data Form
NSW	New South Wales
RCM	Regional Climate Model
SET	South East and Tablelands state planning region
SON	September October November
SRES	Special Report on Emissions Scenarios
WRF	Weather Research and Forecasting

Summary of findings

Projected climate in the NSW and ACT Alpine region

1. Future changes in climate for the Alpine region are much larger for the far future (2060 to 2079) compared to the near future (2020 to 2039), relative to a 1990 to 2009 baseline.

2. The Alpine region will become drier in the future due to a large reduction in precipitation in spring; however, other areas are getting wetter due to more precipitation in summer, winter and autumn.

3. Compared to surrounding regions, the Alpine region will have fewer moderate and heavy rainfall events in the near future, with a more than 60% decrease in seasonal heavy precipitation events projected for some parts in winter. In the far future, increases in heavy precipitation are projected for most areas except some of the Alpine region, where a 10% decrease is projected annually.

4. A larger increase in maximum temperature is projected for the Alpine region compared to other regions, with the greatest projected increase in winter, where a more than 3°C increase is projected in the Alpine region for 2060 to 2079 (relative to 1990 to 2009). Projected increases in minimum temperature are similar across all regions, with 0.5–1°C increases projected for 2020 to 2039, and 2–2.5°C increase projected for most areas for 2060 to 2079 (relative to 1990 to 2009).

5. More hot days are projected for the Murray-Murrumbidgee state planning region. The greatest increase in hot days is projected to occur in summer, where 8–10 more hot days are projected in this region for 2020 to 2039, and 12–32 more for 2060 to 2079 (relative to 1990 to 2009) for the same region. Fewer cold nights are projected across all regions, especially the Alpine region. Winter has the greatest decrease in cold nights in the Alpine region, where more than 20 fewer cold nights are projected for 2060 to 2079. Spring is also projected to have more hot days and fewer cold nights.

6. Mean and maximum wind speed is projected to decrease in the future, mostly in spring, where a more than 8–10% decrease is projected for 2060 to 2079. There is minimal change in strong wind days and gale days in future projections.

7. Overall, seasonal changes are generally larger than annual changes for both the near and far future projection periods.

1. Introduction

1.1 Background

The New South Wales (NSW) and Australian Capital Territory (ACT) Alpine region is located in the south-eastern corner of mainland Australia and is the highest mountain range in Australia. Though it comprises only about 0.16% of Australia in size, it is an important region for ecosystems, biodiversity, energy generation and winter tourism. It forms the southern end of the Great Dividing Range, covering a total area of 1.64 million hectares that extend over 500 kilometres. The highest peak, Mount Kosciuszko, rises to an altitude of 2228 metres.

This report is part of a larger project delivered by the NSW Department of Planning, Industry and Environment on the various impacts from climate change on the NSW and ACT Alpine region, hereafter referred to as the Alpine region. The full study region covers the Murray-Murrumbidgee region (MM), South East and Tablelands (SET) and the ACT, bordering the Victorian border in the south (Figure 1).

The Alpine region is vulnerable to climate change. Observations have shown substantial changes in precipitation and temperature for this area (Di Luca et al. 2018), which have already impacted biodiversity and ecosystems (Hughes 2011). In 2014, the NSW/ACT Regional Climate Modelling (NARCliM) project was delivered. Climate snapshots for each of the 11 NSW planning regions and the ACT were developed to demonstrate observed and projected climate change; however, the snapshots only show changes for some variables and focus on each planning region.

Figure 1   **The study area for the Alpine project, including the NSW and ACT Alpine region, Murray-Murrumbidgee region and South East and Tablelands**

1.2   Objectives

The aim of this study is to provide annual, monthly and seasonal future climate projections for precipitation, temperature and wind for the Alpine region and surroundings. The future climate projections will underpin impact assessments quantifying the magnitude of further impacts for this region under future climate conditions, and direct decisions on adaptation to unavoidable future climate projections for this region.

1.3   Outputs

Output	Details
Precipitation	Bias-corrected, monthly total, dry days, daily totals and heavy rainfall days (>25 mm/d). Network Common Data Form (NetCDF) 10 km^2 gridded data. Provided for reanalysis, near and far future.
Temperature	Maximum, minimum, days over 25°C, days over 35°C, days under 0°C. NetCDF 10 km^2 gridded data. Provided for reanalysis, near and far future.
Wind	Daily average, maximum speed per day, >13 m/s in hours/year, >17 m/s in hours/year. NetCDF 10 km^2 gridded data. Provided for reanalysis, near and far future.

2.   Method

2.1   Source of data

NARCliM simulations from four Coupled Model Intercomparison Project phase 3 (CMIP3) Global Climate Models (GCMs) were used to drive three Regional Climate Models (RCMs) to form a 12-member GCM/RCM ensemble (Evans et al. 2014). The four selected GCMs are MIROC3.2, ECHAM5, CCCMA3.1 and CSIRO-MK3.0. For future projections, the Special Report on Emissions Scenarios (SRES) business-as-usual A2 scenario was used (IPCC 2000). The three selected RCMs are three physics scheme combinations of the Weather Research and Forecasting (WRF) model. Each simulation consists of three 20-year runs (1990 to 2009, 2020 to 2039, and 2060 to 2079). The four GCMs were chosen based on a number of criteria: i) adequate performance when simulating historic climate; ii) most independent; iii) cover the largest range of plausible future precipitation and temperature changes for Australia. The three RCMs correspond to three different physics scheme combinations of the WRF V3.3 model (Skamarock et al. 2008), which were also chosen for adequate skill and error independence, following a comprehensive analysis of 36 different combinations of physics parameterisations over eight significant east coast lows (ECLs) (Evans et al. 2012; Ji et al. 2014). For the selected three RCMs, the WRF Double Moment 5-class (WDM5) microphysics scheme and NOAH land surface scheme are used in all cases. Refer to Evans et al. (2014) for more details on each physics scheme.

We acknowledge that the results are model dependent (as all model studies are) but through the use of this carefully selected ensemble we have attempted to minimise this dependence. By using this model selection process, we have shown that it is possible to create relatively small ensembles that are able to reproduce the ensemble mean and variance from the large parent ensemble (i.e. the many GCMs) as well as minimise the overall error (Evans et al. 2013a).

Some initial evaluation of NARCliM simulations shows that they have strong skill in simulating the precipitation and temperature of Australia, with a small cold bias and overestimation of precipitation on the Great Dividing Range (Evans et al. 2013b; Ji et al. 2016). The differing

responses of the different RCMs confirm the utility of considering model independence when choosing the RCMs. The RCM response to large-scale modes of variability also agrees well with observations (Fita et al. 2016). Through these evaluations we found that while there is a spread in model predictions, all models perform adequately with no single model performing the best for all variables and metrics. The use of the full ensemble provides a measure of robustness such that any result that is common through all models in the ensemble is considered to have higher confidence.

In total, there were four same GCM driven simulations (average of three members) and three same RCM used simulations (average of four members). The analyses in this study are based on the outputs from these simulations.

Available NARCliM bias-corrected data was used for future precipitation and temperature projections. Wind speed projections, for which no bias-corrected data were available, were also produced. An observational dataset known as AWAP (Australian Water Availability Project) was used to evaluate NARCliM simulations for the baseline period.

2.2   Analysis

Bias-corrected monthly precipitation and maximum and minimum temperatures were used to analyse annual and seasonal averages of precipitation and temperature, as well as changes for the near future (2020 to 2039) and far future (2060 to 2079) relative to the baseline period (1990 to 2009).

Bias-corrected daily precipitation and temperature data were used to analyse changes in annual and seasonal dry days (daily precipitation less than 0.2 mm), moderate precipitation days (daily precipitation greater than 10 mm), heavy precipitation days (daily precipitation greater than 25 mm), hot days (maximum temperature above 35°C) and cold nights (minimum temperature below –2°C).

Post-processed monthly average data of daily maximum wind speed are used to calculate changes in annual and seasonal mean and maximum wind speeds. Post-processed daily maximum wind speed is used to calculate changes in strong wind and gale days.

2.3   Quality control

The NARCliM outputs have been subjected to comprehensive data quality assurance/quality control. The method for quantifying future climate projections is widely used. Annual climate projections are similar to those shown on the AdaptNSW Climate projections for your region webpage. Seasonal and monthly future projections use the same method but for finer timescale outputs.

The data have also been evaluated as conference and journal papers (Evans et al. 2013b; Ji et al. 2016; Fita et al. 2016). Similar climate projections from NARCliM have been published as technical reports (Olson et al. 2014; Di Luca et al. 2016) and peer reviewed scientific publications (Olson et al. 2016; Di Luca et al. 2018).

2.4   Data storage and access

All output data were converted to raster format (ArcGIS ESRI grid) and supplied to the MCAS-S (Multi-Criteria Analysis Shell for Spatial Decision Support) datapacks for distribution and storage. All input data to the model and by-products are stored on hard disk drives. All data are in the NARCliM coordinate system. The extent of the datasets includes the MM region, ACT and SET with the boundary at top: –32.671254, left: 143.317445, right: 150.745676, and bottom: –37.505077.

3. Results

This section reports annual and seasonal means for 1990 to 2009 (baseline period), as well as projected annual and seasonal changes for 2020 to 2039 (near future) and 2060 to 2079 (far future) relative to 1990 to 2009.

3.1 Precipitation

Mean precipitation for the 1990 to 2009 baseline period

Mean annual precipitation for the NARCliM baseline period (1990 to 2009) is shown in Figure 2. The map presents the results of the 12 individual models as an average of all 12, referred to as the ensemble mean. Bias-corrected precipitation data were used in the analyses. Grey box areas within the map (Figure 2) indicate no observations available for those over waterbody grids. The bias-correction method is effective at correcting long-term means. Because bias-corrected precipitation was used in this study, the biases are small relative to AWAP observations (Olson et al. 2016).

There is a clear gradient in annual precipitation with 200–400 millimetres/year precipitation in the western MM region and up to 1800 millimetres/year precipitation over the Alpine region (Figure 2). Annual precipitation is generally more than 800 millimetres/year for coastal regions and less than 600 millimetres/year west of the Great Diving Range, especially for areas between the range and Mt Kosciuszko.
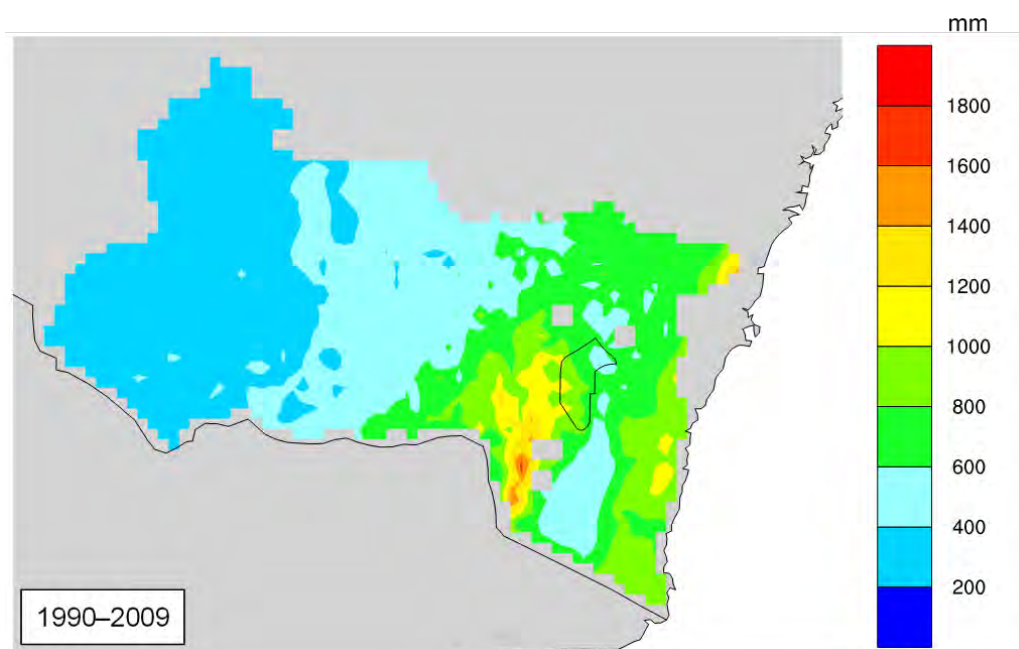
Figure 2   **Mean annual precipitation for the 1990 to 2009 baseline period**

A clear seasonal variation in precipitation is observed for the Alpine and coastal regions with a wet summer and low winter rainfall for the coast, and wet winter and low summer precipitation for the Alpine region (Figure 3). The central and western MM region has uniform rainfall across the different seasons.

For the summer simulated results, a clear east–west gradient is observed with more than 400 millimetres/season precipitation on the coast and less than 150 millimetres/season precipitation in the central and western MM region. Winter is the driest season for regions

along the coast with less than 100 millimetres/season; however, it is the wettest season for the Alpine region with more than 450 millimetres/season precipitation. Spring and autumn are transitional seasons for the Alpine and coastal regions with 200–300 millimetres/season for the coast, and more than 400 and 250 millimetres/season for spring and autumn respectively.
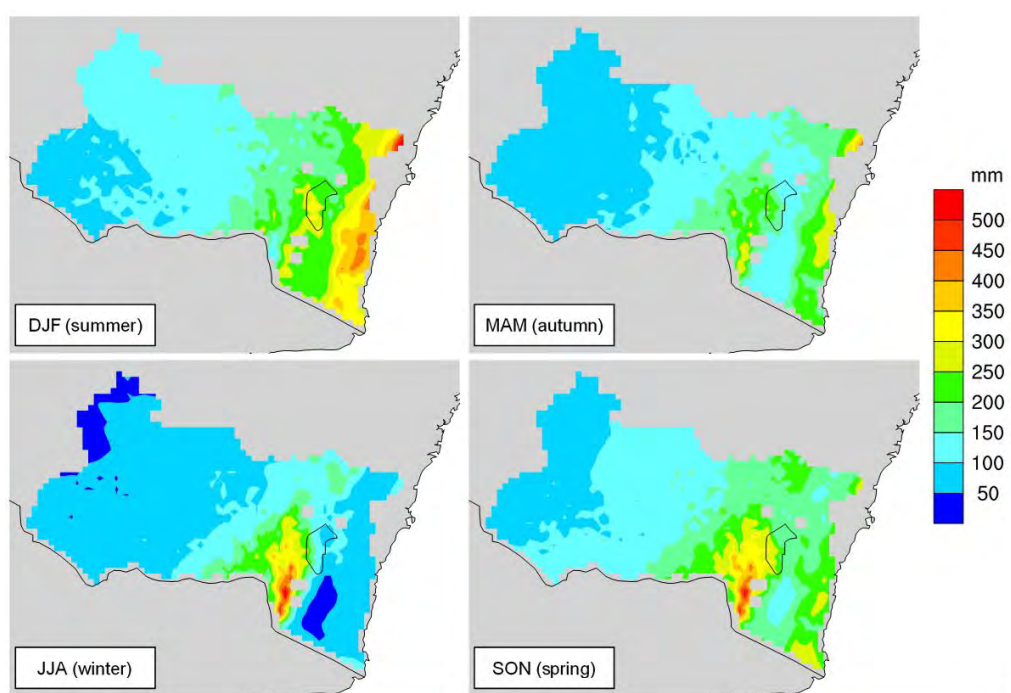
Figure 3   **Mean seasonal precipitation for the 1990 to 2009 baseline period**

Changes in precipitation for 2020 to 2039

A small decrease in annual precipitation is projected for the entire study region, apart from a small increase for some areas in the MM region (Figure 4).
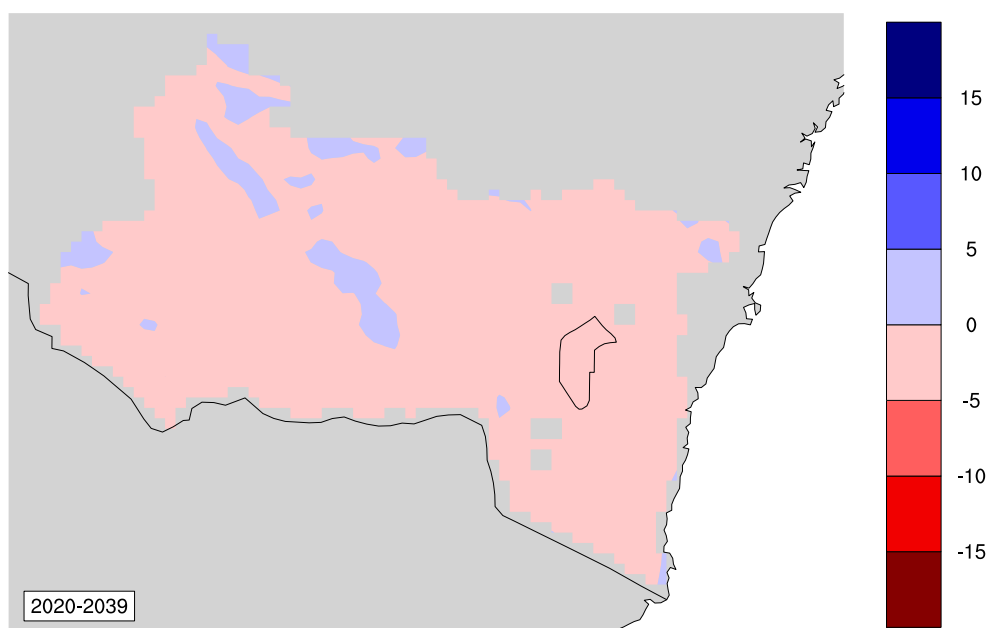
Figure 4   **Changes in annual precipitation (%) for 2020 to 2039 relative to 1990 to 2009**

Projected precipitation changes vary across seasons and regions (Figure 5). In summer, less than 5% increase in precipitation is projected for the MM region and less than 5% decrease for the SET region. In winter, a less than 5% decrease in precipitation is projected from most of the study area, and 5-10% decrease is projected from southwest MM region and eastern SET region. An increase in precipitation is projected in autumn for the study area, especially for the western MM region where is increase is more than 10%. Decreases in spring precipitation are projected for most areas, especially for the MM region, where a 10–20% decrease is projected.
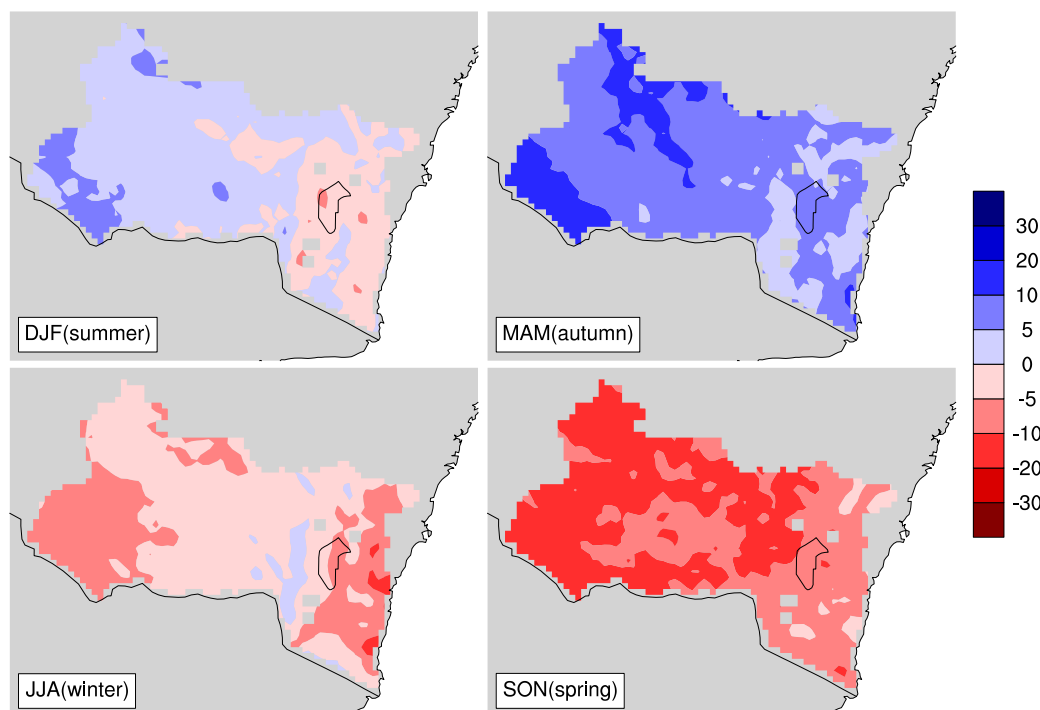
Figure 5   **Changes in seasonal precipitation (%) for 2020 to 2039 relative to 1990 to 2009**

Changes in precipitation for 2060 to 2079

There is a clear difference in changes in annual precipitation in the far future compared with the near future; A small increases in annual precipitation are projected for the study region except for the Alpine region where a up to 10% decrease is expected. Overall, it is getting wetter in 2060 to 2079 compared to the present and 2020 to 2039 period, for most areas except the Alpine region (Figure 6).

Compared to 2020 to 2039, projections for 2060 to 2079 show a large change in seasonal precipitation (Figure 7). The far future is projected to be wetter in summer for all areas, especially for the Alpine region where a small decrease in precipitation is projected. Greater precipitation in autumn is projected for all study areas, especially for the north-west MM and southern SET regions with a greater than10% increase in precipitation. In winter, there is little change for the western region and a 10–20% decrease in precipitation for the Alpine and Southern SET region. During spring, a decrease in precipitation is projected for most areas, especially for the Alpine region where a more than 20% decrease is projected.

Spring and winter will be drier for most areas, while summer and autumn will get wetter, especially for the MM region.
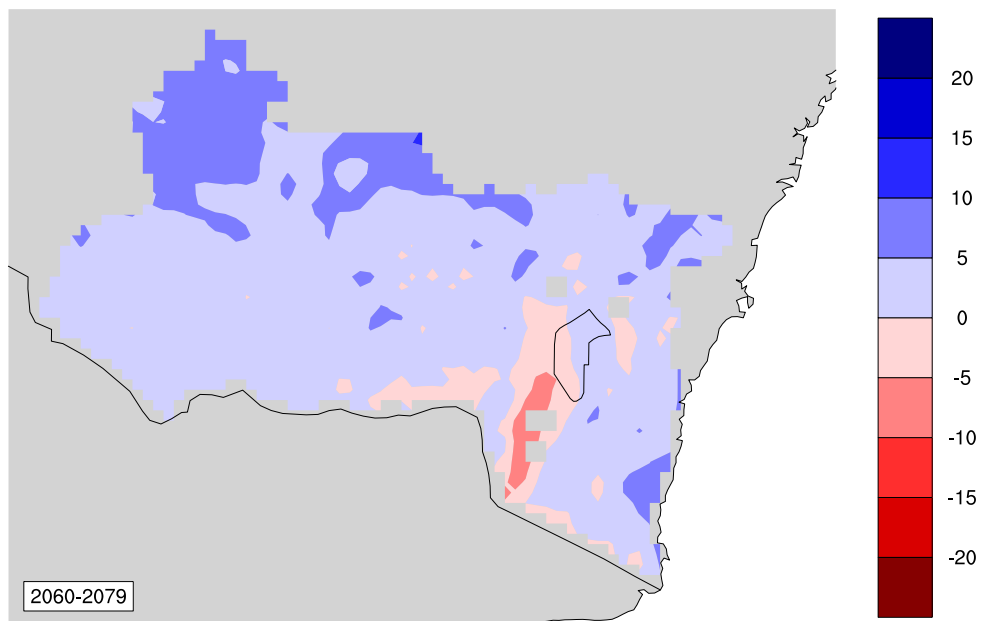
Figure 6   **Changes in annual precipitation (%) for 2060 to 2079 relative to 1990 to 2009**
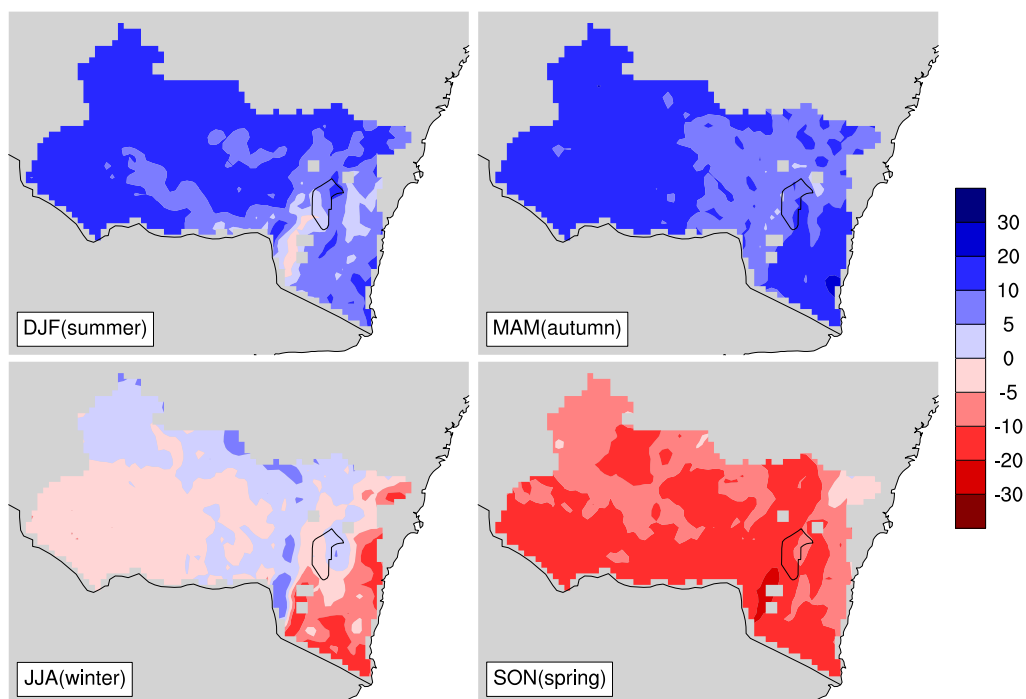
Figure 7   **Changes in seasonal precipitation (%) for 2060 to 2079 relative to 1990 to 2009**

3.2 Dry days (precipitation below 0.2 mm/day)

Mean number of dry days for the 1990 to 2009 baseline period

Dry days for 1990 to 2009 is shown in Figure 8. It is clear that the MM region has far more dry days compared with the other regions. More than 70% of days in the west of the MM region are dry days; however, more than 50% of days in the Alpine region are wet days.
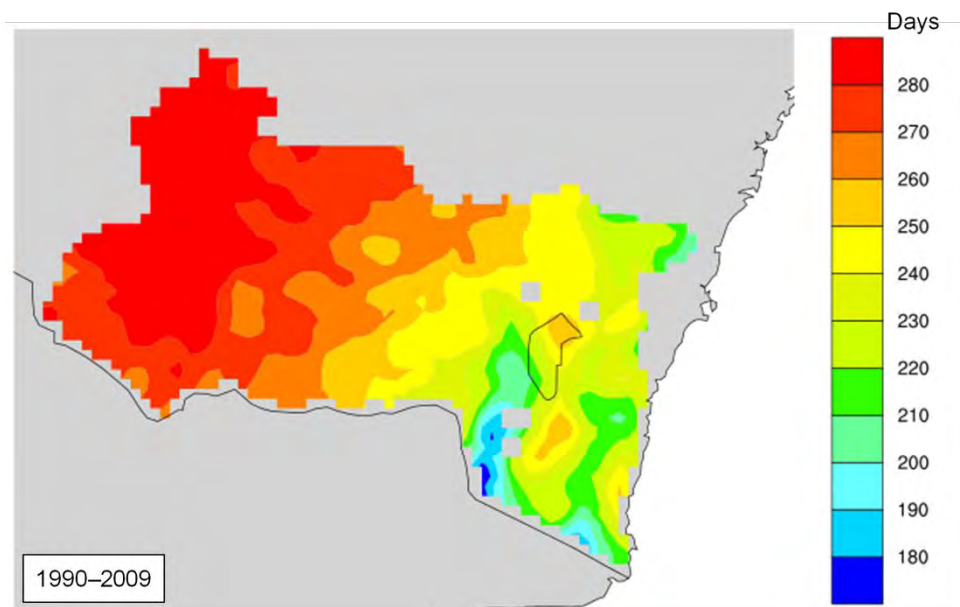
Figure 8   Simulated number of annual dry days for 1990 to 2009

Seasonal variations for different areas are clear (Figure 9). For the MM areas, more dry days are observed in summer, autumn and spring, with relatively few dry days in winter. The least number of dry days are in summer, with the greatest number of dry days for coastal areas being in winter. For the Alpine region, winter has the least number of dry days, with autumn having the most.
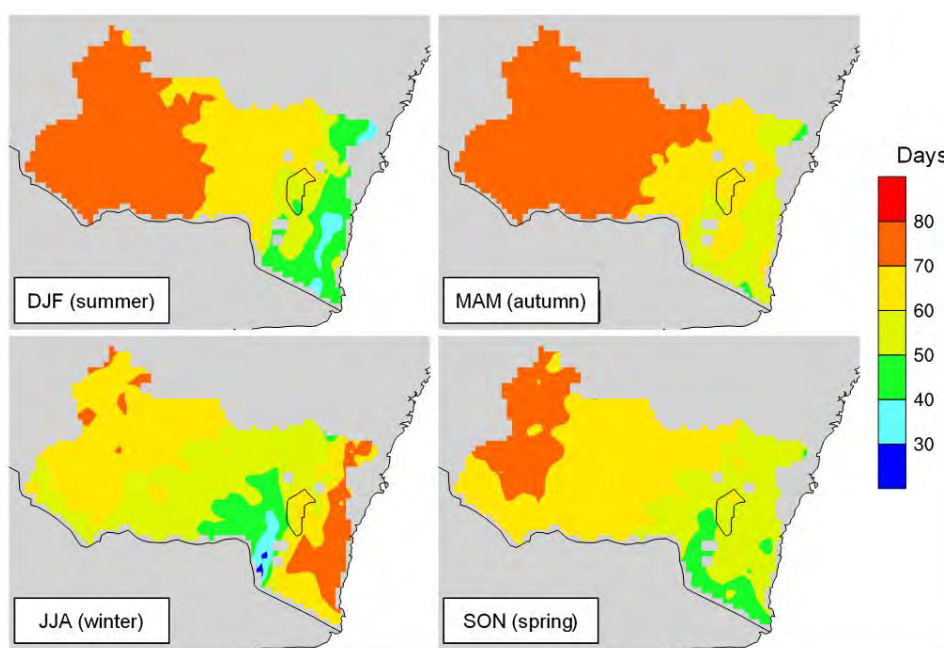
Figure 9   Simulated number of seasonal dry days for 1990 to 2009

Changes in the number of dry days for 2020 to 2039

A small increase in the number of dry days is projected for the 2020 to 2039 period (Figure 10). An up to 2% increase in dry days is projected for the majority of areas, except for the Alpine region where a 2–4% increase is projected. There is seasonal variation in dry day projections with increases in dry days in spring, especially for the Alpine region, where a 6–8% increase in projected (Figure 11). For all other seasons, there are only small changes projected for the number of dry days ranging from –2 to 2%.
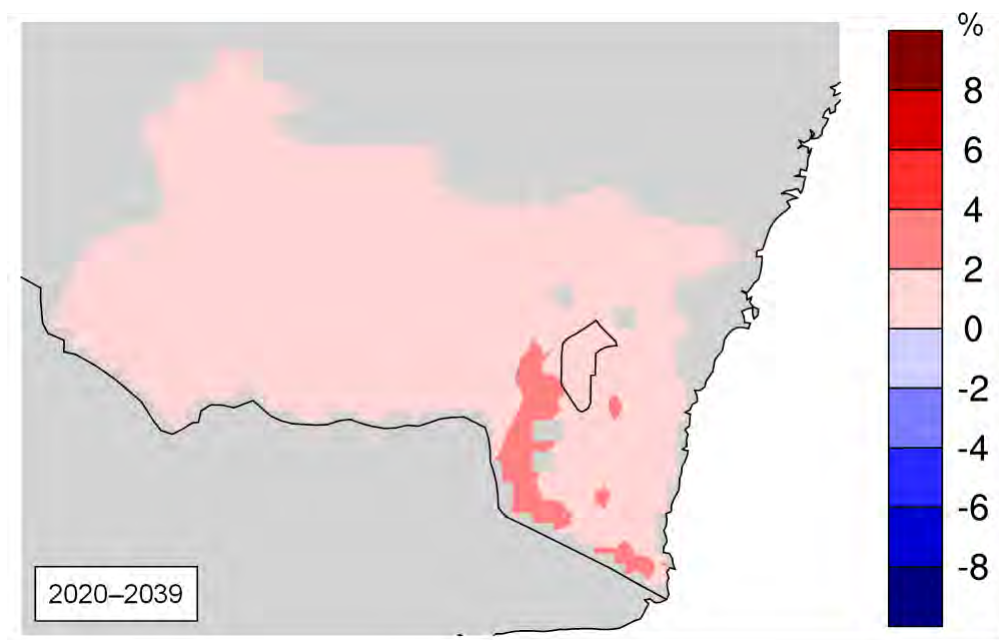
Figure 10   Changes in annual dry days (%) for 2020 to 2039 relative to 1990 to 2009
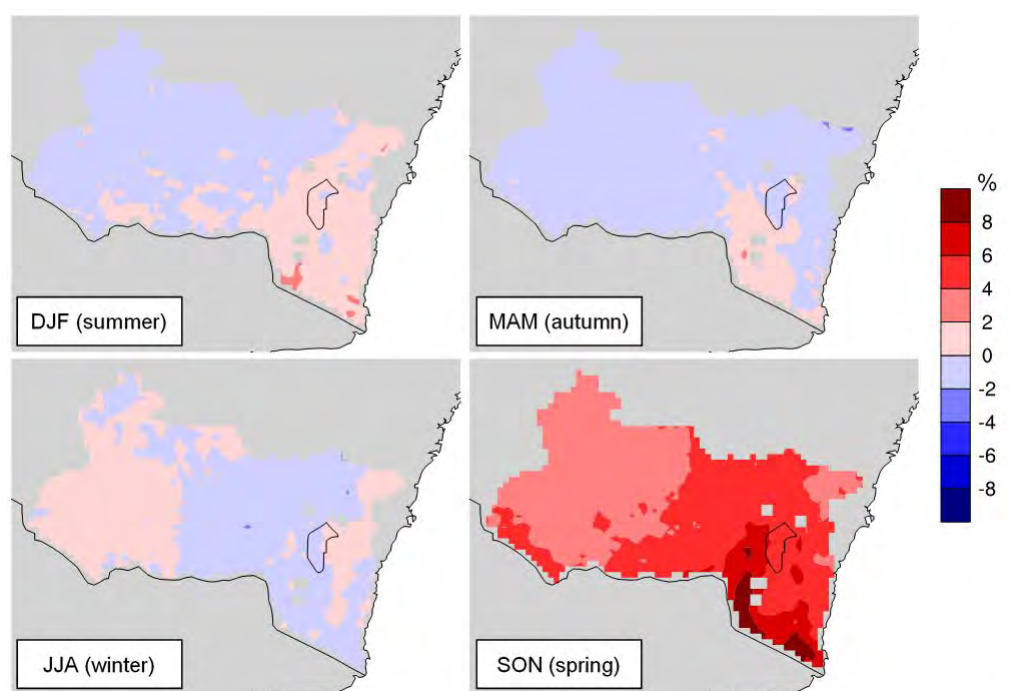
Figure 11   Changes in seasonal dry days (%) for 2020 to 2039 relative to 1990 to 2009

Changes in the number of dry days for 2060 to 2079

More dry days are projected for the 2060 to 2079 projection period when compared to the 2020 to 2039 period, especially for the Alpine region and southern MM area (up to an 8% increase in annual dry days, Figure 12). The northern MM region and coastal regions show mostly small increases in the number of projected dry days.
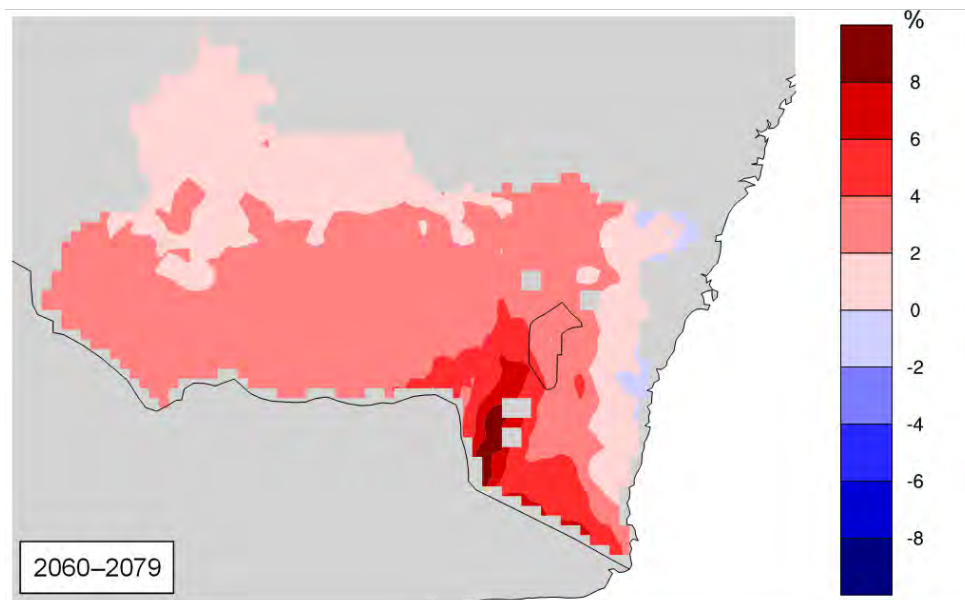
Figure 12   **Changes in annual dry days (%) for 2060 to 2079 relative to 1990 to 2009**

There is clear variation in seasonal dry day projections for the 2060 to 2079 projection period (Figure 13). Spring and winter will have an increased number of dry days over most of the region, especially in the Alpine region during spring, where at least a 12–16% increase in dry days is projected. Summer and autumn mostly have small changes relative to the baseline period, except for the Alpine region where a slightly larger increase (4–6%) is projected in summer.
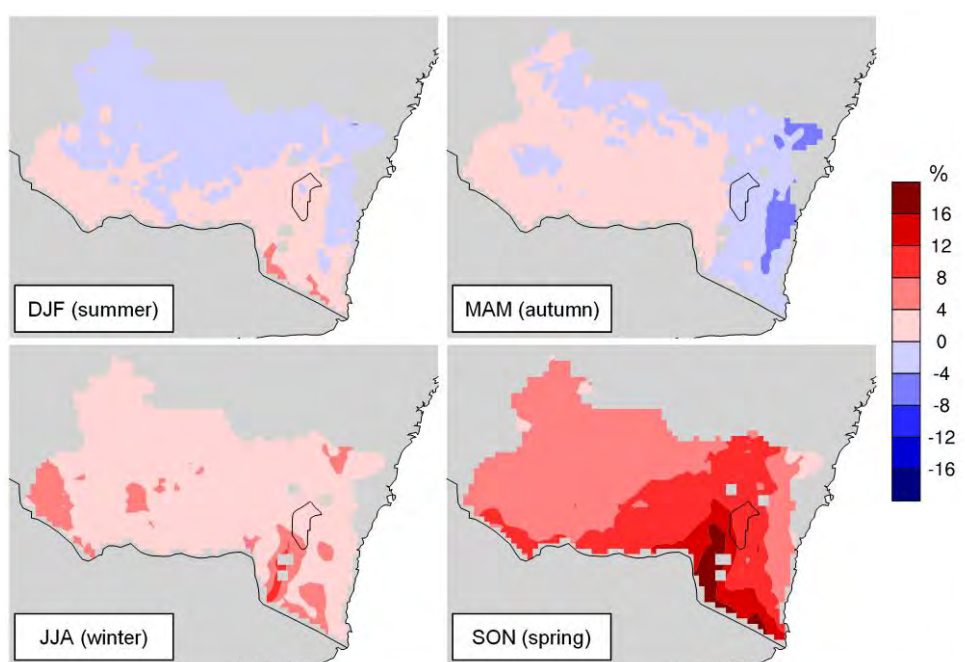
Figure 13   **Changes in seasonal dry days (%) for 2060 to 2079 relative to 1990 to 2009**

3.3 Moderate precipitation days (rainfall above 10 mm/day)

Mean number of moderate precipitation days for the 1990 to 2009 baseline period

For this study we define 'moderate precipitation' as precipitation in excess of 10 millimetres per day. The mean number of days with moderate precipitation is shown in Figure 14. Ten to 20 days with moderate rainfall are shown for most of areas except for the western MM region which has fewer than 10 days, coastal areas where there are 20–30 days with moderate rainfall, and the Alpine region where more than 40 days have moderate rainfall.
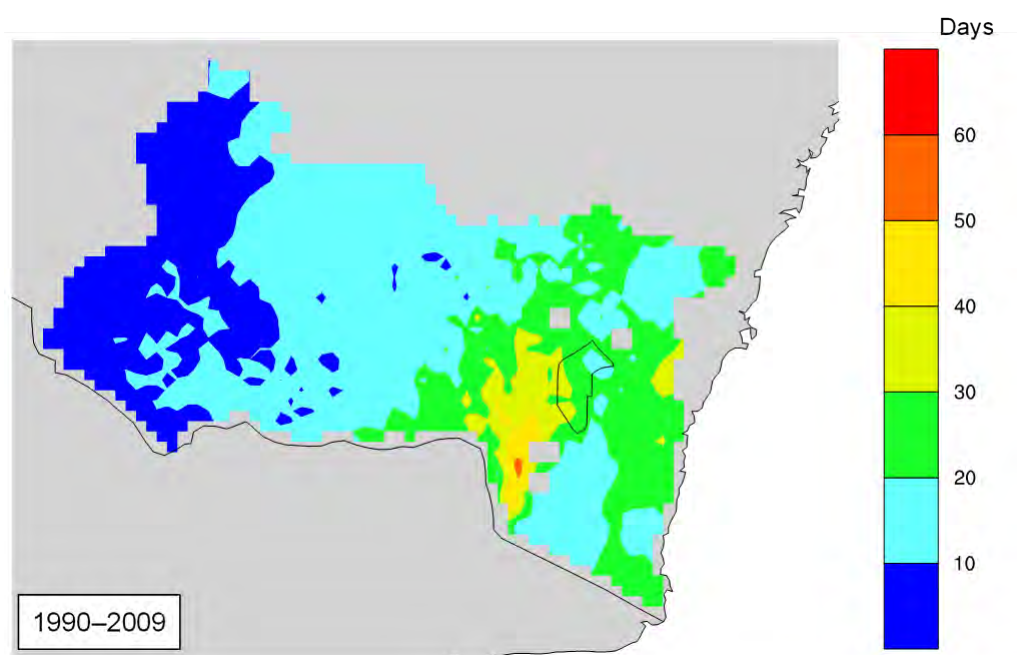
Figure 14   **Annual moderate precipitation days for 1990 to 2009**

There is little difference in seasonal days with moderate precipitation for the western and central MM region; however, there is a clear seasonal variation for the Alpine region where more than 20 days in winter have moderate precipitation while there are only 6–8 days in summer and autumn (Figure 15). For the coast, the most moderate precipitation days are in summer, with the least in winter.
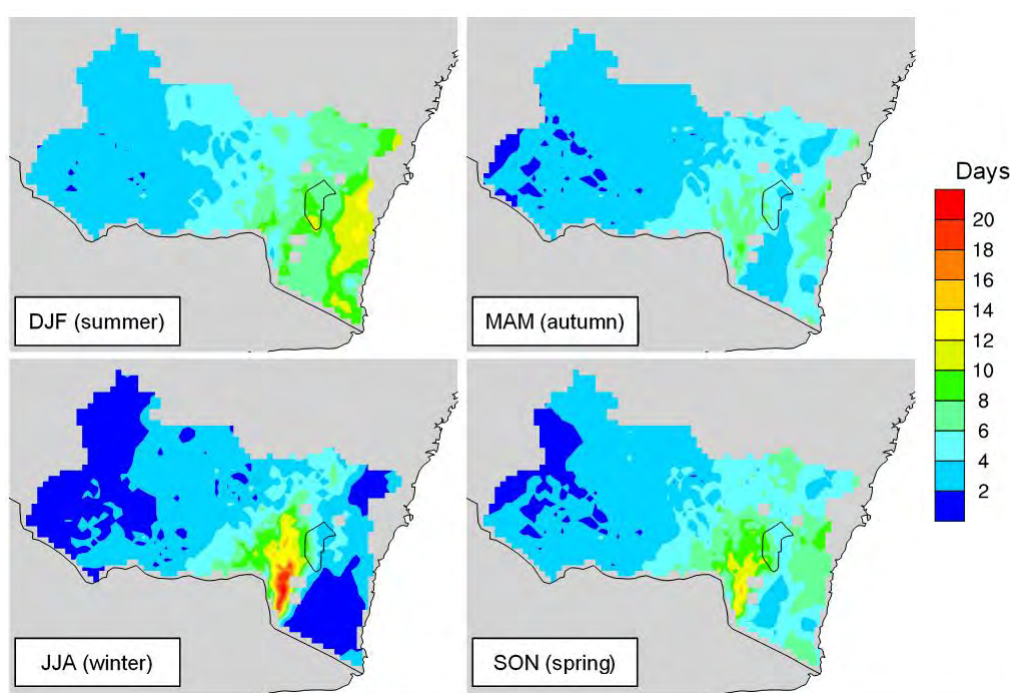
Figure 15 **Seasonal moderate precipitation days for 1990 to 2009**

Changes in the number of moderate precipitation days for 2020 to 2039

Changes in the number of days with moderate precipitation are small with a less than 5% increase for the western domain and a less than 5% decrease for the eastern domain (Figure 16).
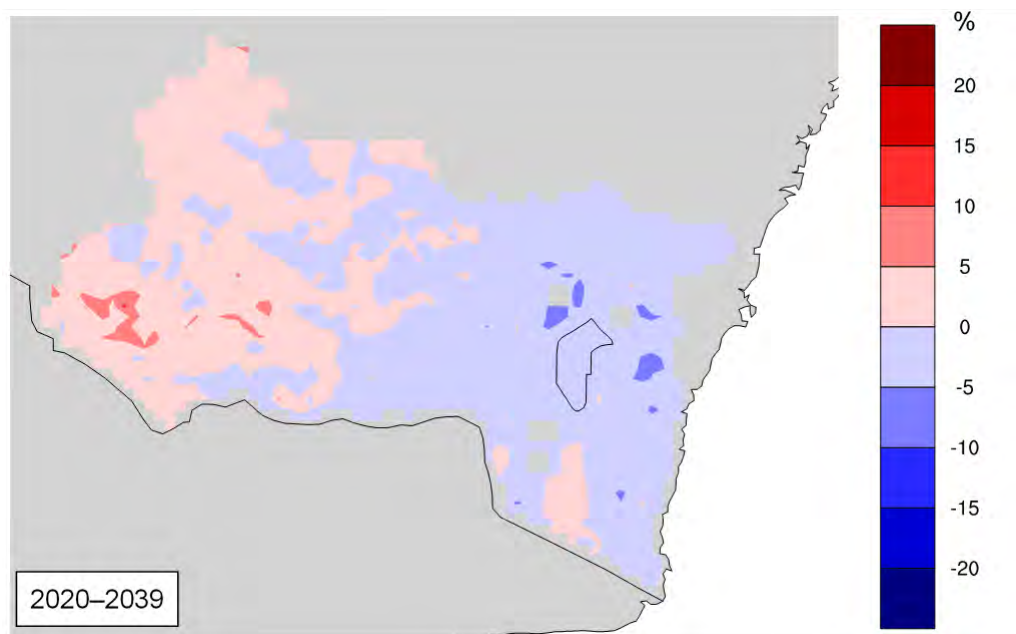
Figure 16 **Changes in annual moderate precipitation days (%) for 2020 to 2039 relative to 1990 to 2009**

There is a clear seasonal variation of changes in days with moderate precipitation (Figure 17). Summer and autumn will generally have more moderate precipitation days, especially for autumn when a more than 20% increase is projected for some areas in the MM region. Winter and spring will have fewer moderate precipitation days, especially in winter when a more than 10% decrease is projected for some parts of the Great Dividing Range.
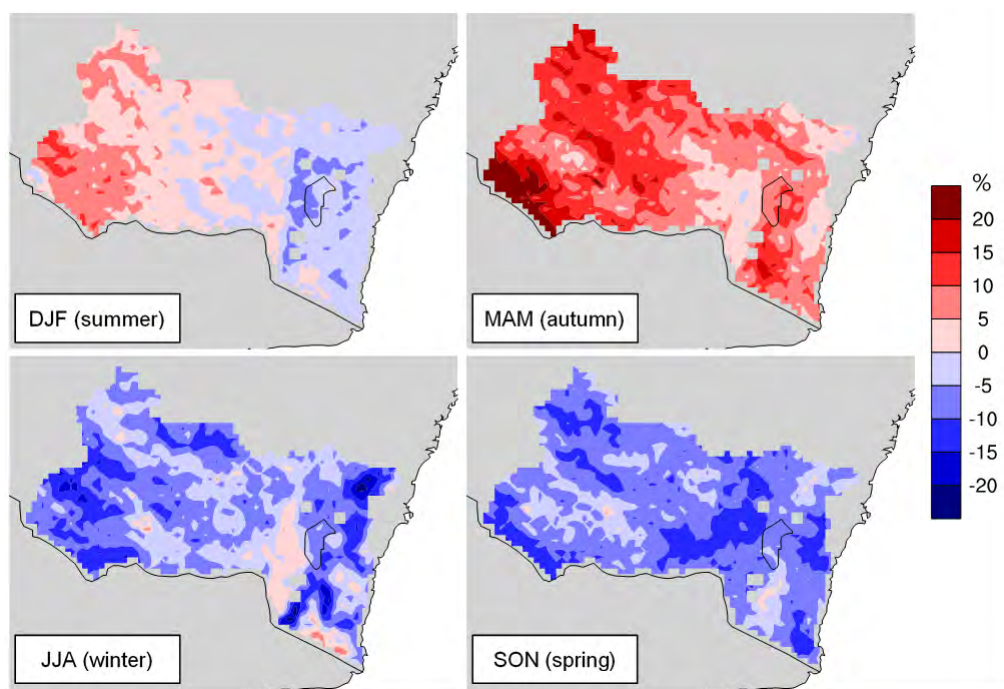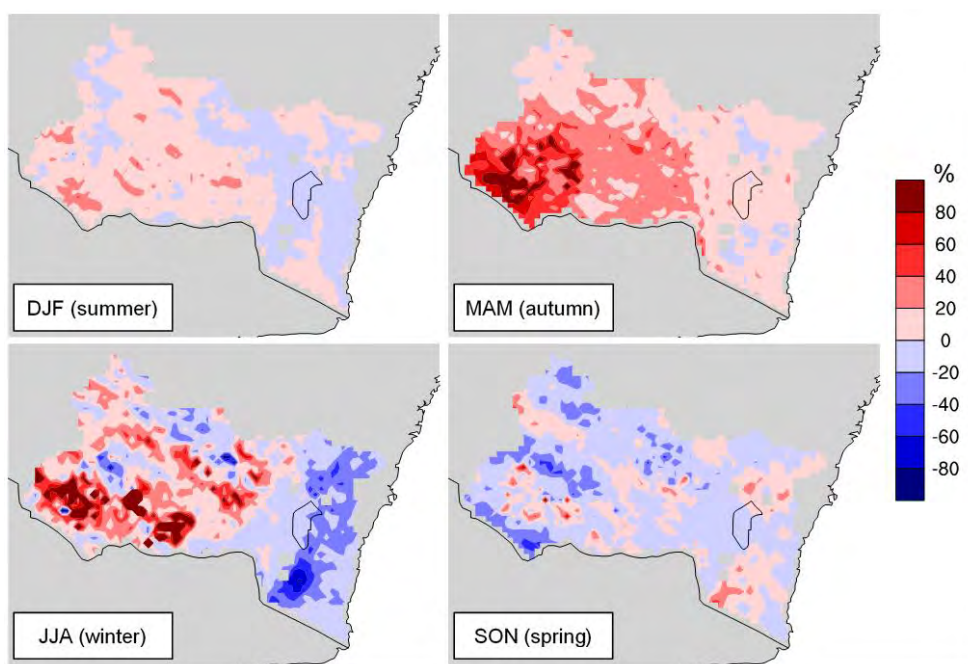

Figure 17   **Changes in seasonal moderate precipitation days (%) for 2020 to 2039 relative to 1990 to 2009**

Changes in the number of moderate precipitation days for 2060 to 2079

Changes in the number of days with moderate precipitation for 2060 to 2079 are much larger relative to 2020 to 2039 (Figure 18). A more than 15% increase is projected for some areas in the western MM region and a more than 10% decrease is projected for some areas in the Alpine region. This indicates that most areas will have more moderate precipitation in the far future, except for the Alpine region where much fewer moderate precipitation days will occur.

Similar to the results for 2020 to 2039, summer and autumn will have more days with moderate precipitation, but the magnitude of change for 2060 to 2079 is much larger than that for 2020 to 2039 when compared with 1990 to 2009 (Figure 19). A more than 10% increase in days with moderate precipitation is projected for most of the study region during summer and autumn. More moderate precipitation days are also projected for winter except for the coastal and Alpine regions where a more than 15% decrease is projected in some areas for 2060 to 2079. Larger decreases are projected for spring, especially in parts of the Alpine region, where a more than 20% decrease in moderate precipitation days is projected.
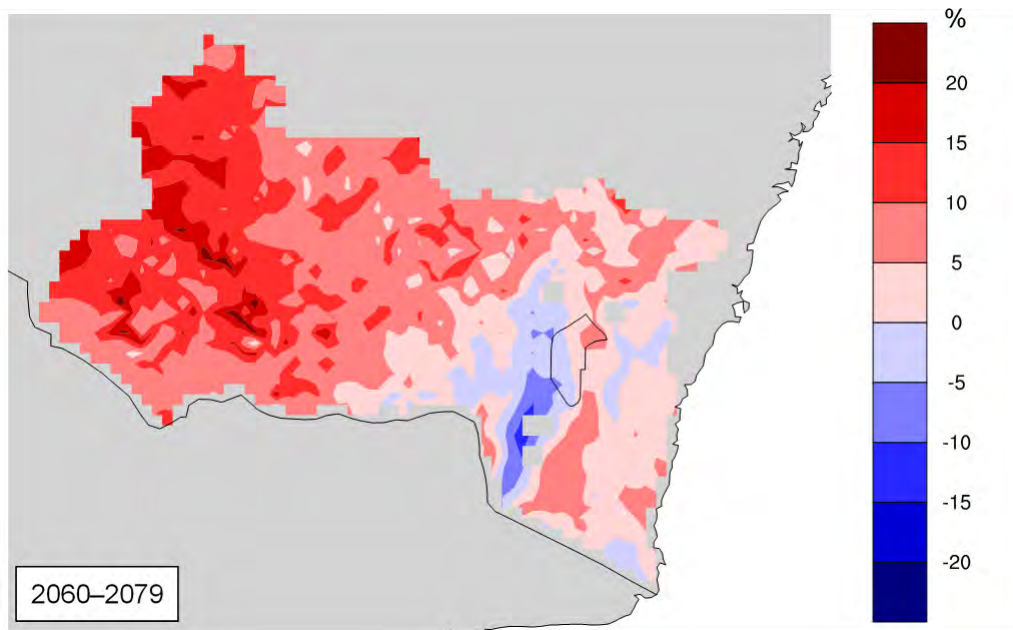
Figure 18   **Changes in annual moderate precipitation days (%) for 2060 to 2079 relative to 1990 to 2009**
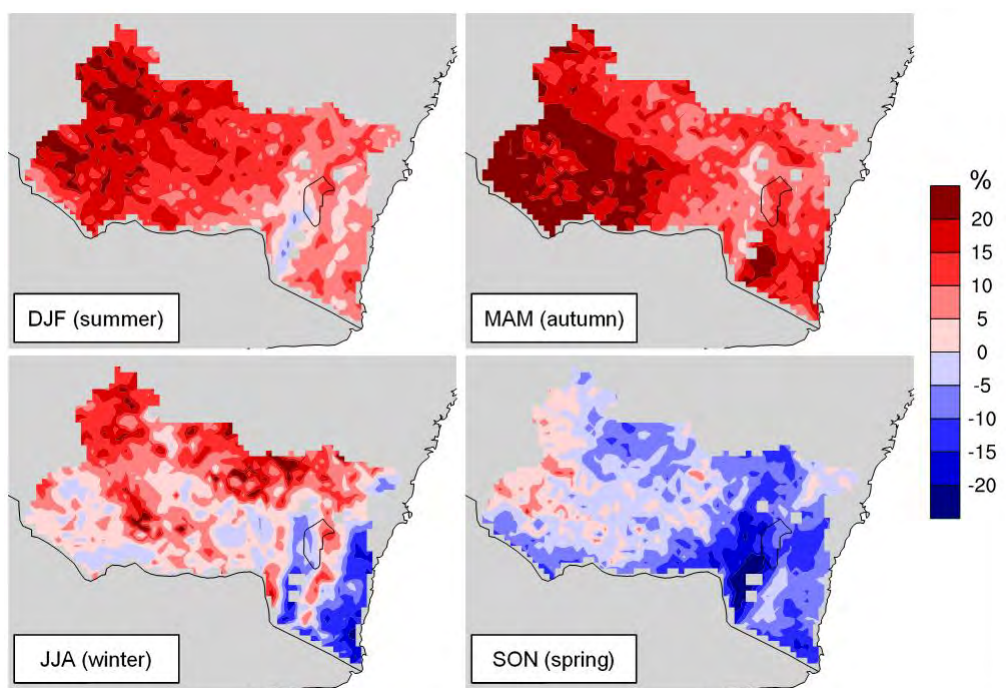
Figure 19   **Changes in seasonal moderate precipitation days (%) for 2060 to 2079 relative to 1990 to 2009**

3.4 Heavy precipitation days (rainfall above 25 mm/day)

Mean number of heavy precipitation days for the 1990 to 2009 baseline period

Precipitation above 25 millimetres/day is taken as a threshold of daily precipitation for a heavy precipitation day. Simulations indicate there are few heavy precipitation days for the western MM region, and a few events for western SET. Most of the heavy precipitation events are shown in the coastal and Alpine regions with 8–15 events in a year (Figure 20).

Heavy precipitation days mostly occur in summer for the coast and in winter for the Alpine region (Figure 21). The Alpine region can have some heavy precipitation events in other seasons, but the coast has no heavy precipitation events in winter.
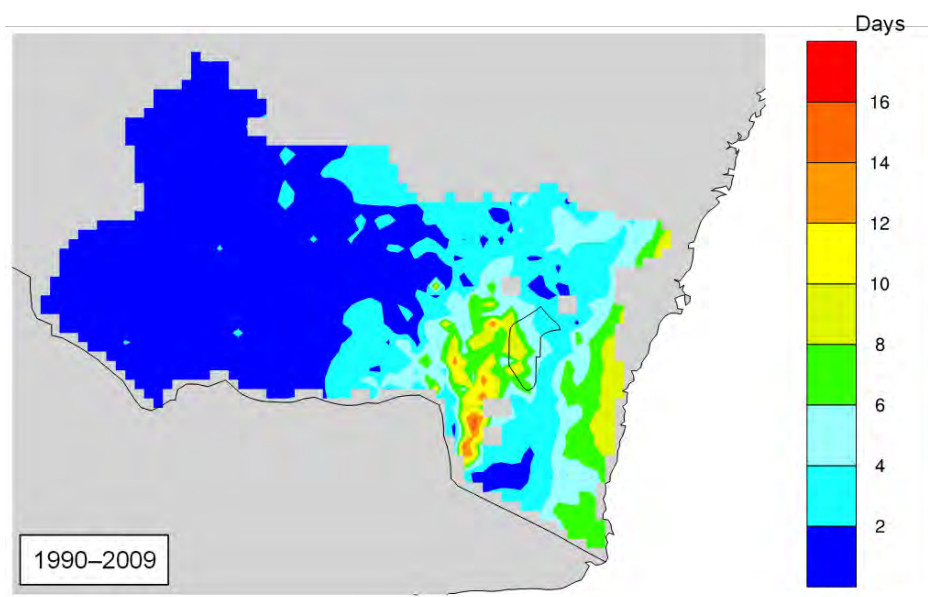
Figure 20   Annual heavy precipitation days for 1990 to 2009
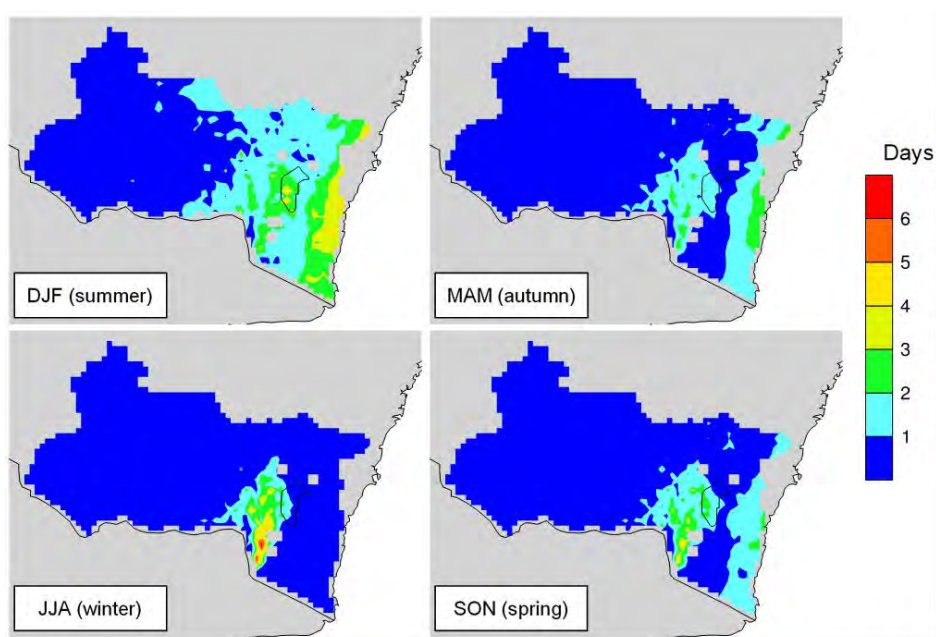
Figure 21   Seasonal heavy precipitation days for 1990 to 2009

Changes in the number of heavy precipitation days for 2020 to 2039

Future projections for heavy precipitation days are summarised in Figure 22. Broadly, the western MM region will expect to have more heavy precipitation events in 2020 to 2039; however, the eastern MM region and SET will have fewer heavy precipitation events in the same period.
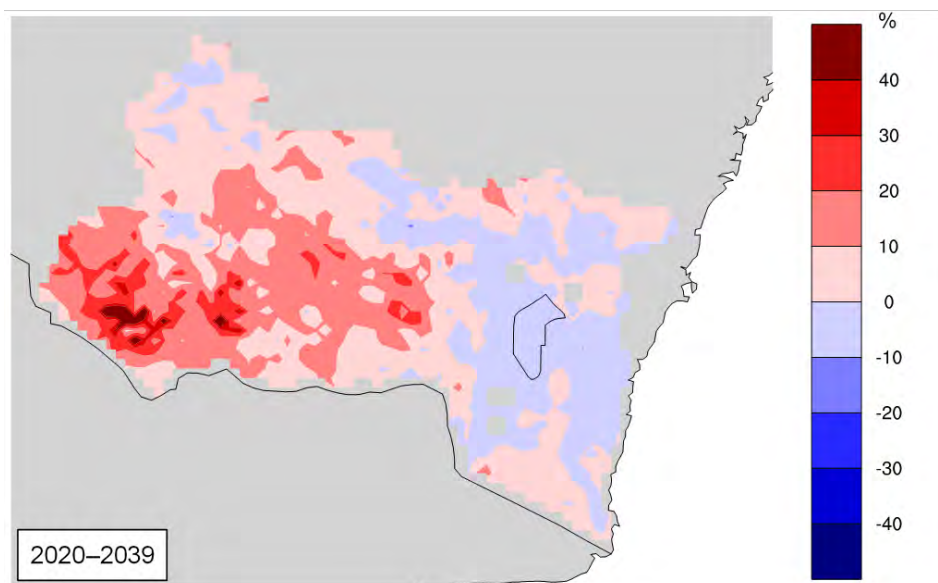
Figure 22   Changes in annual heavy precipitation days (%) for 2020 to 2039 relative to 1990 to 2009

Larger increases in seasonal heavy precipitation events for the western MM region are mostly in autumn and winter, when a more than 60% increase is projected for some areas (Figure 23). A more than 60% decrease in seasonal heavy precipitation events is projected for some parts of the Alpine region in winter. There is little seasonal variation in changes in heavy precipitation days in coastal areas.

Figure 23   Changes in seasonal heavy precipitation days (%) for 2020 to 2039 relative to 1990 to 2009

Changes in the number of heavy precipitation days for 2060 to 2079

For 2060 to 2079 increases in heavy precipitation days are projected for most areas except for some of the Alpine region, where about a 10% decrease is projected. A more than 40% increase can be seen over most of the MM region and a 10–20% increase for coastal regions (Figure 24).
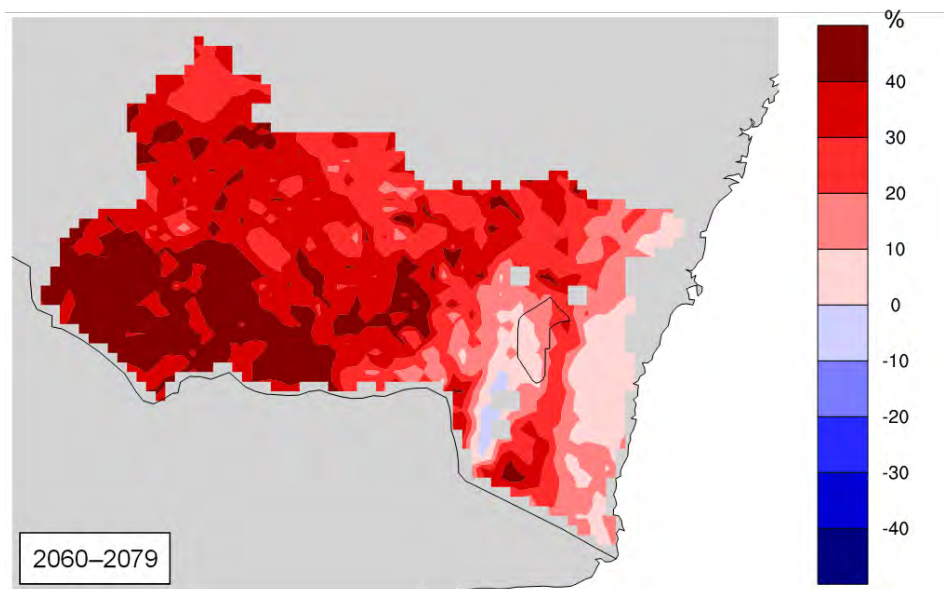
Figure 24   **Changes in annual heavy precipitation days (%) for 2060 to 2079 relative to 1990 to 2009**

A more than 60% increase in heavy precipitation days is projected for autumn and winter in the MM region, where a 20–40% increase is projected for the other two seasons (Figure 25). A 20% increase is projected for the coastal and Alpine regions in summer and autumn, and a 20% decrease is projected for the other two seasons for the same areas.
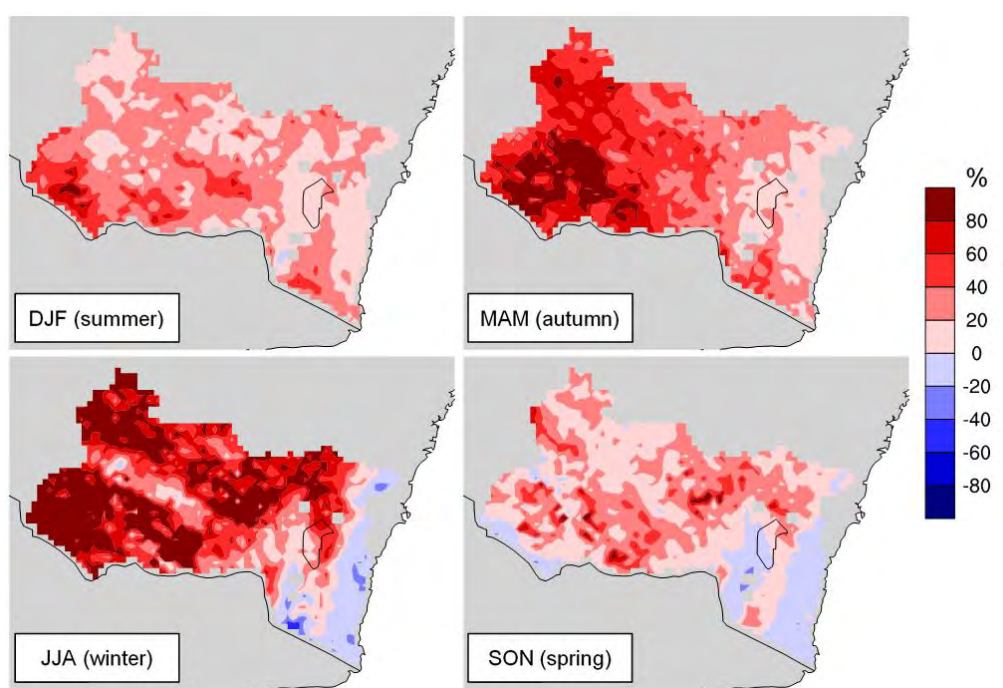
Figure 25   **Changes in seasonal heavy precipitation days (%) for 2060 to 2079 relative to 1990 to 2009**

3.5   Maximum temperature

Mean maximum temperature for the 1990 to 2009 baseline period

There is a clear west–east temperature gradient in the MM region with more than 25°C annual maximum temperature for the north-western MM region and 17–19°C in the east (Figure 26). For the SET region, a weak temperature gradient is shown from the coast to inland, with 20–22°C shown for the coast and 17–19°C inland. The lowest mean annual maximum temperature is observed in the Alpine region where annual mean maximum temperature is below 10°C in some areas.
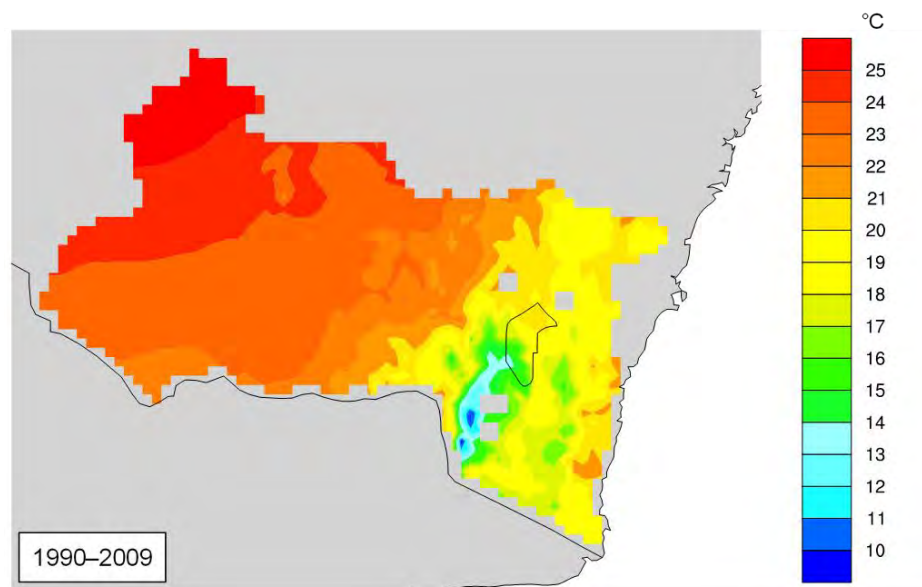
Figure 26   Mean annual maximum temperature for 1990 to 2009

Substantial seasonal variation in maximum temperature can be observed for the MM and Alpine region, but small seasonal variation is observed for the coast (Figure 27). Mean maximum temperature for the western MM region is largely above 32°C in summer; however, it is generally below 8°C in winter for the Alpine region.
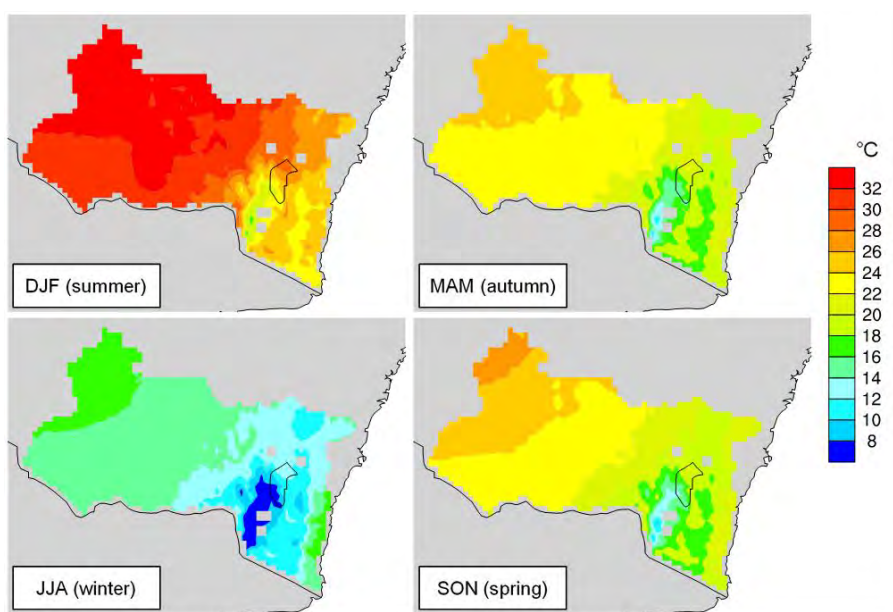
Figure 27   Mean seasonal maximum temperature for 1990 to 2009

Changes in maximum temperature for 2020 to 2039

Changes in maximum temperature for 2020 to 2039 is quite small with a 0.5–0.75°C increase for most of the study area except for the northern Alpine region where 0.75-1°C increase is projected (Figure 28).
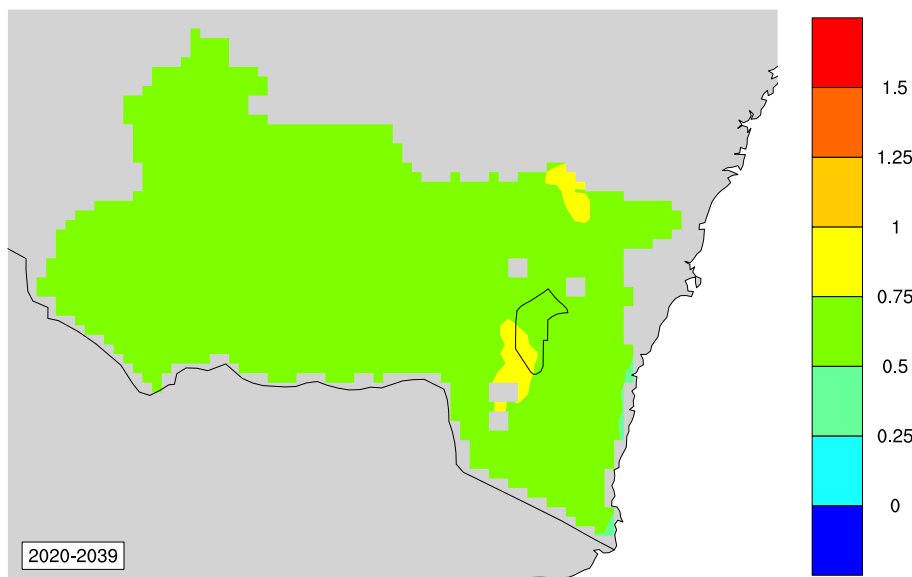
Figure 28   Changes in mean annual maximum temperature for 2020 to 2039 relative to 1990 to 2009

Seasonal increases in maximum temperature are also small with a 0.75–1°C increase in spring and summer and a 0.5-0.75°C increase for the autumn for most areas. Less than 0.5°C increase is expected for winter for majority area except for the Alpine region with 0.5–0.75°C increase (Figure 29).
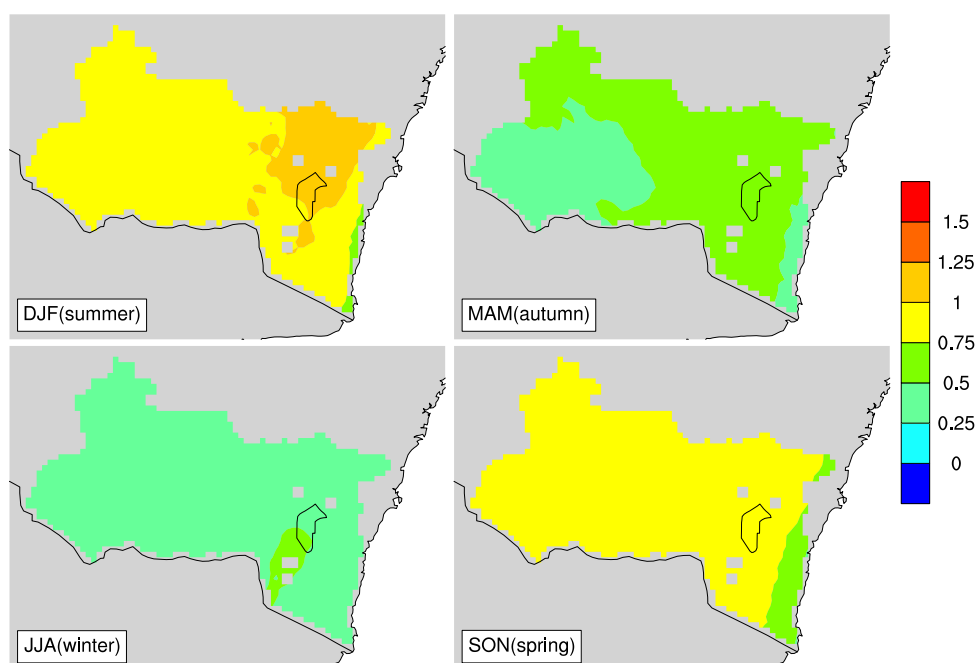
Figure 29   Changes in mean seasonal maximum temperature for 2020 to 2039 relative to 1990 to 2009

19

Changes in maximum temperature for 2060 to 2079

Changes in maximum temperature are much larger for 2060 to 2079 (Figure 30) when compared to changes for 2020 to 2039. A 1.5–2°C increase is projected for eastern SET and southwest MM regions while more than 2°C increase is projected for other regions especially for the Alpine with more than 2.25°C increase.
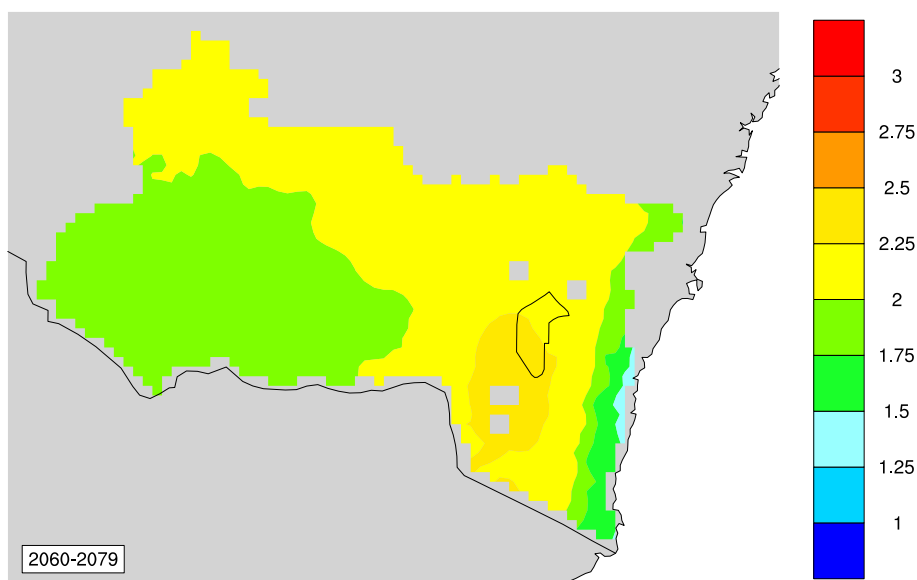
Figure 30   Changes in mean annual maximum temperature for 2060 to 2079 relative to 1990 to 2009

A larger increase in maximum temperature is projected in summer and spring compared with the other two seasons (Figure 31). Little seasonal variation in increases in maximum temperature is projected for the coast. Generally, a larger increase in maximum temperature is projected for the Alpine region than surrounding regions with a more than 2.5°C increase in spring and a 2–2.5°C increase in other three seasons.
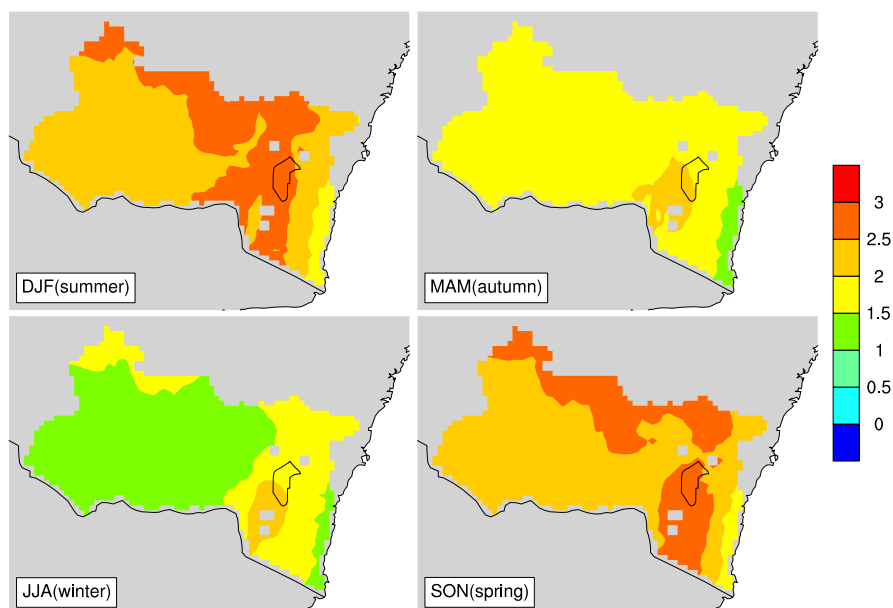
Figure 31   Changes in mean seasonal maximum temperature for 2060 to 2079 relative to 1990 to 2009

3.6   Hot days (maximum temperature above 35°C)

Mean number of hot days for the 1990 to 2009 baseline period

There is a clear north-west to south-east gradient in the number of hot days with more than 50 days in a year for the north-west of the MM region and fewer than five days in a year for the SET and Alpine region (Figure 32).
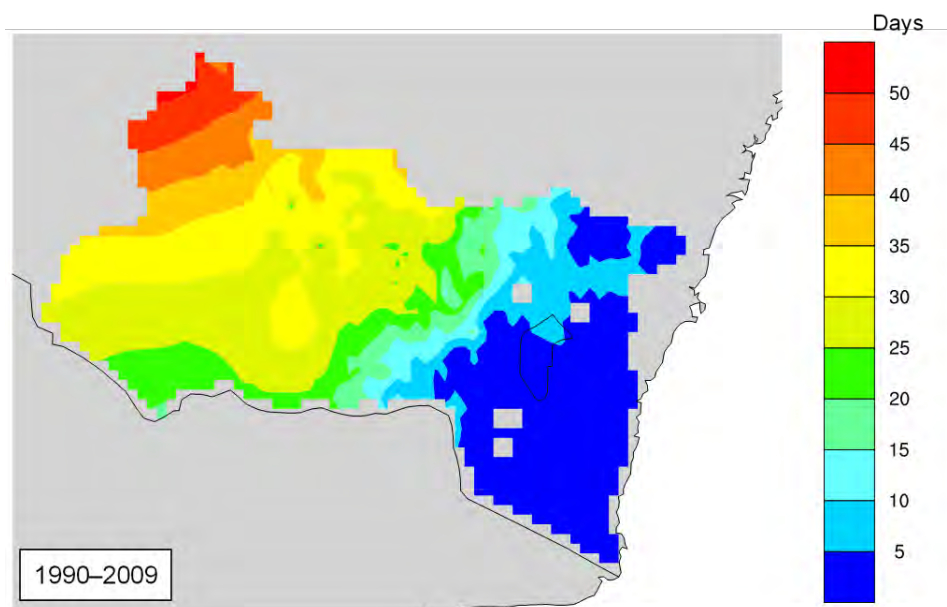
Figure 32   Mean annual number of hot days for 1990 to 2009

Unsurprisingly, the majority of hot days are in summer for the MM region and there are no hot days in winter, but spring and autumn also have a few days with maximum temperature above 35°C, especially for the north-west MM region (Figure 33). Annually, there are few hot days for other regions.
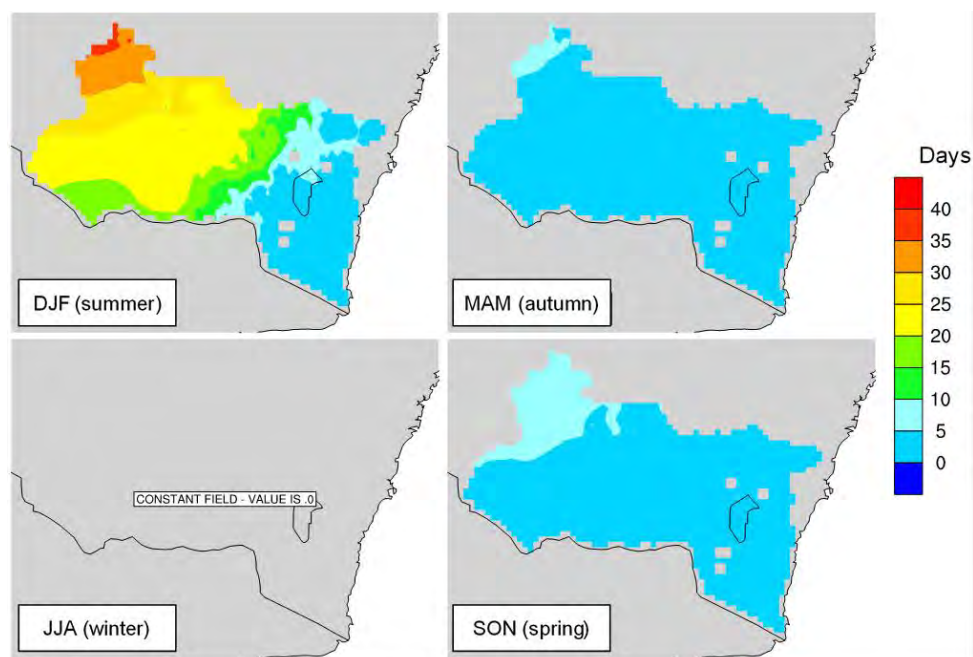
Figure 33   **Mean seasonal number of hot days for 1990 to 2009**

Note that JJA has no values plotted as there are no instances where the maximum temperature exceeds 35°C

Changes in the number of hot days for 2020 to 2039

For most of the MM region, 8–10 more hot days are projected, while 3–5 more hot days are projected for the northern SET region, with only a small increase for the remaining areas (Figure 34).
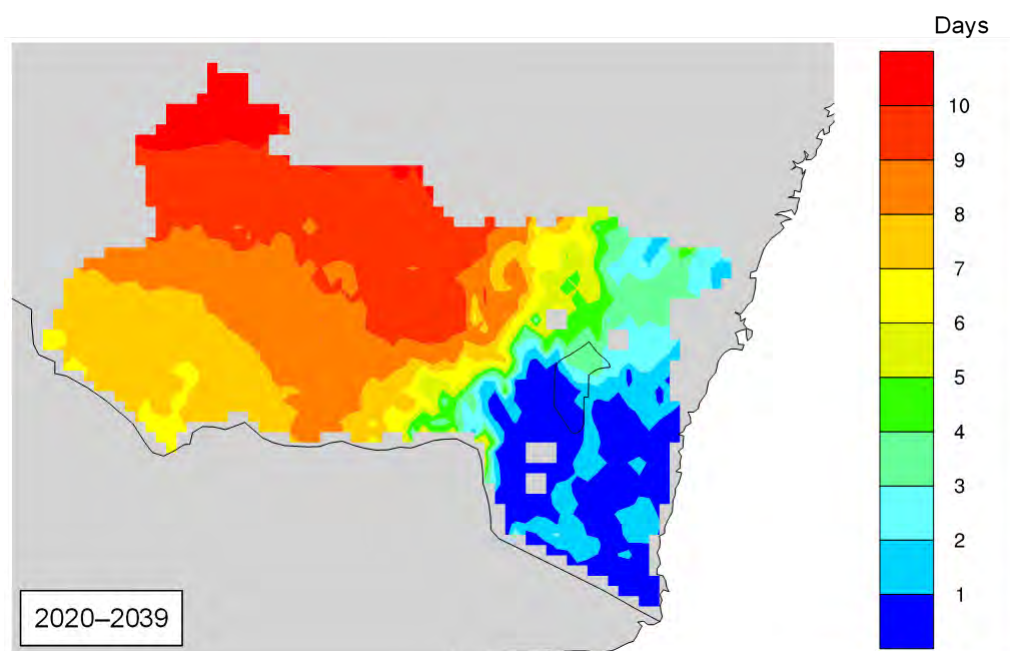
Figure 34   **Changes in annual hot days for 2020 to 2039 relative to 1990 to 2009**

Increases in extreme days are mostly in summer, with some increases in spring, small increases in autumn and no change in winter (Figure 35).
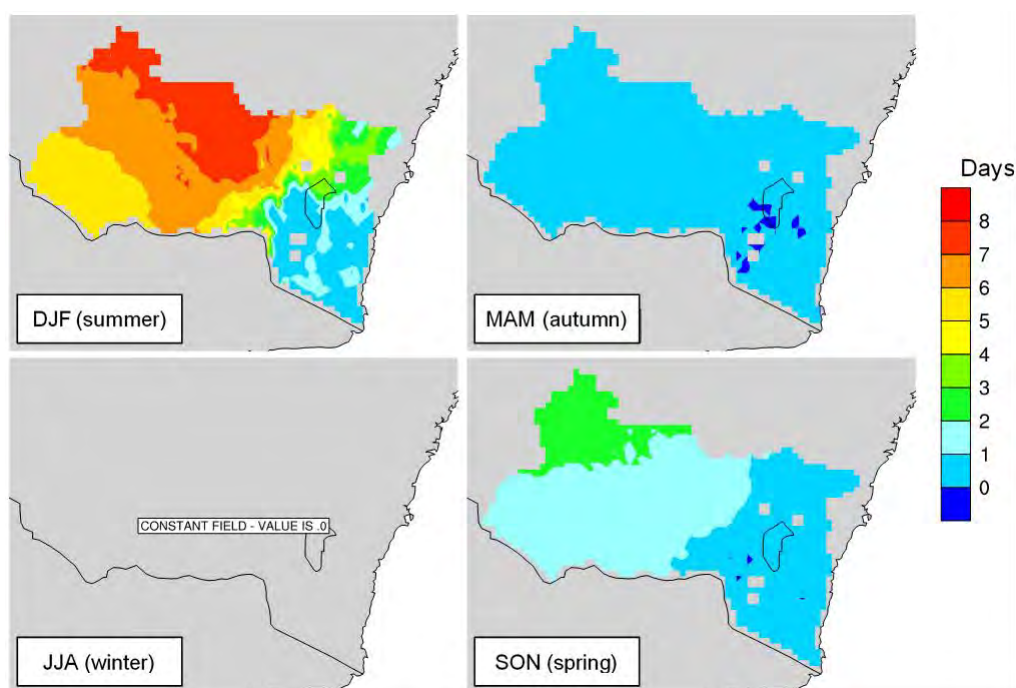
Figure 35   Changes in seasonal hot days for 2020 to 2039 relative to 1990 to 2009

Note that JJA has no values plotted as there are no instances where the maximum temperature exceeds 35°C

Changes in the number of hot days for 2060 to 2079

The change pattern for 2060 to 2079 is similar to that of 2020 to 2039; however, the magnitude of change is much larger in the far future (Figure 36). An increase of more than 24 hot days in a year is projected for 2060 to 2079 for most of the MM region, with 8–12 more hot days for northern SET and fewer than four days for the remaining regions.
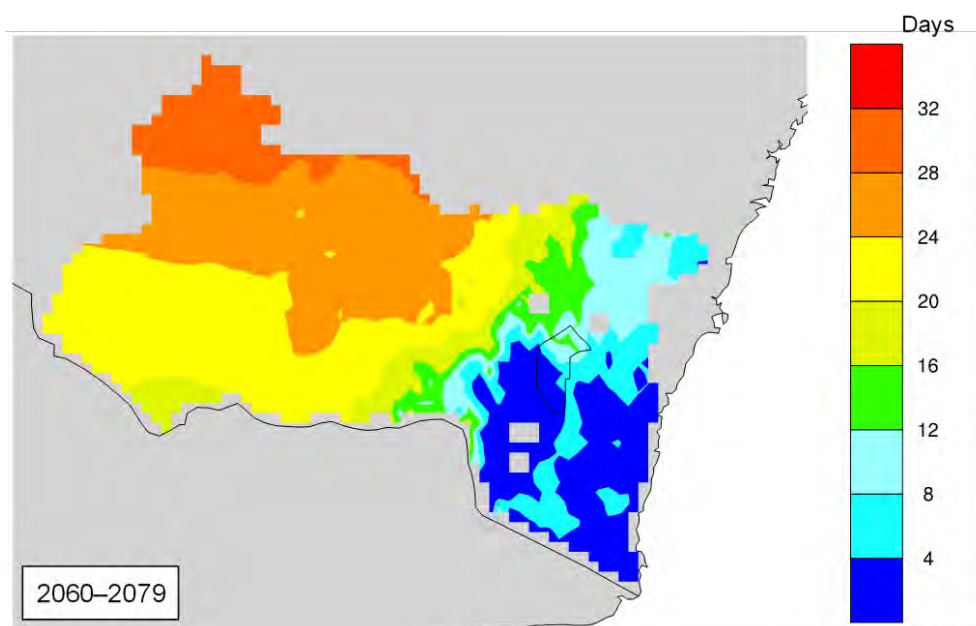
Figure 36   Changes in annual hot days for 2060 to 2079 relative to 1990 to 2009

For the MM region, increases in hot days are mostly in summer, with 4–8 day increases in spring, 2–4 day increases in autumn and no change in winter (Figure 37). For northern SET

8–10 more hot days are projected in summer, as well as a few more hot days in other northern areas. No changes for the Alpine and southern SET regions are projected apart from minor increases in summer in some areas.
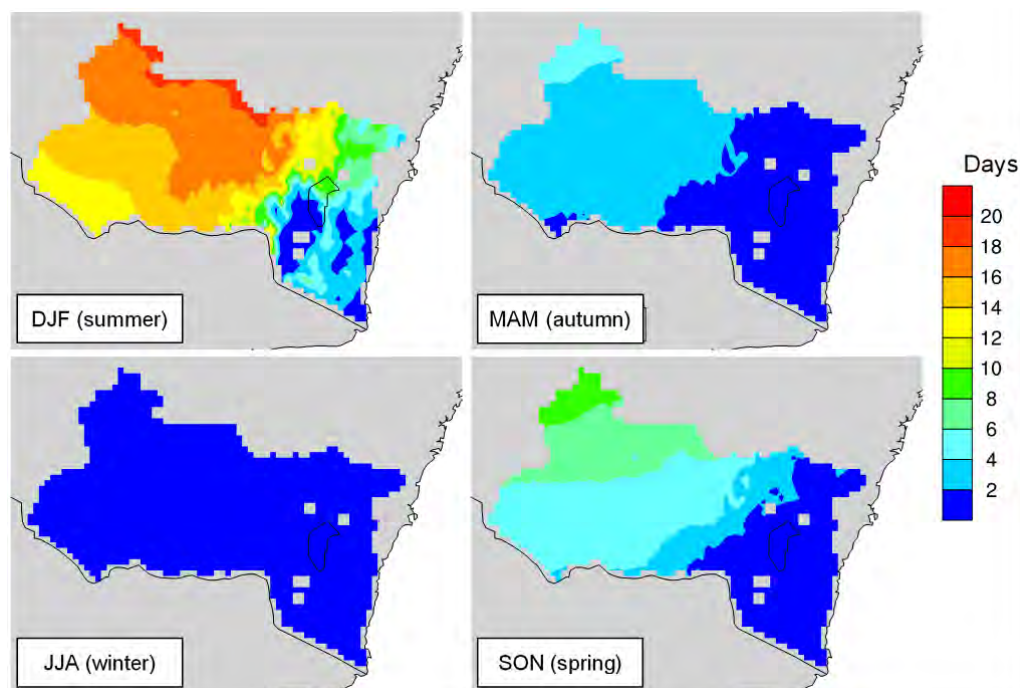
Figure 37   Changes in seasonal hot days for 2060 to 2079 relative to 1990 to 2009

3.7   Minimum temperature

Mean minimum temperature for the 1990 to 2009 baseline period

Annual average daily minimum temperature has a similar pattern of gradients as annual average daily maximum temperature, with more than 10°C minimum temperature in the west MM region and along the coast and less than 2°C minimum temperature in the Alpine region (Figure 38).
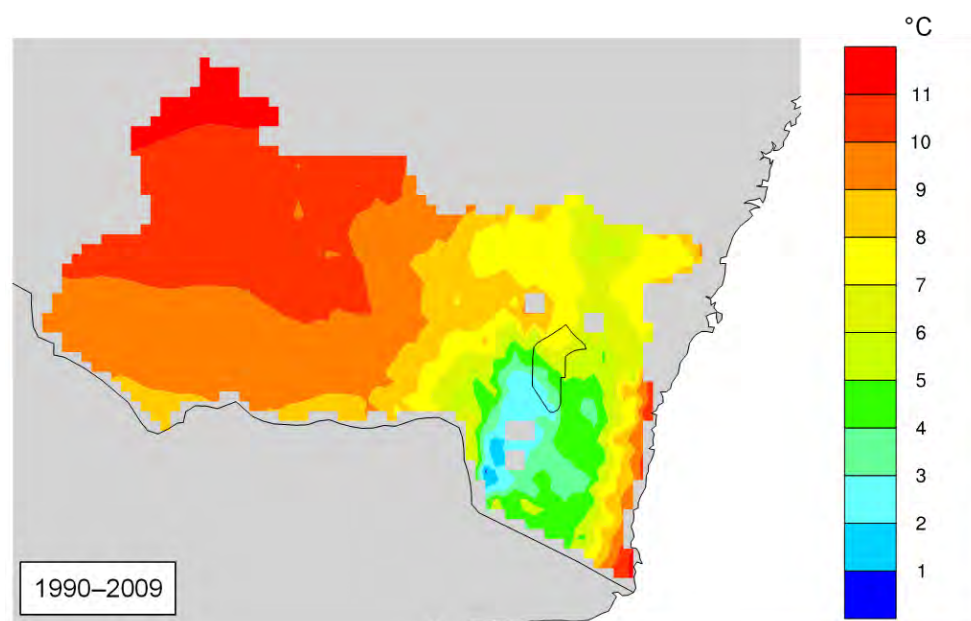
Figure 38   **Mean annual minimum temperature for 1990 to 2009**

There is a clear seasonal variation in minimum temperature with high minimum temperature in summer and low minimum temperature in winter (Figure 39). On average, above 18°C minimum temperature is observed for the north-west MM region in summer, with below –2°C minimum temperature observed for the Alpine region in winter.
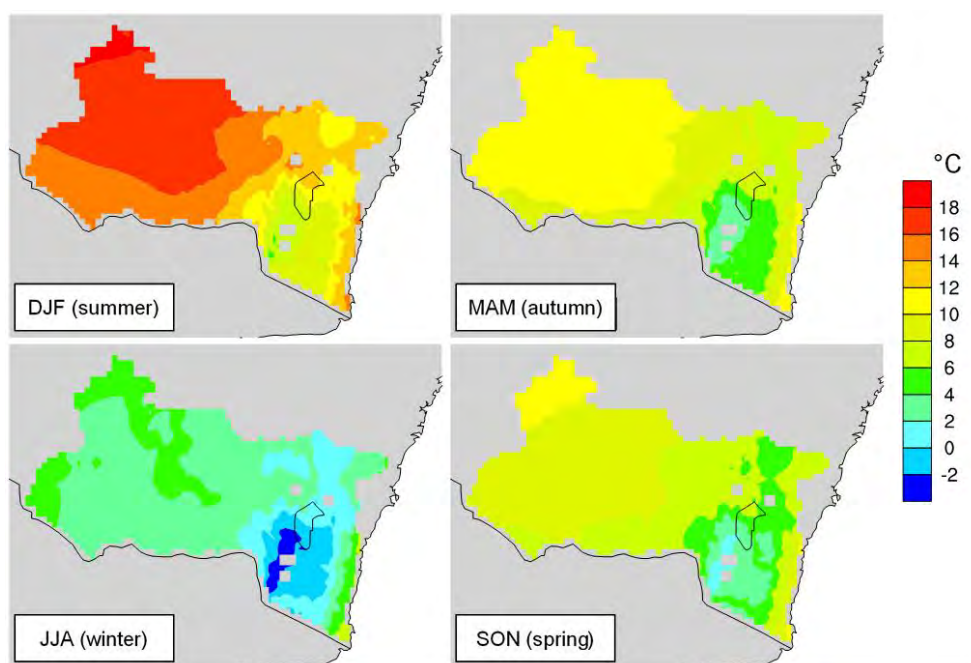
Figure 39   **Mean seasonal minimum temperature for 1990 to 2009**

Changes in minimum temperature for 2020 to 2039

The change in minimum temperature for the 2020 to 2039 projection period is small, with a 0.5–0.75°C increase projected across the study area (Figure 40). The seasonal variation in projected change is also quite small with slightly more increases in summer compared with spring and autumn while winter is projected with the least increase (Figure 41).
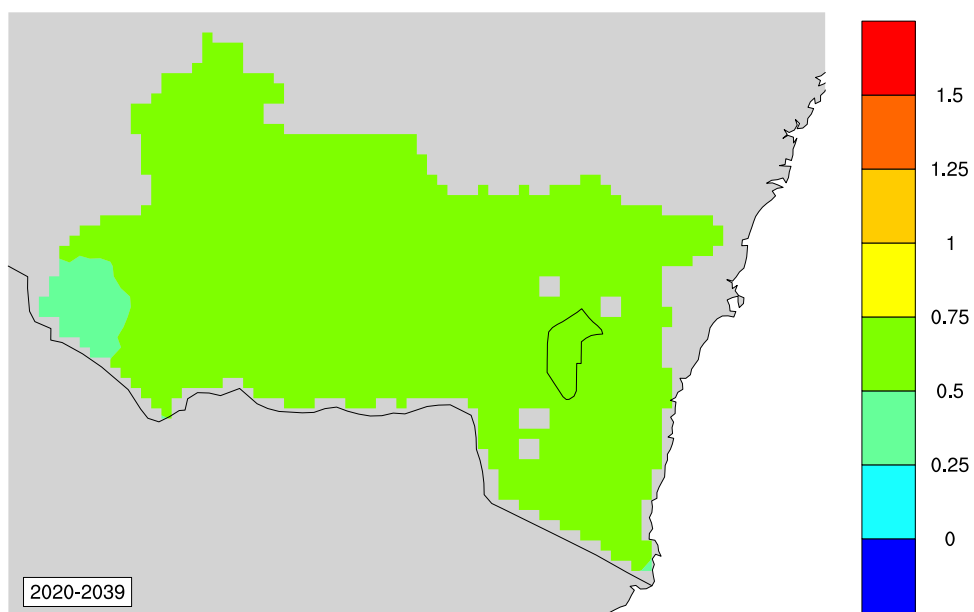
Figure 40   **Changes in mean annual minimum temperature for 2020 to 2039 relative to 1990 to 2009**
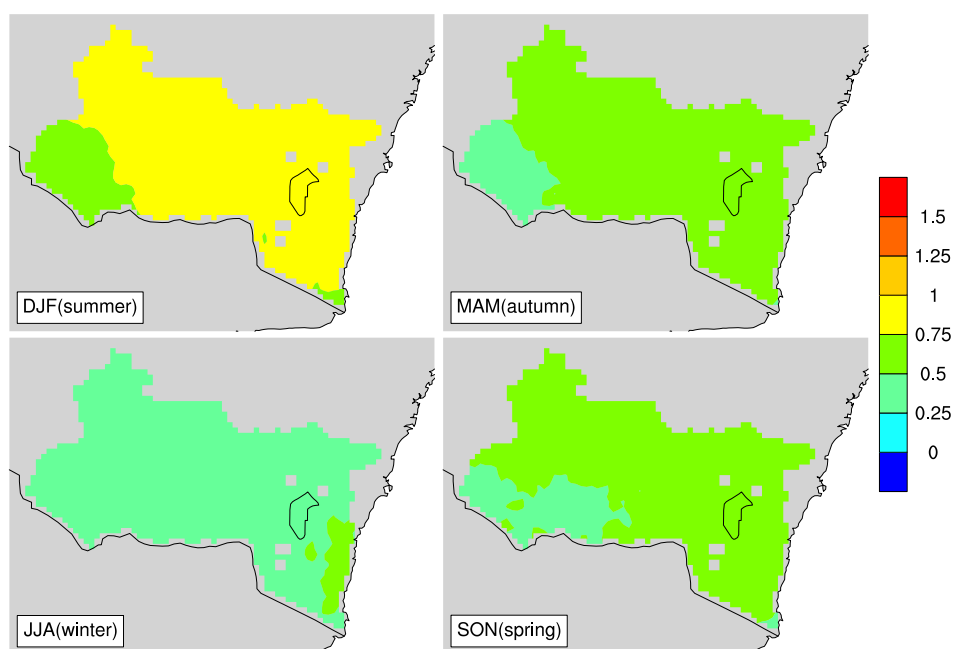
Figure 41   **Changes in mean seasonal minimum temperature for 2020 to 2039 relative to 1990 to 2009**

Changes in minimum temperature for 2060 to 2079

For 2060 to 2079 a 1.5–2°C increase in minimum temperature is projected for most areas, except for the south-SET region where a 2–2.5°C increase is projected (Figure 42).
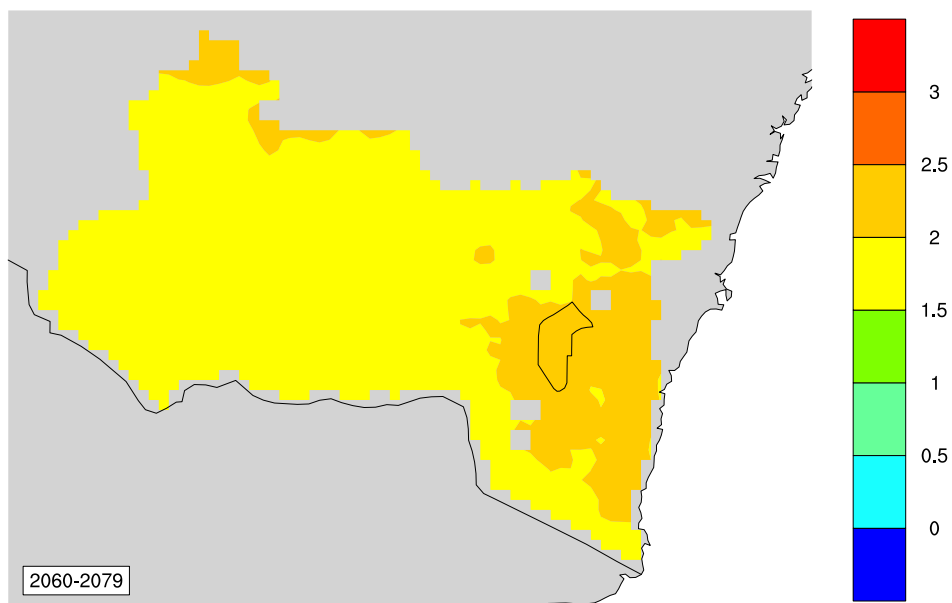
Figure 42   **Changes in mean annual minimum temperature for 2060 to 2079 relative to 1990 to 2009**

Increases in minimum temperature are larger in summer compared with the other three seasons. A 2–2.5°C increase in minimum temperature is projected for most areas (Figure 43). Changes look similar for spring and autumn with a 2–2.5°C increase in SET and northern MM, and a 1.5–2°C increase for the remaining regions. Minimum temperature is projected with least increase in winter with 1-1.5°C increase in the MM region and 1.5-2°C for the SET region.
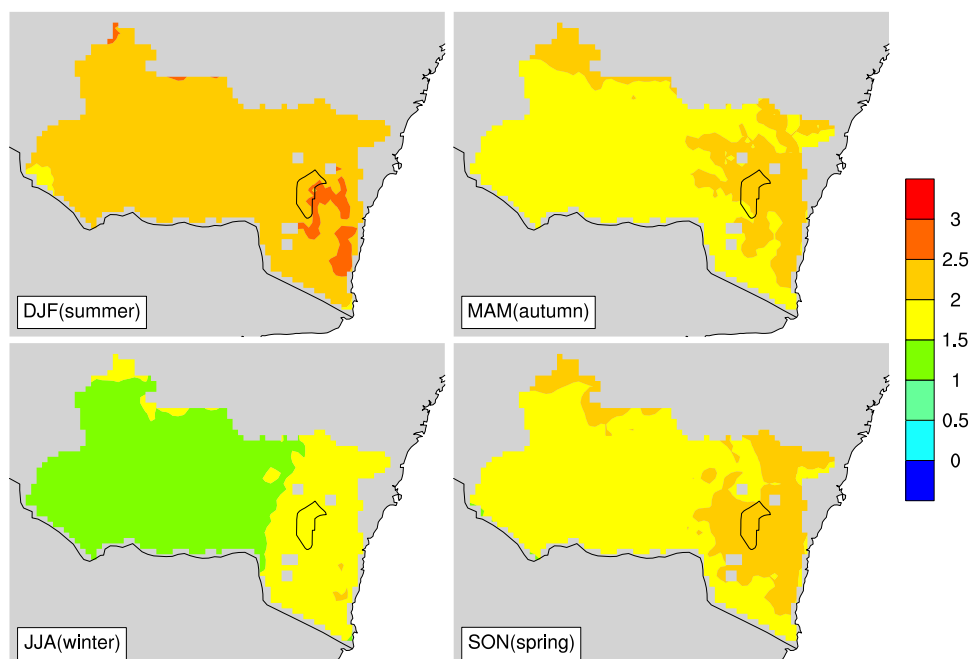
Figure 43   **Changes in mean seasonal minimum temperature for 2060 to 2079 relative to 1990 to 2009**

3.8　　　Cold nights (minimum temperature below –2°C)

Mean number of cold nights for the 1990 to 2009 baseline period

A minimum overnight temperature below –2°C is recorded as a cold night. There are more than 110 cold nights in a year for the Alpine region, 40–60 cold nights in surrounding areas, and fewer than 10 cold nights in a year for coastal areas and most of the MM region (Figure 44).
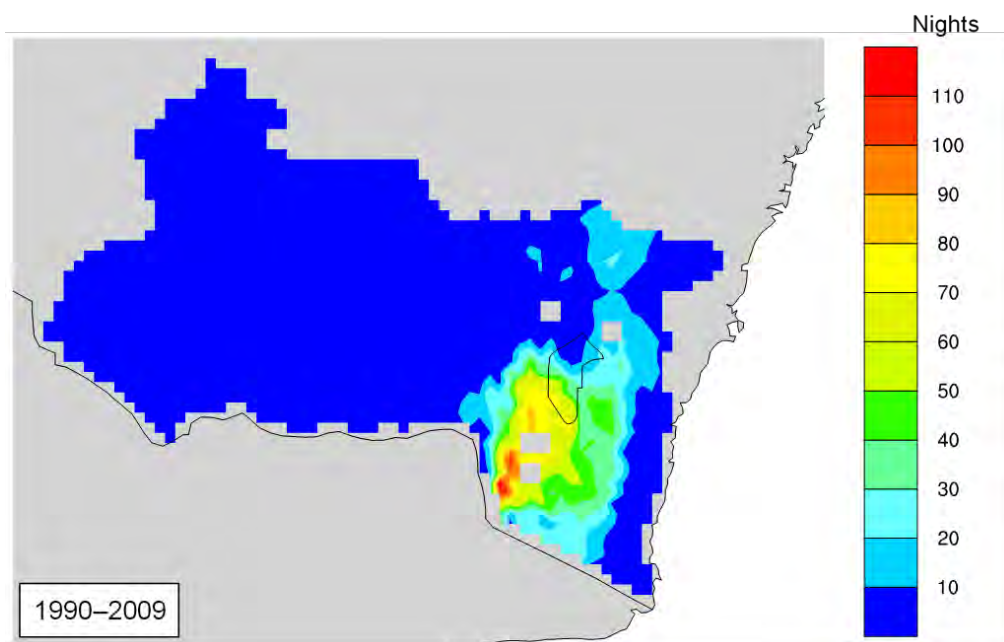
Figure 44　　　Mean annual cold nights for 1990 to 2009

Unsurprisingly, the majority of cold nights are in winter; however, there are 10–20 cold nights in spring and a few cold nights in autumn for the Alpine region and surrounding areas (Figure 45).
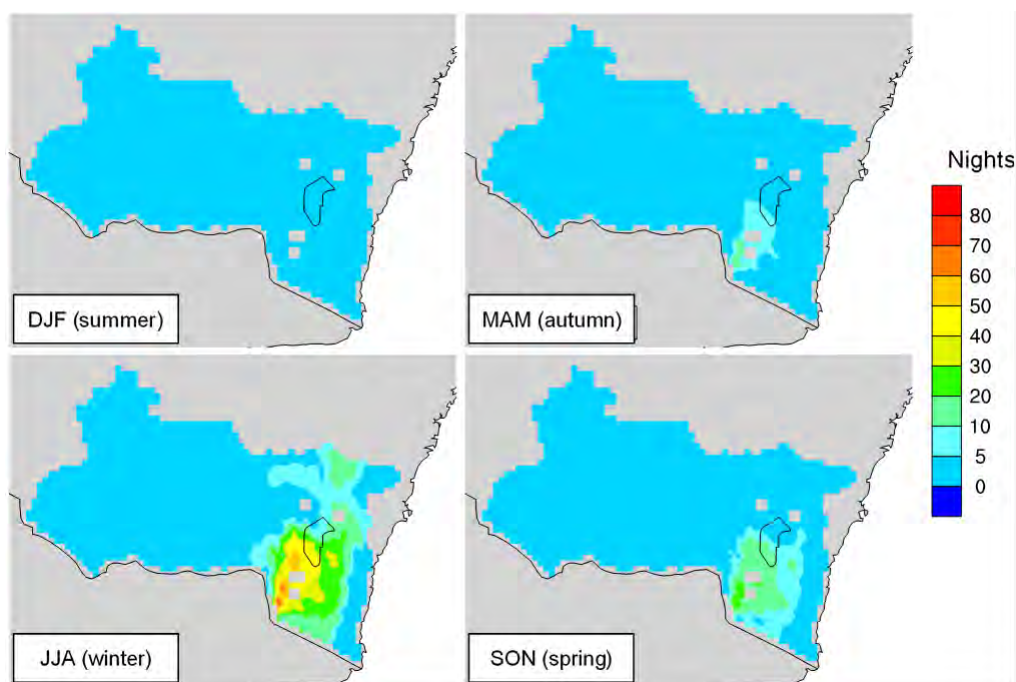
Figure 45　　　Mean seasonal cold nights for 1990 to 2009

Changes in the number of cold nights for 2020 to 2039

Overall, there will be fewer cold nights across the study area in 2020 to 2039. The largest decrease in cold nights is projected for the Alpine region, where a decrease of more than 13 nights a year is projected in some areas (Figure 46).
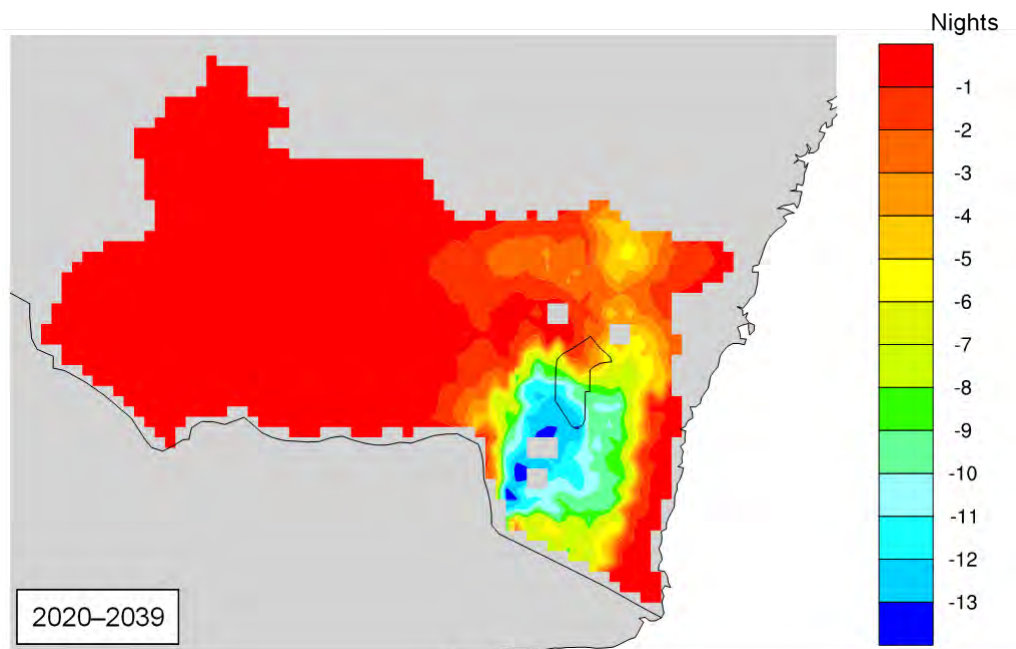
Figure 46   Changes in annual cold nights for 2020 to 2039 relative to 1990 to 2009

Similar to the seasonal distribution of the absolute number of cold nights, the reduction in cold nights will mostly occur in winter, when eight fewer cold nights are projected on average compared with 1990 to 2009 (Figure 47). In addition, some reduction in cold nights is shown in autumn and spring for the Alpine region.
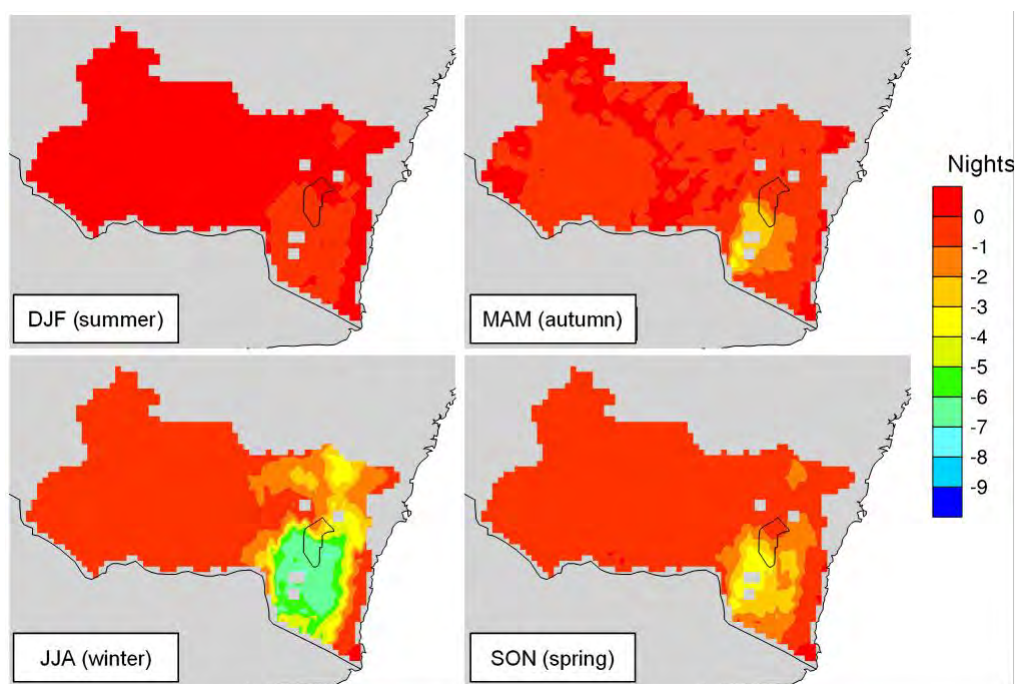
Figure 47   Changes in seasonal cold nights for 2020 to 2039 relative to 1990 to 2009

Changes in the number of cold nights for 2060 to 2079

More than 20 nights a year will no longer be considered a cold night (as per the definition used in this report) for the Alpine region, and more than 40 nights a year for mountain peaks (Figure 48).
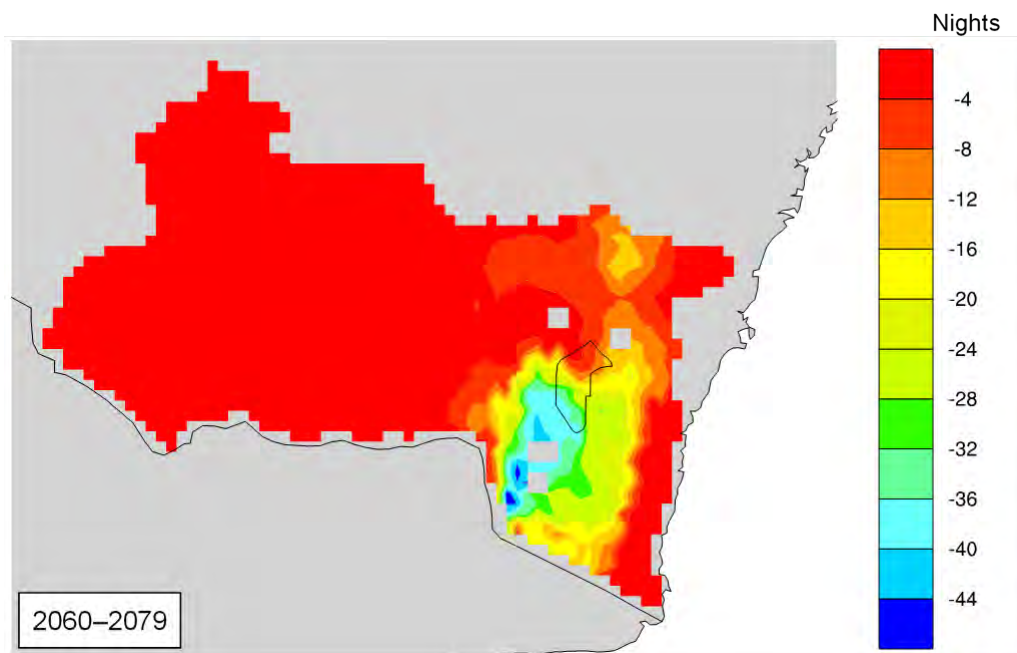

Figure 48   **Changes in annual cold nights for 2060 to 2079 relative to 1990 to 2009**

The largest reduction in cold nights is in winter when 20 fewer cold nights are projected for the Alpine region (Figure 49). Spring will have a more than 10-night reduction in some parts of the Alpine region.
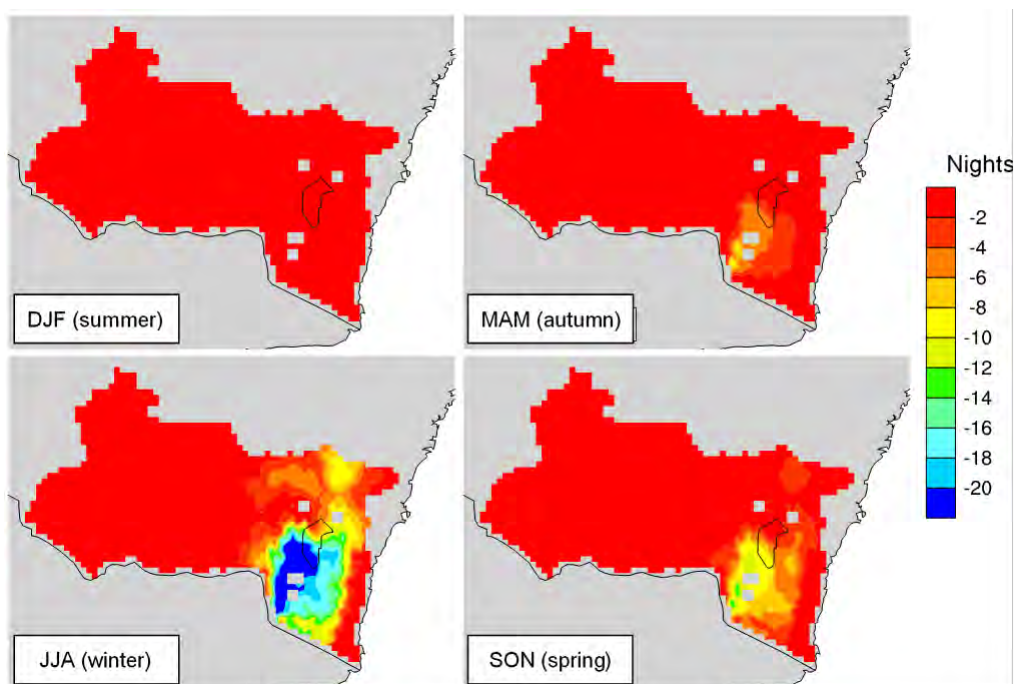
Figure 49   **Changes in seasonal cold nights for 2060 to 2079 relative to 1990 to 2009**

3.9 Mean wind speed

Mean wind speed for the 1990 to 2009 baseline period

The annual mean wind speed using the multi-model mean for the 1990 to 2009 period is shown in Figure 50. More than 8 m/s wind is seen in the Alpine region and 6–7 m/s for high topography areas in SET. Wind speed is generally small (less than 5 m/s) in the MM region as terrain is relatively flat.
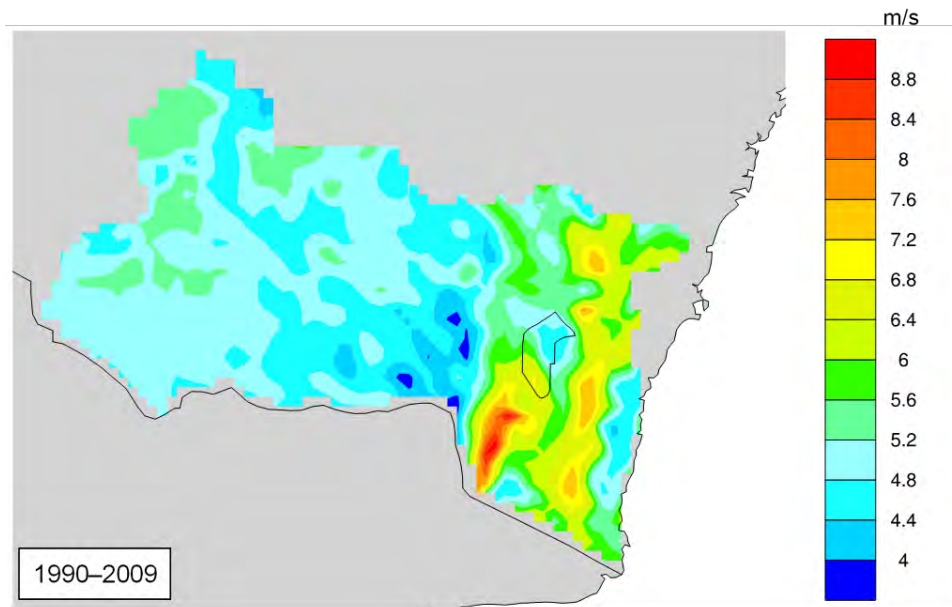

Figure 50   Simulated annual mean wind speed for 1990 to 2009

Seasonal variation in wind speed is seen for different areas (Figure 51). The MM region has higher wind speed in summer and spring compared to winter and autumn; however, the Alpine region and high topography areas in SET have much higher wind speed in winter and spring compared to summer and autumn. The seasonal variation in wind speed along the coast is very small.
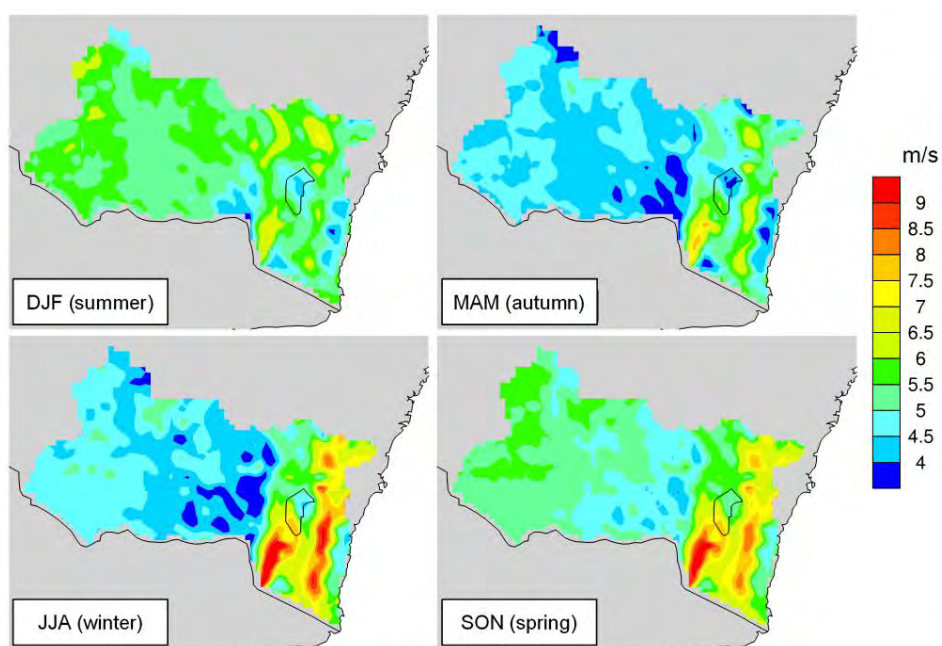

Figure 51   Simulated seasonal mean wind speed for 1990 to 2009

Changes in mean wind speed for 2020 to 2039

A less than 2% decrease in annual mean wind speed is projected for the study area except for the Alpine region and high topography areas in SET where a 2–4% decrease is simulated for 2020 to 2039 (Figure 52).
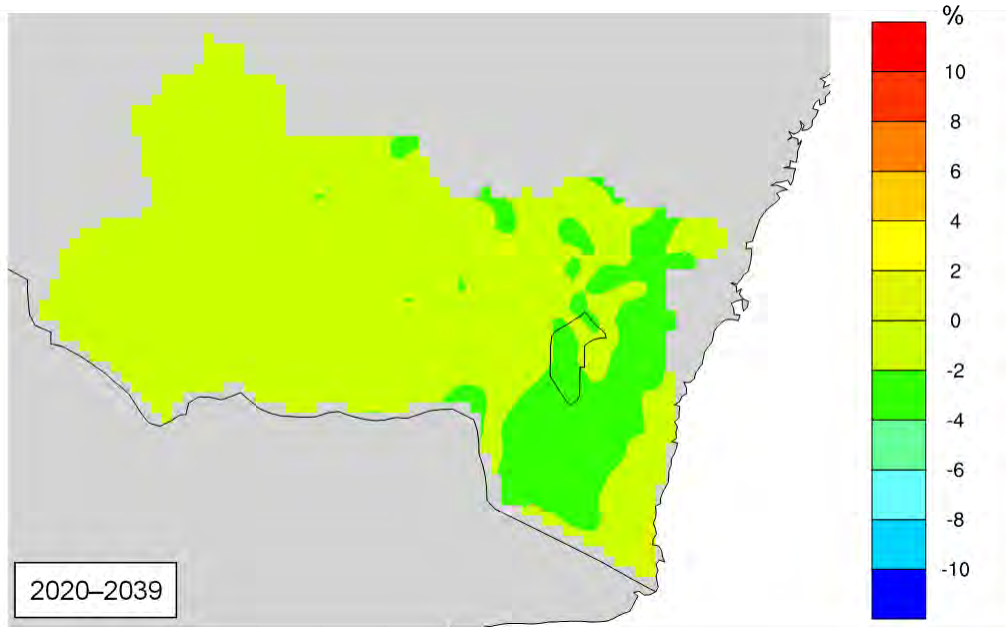

Figure 52   **Changes in annual mean wind speed (%) for 2020 to 2039 relative to 1990 to 2009**

Wind speed generally increases a little across all regions in summer and winter. During spring and autumn, wind speed decreases, especially for the Alpine region and high topography areas in SET, where a more than 4–6% decrease is expected in spring (Figure 53).
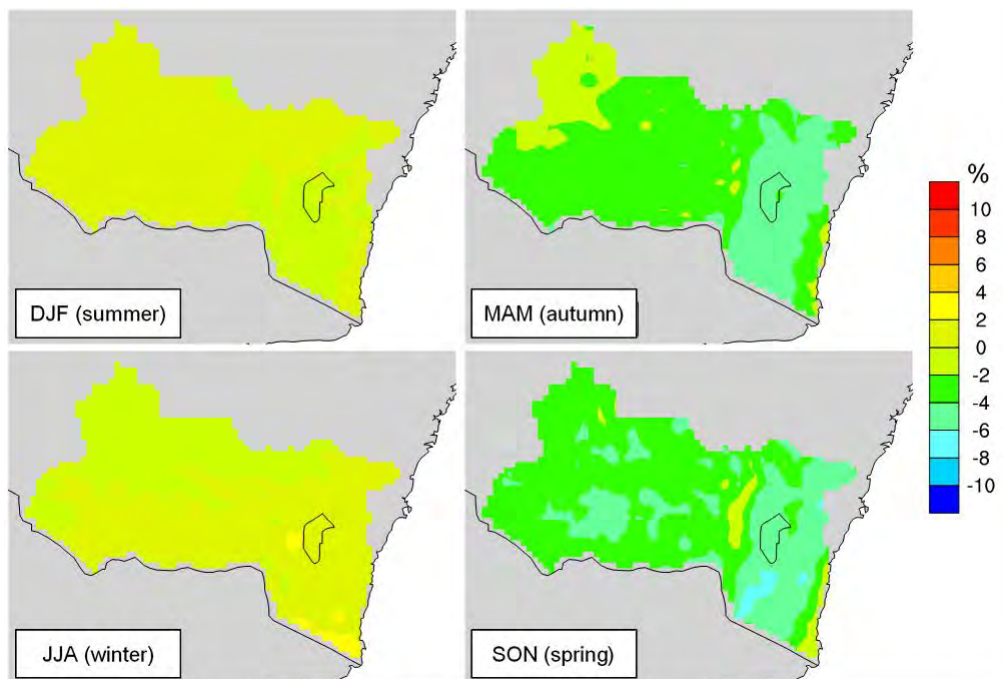

Figure 53   **Changes in seasonal mean wind speed (%) for 2020 to 2039 relative to 1990 to 2009**

Changes in mean wind speed for 2060 to 2079

Wind speed is projected to further decrease by the 2060 to 2079 period. Decreases of 4–6% are projected for most of the study region except for the south-east MM region and the coast where a 2–4% decrease is projected for 2060 to 2079 (Figure 54).
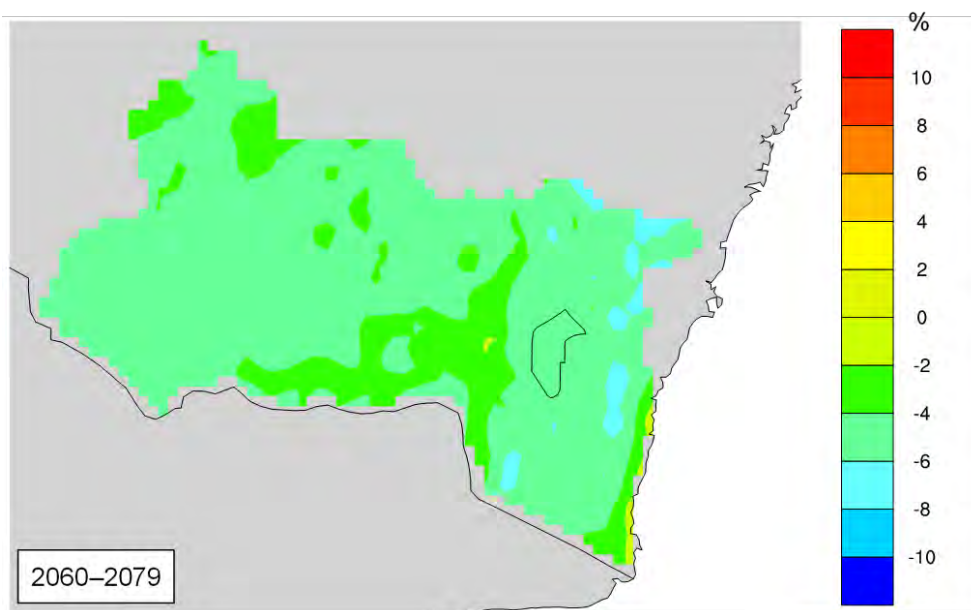

Figure 54 **Changes in annual mean wind speed (%) for 2060 to 2079 relative to 1990 to 2009**

Mean wind speed projected in summer and winter seasons shows little change relative to 1990 to 2009; however, it is projected to have a 6–8% decrease for the Alpine region and high topography areas and a 4–6% decrease for other areas in autumn (Figure 55). A larger decrease is projected for spring when a more than 8–10% decrease in mean wind speed is projected, especially for the Alpine region and high topography areas in SET, where a more than 10% decrease is expected.
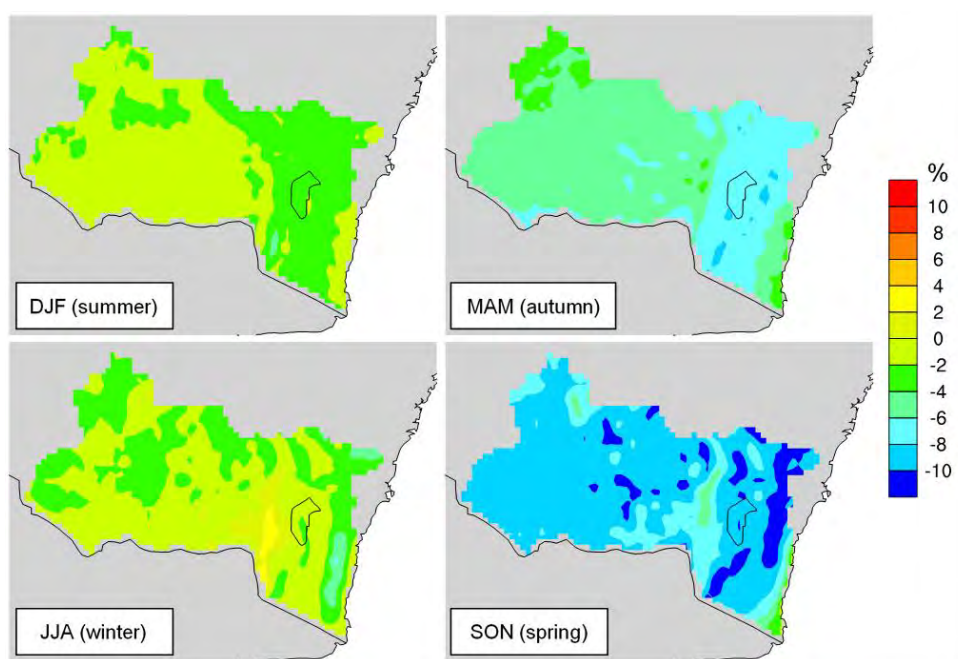

Figure 55 **Changes in seasonal mean wind speed (%) for 2060 to 2079 relative to 1990 to 2009**

3.10   Maximum daily wind speed

Mean maximum wind speed for the 1990 to 2009 baseline period

Maximum wind speed is also larger for the Alpine region and high topography areas in SET, especially for the Alpine region where more than 20 m/s maximum wind speed is simulated (Figure 56). The MM region and coastal areas generally have smaller maximum wind speeds.
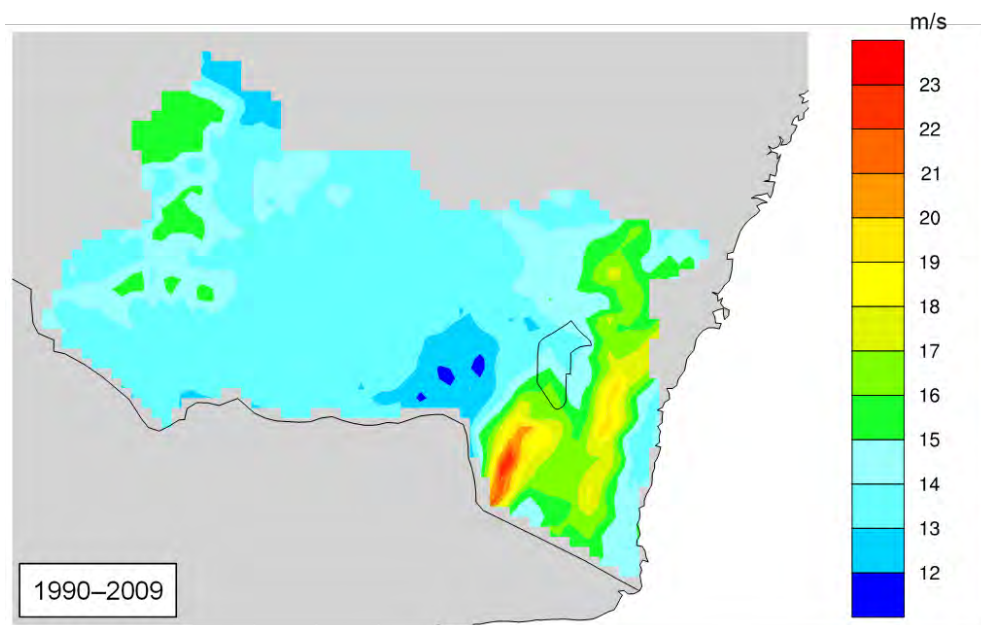

Figure 56   Annual mean maximum wind speed for 1990 to 2009

Maximum wind speed has similar seasonal variation to mean wind speed (Figure 57). Slightly larger maximum wind speed (14–16m/s) is simulated in spring and summer for the MM region. Much larger maximum wind speed (more than 22 m/s) is simulated in winter and spring for the Alpine region and high topography areas in SET relative to summer and autumn.
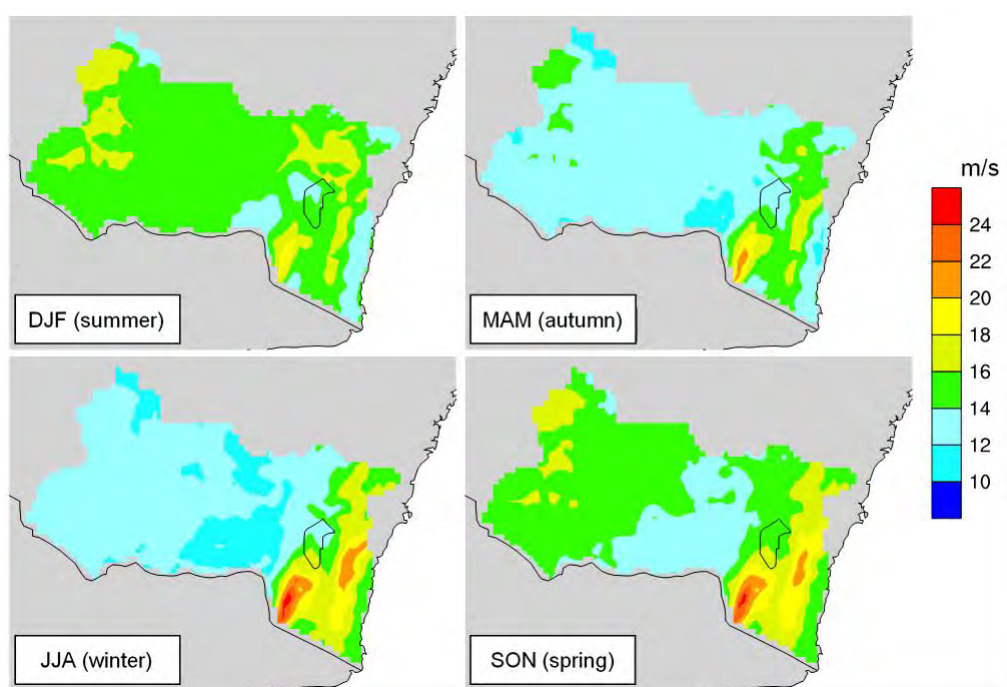

Figure 57   Seasonal mean maximum wind speed for 1990 to 2009

Changes in maximum wind speed for 2020 to 2039

Little change in maximum wind speed is projected for 2020 to 2039 (Figure 58). Overall, a less than 2% decrease in maximum wind speed is simulated for most of the study area, especially for the Alpine region where a slightly larger (2–4%) decrease is projected for some areas.
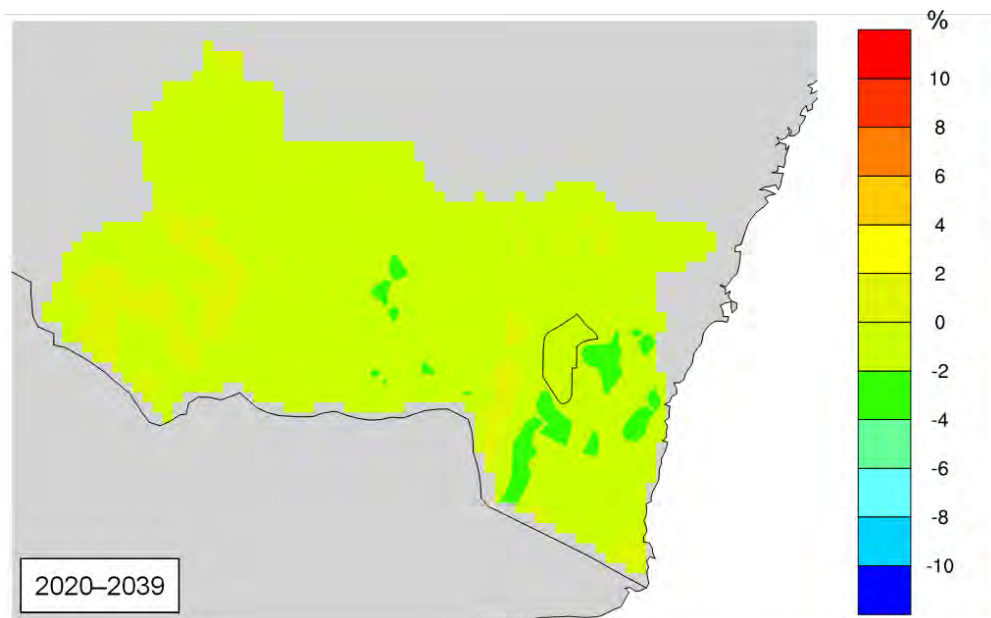

Figure 58   **Changes in annual mean maximum wind speed (%) for 2020 to 2039 relative to 1990 to 2009**

Small seasonal variations in changes in maximum wind speed are projected for 2020 to 2039 (Figure 59). Slightly larger variation is projected for the Alpine region, where a larger decrease is expected in spring and autumn, and a slight increase is projected for summer and winter.
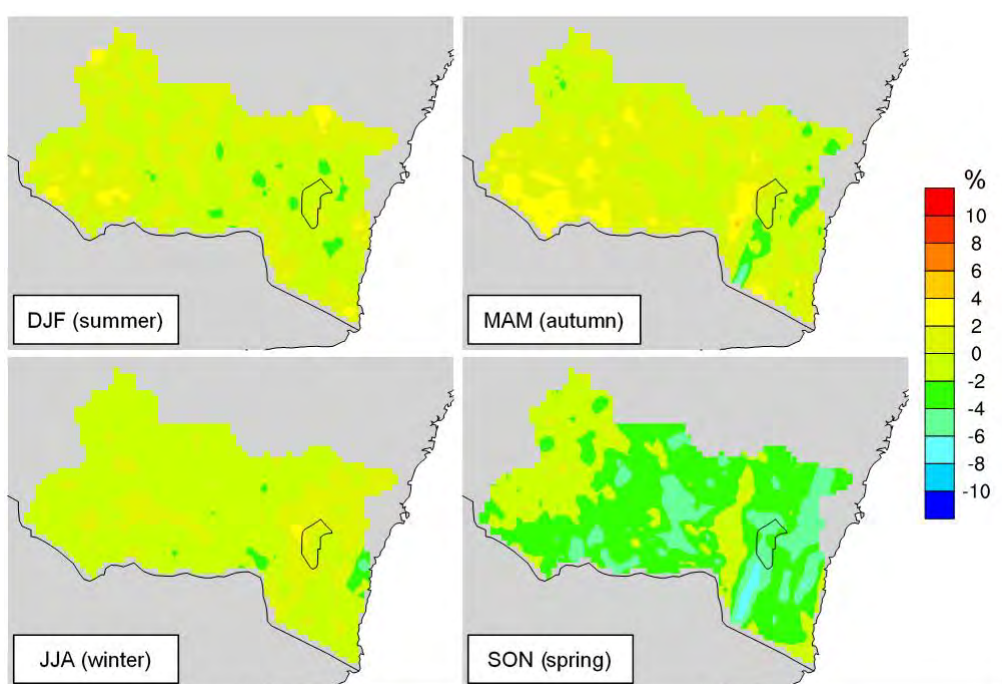

Figure 59   **Changes in seasonal mean maximum wind speed (%) for 2020 to 2039 relative to 1990 to 2009**

Changes in maximum wind speed for 2060 to 2079

Changes in maximum wind speed for 2060 to 2079 are similar to those projected for 2020 to 2039. The only difference is in changes of maximum wind speed for the Kosciuszko National Park, where a slightly larger decrease in maximum wind speed is projected (Figure 60).
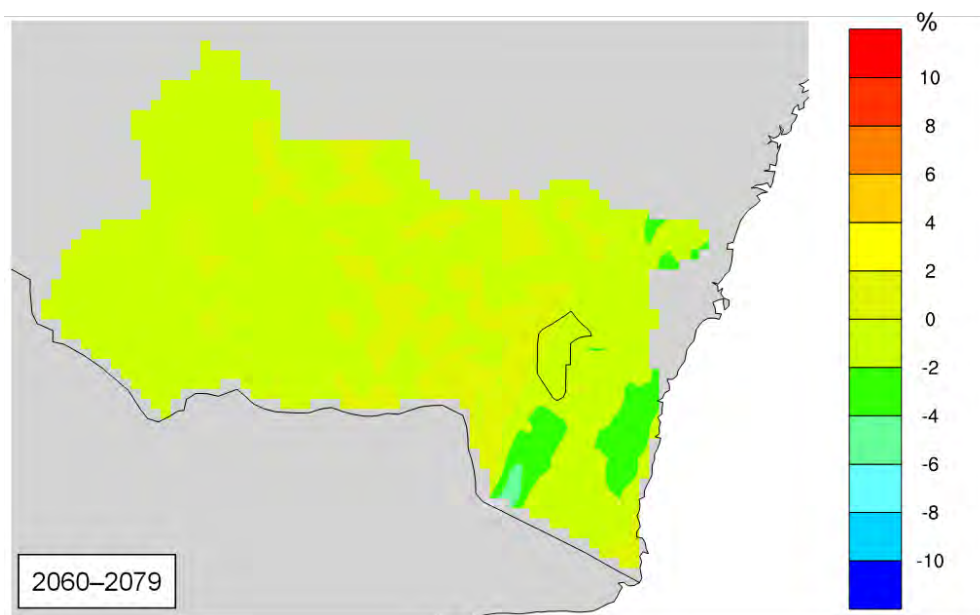

Figure 60   **Changes in annual mean maximum wind speed (%) for 2060 to 2079 relative to 1990 to 2009**

Seasonal variations in changes in maximum wind speed are slightly larger for 2060 to 2079 relative to the 2020 to 2039 period (Figure 61). Some increase in maximum wind speed is projected in the western and eastern MM region in summer and winter respectively; however, decreases will generally be expected for these areas. Relatively larger decreases can be seen in spring and autumn for the Alpine region.
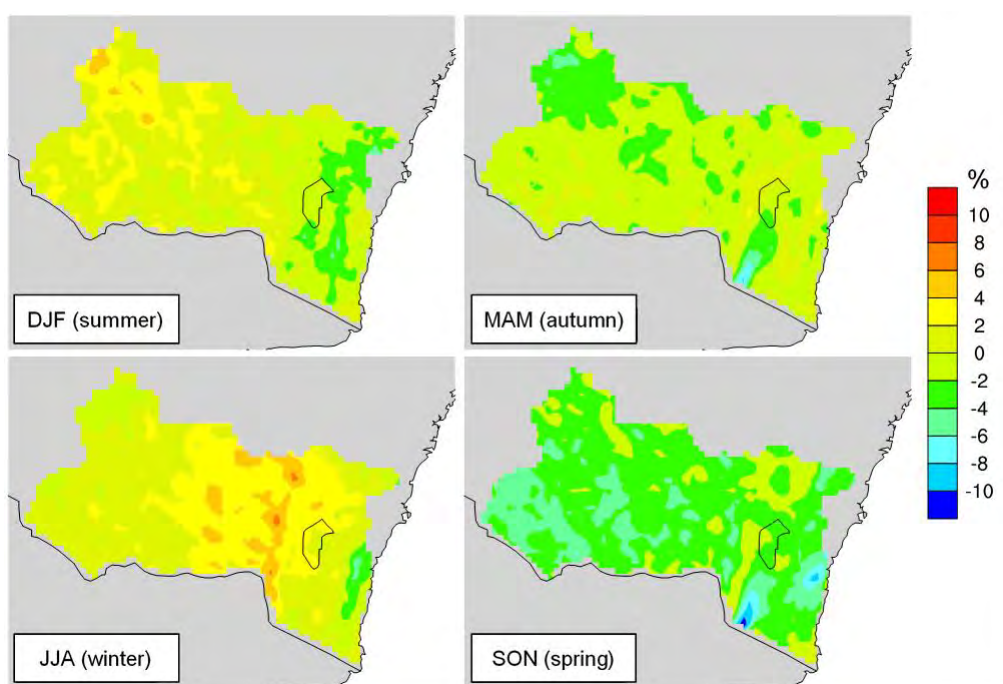

Figure 61   **Changes in seasonal mean maximum wind speed (%) for 2060 to 2079 relative to 1990 to 2009**

3.11   Strong wind days (max. wind speed above 13 m/s)

Mean number of strong wind days for the 1990 to 2009 baseline period

A daily maximum wind speed above 13 m/s is recorded as a strong wind day. It is apparent that strong wind days have a good correlation with the topography of the region. On average, there are more than 120 days a year with strong wind for the Alpine region and 60–80 days a year with strong wind for high topography areas in SET. Fewer than 30 days a year have strong wind for most of the MM region and the coastal region (Figure 62).
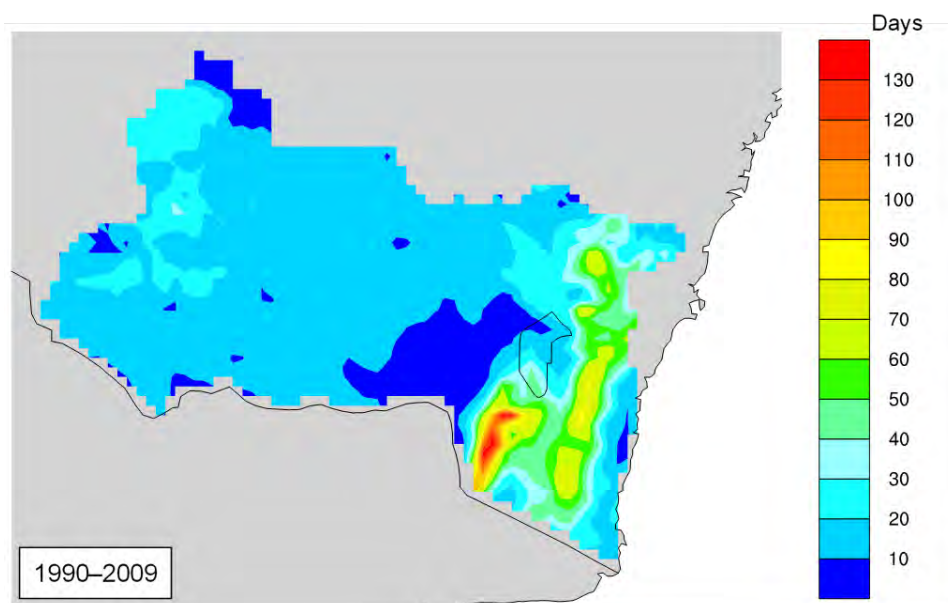

Figure 62   Annual strong wind days for 1990 to 2009

The MM region has a few days with strong wind in winter and autumn, with slightly more strong wind days in the other two seasons. Most of the strong wind days are in winter and spring for the Alpine region and high topography areas, where more than 50 and 20 days, respectively, have strong wind in winter, and more than 30 and 20 days in spring for the Alpine region and high topography areas in SET, respectively (Figure 63).
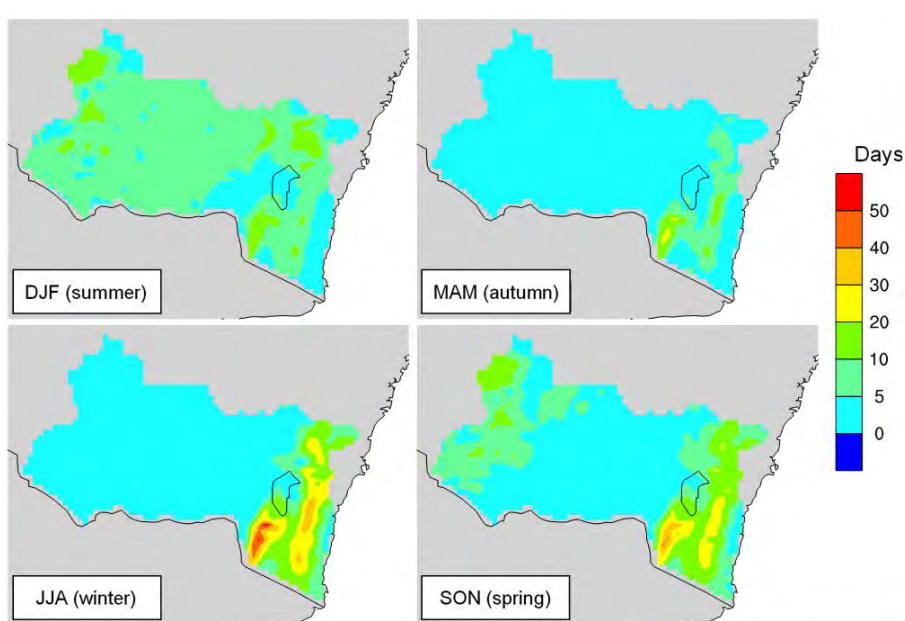

Figure 63   Seasonal strong wind days for 1990 to 2009

Changes in the number of strong wind days for 2020 to 2039

Changes in the number of strong wind days for 2020 to 2039 is very small (Figure 64). On average, about 2–3 more strong wind days are projected for the Alpine region and high topography areas in the SET region, with only around one additional strong wind day projected elsewhere.
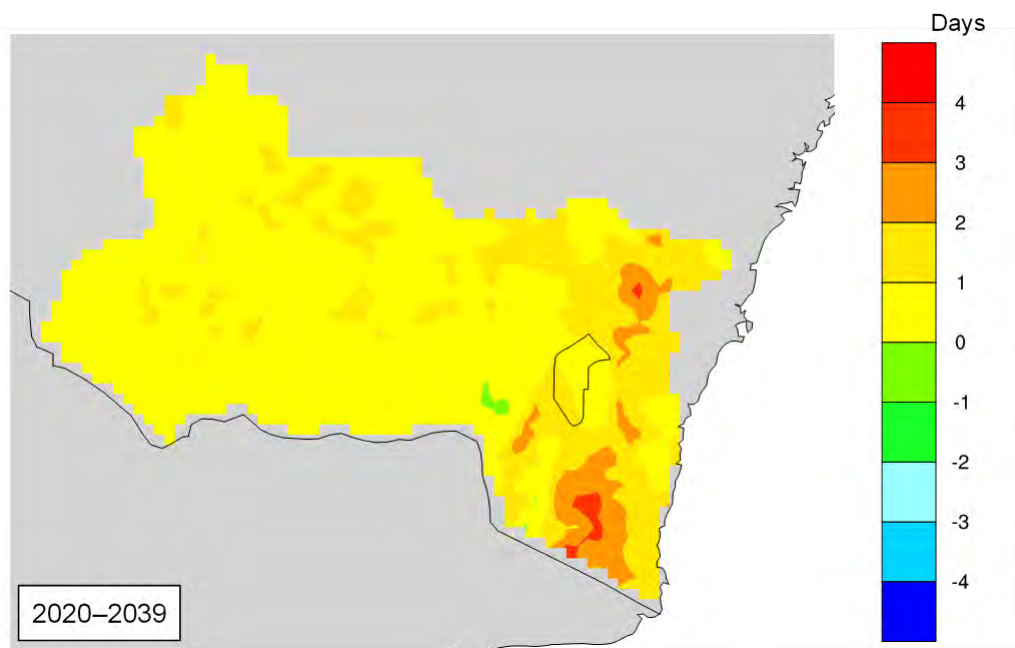

Figure 64   **Changes in annual strong wind days for 2020 to 2039 relative to 1990 to 2009**

Small increases (3–4 days a year) in strong wind days are mainly in winter for the Alpine region and high topography areas in SET (Figure 65), and small decreases (~1–2 days a year) are projected for the other three seasons in the same region. Almost no change is projected for other areas.
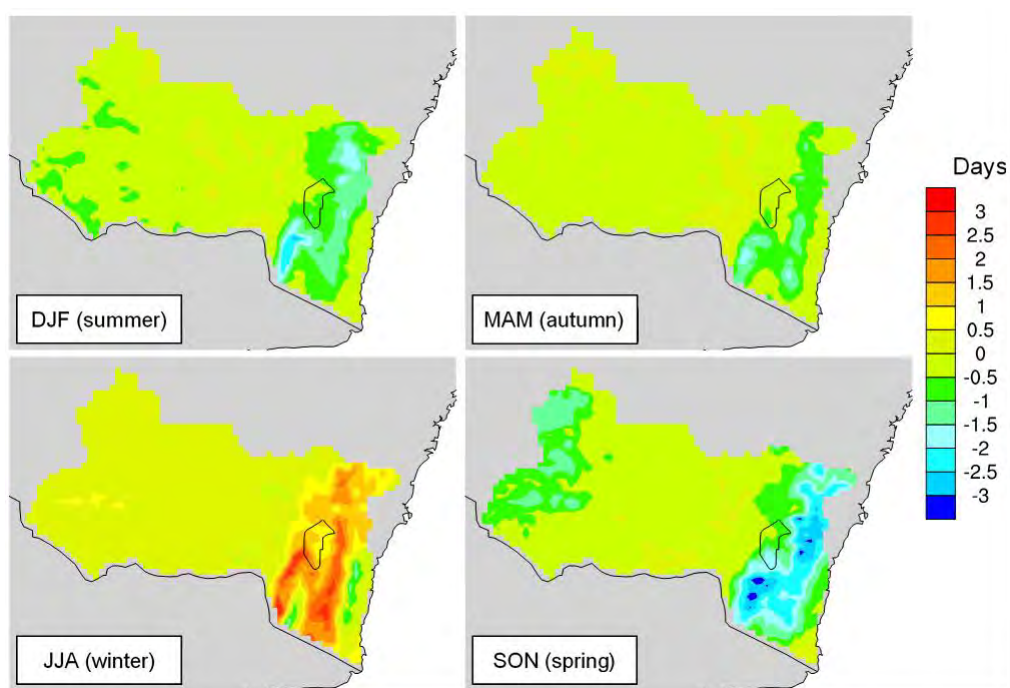

Figure 65   **Changes in seasonal strong wind days for 2020 to 2039 relative to 1990 to 2009**

Changes in the number of strong wind days for 2060 to 2079

A slight decrease in strong wind days is projected for most areas, especially for the Alpine region and high topography areas in the SET region, where 4–6 fewer strong wind days are expected in 2060 to 2079 (Figure 66). The smaller decrease is mostly in spring, summer, and autumn; however, a small increase is projected for winter for the whole study area, which is largest for areas of high topography (Figure 67).
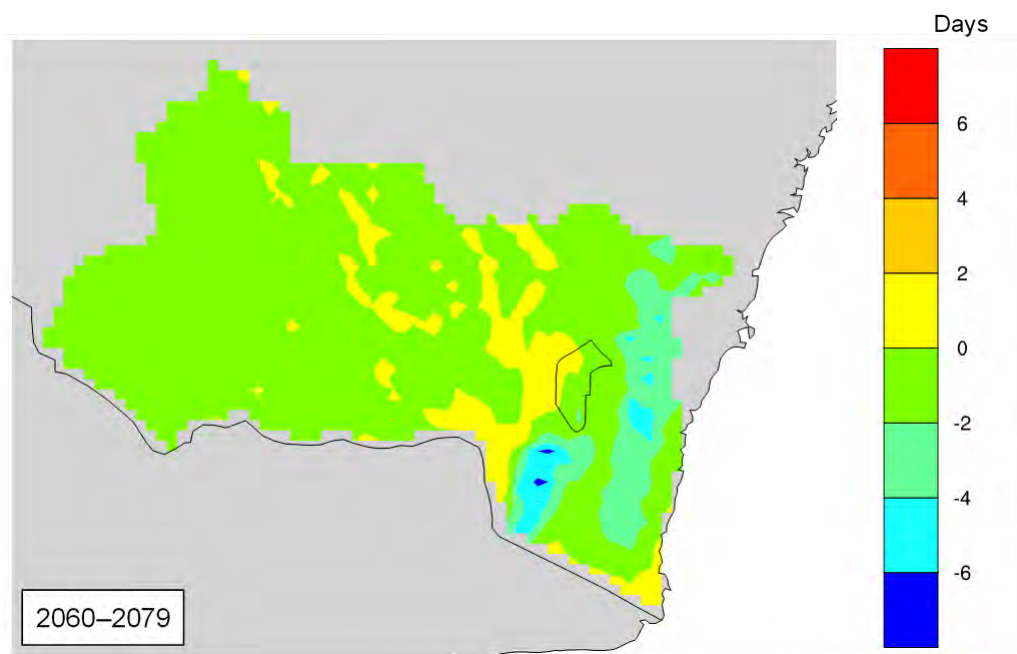
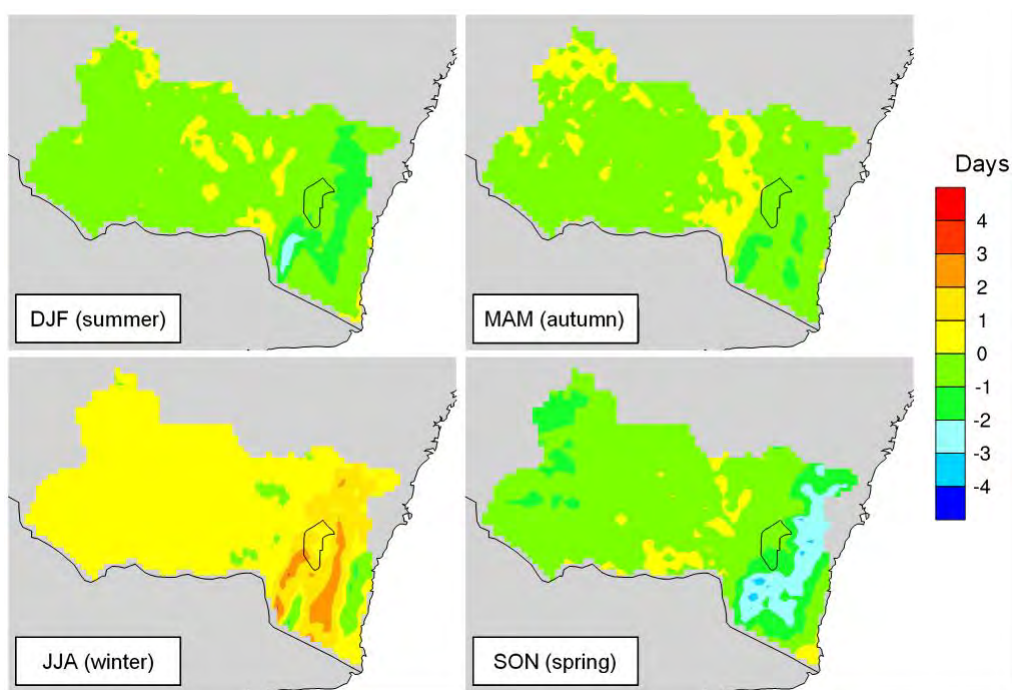**Figure 66**   **Changes in annual strong wind days for 2060 to 2079 relative to 1990 to 2009**

Figure 67   **Changes in seasonal strong wind days for 2060 to 2079 relative to 1990 to 2009**

3.12   Gale days (maximum wind speed above 17 m/s)

Mean number of gale days for the 1990 to 2009 baseline period

Like strong wind days, gale days mostly occur in the Alpine region and high topography areas in the SET region. More than 50 gale days a year are simulated for the Alpine region and more than 20 gale days are simulated for the SET region, with almost no gale days elsewhere (Figure 68). Though gale days can occur at any time, most occur during winter and spring (Figure 69).
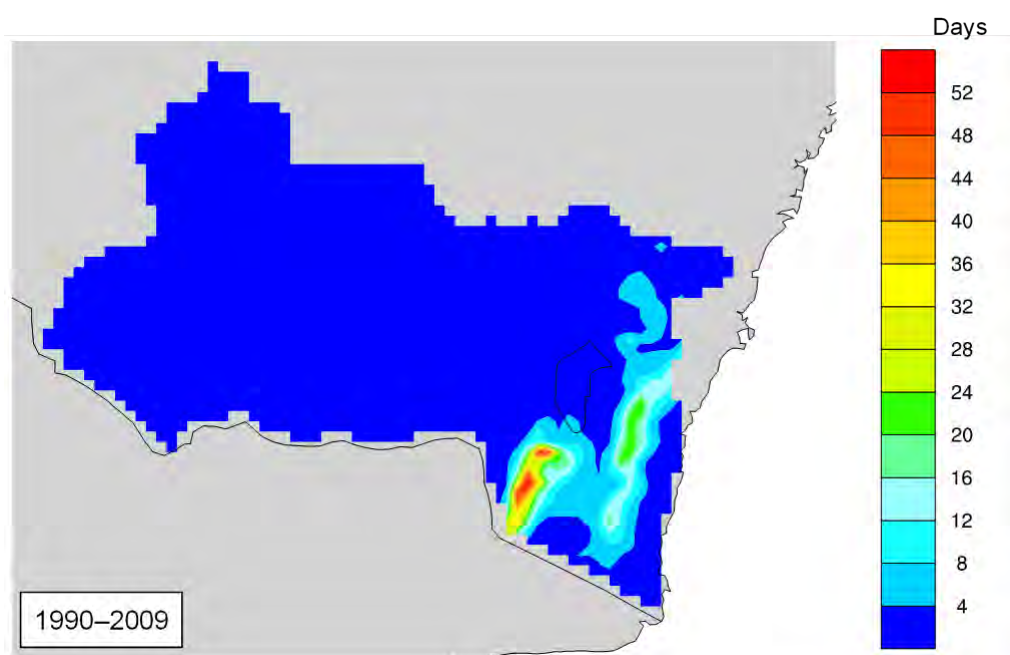

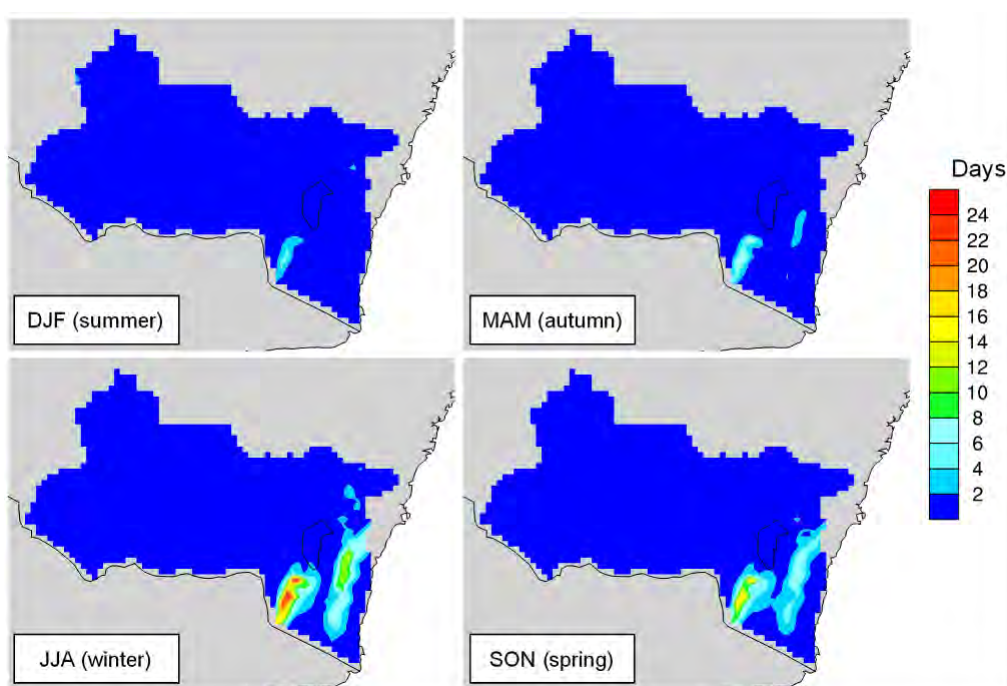**Figure 68   Annual gale days for 1990 to 2009**

Figure 69   Seasonal gale days for 1990 to 2009

Change in the number of gale days for 2020 to 2039

A few more gale days are projected for the Alpine region and high topography areas in the SET region, with almost no changes in other areas for 2020 to 2039 (Figure 70). The few small increases are mostly in winter, with no change in the other seasons (Figure 71).
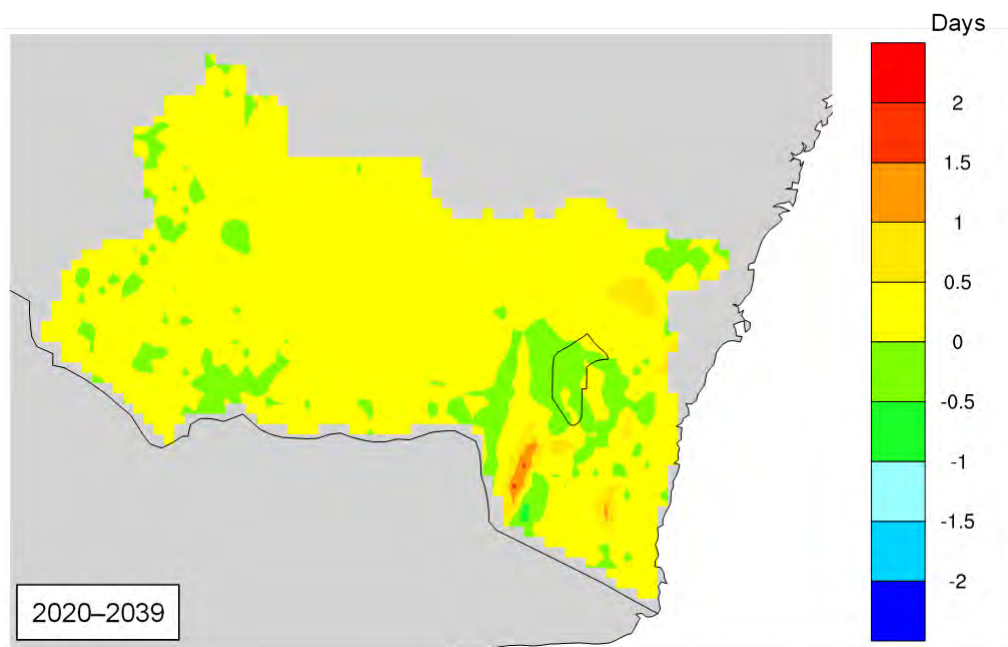

Figure 70   **Changes in annual gale days for 2020 to 2039 relative to 1990 to 2009**

Figure 71   **Changes in seasonal gale days for 2020 to 2039 relative to 1990 to 2009**

Change in the number of gale days for 2060 to 2079

Similar to 2020 to 2039, there is little change in the number of gale days for 2060 to 2079, with 2–4 fewer gale days a year projected at the top of the Alpine region (Figure 72). Projected decreases in the number of gale days are mostly in winter, with almost no change in the other seasons (Figure 73).

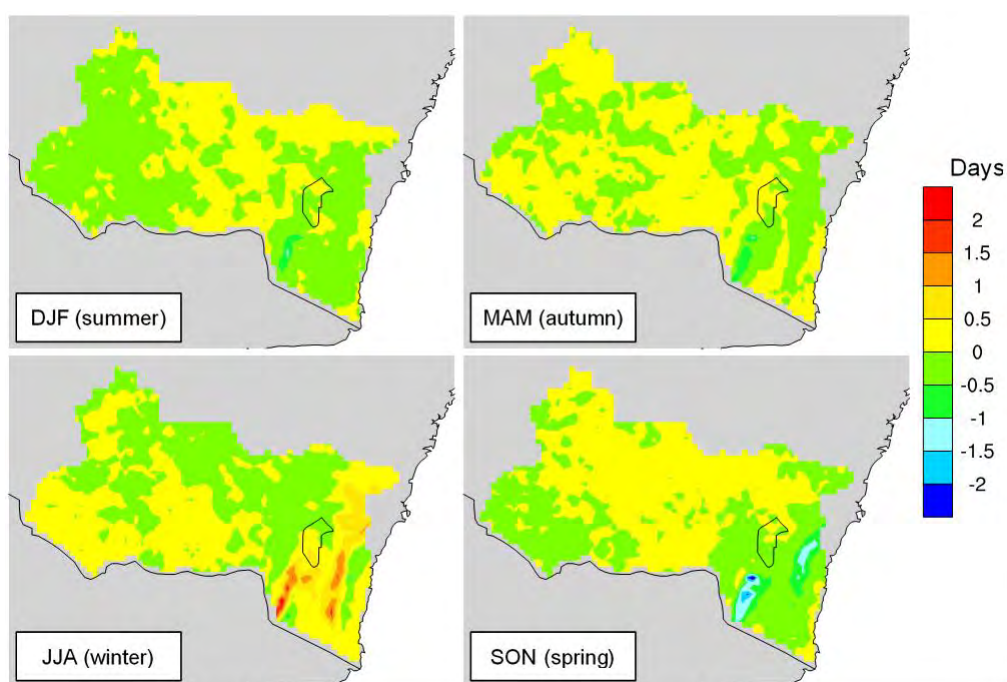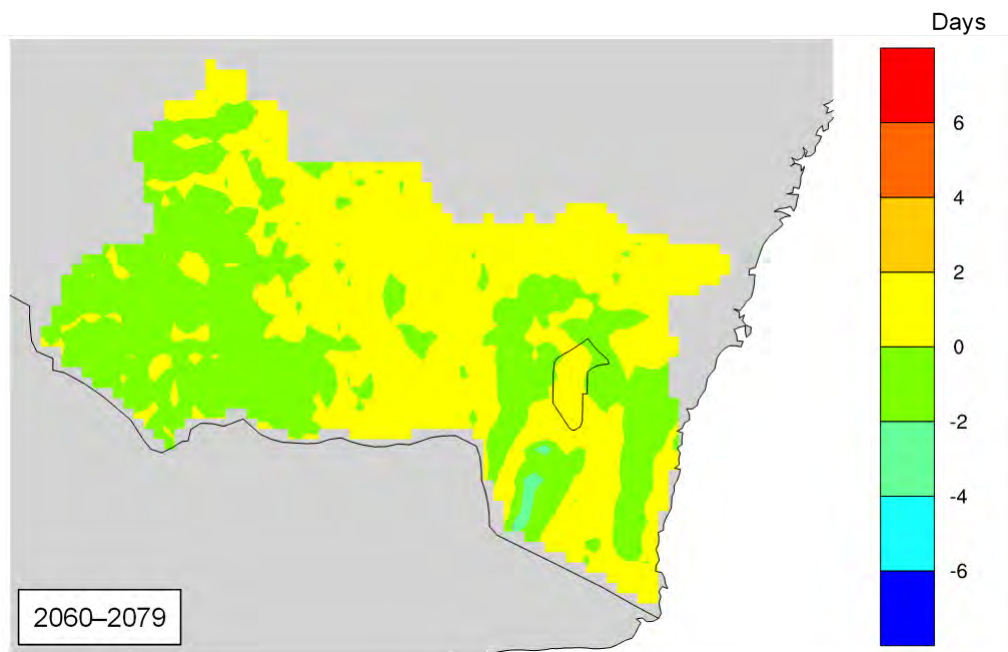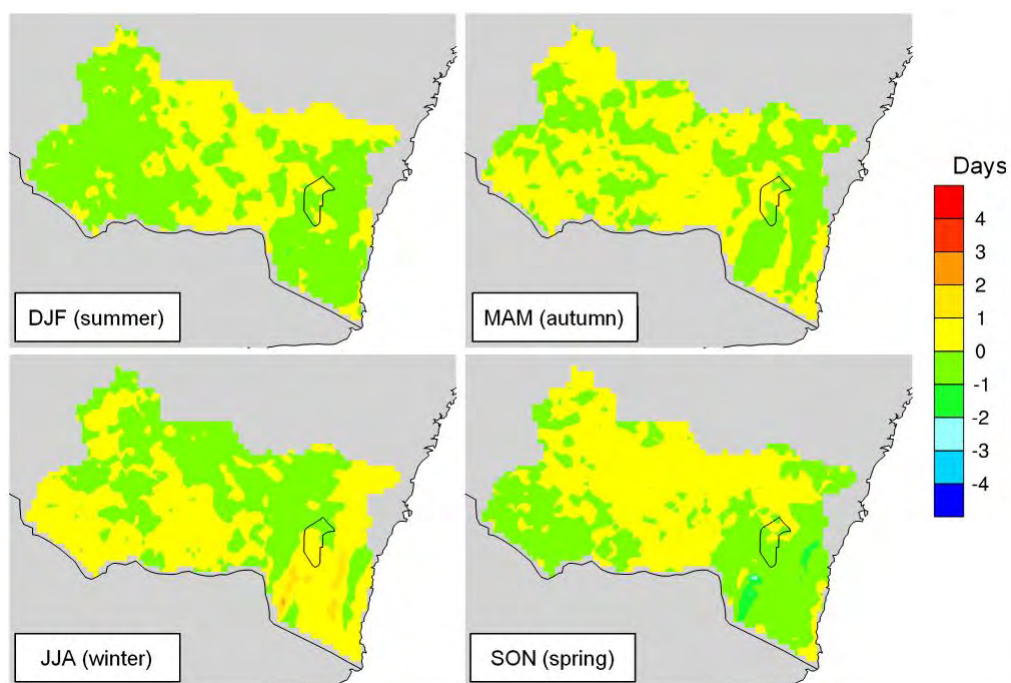**Figure 72**   **Changes in annual gale days for 2060 to 2079 relative to 1990 to 2009**

Figure 73   **Changes in seasonal gale days for 2060 to 2079 relative to 1990 to 2009**

4. Discussion

4.1 Key findings

The results of this report show a number of changes that are projected for the Alpine region and surrounding areas, including changes in precipitation, temperature and wind. The overall key findings indicate:

- The Alpine region will become drier in the future due to a large reduction in precipitation in spring; however, other areas are getting wetter due to more precipitation in summer, winter and autumn.

- The Alpine region will have fewer moderate and heavy rainfall events, which is the opposite of other regions; however, more dry days are expected in the future for all regions.

- Greater increases in maximum temperature are projected for the Alpine region compared with other regions, with the greatest increase occurring in winter. There are no major differences in increases in minimum temperature between the different regions.

- More hot days and fewer cold nights are projected for the MM region and Alpine region, respectively. The greatest of these increases and decreases are in summer and winter respectively; however, spring will also have more hot days and fewer cold nights.

- Mean and maximum wind speed will decrease, mostly in spring; however, little change in strong wind days and gale days are projected for the future.

4.2 Limitations and further research

NARCliM data has its limitations, such as using an older generation CMIP ensemble (i.e. CMIP3), being at a relatively coarse resolution, having limited ensemble members and having only short time periods for analysis.

Only daily rainfall and temperature were bias-corrected on the annual base. Available evaluation (Liu et al. 2018) showed that seasonal or monthly biases are relatively larger even if annual biases are quite small. This has some impacts on threshold-specific variables such as heavy rainfall days, hot days and cold nights.

Results presented in the report are based on the multi-model mean. The same weight was used for each of the 12 GCM/RCM ensemble members. Four GCMs were selected to represent the CMIP3 ensemble. A selected GCM represents different numbers of GCMs in the CMIP3 ensemble. We should consider giving a different weight to each GCM according to the number of GCMs in the ensemble it represents. We should also consider the simulation performance to adjust the weight factor.

Given the short duration of the project, we did not look at the statistical significance and model agreement. This should be assessed in further research.

5.   Conclusion

NARCliM post-processed variables and bias-corrected rainfall and temperature data are used in this study. Results for the multi-model mean, rather than each individual ensemble member, are presented. The results show:

- In the far future, a 2–3°C increase in temperature is projected across the study area. The greatest projected increase in maximum temperature is in the Alpine region during winter, when a more than 3°C increase is expected.

- Less rainfall is projected for the Alpine region in the far future; however, more rainfall is projected for other regions. The reduction in rainfall is mostly due to decreases in spring precipitation, with the increases in rainfall mostly projected to occur in the summer, winter and autumn months.

- More extensive rainfall events are projected for the study area, except for the Alpine region. More dry days are projected across the entire study area.

- Along with larger increases in temperature, more hot days and fewer cold nights are expected in the future.

- Mean and maximum wind speed will decrease; however, little change to the number of strong wind days and gale days is expected in the far future.

6.   References

Di Luca AJ, Evans P and Ji F 2016, *Australian Snowpack: NARCliM ensemble valuation, statistical correction and future projections*, NARCliM Technical Note 7, NARCliM Consortium, Sydney, Australia, 88 pp.

Di Luca AJ, Evans P and Ji F 2018, Australian snowpack in the NARCliM ensemble: evaluation, bias correction and future projections, *Climate Dynamics*, vol.51, no.1–2, pp.639–666.

Evans JP, Ekstrom M and Ji F 2012, Evaluating the performance of a WRF physics ensemble over South-East Australia, *Climate Dynamics*, vol.39, no.6, pp.1241–1258.

Evans JP, Ji F, Abramowitz G, Ekstrom M 2013a, Optimally choosing small ensemble members to produce robust climate simulations, *Environmental Research Letters*, vol.8.

Evans JP, Fita L, Argüeso D and Liu Y 2013b, Initial NARCliM evaluation, in Piantadosi J, Anderssen RS and Boland J (eds), *MODSIM2013, 20th International Congress on Modelling and Simulation*, Modelling and Simulation Society of Australia and New Zealand, December 2013, pp.2765–2771.

Evans J, Ji F, Lee C, Smith P, Argüeso D and Fita L 2014, Design of a regional climate modelling projection ensemble experiment–NARCliM, *Geoscientific Model Development,* vol.7, pp.621–629.

Fita L, Evans JP, Argüeso D, King AD and Liu Y 2016, Evaluation of the regional climate response to large-scale modes in the historical NARCliM simulations, *Climate Dynamics*, pp.1–15, doi: 10.1007/s00382-016-3484-x.

Hughes L 2011, Climate change and Australia: key vulnerable regions, *Regional Environmental Change*, vol.11, no.1, pp.189–195.

IPCC 2000, *Special Report on Emissions Scenarios: A Special Report of Working Group III of the Intergovernmental Panel on Climate Change*, published for the Intergovernmental Panel on Climate Change by Cambridge University Press, Cambridge, UK.

Ji F, Ekstrom M, Evans JP and Teng J 2014, Evaluating rainfall patterns using physics scheme ensembles from a regional atmospheric model, *Theoretical and Applied Climatology*, vol.115, pp.297–304.

Ji F, Evans JP, Teng J, Scorgie Y, Argüeso D and Di Luca A 2016, Evaluation of long-term precipitation and temperature WRF simulations for southeast Australia, *Climate Research*, vol.67, pp.99–115.

Liu DL, Wang B, Evans JP, Ji F, Waters C, Beyer K and Macadam I 2018, Propagation of climate model biases to biophysical modelling can complicate assessments of climate change impact in agricultural systems, *International Journal of Climatology*, vol.39, no.1, pp. 424–444, DOI: 10.1002/joc.5820.

Olson R, Evans JP, Argüeso D, and Di Luca A 2014, *NARCliM Climatological Atlas*, NARCliM Technical Note 4, NARCliM Consortium, Sydney, Australia, 423 pp.

Olson R, Evans JP, Di Luca A, and Argüeso D 2016, The NARCliM project: model agreement and significance of climate projections, *Climate Research*, vol.69, pp.209–227.

Skamarock WC, Klemp JB, Dudhia J, Gill DO, Barker DM, Duda MG, Huang XY, Wang W and Powers JG 2008, *A description of the advanced research WRF Version 3,* NCAR Technical Note, National Center for Atmospheric Research, Boulder Colorado, USA.